DURBAN UNIVERSITY OF TECHNOLOGY

STRUCTURAL, MECHANICAL AND MORPHOLOGICAL ANALYSIS OF SELF ASSEMBLED BIONANOCOMPOSITES

AJAY VASUDEO RANE

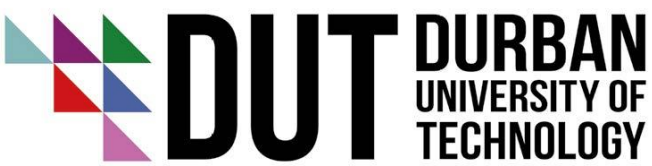

STRUCTURAL, MECHANICAL AND MORPHOLOGICAL ANALYSIS OF SELF ASSEMBLED BIONANOCOMPOSITES

A THESIS SUBMITTED TO THE
DURBAN UNIVERSITY OF TECHNOLOGY
FOR THE DOCTOR OF ENGINEERING DEGREE
(IN MECHANICAL ENGINEERING)
BY

AJAY VASUDEO RANE
DEPARTMENT OF MECHANICAL ENGINEERING
FACULTY OF ENGINEERING AND BUILT ENVIRONMENT
DURBAN 4000, SOUTH AFRICA
2020

FINAL APPROVED SUBMISSION

PROFESSOR KRISHNAN KANNY
(SUPERVISOR)

PROFESSOR SABU THOMAS
(CO-SUPERVISOR)

DR MOHAN TURUP PANDURANGAN
(CO-SUPERVISOR)

DECLARATION

The thesis is being submitted to Durban University of Technology for the award of the degree of Doctor of Engineering (Mechanical Engineering). I declare that the thesis entitled “Structural, Mechanical and Morphological analysis of self-assembled bio nanocomposites” is a record of research work carried out by myself. The content of this thesis, in full or in parts, have not been submitted to any other institute or university for the award of any degree or diploma. I further declare that the only part of this work that has been published is in the form of peer reviewed manuscripts with details provided in “Publications and Conference Presentations”

Signature of Student Date 28 September 2020
(Ajay Vasudeo Rane)

Signature of Supervisor Date 28 September 2020
(Professor Krishnan Kanny)

Signature of Co-supervisor Date 28 September 2020
(Dr Mohan Turup Pandurangan)

Signature of Co-supervisor Date 28 September 2020
(Professor Sabu Thomas)

TO EVERYONE WHO HELPED

ACKNOWLEDGEMENTS

I would express my sincere thanks to Professor Sabu Thomas, Vice Chancellor, Mahatma Gandhi University, Kottayam to arrange a candidature at Durban University of Technology, South Africa, without his kind support it would have never been possible for me to pursue a candidature at Durban University of Technology with Professor Krishnan Kanny. I sincerely thank my research supervisor Professor Krishnan Kanny for providing me with timely help in form of technical advice on research work and financial support during my stay in Durban University of Technology. Many thanks to my co-supervisor Dr Mohan Turup Pandurangan for helping me in all possible perspectives. I would also like to thank the head of department, Dr Festus Maina Mwangi for his support during the submission of this thesis. I would also like to thank good and kind offices of, High Commission of South Africa (New Delhi) and South African Consulate General (Mumbai) for providing study permit. Thanks are extended to CSIR – DST Interbursary Fellowship (Composite) for providing me with a fellowship for a period of three years (2016 – 2019). I would like to place a sincere thanks to staff of department of mechanical engineering, faculty of engineering and built environment, finance department, housing department for their timely support for academic activities. I would sincerely thank, Professor Miroslav Huskic National Institute of Chemistry, Polymer Chemistry and Technology Department, Hajdrihova, 19SI – 1000 Ljubljana, Slovenia and Mahatma Gandhi University, Kottayam in performing dynamic mechanical analysis and spectroscopic analysis. I would like to thank all the authors whose work have been used and well cited in the thesis. I would like to thank all my lab mates in Durban University of Technology and Mahatma Gandhi University for providing me with all the support needed during initial stages of laboratory experiment. I would specially thank my colleagues Ms. Abitha V K, Dr Sajith Rahman, Dr Arool Murugesan, Dr Jemy James and Dr Deepti Yadav for assisting me with my analysis. Special thanks are deserved to Dr Abhishek Guldhe, Ms. Rookmoney Thakur, Dr Lavanya Madhura, Dr Poonam Singh, Dr Nirmal Renuka in giving a support in all respects during my stay in Durban and making my time enjoyable.

THANKS TO MY SWEET FAMILY.

FINALLY THANKS TO ALMIGHTY GOD.

Ajay Vasudeo Rane

TABLE OF CONTENTS

COVER PAGE ..... **i**
TITLE PAGE ..... **ii**
DECLARATION ..... **iii**
DEDICATION ..... **iv**
ACKNOWLEDGEMENTS ..... **v**
TABLE OF CONTENTS ..... **vi**
LIST OF TABLES ..... **xi**
LIST OF FIGURES ..... **xvii**
PUBLICATIONS AND CONFERENCES PRESENTATIONS ..... **xxiv**
PUBLICATIONS xxiv
CONFERENCES xxiv
1 INTRODUCTION **2**
1.1 BACKGROUND AND PROBLEM STATEMENT[1] 2
1.2 AIM 3
1.3 OBJECTIVES OF STUDY 4
1.3.1 PRELIMINARY STUDY 4
1.3.2 PILOT STUDY 4
1.3.3 MAIN STUDY 4
1.4 ASSUMPTIONS 5
1.5 DELIMITATIONS 5
1.6 LIMITATIONS 5
1.7 STRUCTURE OF DISSERTATION 5
2 LITERATURE REVIEW **7**
2.1 INTRODUCTION 7
2.2 CLASSIFICATION OF ENGINEERING MATERIALS 8
2.3 FUNCTIONAL CLASSIFICATION OF MATERIALS 10
2.4 ENGINNERING REQUIREMENT OF MATERIALS 12
2.5 ORGANIC, INORGANIC AND BIOLOGICAL MATERIALS 13

2.6 POLYMER COMPOSITES 15
2.7 POLY (LACTIC ACID) AND POLY (LACTIC ACID) COMPOSITES 20
2.7.1 OVERVIEW OF POLY (LACTIC ACID) 20
2.7.2 SYNTHESIS AND PRODUCTION 21
2.7.3 STRUCTURE – PROPERTY RELATIONSHIP 25
2.7.4 PROPERTIES OF POLY (LACTIC ACID) 26
2.7.5 DEGRADATION AND STABILITY 27
2.7.6 APPLICATIONS 27
2.7.7 OVERVIEW OF POLY (LACTIC ACID) COMPOSITES AND NANOCOMPOSITES 28
2.7.8 CONCLUSION 35
3 MATERIALS AND METHODS 36
3.1 MATERIALS AND METHODS FOR EXTRACTION OF CELLULOSE NANOFIBERS 37
3.1.1 MATERIALS FOR EXTRACTION OF CELLULOSE NANOFIBERS 37
3.1.2 METHOD ADOPTED FOR EXTRACTION OF CELLULOSE NANOFIBERS 37
3.2 MATERIALS AND METHODS FOR PREPRATION OF POLY (LACTIC ACID) COMPOSITES 37
3.2.1 MATERIALS FOR POLY (LACTIC ACID) COMPOSITES 37
3.2.2 METHODS ADOPTED FOR FABRICATION OF POLY (LACTIC ACID) COMPOSITES 38
3.3 CHARACTERIZATIONS 43
3.3.1 CHARACTERIZATIONS FOR TESTING CELLULOSE NANOFIBERS 43
3.3.2 CHARACTERIZATIONS FOR TESTING POLY (LACTIC ACID) COMPOSITES 43
4 PROCESS TECHNIQUE SELECTION & EXTRACTION OF CELLULOSE NANOFIBERS 48
4.1 PROCESS TECHNIQUE SELECTION 48
4.1.1 PHYSICAL AND MECHANICAL PROPERTIES AND MORPHOLOGICAL PROPERTIES 48
4.1.2 FINAL CONCLUSION 79

4.2 EXTRACTION OF CELLULOSE FIBERS AND CONFIRMING ITS NANOFORM .. 79
4.2.1 CHEMICAL COMPOSITION AND NATURE [ATR – FTIR AND XRD]..... 80
4.2.2 PARTICLE SIZE ANALYSIS AND SURFACE CHARGE DETERMINATION [DYNAMIC LIGHT SCATTERING] 81
4.2.3 THERMAL ANALYSIS [THERMAL GRAVIMETRIC ANALYSIS] 81
4.2.4 MORPHOLOGICAL ANALYSIS [SCANNING ELECTRON MICROSCOPY] ... 82
4.2.5 CONCLUSION 83
5 CHARACTERIZING INTERPHASE MODIFICATION 84
5.1 ULTRAVIOLET – VISIBLE SPECTROSCOPY 84
5.1.1 INTRODUCTION..... 84
5.1.2 CONCLUSION 98
5.1.3 LIMITATION OF ULTRAVIOLET – VISIBLE SPECTROSCOPY 98
5.2 DENSITY 98
5.2.1 ABSTRACT 98
5.2.2 CONCLUSION 101
5.3 FINAL CONCLUSION 101
6 STRUCTURAL ANALYSIS 102
6.1 CARBON BLACK 102
6.1.1 ROLE OF ATR – FTIR SPECTROSCOPY 102
6.1.2 INTRODUCTION..... 103
6.1.3 RESULTS AND DISCUSSION 105
6.1.4 CONCLUSION 112
6.2 MULTIWALLED CARBON NANOTUBES..... 112
6.2.1 ABSORTION BANDS OF MULTIWALLED CARBON NANOTUBES AND POLY (LACTIC ACID) COMPOSITES FILLED WITH MULTIWALLED CARBON NANOTUBES 112
6.3 CELLULOSE NANOFIBERS 115
6.3.1 ABSORPTION BANDS OF CELLULOSE NANOFIBERS AND POLY (LACTIC ACID) COMPOSITES FILLED WITH CELLULOSE NANOFIBERS 115

6.4 CARBON BLACK + MULTIWALLED CARBON NANOTUBES 118
6.4.1 ABSORPTION BANDS OF CARBON BLACK + MULTIWALLED CARBON NANOTUBES FILLED POLY (LACTIC ACID) COMPOSITES 118
6.5 CARBON BLACK + CELLULOSE NANOFIBERS 121
6.5.1 ABSORPTION BANDS OF CARBON BLACK + NANOCELLULOSE FILLED POLY (LACTIC ACID) COMPOSITES 121
6.6 FINAL CONCLUSION 124
7 MORPHOLOGICAL ANALYSIS 126
7.1 INTRODUCTION 126
7.2 DISPERSION CHARACTERISTICS [SUBMICROSTRUCTURE] 128
7.2.1 TRANSMISSION ELECTRON MICROSCOPY 128
7.2.2 ATOMIC FORCE MICROSCOPY 133
7.3 FRACTURE STUDIES [MICROSTRUCTURE] 138
7.3.1 OPTICAL MICROSCOPY 138
7.3.2 SCANNING ELECTRON MICROSCOPY 140
7.4 FINAL CONCLUSION 143
8 PHYSIO-MECHANICAL PROPERTIES 145
8.1 DENSITY 145
8.2 HARDNESS 145
8.3 TENSILE TEST 154
8.4 NOTCHED IZOD IMPACT 191
8.5 FLEXURAL TEST 200
8.5.1 FLEXURAL STRENGTH 200
8.5.2 FLEXURAL MODULUS 209
8.6 HEAT DEFLECTION TEST 218
8.7 CONCLUSION 226
9 CONSTRAINED REGION ESTIMATION 227
9.1 DISCUSSION 227
9.2 CONCLUSION 228

10 GENERAL CONCLUSION AND FUTURE OUTLOOK 229

10.1 GENERAL CONCLUSION 229

10.2 FUTURE OUTLOOK 230

APPENDIX 1 – SYNTHESIZED CELLULOSE NANOFIBERS..... 231

APPENDIX 2 – PERCENT CHANGE..... 232

REFERENCES..... 235

LIST OF TABLES

Table 6.1: Absorption peaks in neat poly (lactic acid) and its carbon black filled poly (lactic acid) composites 108
Table 6.2: %Transmittance and Area for characteristics peaks of neat poly (lactic acid) and its shifts in carbon black filled poly (lactic acid) composites..... 110
Table 6.3: Absorption peaks in neat poly (lactic acid) and its multiwalled carbon nanotubes filled poly (lactic acid) composites 113
Table 6.4: %Transmittance and Area for characteristics peaks of neat poly (lactic acid) and its shifts in multiwalled carbon nanotubes filled poly (lactic acid) composites..... 114
Table 6.5: Absorption peaks in neat poly (lactic acid) and its cellulose nanofibers filled poly (lactic acid) composites 115
Table 6.6: Transmittance and Area for characteristics peaks of neat poly (lactic acid) and its shifts in cellulose nanofibers filled poly (lactic acid) composites 117
Table 6.7: Absorption peaks in neat poly (lactic acid) and its carbon black + multiwalled carbon nanotubes filled poly (lactic acid) composites 118
Table 6.8: Transmittance and Area for characteristics peaks of neat poly (lactic acid) and its shifts in carbon black + multiwalled carbon nanotubes filled poly (lactic acid) composites.. 120
Table 6.9: Absorption peaks in neat poly (lactic acid) and its carbon black + cellulose nanofibers filled poly (lactic acid) composites 121
Table 6.10: Transmittance and Area for characteristics peaks of neat poly (lactic acid) and its shifts in carbon black + cellulose nanofibers filled poly (lactic acid) composites 123
Table 8.1. Descriptive Statistics of Hardness for Carbon black filled Poly (lactic acid) composites..... 145
Table 8.2. Descriptive Statistics of Hardness for multiwalled carbon nanotubes filled Poly (lactic acid) composites 145
Table 8.3. Descriptive Statistics of Hardness for cellulose nanofibers filled Poly (lactic acid) composites..... 146
Table 8.4. Descriptive Statistics of Hardness for 2.5carbon black + multiwalled carbon nanotubes and 2.5carbon black + cellulose nanofibers filled Poly (lactic acid) composites. 147
Table 8.5. Means Comparison of hardness by Bonferroni Test for carbon black filled poly (lactic acid) composites 148
Table 8.6. Means Comparison of hardness by Bonferroni Test for multiwalled carbon nanotubes filled poly (lactic acid) composites 149

Table 8.7. Means Comparison of hardness by Bonferroni Test for cellulose nanofibers filled poly (lactic acid) composites 150
Table 8.8. Means Comparison of hardness by Bonferroni Test for 2.5carbon black + multiwalled carbon nanotubes filled poly (lactic acid) composites 151
Table 8.9. Means Comparison of hardness by Bonferroni Test for 2.5carbon black + cellulose nanofibers filled poly (lactic acid) composites 152
Table 8.10. Descriptive Statistics of tensile modulus for Carbon black filled Poly (lactic acid) composites 154
Table 8.11. Descriptive Statistics of yield strength for Carbon black filled Poly (lactic acid) composites 154
Table 8.12. Descriptive Statistics of tensile strength for Carbon black filled Poly (lactic acid) composites 155
Table 8.13. Descriptive Statistics of tensile elongation for Carbon black filled Poly (lactic acid) composites 156
Table 8.14. Descriptive Statistics of tensile modulus for multiwalled carbon nanotubes filled Poly (lactic acid) composites 157
Table 8.15. Descriptive Statistics of tensile modulus for cellulose nanofibers filled Poly (lactic acid) composites 158
Table 8.16. Descriptive Statistics of tensile modulus for 2.5carbon black + multiwalled carbon nanotubes and 2.5carbon black + cellulose nanofibers filled Poly (lactic acid) composites. 159
Table 8.17. Descriptive Statistics of yield strength for multiwalled carbon nanotubes filled Poly (lactic acid) composites 159
Table 8.18. Descriptive Statistics of yield strength for cellulose nanofibers filled Poly (lactic acid) composites 160
Table 8.19. Descriptive Statistics of yield strength for 2.5carbon black + multiwalled carbon nanotubes and 2.5carbon black + cellulose nanofibers filled Poly (lactic acid) composites. 161
Table 8.20. Descriptive Statistics of tensile strength for multiwalled carbon nanotubes filled Poly (lactic acid) composites 161
Table 8.21. Descriptive Statistics of tensile strength for cellulose nanofibers filled Poly (lactic acid) composites 162
Table 8.22. Descriptive Statistics of tensile strength for 2.5carbon black + multiwalled carbon nanotubes and 2.5carbon black + cellulose nanofibers filled Poly (lactic acid) composites. 164
Table 8.23. Descriptive Statistics of tensile elongation for multiwalled carbon nanotubes filled Poly (lactic acid) composites 166

Table 8.24. Descriptive Statistics of tensile elongation for cellulose nanofibers filled Poly (lactic acid) composites 167
Table 8.25. Descriptive Statistics of tensile elongation for 2.5carbon black + multiwalled carbon nanotubes and 2.5carbon black + cellulose nanofibers filled Poly (lactic acid) composites 167
Table 8.26. Means Comparison of tensile modulus by Bonferroni Test for carbon black filled poly (lactic acid) composites 168
Table 8.27. Means Comparison of tensile modulus by Bonferroni Test for multiwalled carbon nanotubes filled poly (lactic acid) composites 169
Table 8.28. Means Comparison of tensile modulus by Bonferroni Test for cellulose nanofibers filled poly (lactic acid) composites 170
Table 8.29. Means Comparison of tensile modulus by Bonferroni Test for 2.5carbon black + multiwalled carbon nanotubes filled poly (lactic acid) composites 171
Table 8.30. Means Comparison of tensile modulus by Bonferroni Test for 2.5carbon black + cellulose nanofibers filled poly (lactic acid) composites 172
Table 8.31. Means Comparison of yield strength by Bonferroni Test for carbon black filled poly (lactic acid) composites 173
Table 8.32. Means Comparison of yield strength by Bonferroni Test for multiwalled carbon nanotubes filled poly (lactic acid) composites 174
Table 8.33. Means Comparison of yield strength by Bonferroni Test for cellulose nanofibers filled poly (lactic acid) composites 175
Table 8.34. Means Comparison of yield strength by Bonferroni Test for 2.5carbon black + multiwalled carbon nanotubes filled poly (lactic acid) composites 176
Table 8.35. Means Comparison of yield strength by Bonferroni Test for 2.5carbon black + cellulose nanofibers filled poly (lactic acid) composites 177
Table 8.36. Means Comparison of tensile strength by Bonferroni Test for carbon black filled poly (lactic acid) composites 178
Table 8.37. Means Comparison of tensile strength by Bonferroni Test for multiwalled carbon nanotubes filled poly (lactic acid) composites 179
Table 8.38. Means Comparison of tensile strength by Bonferroni Test for cellulose nanofibers filled poly (lactic acid) composites 180
Table 8.39. Means Comparison of tensile strength by Bonferroni Test for 2.5carbon black + multiwalled carbon nanotubes filled poly (lactic acid) composites 181

Table 8.40. Means Comparison of tensile strength by Bonferroni Test for 2.5carbon black + cellulose nanofibers filled poly (lactic acid) composites 182
Table 8.41. Means Comparison of tensile elongation by Bonferroni Test for carbon black filled poly (lactic acid) composites..... 183
Table 8.42. Means Comparison of tensile elongation by Bonferroni Test for multiwalled carbon nanotubes filled poly (lactic acid) composites 184
Table 8.43. Means Comparison of tensile elongation by Bonferroni Test for cellulose nanofibers filled poly (lactic acid) composites..... 185
Table 8.44. Means Comparison of tensile elongation by Bonferroni Test for 2.5carbon black + multiwalled carbon nanotubes filled poly (lactic acid) composites..... 186
Table 8.45. Means Comparison of tensile elongation by Bonferroni Test for 2.5carbon black + cellulose nanofibers filled poly (lactic acid) composites 187
Table 8.46. Descriptive Statistics of notched Izod impact for Carbon black filled Poly (lactic acid) composites 192
Table 8.47. Descriptive Statistics of notched Izod impact for Multiwalled carbon nanotubes filled Poly (lactic acid) composites..... 192
Table 8.48. Descriptive Statistics of notched Izod impact for Cellulose nanofibers filled Poly (lactic acid) composites..... 193
Table 8.49. Descriptive Statistics of notched Izod impact for 2.5carbon black + multiwalled carbon nanotubes and 2.5carbon black + cellulose nanofibers filled Poly (lactic acid) composites..... 193
Table 8.50. Means Comparison of notched Izod impact by Bonferroni Test for carbon black filled poly (lactic acid) composites 194
Table 8.51. Means Comparison of notched Izod impact by Bonferroni Test for multiwalled carbon nanotubes filled poly (lactic acid) composites 195
Table 8.52. Means Comparison of notched Izod impact by Bonferroni Test for cellulose nanofibers filled poly (lactic acid) composites..... 196
Table 8.53. Means Comparison of notched Izod impact by Bonferroni Test for 2.5carbon black + multiwalled carbon nanotubes filled poly (lactic acid) composites..... 197
Table 8.54. Means Comparison of notched Izod impact by Bonferroni Test for 2.5carbon black + cellulose nanofibers filled poly (lactic acid) composites..... 198
Table 8.55. Descriptive Statistics of flexural strength for Carbon black filled Poly (lactic acid) composites..... 201

Table 8.56. Descriptive Statistics of flexural strength for multiwalled carbon nanotubes filled Poly (lactic acid) composites 201
Table 8.57. Descriptive Statistics of flexural strength for cellulose nanofibers filled Poly (lactic acid) composites 202
Table 8.58. Descriptive Statistics of flexural strength for 2.5carbon black + multiwalled carbon nanotubes and 2.5carbon black + cellulose nanofibers filled Poly (lactic acid) composites. 202
Table 8.59. Means Comparison of flexural strength by Bonferroni Test for carbon black filled poly (lactic acid) composites..... 203
Table 8.60. Means Comparison of flexural strength by Bonferroni Test for multiwalled carbon nanotubes filled poly (lactic acid) composites 204
Table 8.61. Means Comparison of flexural strength by Bonferroni Test for cellulose nanofibers filled poly (lactic acid) composites 205
Table 8.62. Means Comparison of flexural strength by Bonferroni Test for 2.5carbon black + multiwalled carbon nanotubes filled poly (lactic acid) composites..... 206
Table 8.63. Means Comparison of flexural strength by Bonferroni Test for 2.5carbon black + cellulose nanofibers filled poly (lactic acid) composites 207
Table 8.64. Descriptive Statistics of flexural modulus for Carbon black filled Poly (lactic acid) composites..... 210
Table 8.65. Descriptive Statistics of flexural modulus for multiwalled carbon nanotubes filled Poly (lactic acid) composites 210
Table 8.66. Descriptive Statistics of flexural modulus for cellulose nanofibers filled Poly (lactic acid) composites 211
Table 8.67. Descriptive Statistics of flexural modulus for 2.5carbon black + multiwalled carbon nanotubes and 2.5carbon black + cellulose nanofibers filled Poly (lactic acid) composites. 211
Table 8.68. Means Comparison of flexural modulus by Bonferroni Test for carbon black filled poly (lactic acid) composites..... 212
Table 8.69. Means Comparison of flexural modulus by Bonferroni Test for multiwalled carbon nanotubes filled poly (lactic acid) composites 213
Table 8.70. Means Comparison of flexural modulus by Bonferroni Test for cellulose nanofibers filled poly (lactic acid) composites 214
Table 8.71. Means Comparison of flexural modulus by Bonferroni Test for 2.5carbon black + multiwalled carbon nanotubes filled poly (lactic acid) composites..... 215
Table 8.72. Means Comparison of flexural modulus by Bonferroni Test for 2.5carbon black + cellulose nanofibers filled poly (lactic acid) composites 216

Table 8.73. Descriptive Statistics of heat deflection test for Carbon black filled Poly (lactic acid) composites 219
Table 8.74. Descriptive Statistics of heat deflection test for multiwalled carbon nanotubes filled Poly (lactic acid) composites 219
Table 8.75. Descriptive Statistics of heat deflection test for cellulose nanofibers filled Poly (lactic acid) composites 220
Table 8.76. Descriptive Statistics of heat deflection test for 2.5carbon black + multiwalled carbon nanotubes and 2.5carbon black + cellulose nanofibers filled Poly (lactic acid) composites 220
Table 8.77. Means Comparison of heat deflection test by Bonferroni Test for carbon black filled poly (lactic acid) composites 221
Table 8.78. Means Comparison of heat deflection test by Bonferroni Test for multiwalled carbon nanotubes filled poly (lactic acid) composites 222
Table 8.79. Means Comparison of heat deflection test by Bonferroni Test for cellulose nanofibers filled poly (lactic acid) composites 223
Table 8.80. Means Comparison of heat deflection test by Bonferroni Test for 2.5carbon black + multiwalled carbon nanotubes filled poly (lactic acid) composites 224
Table 8.81. Means Comparison of heat deflection test by Bonferroni Test for 2.5carbon black + cellulose nanofibers filled poly (lactic acid) composites 225

LIST OF FIGURES

Figure 2.1. Schematic representation of molecular dimensions zones in filled polymer composites (Interface and Interphase) 16
Figure 2.2. Schematic representation of phases in polymer composite “Macrostructure of a polymer composite” 17
Figure 2.3: General routes for poly (lactic acid) synthesis and production 21
Figure 2.4: Classification of poly (lactic acid) based on synthesis 22
Figure 2.5: Applications of poly (lactic acid) 28
Figure 3.1: Poly(lactic acid) dissolution stages 38
Figure 3.2: Preparation of Filler Dispersion 39
Figure 3.3: Preparation of PLA - filler Suspension 40
Figure 3.4: Preparation of oligomeric dispersion 41
Figure 3.5: Preparation of PLA mixture 42
Figure 4.1: Effect of carbon black on the relative density of carbon black filled poly (lactic acid) composites (unit of measurement – g/cm^3) 49
Figure 4.2: Effect of carbon black on the hardness of carbon black filled poly (lactic acid) composites 51
Figure 4.3: Stress-Strain Curve for DDCS poly (lactic acid) composites 52
Figure 4.4: Stress-Strain Curve for MMCM poly (lactic acid) composites 53
Figure 4.5: Effect of wt% of carbon black on the tensile yield strength of carbon black filled poly (lactic acid) composites 54
Figure 4.6: Effect of wt% of carbon black on elongation at break of carbon black filled poly (lactic acid) composites 57
Figure 4.7: Effect of carbon black on Young Modulus of carbon black filled poly (lactic acid) composites and theoretical modeling for Young Modulus 59
Figure 4.8: Effect of carbon black on notched Izod impact of carbon black filled poly (lactic acid) composites 60
Figure 4.9: Effect of carbon black on Flexural strength of carbon black filled poly (lactic acid) composites 62
Figure 4.10: Effect of carbon black on Flexural Modulus of carbon black filled poly (lactic acid) composites and theoretical modeling for Flexural Modulus 63
Figure 4.11: Effect of carbon black on heat deflection of carbon black filled poly (lactic acid) composites 65

Figure 4.12: Carbon black particles dispersed in poly (lactic acid) matrix at (a) 0.5wt% (b) 1.5wt% (c) 2.5wt% and (d) 10.0wt% (black color indicates carbon black particles and rest as poly (lactic acid) matrix)..... 67
Figure 4.13: Relative Swelling – Kraus Plot..... 68
Figure 4.14: Transmission electron microscopic images for carbon black, ultra-microtomed specimens of poly (lactic acid) and carbon black filled poly (lactic acid) composites..... 71
Figure 4.15: : Particle size distribution in transmission electron microscopic images for carbon black filled poly (lactic acid) composites. (0.2 wt %, 1.5 wt %, 2.5 wt %, 5.0 wt % and 10.0wt %) (Particle size was determined using ImageJ Software) 72
Figure 4.16: Atomic force microscopic images for microtomed specimens of poly (lactic acid) and carbon black filled poly (lactic acid) composites..... 73
Figure 4.17: Roughness Average Values in Atomic Force Microscopic images for carbon black filled poly (lactic acid) composites (0.2 wt %, 0.5 wt %, 1.5 wt %, 2.5 wt %, 5.0 wt % and 10.0wt %)..... 74
Figure 4.18: Optical microscopic images for tensile fractured specimens of poly (lactic acid) specimen and carbon black filled poly (lactic acid) composites (at X200 magnification)) 76
Figure 4.19: Scanning electron microscopic images for tensile fractured specimens of poly (lactic acid) specimen and carbon black filled poly (lactic acid) composites (at X1000 magnification))..... 77
Figure 4.20: Structural Characterization by Infrared Spectroscopy(ATR - FTIR) and X Ray Diffraction (XRD) – of cellulose nanofibers (a) (b) (c) ATR - FTIR spectra and (d) XRD spectra 79
Figure 4.21: Particle size analysis of cellulose nanofibers by Dynamic Light Scattering (DLS) 80
Figure 4.22: Surface charge determination on cellulose nanofibers by Zeta Potential 81
Figure 4.23: Thermal Gravimetric Thermograph for cellulose nanofibers..... 82
Figure 4.24: Scanning electron microscopic images of cellulose nanofibers..... 83
Figure 5.1: Comparison of UV-VIS absorption spectra for carbon black filled poly (lactic acid) composites (a) PLA/CB/0.5C/0.5O (b) PLA/CB/10.0C/10.0O (c) DD poly(lactic acid) composites with 0.5, 1.0, 1.5, 2.0, 2.5 and 10.0wt% of carbon black and (d) OD poly(lactic acid) composites with 0.5,1.0, 1.5, 2.0, 2.5 and 10.0wt% of carbon black (“C” represents DD and “O” represent DD)..... 84

Figure 5.2: Comparison of UV-VIS absorption spectra for carbon black filled poly (lactic acid) composites (a) 0.5 (b) 1.0 (c) 1.5 (d) 2.0 (e) 2.5 and (f) 10wt% prepared via DD and OD (“C” represents DD and “O” for OD)..... 85
Figure 5.3: Comparison of UV-VIS absorption spectra for multiwalled carbon nanotubes filled poly (lactic acid) composites (a) PLA/MWCNT/0.2MC/0.2MO (b) PLA/MWCNT/2.0MC/2.0MO (c) DD poly(lactic acid) composites with 0.2, 0.4, 0.6, 0.8, 1.0,1.5 and 2.0wt% of multiwalled and (d) OD poly(lactic acid) composites with 0.2, 0.4, 0.6, 0.8, 1.0,1.5 and 2.0wt% of multiwalled carbon nanotubes (“C” represents DD, “O” for OD and “M” for multiwalled carbon nanotubes) 87
Figure 5.4: Comparison of UV-VIS absorption spectra for multiwalled carbon nanotubes filled poly (lactic acid) composites (a) 0.2 (b) 0.4 (c) 0.6 and 0.8 (d) 1.0 (e) 1.5 and (f) 2.0wt% in comparison to equally filled [for 1.0, 1.5 and 2.0wt% in (d), (e) and (f)] carbon black poly (lactic acid) composites prepared via DD and OD. (“C” represents DD, “O” for OD and “M” for multiwalled carbon nanotubes) 89
Figure 5.5: UV-VIS absorption spectra for hybrid poly (lactic acid) composites (a) DD and (b) OD 2.5wt% carbon black + (0.2, 0.4, 0.6, 0.8, 1.0 and 2.0wt%) of multiwalled carbon nanotubes filled poly (lactic acid) composites and (c) DD and (d) OD 2.5wt% carbon black + (0.2, 0.4, 0.6, 0.8, 1.0 and 2.0wt%) of cellulose nanofibers filled poly (lactic acid) composites (first “C” stands for 2.5wt% of carbon black, “M” for multiwalled carbon nanotubes, “F” for cellulose nanofibers and second “C” represents DD and “O” for OD) 92
Figure 5.6: Comparison of UV-VIS absorption spectra for hybrid poly (lactic acid) composites, i.e., 2.5wt% carbon black with (a) 0.2 (b) 0.4 (c) 0.6 (d) 0.8 (e) 1.0 and (f) 2.0 multiwalled carbon nanotubes prepared via DD and OD in comparison to 2.5wt% filled poly (lactic acid) composites prepared via OD 93
Figure 5.7: Comparison of UV-VIS absorption spectra for hybrid poly (lactic acid) composites, i.e., 2.5wt% carbon black with (a) 0.2 (b) 0.4 (c) 0.6 (d) 0.8 (e) 1.0 and (f) 2.0 cellulose nanofibers prepared via DD and OD in comparison to 2.5wt% filled poly (lactic acid) composites prepared via OD 95
Figure 5.8: Comparison of UV-VIS absorption spectra for hybrid poly (lactic acid) composites with an equal concentration of second filler [MWCNT’s and CNF] prepared using OD 96
Figure 5.9: Comparison of density values for poly (lactic acid) composites prepared by dissolution dispersion [DD] and oligomeric dispersion [OD] [“C” represents DD, “O” for OD and “T” for Theoretical density] filled with (a) carbon black (C) (b) multiwalled carbon

nanotubes (M) (c) cellulose nanofibers (F) (d) comparison between multiwalled carbon nanotubes and cellulose nanofibers 99
Figure 5.10: Comparison of density values for hybrid poly (lactic acid) composites prepared by dissolution dispersion [DD] and oligomeric dispersion [OD] filled with (a) 2.5wt% carbon black + multiwalled carbon nanotubes (0.2, 0.4, 0.6, 0.8, 1.0, 1.5 and 2.0wt%) (b) 2.5wt% carbon black + cellulose nanofibers (0.2, 0.4, 0.6, 0.8, 1.0, 1.5 and 2.0wt%) (c) comparison between hybrid poly (lactic acid) composites prepared by DD (d) comparison between hybrid poly (lactic acid) composites prepared by OD..... 100
Figure 6.1: Intramolecular and Intermolecular forces of attraction existing within polymer composites..... 102
Figure 6.2: Schematic representation of Carbon black filled poly (lactic acid) at 0.5, 1.0, 1.5, 2.0 and 2.5wt% 104
Figure 7.1: PLA Composites with (a) 0.5 (b) 1.5 (c) 2.0 (d) 2.5 (e) 5.0 (f) 10.0 of carbon black (X1000) 128
Figure 7.2: PLA Composites with (a) 0.2 (b) 0.4 (c) 0.6 (d) 0.8 (e) 1.5 (f) 2.0 of multiwalled carbon nanotubes (X1000) 129
Figure 7.3: PLAC with (a) 0.2 (b) 0.4 (c) 0.6 (d) 0.8 (e) 1.5 (f) 2.0 of cellulose nanofibers (X1000) 130
Figure 7.4: PLAC with 2.5CB + (a) 0.2MWCNT (b) 1.0MWCNT (c) 1.5MWCNT (d) 2.0MWCNT (X1000)..... 131
Figure 7.5: PLAC with 2.5CB + (a) 0.2CNF (b) 1.0CNF (c) 1.5CNF (d) 2.0CNF (X1000).... 132
Figure 7.6: PLA Composites with (a) 0.5 (b) 1.5 (c) 2.0 (d) 2.5 (e) 5.0 (f) 10.0 of carbon black 133
Figure 7.7: PLA Composites with (a) 0.2 (b) 0.4 (c) 0.6 (d) 0.8 (e) 1.5 (f) 2.0 of multiwalled carbon nanotubes 134
Figure 7.8: PLA Composites with (a) 0.2 (b) 0.4 (c) 0.6 (d) 0.8 (e) 1.5 (f) 2.0 of cellulose nanofibers 135
Figure 7.9: PLAC with 2.5CB + (a) 0.2MWCNT (b) 1.0MWCNT (c) 1.5MWCNT (d) 2.0MWCNT 136
Figure 7.10: Roughness average value (Ra) for single filler poly (lactic acid) composites (a) and hybrid composites (b) 136
Figure 7.11: PLAC with 2.5CB + (a) 0.2CNF (b) 1.0CNF (c) 1.5CNF (d) 2.0CNF 137
Figure 7.12:Poly (lactic acid) composites with (a) 0.5wt%, (b) 2.5wt% and (c) 10wt% of carbon black..... 138

Figure 7.13: Poly (lactic acid) composites (a) 0.2wt% (b) 0.8wt% and (c) 2.0wt% of Cellulose nanofibers (d) 0.2wt%, (e) 0.8wt% and 2.0wt% of multiwalled carbon nanotubes (X100) ... 139
Figure 7.14: Poly (lactic acid) composites 2.5wt% Carbon black +[(a) 0.2wt% (b) 0.8wt% and (c) 2.0wt%] of Multiwalled carbon nanotubes 2.5wt% Carbon black + [(d) 0.2wt%, (e) 0.8wt% and 2.0wt%] of cellulose nanofibers (X100)..... 139
Figure 7.15: Poly (lactic acid) composites with (a) 0.5wt%, (b) 2.5wt% and (c) 10wt% of carbon black (X1000) 141
Figure 7.16: Poly (lactic acid) composites (a) 0.2wt% (b) 0.8wt% and (c) 2.0wt% of Multiwalled carbon nanotubes (d) 0.2wt%, (e) 0.8wt% and 2.0wt% of cellulose nanofibers (X1000) 142
Figure 7.17: Poly (lactic acid) composites 2.5wt% Carbon black +[(a) 0.2wt% (b) 0.8wt% and (c) 2.0wt%] of Multiwalled carbon nanotubes 2.5wt% Carbon black + [(d) 0.2wt%, (e) 0.8wt% and 2.0wt%] of cellulose nanofibers (X1000)..... 143
Figure 8.1. Hardness for poly (lactic acid) composites filled with (a) carbon black (b) multiwalled carbon nanotubes (c) cellulose nanofibers (d) multiwalled carbon nanotubes + 2.5carbon black (e) cellulose nanofibers + 2.5carbon black 146
Figure 8.2. Comparative hardness for (a) multiwalled carbon nanotubes + 2.5 carbon black (b) cellulose nanofibers + 2.5 carbon black with 2.5carbon black poly (lactic acid) composites and specific nanofiller loaded poly (lactic acid) composites. 147
Figure 8.3. (a) Tensile Modulus (b) Yield Strength (c) Tensile Strength (d) Tensile Elongation of Carbon black filled poly (lactic acid) composites..... 155
Figure 8.4. (a) Stress Strain Curves, Comparative properties of (b) Tensile Modulus (c) Yield Strength (d) Tensile Strength of carbon black filled poly (lactic acid) composites. 156
Figure 8.5. Stress Strain Curves for poly (lactic acid) composites filled with (a) multiwalled carbon nanotubes (b) cellulose nanofibers (c) multiwalled carbon nanotubes + 2.5carbon black (d) cellulose nanofibers + 2.5carbon black 157
Figure 8.6. Tensile Modulus for poly (lactic acid) composites filled with (a) multiwalled carbon nanotubes (b) cellulose nanofibers (c) multiwalled carbon nanotubes + 2.5carbon black (d) cellulose nanofibers + 2.5carbon black..... 158
Figure 8.7. Comparative tensile modulus for (a) multiwalled carbon nanotubes (b) cellulose nanofibers (c) multiwalled carbon nanotubes + 2.5 carbon black (d) cellulose nanofibers + 2.5 carbon black with aspect ratio for multiwalled carbon nanotubes and cellulose nanofibers and 2.5carbon black poly (lactic acid) composites and specific nanofiller loaded poly (lactic acid) composites. 160

Figure 8.8.Yield strength for poly (lactic acid) composites filled with (a) multiwalled carbon nanotubes (b) cellulose nanofibers (c) multiwalled carbon nanotubes + 2.5carbon black (d) cellulose nanofibers + 2.5carbon black..... 162
Figure 8.9.Comparative yield strength for (a) multiwalled carbon nanotubes (b) cellulose nanofibers (c) multiwalled carbon nanotubes + 2.5 carbon black (d) cellulose nanofibers + 2.5 carbon black with predicted values for multiwalled carbon nanotubes and cellulose nanofibers filled poly (lactic acid) composites and 2.5carbon black poly (lactic acid) composites and specific nanofiller loaded poly (lactic acid) composites. 163
Figure 8.10.Tensile strength for poly (lactic acid) composites filled with (a) multiwalled carbon nanotubes (b) cellulose nanofibers (c) multiwalled carbon nanotubes + 2.5carbon black (d) cellulose nanofibers + 2.5carbon black..... 164
Figure 8.11.Comparative tensile strength for (a) multiwalled carbon nanotubes (b) cellulose nanofibers (c) multiwalled carbon nanotubes + 2.5 carbon black (d) cellulose nanofibers + 2.5 carbon black with predicted values for multiwalled carbon nanotubes and cellulose nanofibers filled poly (lactic acid) composites and 2.5carbon black poly (lactic acid) composites and specific nanofiller loaded poly (lactic acid) composites. 165
Figure 8.12.Tensile elongation for poly (lactic acid) composites filled with (a) multiwalled carbon nanotubes (b) cellulose nanofibers (c) multiwalled carbon nanotubes + 2.5carbon black (d) cellulose nanofibers + 2.5carbon black 166
Figure 8.13. Comparative tensile elongation for (a) multiwalled carbon nanotubes + 2.5 carbon black (b) cellulose nanofibers + 2.5 carbon black with 2.5carbon black poly (lactic acid) composites and specific nanofiller loaded poly (lactic acid) composites. 167
Figure 8.14. Notched Izod Impact for poly (lactic acid) composites filled with (a) carbon black (b) multiwalled carbon nanotubes (c) cellulose nanofibers (d) multiwalled carbon nanotubes + 2.5carbon black (e) cellulose nanofibers + 2.5carbon black 191
Figure 8.15. Comparative notched Izod impact for (a) multiwalled carbon nanotubes + 2.5 carbon black (b) cellulose nanofibers + 2.5 carbon black with 2.5carbon black poly (lactic acid) composites and specific nanofiller loaded poly (lactic acid) composites. 192
Figure 8.16. Flexural Strength for poly (lactic acid) composites filled with (a) carbon black (b) multiwalled carbon nanotubes (c) cellulose nanofibers (d) multiwalled carbon nanotubes + 2.5carbon black (e) cellulose nanofibers + 2.5carbon black 200
Figure 8.17. Comparative flexural strength for (a) multiwalled carbon nanotubes + 2.5 carbon black (b) cellulose nanofibers + 2.5 carbon black with 2.5carbon black poly (lactic acid) composites and specific nanofiller loaded poly (lactic acid) composites. 201

Figure 8.18. Flexural Modulus for poly (lactic acid) composites filled with (a) carbon black (b) multiwalled carbon nanotubes (c) cellulose nanofibers (d) multiwalled carbon nanotubes + 2.5carbon black (e) cellulose nanofibers + 2.5carbon black 209
Figure 8.19. Comparative flexural modulus for (a) multiwalled carbon nanotubes + 2.5 carbon black (b) cellulose nanofibers + 2.5 carbon black with 2.5carbon black poly (lactic acid) composites and specific nanofiller loaded poly (lactic acid) composites. 210
Figure 8.20. Heat Deflection Test for poly (lactic acid) composites filled with (a) carbon black (b) multiwalled carbon nanotubes (c) cellulose nanofibers (d) multiwalled carbon nanotubes + 2.5carbon black (e) cellulose nanofibers + 2.5carbon black. 218
Figure 8.21.Comparative heat deflection test for (a) multiwalled carbon nanotubes + 2.5 carbon black (b) cellulose nanofibers + 2.5 carbon black with 2.5carbon black poly (lactic acid) composites and specific nanofiller loaded poly (lactic acid) composites. 219
Figure 9.1. Constrained region (a) MWCNT filled hybrid poly (lactic acid) composites (b) CNF filled hybrid poly (lactic acid) composites (c) Comparative between MWCNT and CNF filled hybrid poly (lactic acid) composites 227

PUBLICATIONS AND CONFERENCES PRESENTATIONS

PUBLICATIONS

Rane, A.V., Kanny, K., Mathew, A., **Mohan, T.P**. and **Thomas, S**., **2019**. Comparative Analysis of Processing Techniques' Effect on the Strength of Carbon Black (N220)-Filled Poly (Lactic Acid) Composites. Strength of Materials, *51*(3), pp.476-489.

Rane, A.V., Mathew, L., **Kanny, K**., Mlowe, S., Revaprasadu, N. and **Thomas, S**., **2019**. Attenuated Total Reflectance Fourier Transform Infrared Spectroscopy: A Tool to Determine Reinforcement of Carbon Black in Polylactic Acid Composites. Materials Performance and Characterization, *8*(1), pp.617-625.

Ajay Vasudeo Rane, **Krishnan Kanny**, Anitha Mathew, **Mohan Turup Pandurangan**, **Sabu Thomas**, **2019**. Microstructural features affecting mechanical properties: Effect of processing on dispersion of carbon black (N220) nanoparticles reinforcement in poly (lactic acid). Surfaces and Interfaces, 18 (Article no: 100451), pp.1-9.

Abitha, V.K.., **Rane, A.V**., **Kanny, K**., Kaushik, P., **Thomas, S**., **2019**. Polymer/Filler Interactions: A Critical Review. The Journal of Plastic and Rubber Institute of Sri Lanka, 18, pp. 69 – 71.

Ajay Vasudeo Rane, **Krishnan Kanny**, Merlin Biju, Sudhikuttan Akkattil Sudhakaran, Ammu Aravind, **Sabu Thomas**, **2020**. Ultraviolet-Visible Spectroscopy: A qualitative tool to predict dispersion and interphase characteristics in carbon-based particulate filled poly (lactic acid) composites. Materials Performance and Characterization,(1), pp.518-530

CONFERENCES

Ajay Vasudeo Rane, **Krishnan Kanny**, **Sabu Thomas**. Role of Nanofillers in Improving Structural Properties of Polymer Composites, International Conference on Natural Polymers 6^{th} – 8^{th} December 2019.

Rane, A.V., Kanny, K., and **Thomas, S**. Interaction In Multiwalled Carbon Nanotubes Filled Poly (Lactic Acid) By Attenuated Total Reflectance Fourier Transform Infrared Spectroscopy. Third Interdisciplinary Research and Innovation Conference 2018. 18 – 20 September 2018.

Ajay Vasudeo Rane, Lithu Mathew, **Krishnan Kanny**, **Sabu Thomas**. Concept of reinforcement in composites based on carbon black and poly (lactic acid) by vibrational – rotational spectra via infrared spectroscopy. Third International Conference on Composites, Bio composites and Nanocomposites 2018. 7 – 9 November 2018.

R Thakur, **A .V. Rane**, **K Kanny**, G Harris. Poly (lactic acid) dense membranes for water disinfection. Third International Conference on Composites, Bio composites and Nanocomposites 2018. 7 – 9 November 2018.

Philasande Matwasa, **Ajay Vasudeo Rane**, **Mohan Turup Pandurangan**, **Krishnan Kanny**. Electromagnetic interference shielding using nanocellulose. Third International Conference on Composites, Bio composites and Nanocomposites 2018. 7 – 9 November 2018.

Sanele Kervin Ntuli, **Ajay Vasudeo Rane**, **Mohan Turup Pandurangan**, **Krishnan Kanny**. Extraction of nanocellulose. Third International Conference on Composites, Bio composites and Nanocomposites 2018. 7 – 9 November 2018.

1 INTRODUCTION

1.1 BACKGROUND AND PROBLEM STATEMENT[1]

The wide usage of polymeric materials in engineering is largely due to their valuable mechanical properties. Fracture is a rupture of the bonds between elements of a body (atoms, molecules or ions) resulting in breakage or cleavage of the specimen into parts. The resistance of a material to fracture is called strength or mechanical strength. Since the mechanical properties of polymers largely depend on their structure, it is necessary to create a structure ensuring an optimal set of mechanical properties which do not vary with time. The structure of the polymer is established during processing. Processing not only imparts certain shape to the material but also plays an important role in the creation and determination of its structure, i.e. microstructures. Structures are often conceived in the melts or solutions from which the polymers are fabricated. An interesting method of structure control is by introducing artificial nuclei into the polymer melt, which then becomes crystallization centers. Growing attention in PLA is because of some distinctiveness that is deficient in other polymers, specifically concerning renewability, biocompatibility, processability, and energy saving. PLA is derivative from renewable and biodegradable resources, and its degradation products are non-pollutant and non-toxic. Therefore, PLA may be a substitute for petrochemical plastics. Furthermore, PLA has several bio applications, such as biodegradable matrix for surgical implants, and in drug delivery systems. On the other hand, for structural use, it is required that some of its properties be improved, namely in terms of thermo-mechanical and electrical performance. To rise above these limitations, approaches, like blending with other polymers, functionalization, and adding of fillers, are practiced. Adding up of nanofillers is an appealing approach, as with small quantity of filler, it is achievable to improve desired features, keeping key properties of PLA unharmed. The most reported nanofillers are clays, silica's, and carbon nanomaterials as incorporating nanofillers is a common approach to attain this goal. Exceptional properties of carbon-based nanomaterials have increased research works dealing with PLA composites. To discuss in brief, poly (lactic acid) originally is a brittle material with low impact strength and its elongation at break is similar to other brittle polymer such as polystyrene. On the contrary, its tensile strength and modulus are comparable to poly (ethylene terephthalate). The inability of poly (lactic acid) to plastically deform at high-stress levels limits its application; hence several modifying techniques have been used to enhance its deformation properties, as discussed above. From the available literature, has been confirmed that crystallinity is an important characteristic affecting the strength properties of

poly (lactic acid) and its composites. Carbon black acts as a nucleating agent, increasing crystallization rate of polymers, which has been proved in a work by Su et al. wherein non-isothermal crystallization process of poly (lactic acid), poly (lactic acid)/carbon black and poly (lactic acid)/modified carbon black composites were studied by Jeziorny equation, Ozawa Model and MO equation. Wang et al. fabricated high-performance poly (lactic acid)/ carbon black composites via melt blending, using acetyl tributyl citrate and poly (1, 3 – butylene adipate as a plasticizer, which improved the interaction between poly (lactic acid) chains and carbon black. Physical interaction in polymer composites relates to entanglements in polymer chains, absorption of polymer chains on fillers surface, the formation of crystallites, coalescence of ionic centers or of glassy blocks. Chemical interactions involve randomly joining segments of pre-existing chains; random copolymerization or end linking functionally terminated chain ends. Xiu et al. reported co-continuous-like structure by incorporating small quantities of filler particles with self-networking capability with a balance between stiffness and toughness. As mentioned earlier fillers of particle size ranging from 20nm to 30nm, shall act as a stress concentrator and contribute to increase in mechanical properties of poly (lactic acid) composites, on better dispersion within poly (lactic acid) matrix To the best of our knowledge, reports on applications of thermoplastics like polypropylene, polyethylene, and polystyrene filled with carbon black for magneto strictive, microwave, liquid sensing, solar absorbers, electrodes, electromagnetic interference shielding, vapor sensitivity, shape memory effect are available Likewise, applications of poly (lactic acid) include composites in medical, packaging, textile, environmental and other commercial applications including agricultural and engineering materials, electrical appliances and automotive parts are also reported As per our findings from the literature, the influence of the low quantity filler on mechanical properties of poly (lactic acid) for structural applications has not been practiced and no detailed study is reported to date. Hence in this study, we fabricate poly (lactic acid) samples, poly (lactic acid) composites and hybrid composites by incorporating small quantities of fillers. In-depth analysis for change in mechanical properties is reported with comparison to structural and morphological analysis The experimental results have been compared with theoretical predictions[1].

1.2 AIM

To investigate the suitability of processing, considering the shape factor and concentration of particulate fillers in poly (lactic acid) and hybrid filler poly (lactic acid) composites on

mechanical, structural and morphological properties of poly (lactic acid) composites with respect to interphase characteristics

1.3 OBJECTIVES OF STUDY

1.3.1 PRELIMINARY STUDY

To extract good quality of cellulose nanofibers from raw kenaf fibers, using steam explosion and then characterizing them using the materials and methods as listed in **Section 3.1.1** and **3.1.2** are used for fabrication of poly (lactic acid) composites and hybrid filler poly (lactic acid) composites.

To select a processing technique to fabricate poly (lactic acid) composites. In order to select the processing technique carbon black filler with various concentrations was blended with poly (lactic acid) via dissolution dispersion [DD] and melt mixing compression molding [MMCM] and tested for mechanical properties and morphological evidence.

1.3.2 PILOT STUDY

To determine the dispersion and interphase characteristics of poly (lactic acid) composites and hybrid filler poly (lactic acid) composites prepared by dissolution dispersion [DD] and oligomeric dispersion [OD].

To select/modify a process based on interphase characteristics which suits our requirement of optimization between strength and stiffness.

1.3.3 MAIN STUDY

To fabricate the poly (lactic acid) composites and hybrid filler poly (lactic acid) composites out of the process selected in pilot study.

To determine the physical and mechanical properties of poly (lactic acid) composites and hybrid filler poly (lactic acid) composites.

To determine the structural properties of poly (lactic acid) composites and hybrid filler poly (lactic acid) composites.

To determine the morphological properties of poly (lactic acid) composites and hybrid filler poly (lactic acid) composites.

To determine the constrained region formed within poly (lactic acid) composites and hybrid filler poly (lactic acid) composites.

1.4 ASSUMPTIONS

Data collection equipment and instruments were deemed valid and reliable based on their use and calibration period in the university and other institutions.

Testing standards selected for property determination were applicable to and suitable for the type of materials being tested.

1.5 DELIMITATIONS

Although there were many natural fibers available in the market, only kenaf fiber was used in this study.

While there were many chemicals and methods to extract cellulose nanofibers from raw natural fibers, conventional step method of alkali, bleaching and acid treatment with steam explosion was adopted due to its ease in extracting cellulose nanofibers from raw natural fibers.

1.6 LIMITATIONS

Conclusions drawn from the results of this study are solely related to the materials used for fabrication and preparation under a similar methodology. Hence results cannot be generalized to all poly (lactic acid) particulate filler composites that are prepared using different methodologies.

While the results of this study may have application, as structural and functional composites.

1.7 STRUCTURE OF DISSERTATION

Chapter 1, titled as Introduction presents the context of the study by highlighting the advantages and disadvantages of poly (lactic acid) and the efforts made to improve the disadvantages are mentioned. In the art of processing a method which combines use of fillers and monomers, i.e. oligomeric dispersion leads to statement of problem, aim and objectives, assumptions, delimitations, limitations and scope of the study.

Chapter 2, titled as Literature Review presents the overview of the literature related to poly (lactic acid) composites. This includes review of particulate filled poly (lactic acid) composites, their properties, processing and applications. Discussion on polymer/filler interactions and challenges in optimizing the strength and stiffness in polymer composites are discussed.

Chapter 3, titled as Materials and Methods, describes the research approach and methodology adopted in fabrication, testing and analyzing the data for poly (lactic acid) composites and hybrid filler poly (lactic acid) composites.

Chapter 4, titled as Process technique selection and extraction of cellulose nanofibers is a preliminary research work, describing the quality of cellulose nanofibers extracted from raw kenaf fibers. Process selection for fabrication of poly (lactic acid) composites is experimented and characterized for mechanical and morphological properties.

Chapter 5, titled as Modification of Interphase describe the modification technique used to fabricate a poly (lactic acid) composites and hybrid filler poly (lactic acid) composites with balance between strength and stiffness, i.e. strength and elongation.

Chapter 6, titled as Structural properties, showcases the molecular interactions i.e. intermolecular and intramolecular interactions, physical and chemical interactions existing within poly (lactic acid) composites and hybrid filler poly (lactic acid) composites.

Chapter 7, titled Morphological properties evidences the type of fracture which determines the nature of deformation via optical microscopy and scanning electron microscopy. Also morphological evidences obtained from transmission electron microscopy and atomic force microscopy determines the level of dispersion of particulate fillers in poly (lactic acid) composites and hybrid filler poly (lactic acid) composites.

Chapter 8, titled as Physical and Mechanical properties, showcases the values of numerical data of density, hardness, tensile test, flexural test, Izod impact, heat distortion/deflection temperature of poly (lactic acid) composites and hybrid filler poly (lactic acid) composites with their statistical data.

Chapter 9, titled as Constrained region estimation, makes use of dynamic mechanical analysis to determine constrained region within 2.5wt% CB filled poly (lactic acid) composites and hybrid filler poly (lactic acid) composites in comparison to neat poly (lactic acid).

Chapter 10, titled as General Conclusion and Future outlook draws the conclusion from the entire set of experiments and also mentions the future directions.

Note: Background and Problem statement (**Section 1.1**) is published in Rane, A.V., Kanny, K., Mathew, A., Mohan, T.P. and Thomas, S., 2019. Comparative Analysis of Processing Techniques' Effect on the Strength of Carbon Black (N220)-Filled Poly (Lactic Acid) Composites. Strength of Materials, *51*(3), pp.476-489.

2 LITERATURE REVIEW

Literature review for the present study has been published in “The Journal of the Plastics and Rubber Institute of Sri Lanka (2019) Volume 18” 69 – 71; as Polymer/Filler Interactions: A Critical Review” and Accepted for publishing as book chapter titled “Green Composites based on Poly(lactic acid) Pan Stanford Publishing House; Edited by: Sabu Thomas, Abitha V K and Hanna J Maria”

2.1 INTRODUCTION

Material science and engineering is an interdisciplinary area concerned with invention of new materials and improving the already known and existing materials for their better use in present scenario. This improvement in known materials is achieved by deeper understanding of the microstructure – composition – synthesis and processing, relationship. By term composition we mean chemical makeup of a material. By term structure we mean arrangement of atoms seen at different levels. By synthesis and processing we mean production of components. The term synthesis refers to how materials are made from naturally occurring or man – made chemicals. The term processing refers how materials are shaped as desired or required by making changes in properties of materials[2].

A vast range of materials is available to the engineer and all these materials possess widely different properties. Glass, concrete, rubber, timber, metals, alloys, plastics or ceramics are all used by engineers, but their characteristics and properties are completely different from each other. Also within one group of materials, the range of properties may be quite wide, i.e. the properties may range from soft and easily deformed materials (lead), to hard and tough material (tool steel)[2].

All engineers are concerned with the optimum use of materials and they have to select the most suitable material for their job. The material can be for civil engineering structure, electrical transmission power plant, modern cutting machines or perhaps an electric component. While making the selection, he has to consider many factors. He has to think all the facts concerning the job, such as “will the properties of material change during service?” “can the finished component be produced at the economic cost?” “can the finished component be imparted versatile properties?” “will the material withstand corrosion in varying conditions?” “can the material be easily formed to the desired shape?” “does the material possess required, mechanical, electrical, thermal, magnetic and optical properties?” “can the material withstand static or dynamic load” etc.

As there are thousands and thousands of materials available and it is not possible for an engineer to possess a detailed knowledge of all of them. But a good grasp of the fundamental principles which control the properties of materials will help him to make the optimum selection of material[2].

One thing which is common in all materials is that all of them are composed of atoms. The atoms, of course, differ from each other but all the atoms of known elements are made of three basic particles i.e., protons, electrons and neutrons. The atoms largely control the final properties of the engineering materials by the way in which they are bonded to each other and also in the manner in which protons, neutrons and electrons assembled into atoms[2].

2.2 CLASSIFICATION OF ENGINEERING MATERIALS

The fundamental knowledge which can be ordered and structured in some logical manner, called classification. Classification can be made from the existing knowledge as well as from the various theories as speculations of the persons working in the concerned area. In material science or engineering materials, the following factors form the basis of the various systems of classifications are as follows: the chemical composition of the material, the mode of occurrence of the material in nature, the refining and the manufacturing process to which the material is subjected before it gets the required properties, the atomic and crystalline structure of material, the industrial use of material. The broad spectrum of engineering materials is listed below. In general, in each and every engineering applications, we find materials from all the three basic types of materials. Material groups written below possess different structure and properties like deficiencies in strength.

Metals and Alloys: These include steels, aluminium, zinc, magnesium, iron, titanium, copper and nickel etc. In general, metals have good electrical and thermal conductivity. Metals and Alloys have relatively high strength, high stiffness, ductility or formability and are more shock resistance.

Metals and Alloys are particularly useful for structural and load bearing applications in industries. Pure metals are occasionally used but their alloys (with combination of metals) provide improvement in properties for desired use.

Ceramic and Glasses: Ceramics are inorganic crystalline materials and probably the most natural materials. Beach sand and rocks are examples of naturally occurring ceramics. Advanced ceramic materials are made by refining the naturally occurring ceramics. Advanced ceramics find use in computer chips, sensors and actuators, capacitors, wireless communication system, conductor and insulators.

Some ceramics are used in consumer products like paints, plastics and tires. Some ceramics are used as barrier coatings to protect metallic substrates in turbine engines.

In general ceramics do not conduct heat due to presence of porosity (small holes) so they must be heated to very high temperature before melting. Ceramics are strong and hard but are very brittle. Ceramics are first powdered and then converted to different shapes. New processing techniques are able to make ceramics sufficiently resistant to fracture that make them useful for load bearing applications. Ceramics have exceptional strength under compression.

Glass: According to American Society for Testing and Materials glass is an inorganic product of fusion which has been cooled to a rigid condition without crystallizing. It is an amorphous material often but not always, the term amorphous refer to materials that do not have a regular periodic arrangement. Glass is widely used in houses, automobiles, computers, television screens and hundreds of other applications. Optical fibers based on high purity silica glass established their importance in communication industry. Glasses can be thermally treated (tempered) to make them stronger. Glass – ceramics are formed by nucleating small crystals within glass by a special thermal process. Zerodur is an example of glass – ceramic material used to make mirror substrates for large telescopes.

Polymers: There are organic materials prepared by polymerization reactions in which small molecules are chemically combined into long chain molecules or three-dimensional structures. Polymeric materials include rubber have lower specific gravity and good strength. Many polymers have very good electrical resistivity. Polymers can also provide good thermal insulation.

Polymers have lower strength but have a very good strength to weight ratio. They are not used at high temperatures. Polymers have thousands of applications from bullet proof vests, compact disks, ropes and liquid crystal displays LCD's to clothes and teacups and utensils.

The important polymers are:

Thermoplastic: In which the long molecular chains are not rigidly connected have good ductility and formability, e.g. Nylon, Polyethylene.

Thermosetting: These are stronger polymers but are more brittle because the molecular chains are tightly linked, e.g., Urea formaldehyde and phenol formaldehyde. Thermoset polymers have wide use in electronic industries.

Semiconductors: These are materials which behave as insulators at 0°K but develop significant conductivity as the temperature rises. They have resistivities between 10^{-1} and 10^{5}ohm. Silicon – germanium and gallium – arsenide based semiconductors, those used in

computers and electronics are part of a broader class of materials known as electronic materials.

Carbon, silicon, germanium, zinc sulphide, magnesium oxide, grey tin and selenium are common materials termed as semiconductors.

Composite materials: Main idea behind developing composite materials is to have some specific physical characteristics like high strength, stiffness and heat resistance than one individual material. Composites are combination of metals, ceramics, plastics and other materials. Concrete, plywood and fiber glass are examples of composites materials. Fiber glass is made by dispersing glass fiber in a polymer matrix. The glass fiber makes the polymers stiffer, without increasing its density. With composites we can produce light weight, strong, ductile, high temperature resistant materials or we can produce hard, shock resistance cutting tools that would otherwise shatter. Today's space science rely heavily on composites for its aircraft and vehicles[2].

2.3 FUNCTIONAL CLASSIFICATION OF MATERIALS

A functional classification of materials can also be useful. We can classify materials based on whether the most important function they perform is mechanical (structural), biological, electrical, magnetic or optical. These categories can be broken down further into subcategories.

Aerospace: Light materials such as wood and an aluminium alloy (that accidentally strengthened the engine even more by picking up copper from the mold used for casting) were used in the Wright brothers historic flight. Today, NASA's space shuttle makes use of aluminium powder for booster rockets. Aluminium alloys, plastics, silica for space shuttles tiles and many other materials belong to this category. Some examples of aerospace are C – C composites, Amorphous silicon, Al – alloys etc.

Biomedical: Our bones and teeth are made in part from a naturally formed ceramic known as hydroxyapatite. A number of artificial organs, bone replacement parts, cardiovascular stents, orthodontic braces and other components are made using different plastics, titanium alloys, and non – magnetic stainless steels. Ultrasonic imaging systems make use of ceramics known as PZT (lead zirconium titanate). Magnets used for magnetic resonance imaging make use of metallic niobium – tin based superconductors. Some examples of biomedical are hydroxyapatite, titanium alloys, stainless steels etc.

Electronic materials: Semiconductors, such as those made from silicon are used to make integrated circuits for computer chips. Barium titanate, tantalum oxide and many other

dielectric materials are used to make ceramic capacitors and other devices. Superconductors are used in making powerful magnets. Copper, aluminium and other metals are used as conductors in power transmission and in microelectronics. Some examples of electronic materials are Si, GaAs, Ge, PZT, Al, Cu, conducting polymers etc.

Energy technology and environmental technology: The nuclear industry uses materials such as uranium dioxide and plutonium as fuel. Numerous other materials, such as glasses and stainless steels are used in handling nuclear materials and managing radioactive waste. New technologies related to batteries and fuel cells make use of many ceramic materials such as zirconia and polymers. The battery technology has gained significant importance owing to the need for many electronic devices that require longer lasting and portable power. Fuel cells will also be used in electric cars. The oil and petroleum industry widely use zeolites, alumina, and other materials as catalyst substrates. They use Pt, Pt/Rh and many other metals as catalyst. Many membrane technologies for purification of liquids and gases make use of ceramic and plastics. Solar power is generated using materials such as amorphous silicon. Some examples of energy technology and environment technology are UO_2, Ni – Cd, LiCo O_2, amorphous SiH etc.

Magnetic materials: Computer hard disk and audio and video cassettes make use of many ceramic, metallic and polymeric materials. For example, particles of a spherical form of iron oxide, known as gamma iron oxide, are deposited used for making video – tapes. Computer hard disks are made using alloys based on cobalt – platinum – tantalum – chromium. Many magnetic ferrites are used to make inductors and components for wireless communication. Steels based on iron and silicon are used to make transformers cores. Some examples of magnetic materials are Fe, Fe – Si, NiZn and MnZn ferrites.

Photonic or optical materials: Silica is used for making optical fibers. More than fifteen million kilometers of optical fiber has been installed around the world. Optical materials are used for making semiconductor detectors and lasers used in fiber optic communications systems and other applications. Similarly alumina and yttrium aluminium garnets are used for making lasers. Amorphous silicon is used to make solar cells and photovoltaic modules. Polymers are used to make liquid crystal displays. Some examples of optical materials are SiO2, GaAs, glasses, indium tin oxide etc.

Smart materials: A smart material can sense and respond to an external stimulus such as change in temperature, the application of a stress, or a change in humidity or chemical environment. Usually a smart – material based system consists of sensors and actuators that read changes and initiate an action. An example of a passively smart material is lead

zirconium titanate and shape memory alloys. When properly processed PZT can be subjected to a stress and a voltage is generated. This effect is used to make such devices as spark generators for gas grills and sensors that can detect under water objects such as fish and submarines. Other examples of smart materials include magnetorheological fluids. These are magnetic paints that responds to magnetic fields. These materials are being used in suspension systems of automobiles. Other examples of smart materials and systems are photochromic glasses and automatic dimming mirrors, Ni – Ti shape memory alloys, polymer gels etc.

Structural materials: These materials are designed for carrying some type of stress. Steels, concrete and composites are used to make buildings and bridges. Steels, glasses, plastics and composites are also used widely to make automotive. Often in these applications, combinations of strength, stiffness and toughness are needed under different conditions of temperature and loading. Some examples of structural materials are aluminium alloys, fiber glass, wood and plastics etc.[2].

2.4 ENGINNERING REQUIREMENT OF MATERIALS

The practical application of all types of engineering materials depends upon a thorough knowledge of their particular properties under a wide range of conditions. The range of properties found in different classes of materials is very large. Some of the most important properties of materials are discussed below.

Mechanical: Strength, stiffness, ductility, elasticity, plasticity, toughness, brittleness, hardness, malleability, creep, fatigue

Electrical: Conductivity, resistivity, dielectric permittivity, dielectric strength

Magnetic: Permeability, coercive force, hysteresis

Thermal: Specific heat, thermal expansion, conductivity

Chemical: Corrosion resistance, acidity or alkalinity, composition

Physical: Dimension, density, porosity, structure

Acoustical: Sound transmission, sound reflection

Optical: Color, light transmission, light reflection

A more meaningful classification for the purpose is to distinguish between those properties that are determined by the actual crystal structure, the so called structure sensitive properties and those that are independent of the crystal structure namely the structure insensitive properties[2].

2.5 ORGANIC, INORGANIC AND BIOLOGICAL MATERIALS

Organic compounds are available in a wide range because hundreds and hundreds of hydrocarbon compounds and their derivatives are there in existence. It is important to study organic compounds because all biological systems are composed of carbon compounds. But some of the materials of biological origin do not possess organic composition, e.g. limestone.

Organic materials: These materials consist of carbon, which is chemically bonded with hydrogen, oxygen and other non – metallic substances. They have complex structures. Wood, many types of waxes, plastics and petroleum derivatives are organic materials.

Some common engineering organic materials are synthetic rubber and plastics are termed as polymers because they are prepared by polymerization reactions. In such reactions, simple molecules are chemically combined into long chain molecules or three-dimensional structures. Most of the polymers and solid materials, have chemical combination of carbon and hydrogen, nitrogen, oxygen and other elements. These materials have lower specific gravity and good strength. Two important polymers are: Thermoplastics and Thermosets. Many plastics are very good electrical and thermal insulators as well as possess high resistance to abrasion. Because of their high strength to weight ratio, they are widely used in many situations. They are used for reducing weight for mobile objects, such as cars, aircrafts and rockets.

Another thermoplastic material is the natural rubber which is organic material of biological origin. It is prepared from a fluid which is provided by rubber trees. Such rubber materials are used for tyres of automobiles, insulation of metal components, toys and other rubber products.

Inorganic materials: Inorganic materials are not biological materials they are not formed due to natural growth and development of living organism. Inorganic materials are metals, clays, sand rocks, gravels, minerals and ceramics. They have mineral origin.

Rocks are the units which form the crust of the earth. There are three major groups of rocks: Igneous rock are formed by the consolidation of semi liquid or liquid material (magma). The rocks are called plutonic if consolidation takes place deep within the earth and they are called volcanic if lava or magma solidifies on the earth's surface, Basalt is igneous volcanic, and granite is igneous plutonic. When broken down remains of existing rocks are consolidated under pressure, the rocks so formed are called sedimentary rocks. Shale and sandstone are sedimentary rocks. The required pressure is supplied by the overlying rocky material. Metamorphic rocks are basically sedimentary rocks which are changed by heat and intense

pressure into new rocks. Their structure is in between igneous rock and sedimentary rocks. Marble and slates are examples of metamorphic rocks.

Rock materials are used for the construction of the monuments, houses, arches, tombs, buildings, bridges etc. Even today, slate, which has great hardness is used as roofing material. Basalt dolerite, rhyolite is crushed into stones and used for road construction material and concrete aggregate. Another type of material which is of particular interest to an engineer is pozzolanic material. They are naturally occurring or synthetic siliceous materials that will hydrate to form cement. Blast furnace slag, volcanic ash, some shales and fly ash are some common examples of pozzolanic materials. The cement which contains 10-20% ground blast furnace slag is called pozzolans – portland cement. It sets more slowly than ordinary Portland cement. It has greater resistance to sulphate solutions and sea water.

Some materials exist in nature in the form in which they are to be used. These are called naturally occurring materials. These materials are rocks, stone, wood, copper, silver, gold etc. They are not many in number. In modern times however most of the materials are manufactured so that they may possess a particular property to meet a particular condition. Thus, the study of engineering materials is also connected with the manufacturing process by which the materials are produced to acquire the desired properties.

The metals which occur in nature, in their free state are mostly chemically inert. Such metals e.g., copper, silver, gold, etc. are highly malleable and ductile as well as extremely corrosion resistant. Their alloys are harder than their basic metals. The more reactive metals are found as carbonates, sulphates and sulphide ores.

Biological materials: The engineer is also very much interested in biological materials such as leather, limestone, bone, horn, wax, wood etc. Ancient man used wood for many purposes. Wood is a fibrous composition of hydrocarbons, cellulose and lignin. Apart from these components a small amount of gum, starch, resin, wax and organic acids are also present. Wood is classified as soft wood and hard wood. Fresh wood contains high percentage of water and seasoning is done to dry out the wood. The defects such as cracks, twist, warp etc. may occur if proper seasoning is not done.

The skin of animals, after cleaning and tanning operations is called leather. Leather was used as clothing by ancient man and today also it is used for making belts, boxes, purses, shoes etc. Tanning is used for preserving leather. Two tanning techniques are used popularly used: Vegetable tanning consists of soaking the skin in tanning liquor for many days and then drying to condition the leather. Chrome tanning involves pickling the skin in acid solution and

then revolving in a drum which contains chromium salt solution. After that leather is dried and rolled.

An important material which is not organic but has biological origin is limestone. It chiefly consists of calcium carbonate and limestone. This is used to manufacture cement. Limestone in the pure form is used as flux in iron and steel industries.

Bones of animals were used to make tools and weapons in early days. They are laminate of organic substance and phosphates and carbonates of calcium. Bones are stronger in compression as compared to tension. In modern days bones are used for the manufacture of rule, gelatin etc.

Above paragraphs gave a general idea on brief introduction to the materials, considering its classification, functional classification, engineering requirement and nature of materials. Let us now look at the area focused on in the thesis, i.e. polymer composites specifically particulate filled polymer composites.

Our main motive for writing this literature survey was to consolidate the most relevant information on poly (lactic acid) (PLA) and PLA composites into a write up that serves as a one-source reference who are keen on this unique biodegradable polymer specific to synthesis and production, structure, properties and applications[2].

2.6 POLYMER COMPOSITES

Development in the era, needs cost effective structural and functional materials with diverse properties. Material science is an interdisciplinary area concerned with invention of new materials and improving the already known and existing materials for their better use in present scenario. Materials form the basis of human life with more emphasis given to polymer composites. In this section of review we describe the role of fillers in enhancing properties of polymer composites with principles governing their distribution and interaction within polymer composite materials.

Fillers [particulate fillers and fibers] irrespective of their sources are gaining importance in manufacturing of technical goods and products for structural and functional applications. The increase in their importance is attributed to their fundamental and practical behaviour. Hence it is vital to understand the complex behaviour of fillers when they are practically used in solid [polymer], liquid or gaseous media[3] This short review focuses on the behaviour of these fillers particularly to polymers. Behaviour of fillers with polymers requires the knowledge on physical and chemical characteristics of fillers; as these characteristics determine the enhancement level in performance of the final product[4]. In general, polymer mixed with

fillers [with respect to concentration] is termed as polymer composite material. There are various classifications for polymer composite materials depending upon the source of polymers and fillers, but in this review we shall only focus on the organization of phases within polymer composite material and principles governing filler distribution and interaction.

“Interface”[3] and “Interphase” are two molecular dimensions within the polymer composite material and are used sometimes in replacement to each other or as a synonym to each other; but rather there is a huge difference between their actual presence in the polymer composite material, as seen in **Figure 2.1**. The molecular dimension in the vicinity of the polymer is termed as “interface” and the dimension extending from the polymer surface which is influenced by the polymer surface is “interphase”. “Interface” and “Interphase” are the two molecular dimensions within polymer composite materials responsible for properties of the final polymer composite material under stress during application.

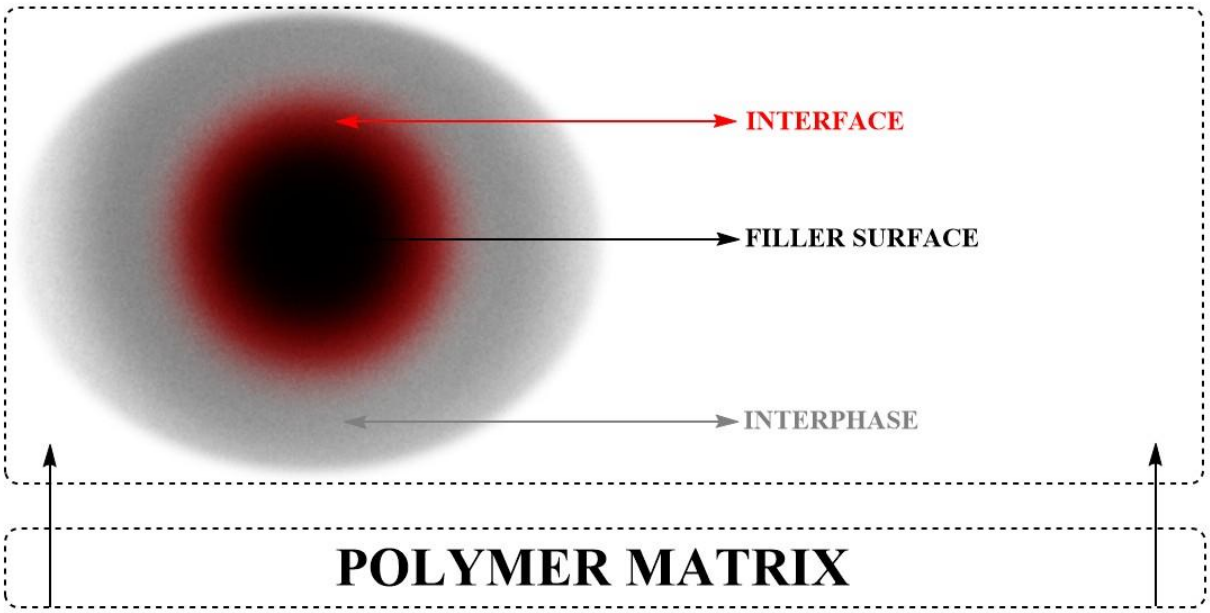

Figure 2.1. Schematic representation of molecular dimensions zones in filled polymer composites (Interface and Interphase)

Filling polymers with fillers is one of the most widely used methods in manufacturing of structural and functional materials with required set of mechanical, physical and functional properties for any practical application[4]. Fillers are those materials in polymer composite which are distributed near to uniformity (with isotropic and anisotropic alignments) as shown in **Figure 2.2**, with appropriate means of processing, after knowing the physical and chemical properties of the polymers as well as fillers.

Reinforcement of polymers with fillers is a process that indicates the compatibility of the fillers with the polymers, thereby having a distinct phases (i.e. interface and interphase) with the polymer phase[4]. As we already discussed, polymer composite materials are “heterophasic” [two or more phases] wherein phases interact with each other. Proportion of the constituents phase is an important parameter, giving rise to different properties in polymer composite materials, but formation of two molecular dimensions (i.e. interface and interphase) cannot be neglected. Following the definition of composites, on a broader aspect the polymer composite materials may be ordered and structured into “particulate or fibrous filled polymer composite” and “long fiber reinforced polymer composite”. Further on following the dimensional aspects, of fillers as we can order polymer composites into “dispersed particles”, “short cut fibers” and “long fibers”[4]. Several physical characteristics of fillers influence the properties of the polymer composite materials, to name a few - shape, dimension, size distribution, orientation and composition, out of which “mean values of particle size” is considered as the important property relating to the property of polymer composite material; that contributes to the total surface of the phase border between phases[4]. Particle size along with the shape predicts the performance of the polymer composite material.

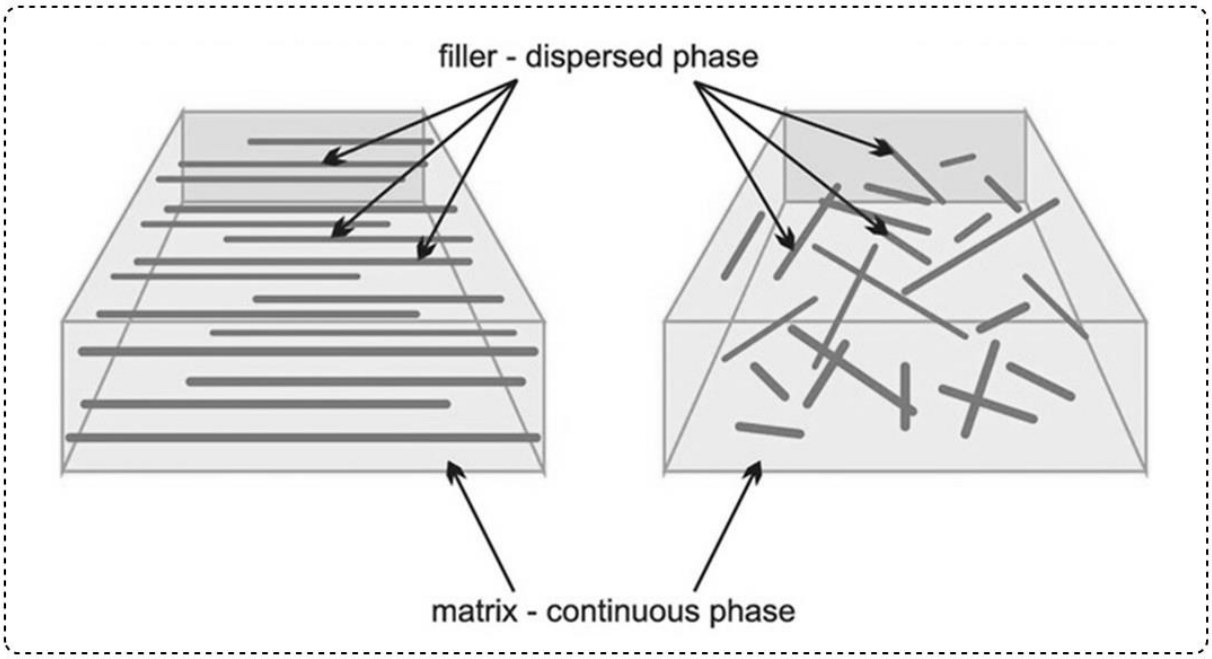

Figure 2.2. Schematic representation of phases in polymer composite “Macrostructure of a polymer composite”

Effectiveness of the filler action is determined by the “specific surface area” of the filler; specific surface is important wherein fillers are modified by utilizing any of the available chemical methodologies of modification. Packing of fillers within the polymer composite

material is dependent on the shape of filler used, i.e. hybrid effect wherein smaller size fillers are used to fill in gaps between larger size fillers within polymer composites. Fillers having tendency to enhance the mechanical properties of base polymer are termed as “active fillers”[4]. “Inactive fillers” intend to give a particular color or rather makes the final product cost effective[4]. As physical properties are important, chemical characteristics of the fillers also have an important role in determining the final properties of the polymer composite material; free surface energy is one such chemical property – as interfacial interactions [between polymer and filler] within polymer composite is dependent on the ratio of “free surface energy” of polymer and filler. Fillers in polymer cannot introduce change in only one particular property as addition of filler into polymer results in formation of new material, with properties completely different from the polymer, it shall be accounted to “micro and macro heterogeneities” and “physical and chemical interactions at molecular dimensions zones”. Strong chemical interactions (strength of interface) within polymer composite material increases the stiffness of polymer composite material. Strong physical interactions (strength of interphase) contributes to elastic modulus within polymer composite material and enhances toughness. Having a balance between “stiffness” and “toughness” is of great importance in research area of polymer composite materials. Distribution of phases within polymer composites has a great influence on the properties of the polymer composite materials. Polymer matrix in any polymer composite material is “primary continuous phase”; continuous fibers in a polymer composite material is termed as “secondary continuous phase” whereas particulate fillers in polymer composites are termed as “secondary dispersed phase”[4]. As mentioned about the properties of fillers for polymer composite material, polymer material should possess properties to be used in polymer composite material out of which “good ability to wet the filler surface” is essential. “Area of application” of polymer composite material, determines the choice of polymer and fillers. Fillers activity into polymers, can be classified as “structural” “kinetic” and “thermodynamic”. Changes in polymer structure on a molecular or sub molecular level by a filler is termed as structural activity; ability to change the viscoelastic and relaxation properties of polymer chains in contact with filler (i.e. chain mobility) is kinetic activity and ability of filler to influence the phase state and thermodynamic parameters (enthalpy and entropy) important for filled “polymer blend” is termed as thermodynamic activity of filler. “Influence of filler” can be arbitrarily determined by relating the changes in properties per unit content of filler[4]. In the above text we described the important physical and chemical factors of fillers and polymers, formation of molecular dimension zone and their influence on properties of polymer composite materials, now in the

further text we shall discuss on the principles governing filler distribution and interaction within polymer composite materials.

Factors governing the organization of fillers within the polymer composite materials are related to physical and chemical nature of the fillers and the polymers, and further determine the performance and properties of the polymer composite materials. Through this mini review we attempt to discuss interactions and the factors governing them, within a polymer composite material, for readers to consider them during their next additive formulation of polymers with fillers. First of all it is the particle size distribution[5][6] of filler within the matrix, that depends on the surface availability and potential for interaction with the polymer matrix with respect to filler; with considerations for polymer – polarity, crystallinity and viscosity are the parameters; finally processing methods also determines the filler distribution within polymer matrix. Filler distribution in polymer matrix is subjected to “area of application”, polymer composite materials intended to be used in electrical conduction, adhesive may decrease in performance if uniform distribution of fillers occurs in polymer matrix. Morphological analysis for distribution of filler in polymer matrix may appear identical but may differ in their properties, this may be attributed to the molecular motions within the polymer matrix. The “intensity” and “extensity” factors should be considered to have a uniform distribution of filler within polymer, intensity factor i.e. reduction to the smallest particle size determining the property; and extensity factor i.e. uniform inter particle distance determining the uniformity of the properties[5]. Then comes the orientation of fillers in a polymer matrix. Particle shape and concentration of filler and viscosity of polymer matrix are the material factors determining the orientation of fillers in a polymer matrix. Orientation of fillers within polymer matrix is also determined by the processing as distribution of fillers is. Processing factors like rate of flow, characteristics of die, residence time and mold characteristics also effect orientation of fillers within polymer matrix. Orientation within polymer matrix can be induced by controlling the shear forces or by simultaneous shearing and electric fields. “Area of application” also determines the best orientation of fillers within the polymer composite materials. Further comes important dimension in the polymer composites “Void”, void if “macro” sized would reduce the mechanical performance of the polymer composites, hence void minimization is taken care of; in some applications “micro” voids are created to enhance the toughness of the polymer composite materials. “Polymer – filler interaction” forms the basis of all set of experimental observation through any means of characterization as reported in past and current literatures. Physical interaction and chemical interaction within the polymer composites are responsible factor for “polymer – filler interaction”[5]. Chemical

interaction between polymer functional groups and surface groups on fillers, physical interaction through Vander Wal forces and hydrogen bonding between polymer – polymer, polymer – filler and filler – filler, mechanical interlocking between polymer chains are responsible factors for “polymer – filler interaction”. Ionic interactions, acid base interactions are other interactions responsible. Changes in morphology of interacting components also confirms the “polymer – matrix interaction”. Molecular dimension zones (interface and interphase) formed due to molecular transformation is a static phenomenon dependent on the concentration of fillers. These molecular transformation forms molecular dimension zones which have properties different from the bulk of the polymer and hence usually improves the material properties. Chemical interactions also play a role in organization of fillers within polymer matrix. Chemical interactions are chemical reactions occurring at the surface of filler and with filler surface. Interactions within polymer composites materials are complex and their quantification is difficult; however the structural characterizations e.g. FTIR, RAMAN, NMR and ESCA are used to determine the type of interactions i.e. physical or chemical, occurring within polymer composite materials[5][7]. All the factors governing filler distribution and interactions are inter – related to each other. Further interfacial adhesion and interphase thickness can be roughly estimated through tensile test. Filler chain links, polymer chain dynamics and bound polymer are few experiments which may give an inference on organization of fillers within the polymer matrix.

2.7 POLY (LACTIC ACID) AND POLY (LACTIC ACID) COMPOSITES

2.7.1 OVERVIEW OF POLY (LACTIC ACID)

Poly(lactic acid) (PLA) cannot be considered as a new polymer. In early 1845, Theophile-Jules Pelouze synthesized PLA by the condensation of lactic acid . Wallace Hume Carothers et al. in 1932 developed a method to polymerize lactide to produce PLA and was later patented by DuPont in 1954 . Although PLA existed for several decades, its use was limited to biomedical applications (e.g., biocompatible sutures, implants, biologically active controlled release devices) due to its high cost. The low molecular weight PLA polymers obtained also hampered their wide-ranging applications. The breakthrough occurred in the early 1990s when Cargill Inc. succeeded in polymerizing high molecular weight PLA using a commercially viable lactide ring opening reaction . In 1997, Cargill Dow LLC, a joint venture between Cargill Inc. and The Dow Chemical Company, was formed to begin truly commercially significant production of PLA resins under the trade name NatureWorks™. This is a major landmark in PLA’s history because it signifies the beginning of a large-scale use of this bio-based

polymer, transforming PLA from a specialty material to a commodity thermoplastic. The increased availability of PLA stimulated an increase in its research and development activities. A survey of the literature revealed that the number of published articles related to PLA increased exponentially over the past decade, which can be also partly attributed to the escalating .green. movement that is stimulating the use of bio-based polymers. To date, the major PLA resin suppliers have been Cargill (in the United States known as Ingeo™), Mitsui Chemicals, Inc. (in Japan known as LACEA™), Purac (The Netherlands), and Teijin Limited (in Japan known as Biofront®)[8].

2.7.2 SYNTHESIS AND PRODUCTION

Poly(lactic acid) (PLA) is produced from the monomer of lactic acid (LA). PLA can be produced by two well-known processes the direct polycondensation (DP) route and the ring-opening polymerization (ROP) route.

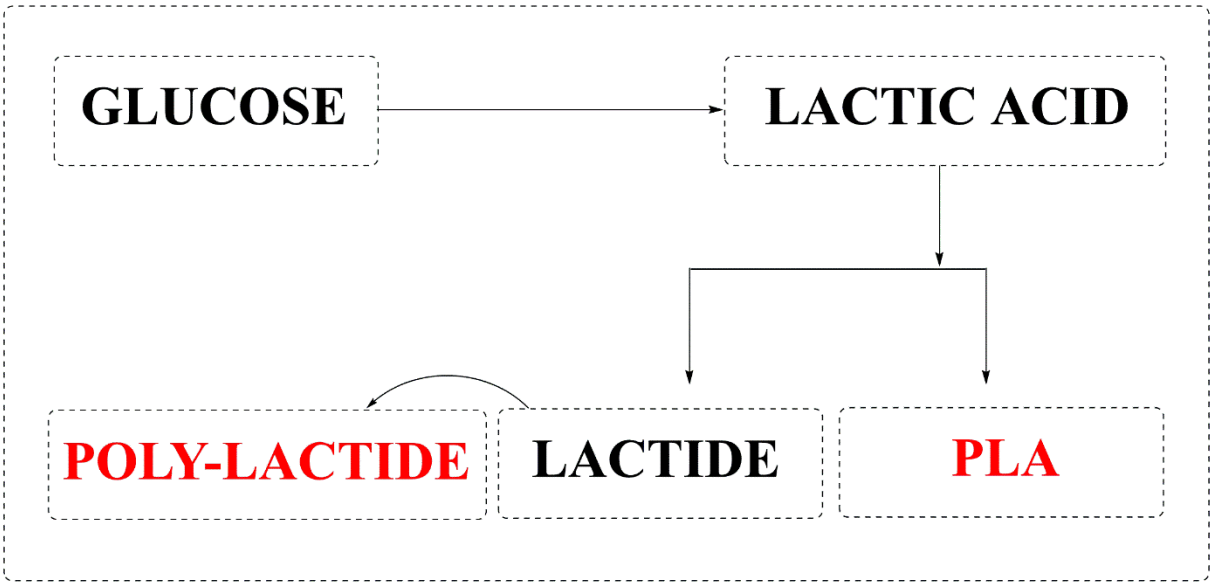

Figure 2.3: General routes for poly (lactic acid) synthesis and production

Although DP is simpler than ROP for the production of PLA, ROP can produce a low-molecular-weight brittle form of PLA. Generally, several substances are involved in the production of PLA, and these relationships have been summarized in **Figure 2.3.** The lactic acid for the process is obtained from the fermentation of sugar. Lactic acid is converted to lactide and eventually to PLA. It should be noted that there are two different terms, ‘poly(lactic acid)’ and ‘polylactide’, for the polymer of lactic acid. Both terms are used interchangeably; however, scientifically there is a difference because polylactide is produced through the ROP

route whereas poly(lactic acid) is generated using the DP route. Generally speaking, the term 'poly(lactic acid)' is widely used to mean the polymer that is produced from lactic acid[9].

2.7.2.1 SYNTHESIS - HOMOPOLYMERS OF POLY (LACTIC ACID)

L-Lactic acid is metabolic intermediate and can be obtained at low cost from the fermentation of agriculture and food by products containing carbohydrates. Thermal dehydration polymerisation of L-lactic acid gives poly(L-lactic acid) (PLLA). This requires high energy and PLLA of low molecular weight (MW)(few thousands) is obtained. Ring opening polymerisation of lactic acid dimer, lactide, with a suitable catalyst results in high molecular PLLA with useful properties. These can proceed through coordination, anionic, or cationic mechanisms. Among the effective catalysts/initiators are Lewis acids in form of metal salts of aluminium, tin, titanium and zinc, and rare earth metals; alkali metal alkoxides and supermolecular complexes ; and acids . **Figure 2.4** classifies the different poly (lactic acid) based on their chemical composition.

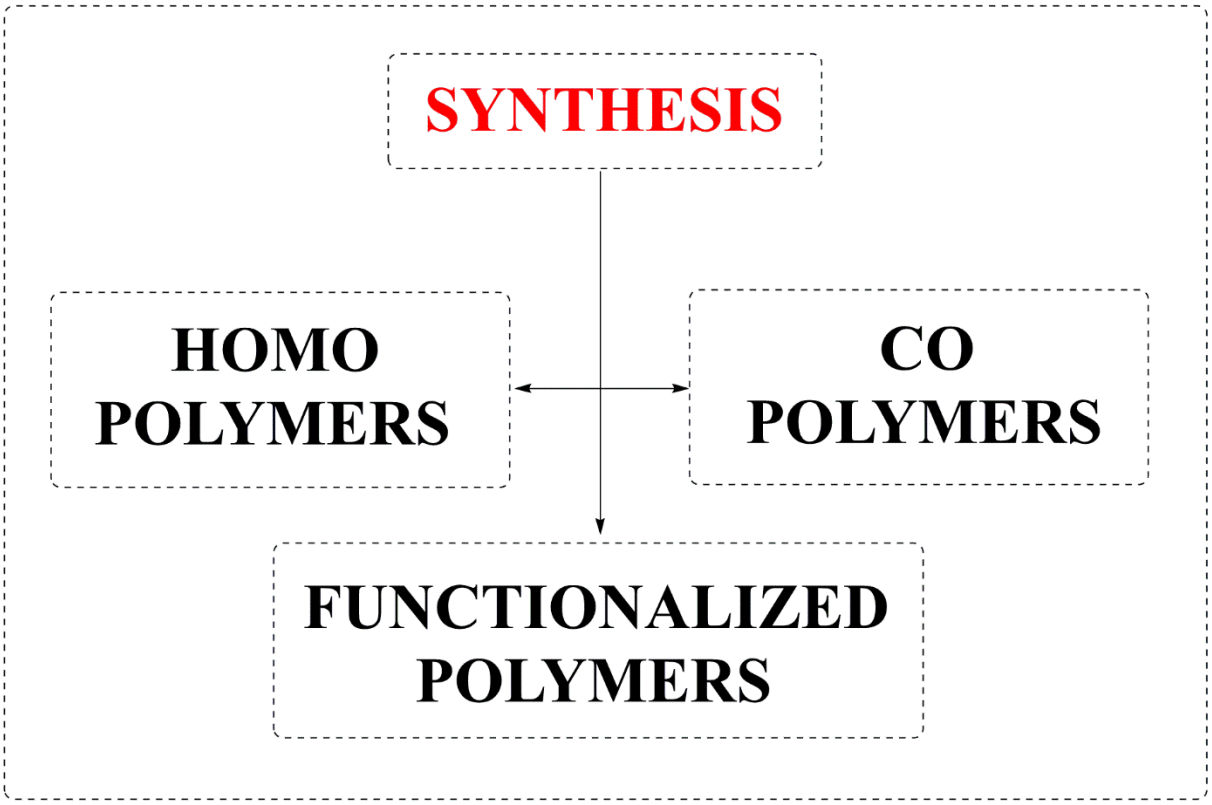

Figure 2.4: Classification of poly (lactic acid) based on synthesis

Coordination ring opening polymerisation is the most effective route for the bulk polymerisation of lactide. It is generally agreed by researchers that transition metal ions such as tin catalyse the polymerisation proceed via an insertion mechanism. At temperatures

above 150 °C the transesterification between cyclic lactide and PLA proceeds through acyl cleavage and results in high degree of retention of the stereo-chemistry of the lactide monomers. Tin catalysts are easily available and effective. They can be used for large scale producers of PLA. Stannous (II) chlorides and stannous (II) 2-ethylhexanoate are approved for food additives and are thus more often used than the others. Glycols are often used as co-initiators to obtain polyester chain growth from both hydroxy terminals of the glycols. Multi-functional glycol co-initiators can be used to obtain star shaped and highly branched PLA. Sufficient reaction time generally results in PLA with molecular weight dispersity of 1.5-2.0. Better polymerisation of lactic acid with tin salts as catalysts can be carried out in multiple steps. Lactic acid is heated at 150 °C with tin catalyst to obtain oligomeric PLA (with a degree of polymerisation of 1-8). The oligomers are then heated at 180 °C under vacuum (1333 Pa) for 5 hours to give PLA of high MW (100,000). Finally the third step is carried out at solid state above the crystallization temperature, T_c, (105 °C, 66 Pa, 0.5-2 hours) and annealing 150 °C for 10-30 hours. A PLA of MW up to 600,000 is obtained. Solution polymerisation in diphenyl ether results in a PLA of MW of 140,000. A considerable amount of effort has been directed towards the research on catalysts for ring opening polymerisation of lactide. Alkoxides such as aluminium triisopropoxide are effective catalysts. The anionic polymerisation gives PLA of MW up to 100,000 with MW/M_n around 1.4. When this polymerisation is carried solvent dispersion systems microspheres of well-defined size of PLA can be obtained. Direct condensation of lactic acid with high boiling point solvent and ring opening polymerisation of lactide were studied and both were found to be effective and PLA of MW of 300,000 was obtained.

PLA from obtained by using different methods were compared and found to have different properties. Both had glass transition temperature (T_g) of around 58-59 °C but the direct process PLA had melting temperature, T_m, 163 °C and was relatively stable whereas the PLA prepared by ring opening had a higher T_m of 178 °C but was less stable. This was attributed to the presence of catalyst and impurities[8].

2.7.2.2 SYNTHESIS - COPOLYMERS OF POLY(LACTIC ACID)

High MW PLA from prepared from PLLA, are partially crystalline with a T_m of 175-180 °C, T_g of 60 °C and a crystallization temperature (T_c) of 100-105 °C, and a decomposition temperature (T_d) of 185-190 °C. It is brittle and undergoes unzipping to lactide when thermally processed. Copolymerization with D-lactic acid and other hydroxy acids to obtain polyesters with a lower T_m and thus better thermal processing characteristics has been the common

approach to obtain useful PLA. Stereo copolymers of L-lactic acid and D-lactic acid have lower crystallinity and T_m than the homopolymer of L-lactic acid and the polyester properties vary with the optical purity with the 50/50 DL polylactic acid (PDLLA) having no crystallinity at all. Variation of the optical purity is the most commonly used means to produce PLA of different property.

Copolymers of lactic acid with glycolic acid were the first commercialized biodegradable polymers to be used as biomaterials and are used as sutures, wound dressings, and drug release systems since the 1970s. Copolymers of lactic acid with other aliphatic polyesters specially those with cyclic esters, ethers, and anhydrides have become the most studied biodegradable polymers. Ring opening polymerisation with other cyclic monomers is the best method. Thermal polymerisation with mixtures of monomers generally gives copolymers with random sequence with less crystallinity and lower T_m and T_g than PLLA. Sequential addition of monomers into the polymerisation, in some cases, results in block copolymers. Most of these aliphatic polyesters are compatible with each other at low MW but tend not to be compatible at high MW and thus complex morphology is observed for many block copolymers of PLA.

Poly(ε-caprolactone) (PCL) with T_g at –60 °C and T_m at 60 °C, are commercially available in large quantity and its biodegradation was studied in detail in terms of morphology and microbial variety. It is more flexible and hydrophobic than PLA. It was reasoned that copolymers of PLA and PCL with the proper compositions and sequences could be prepared which would have better flexibility, hydrophilic/hydrophobic balance, and impact strength than homopolymers of PLA. The need for a biodegradable replacement for poly(dimethyl siloxane) as a sustainable drug release systems was behind research on PLA/PCL copolymers as biomaterials. Block copolymers of PLA and PCL are easily obtained by using PCL-diols as co-initiator with stannous catalysts in lactide ring opening polymerisation. The expected trends in T_m, Young's moduli, material strength and ultimate elongation were observed up to 50 wt% of PCL. Bulk polymerisation of mixtures of lactides and caprolactone with stannous 2-ethylhexanoate catalyst resulted in copolymers with thermal properties of phase-separated block structures. Chain extensions can be used to expand the range of MW, composition and properties. Solution polymerisation with aluminium tris(isopropoxide) catalyst have been studied. Anionic initiators, including lithium *t*-butoxide, were also studied. Results from different research groups do not agree, and this is likely to be due to the different extents of ester exchange reaction during the polymerisation. Using poly(ethylene glycol) (PEG), as co-initiator block copolymers of PLA/PEG have been prepared. Copolymers of L-lactide and 1,5-

dioxepan-2-one were prepared with a tin catalyst. These tri-block copolymers behave like elastomers[8].

2.7.2.3 SYNTHESIS – FUNCTIONLIZED POLY (LACTIC ACID)

It is acknowledged by researchers that the practice of using metallic implants for bone fracture fixation has serious problems. Most serious ones are osteoporosis due to stress shielding caused by the mismatch of the metallic properties with that of bones and necessitate second operations for the removal of the implants. To alleviate problems, use of biodegradable polyesters were explored. Although it can be used as a suture poly(glycolic acid) undergoes hydrolysis too fast in various forms to be effective as implants. The presence of methyl side groups in PLA as the longer methylene unit in PCL slows down the rate of hydrolysis for PCL and PLA as compared with polyglycolic acid (PGA) and use of various copolymers of PLA with PGA and PCL have been explored as implant materials. These copolymers are generally partially crystalline. During hydrolysis and biodegradation the amorphous regions are degraded faster than the crystalline regions resulting in the formation of highly crystalline fragments and catastrophic loss of mechanical properties. It was reasoned that polyester networks will be less crystalline and also suffer less loss of mechanical properties during degradation. Crosslinkable polyesters and copolyesters with unsaturated maleic acid, fumaric acid, and itaconic acid units were synthesized from reactions of corresponding unsaturated anhydrides for networks and composites formation. Methacrylate terminated oligomeric polyesters can be obtained from polymerizations with co-initiators with a methacrylate group. These are starting materials for the graft copolymer of PLA. Hydroxy groups containing terminals are generally present in PLA polymerized with glycols as co-initiator. Those with hydroxy side groups were obtained from copolymerization of lactide with tartaric acid and cyclic carbonate with ketal groups which upon hydrolysis yields hydroxy groups. PLA with hydroxy terminals have been converted into degradable polyurethanes. PLA with amino, carboxylic, and chloro terminals were prepared from the PLA with hydroxy terminals[8].

2.7.3 STRUCTURE – PROPERTY RELATIONSHIP

Stereocomplex (sc)-type polylactides (sc-PLA), consisting of both enantiomeric poly(L-lactic acid) (PLLA) and poly(D-lactic acid) (PDLA), can potentially act as high performance polymers because their melting temperature (T_m = 230°C) is 50°C higher than that of the single PLLA or PDLA polymer (180°C). The stereocomplex (sc) crystal form of sc-PLA is triclinic or trigonal with both 3_1 (or 3_2 and 3_1) helical PLLA and PDLA chains packed side by

side, which is quite different from the **homochiral (hc)** pseudo-orthorhombic or orthorhombic crystal forms. Since their improved thermal and mechanical properties facilitate a wider application, various trials of the formation of sc-PLA have been done. Simple mixing of high molecular weight PLLA and PDLA, however, is likely to lead to hc crystallization rather than sc crystallization to retard the thermal stability of the resultant polymer blends. To promote sc crystallization, **stereo-block (sb)** type PLA (sb-PLA), a block copolymer of PLLA and PDLA, has been developed. The covalent bond of the enantiomeric sequences of PLLA and PDLA favor sc crystallization of the copolymer. The sb-PLA can be synthesized by solid-state polycondensation (SSP) of a mixture of PLLA and PDLA having medium molecular weight as well as by stepwise ring-opening polymerization (ROP) of D- and L-lactides[8].

2.7.4 PROPERTIES OF POLY (LACTIC ACID)

2.7.4.1 PHYSICAL PROPERTIES

Properties of PLA are greatly dependent on the optical purity. PLA with 100% L-unit, PLA 100, is partially crystalline (45-70%) with a T_m of around 180℃-184℃). The degree of crystallinity and T_m of PLA decrease with decreasing optical purity. PLA of less than 87.5% optical purity are amorphous. PLA of high optical purity has similar T_m to that of two other polymers with methyl side groups, microbial PHB, and isotactic polypropylene (iPP). All three polymers are helical in the crystalline form. The T_g of high MW PLA with different optical purity is within 55℃-61.5℃ range, which is higher than that of PHB and iPP. PLA is strong but brittle. Although PLA is soluble in chlorinated organic solvents and can be solution processed thermal processing of PLA with 96% or less optical purity (injection moulding or extrusion) are preferred. Star-shaped PLA have lower crystallinity than linear PLA with the same optical purity. The T_c of PLA with various structures are around 115℃-125℃. Stereo-complexation have been observed for L-and D-PLA. The complex has a T_m at 220℃. High MW PLA (100,000 and up) can be processed into fibres, non-woven, and articles with rigidity and strength, which are potentially useful at commodity scale if the initial high costs can be reduced as the volume increases . A considerable amount of effort has been directed toward packaging films of PLA with mixed results. The addition of suitable plasticizer to lower the T_g of PLA is necessary for obtaining flexible films[10].

2.7.4.2 CHEMICAL PROPERTIES

The most important degradation of PLA is hydrolysis. Under dry conditions pure PLA 100 can last more than 10 years . In thin film rapid changes due to hydrolysis were observed in 35

days and the changes levelled off. Increase in crystallinity can be attributed to in the increase of mobility of oligomers formed which can crystallize themselves or induce the crystallisation of larger size PLA. The hydrolysis of PLA with smaller surface/volume ratios is much m slower and complicated. PLA/GA copolymers are hydrolyzed much faster than PLA and have become the main biodegradable polymeric materials for biomedical applications such as sutures, implants, tissue engineering and drug release when fast rates of hydrolysis are desirable whereas poly(lactide-*co*-caprolactone), PLA/CL, are more suitable for slower hydrolysis than PLA. The hydrolysis of PLA, PLA/CL, and poly(lactide-*co*-glycolide), PLA/GA, like that of many hydrophobic aliphatic polyesters, is rather complex. The hydrolysis of the amorphous regions are much faster than the crystalline regions. The crystallinity of copolymers decreases rapidly with increasing amount of the second component in the copolymers. Typically little crystallinity is observed for copolymers with less than 80% PLA and the rate of hydrolysis increases accordingly[10].

2.7.5 DEGRADATION AND STABILITY

Biodegradations of PLA have been a subject of interest and so far proteinase K (EC 3.4.21.64) is the only reported enzyme that will degrade PLA amorphous regions of low MW . Microbial degradation studies of PLA have been inclusive .

Although most microorganisms studied can utilize lactic acid and its dimer, microbial degradation of oligomers and polymers of PLA have not yet been observed at appreciable rates. Thermal degradation of PLA can proceed via different mechanisms. Hydroxy-terminated PLA might undergo ‘back-biting’ transesterification resulting in ‘unzipping’ of the PLA to lactide. A common method of forming lactide is the thermal decomposition of oligomeric PLA. Inter- and intra-molecular transesterifications, both facilitated by the presence of polymerisation catalysts, is commonly observed. Finally, fragmentation of PLA, might also happen. Stabilization by the addition of suitable stabilizers is an area of ongoing research as biocompatible additives for polymers are not commonly available[8].

2.7.6 APPLICATIONS

Hydrogels have received increasing interest (**see Figure 2.5**) specially for biomedical and consumer products application. PLA and PEG hydrophilic/hydrophobic block copolymers are especially promising for soluble hydrophilic/hydrophobic system that becomes an insoluble microsphere when injected into the body as drug release systems . The hydrolysis and biodegradation of these copolymers are subjects of ongoing research. As is generally true for

new polymers, costs for PLA and copolymers are relatively high for large volume applications. However, they are from renewable resources and environmentally compatible. All factors considered they are polymers for the future. Mixing with low cost biopolymers such as starch to lower the cost and increase biodegradation rates, was successfully done for PCL and cellulose esters , has had only mixed results as PLA and copolymers are not hydrolytically stable enough at high temperatures when the mixing has to be carried out. Reactive coupling of PLA with starch unfortunately adds to the cost[8] .

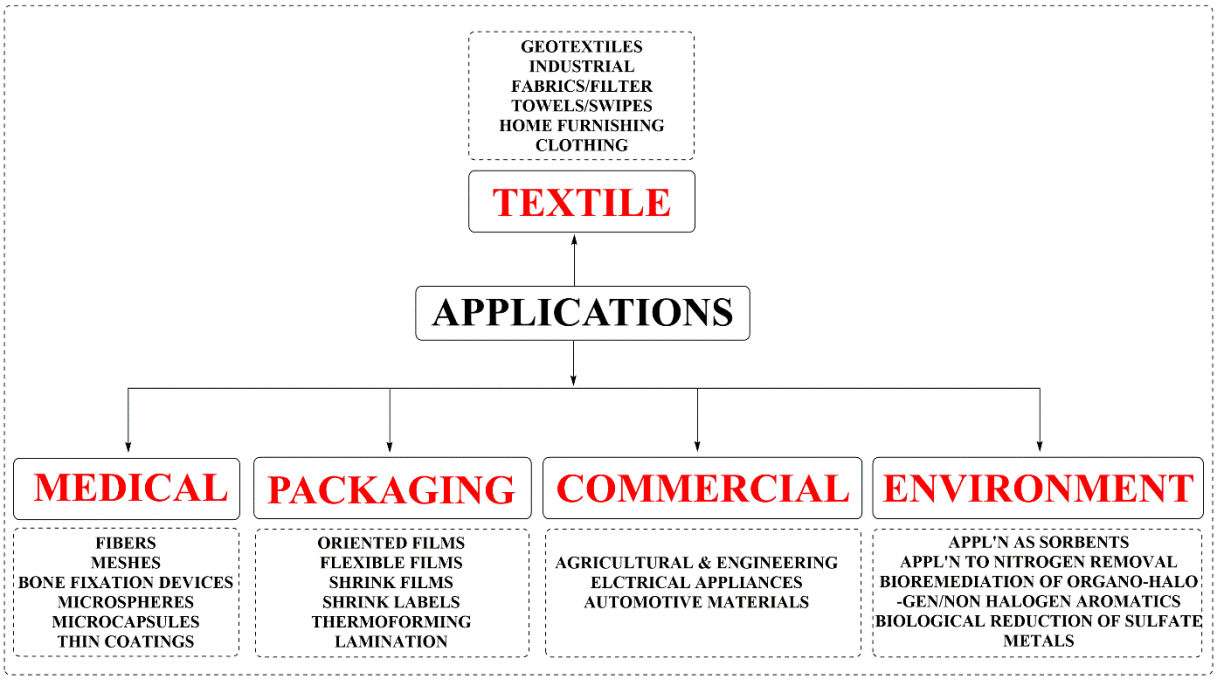

Figure 2.5: Applications of poly (lactic acid)

2.7.7 OVERVIEW OF POLY (LACTIC ACID) COMPOSITES AND NANOCOMPOSITES

A composite is defined as a material that combines two or more distinct constituents or phases, where one or more of the discontinuous phases (reinforcements) are dispersed in another continuous phase (matrix) in order to obtain tailormade characteristics and properties. The reinforcing agent can be either particle or fibrous material. The most common form of reinforcement is the fiber. The difference is that a particle has almost equal dimensions in all directions while a fiber has a much greater length than its cross section. Both of these types of reinforcements have been used to produce polymer composites. In fiber-reinforced polymer composite materials, fibers are used to carry the load while the polymeric matrices are used to bind the fibers together, transfer the stresses from one fiber to the next, and keep them in the desired location and orientation; the matrices also protect the fibers from abrasion and environmental damage upon exposure to elevated temperature and

humidity. Because of the distinct advantages that they have over traditional materials, polymer composites are being used in an increasing number of engineering applications. Although a number of conventional thermoset and thermoplastic matrices are used in composite production, depletion of petroleum resources, disposal problems after use, and the introduction of new stringent legislations have created a surge of interest in bio-derived matrix materials. Polylactic acid (PLA) is one such biopolymer, which apart from being used in the packaging industries has gained a lot of attention as a matrix in composites . It is one of the most promising biodegradable polymers owing to its mechanical property profile, thermoplastic processability, and biological properties, such as biocompatibility and biodegradability. However, widespread application of PLA is limited because of high cost compared to commodity thermoplastics such as polyethylene (PE) and polypropylene (PP), brittleness, and low thermal stability . One approach to increase the usability of PLA is to add fibrous reinforcements in order to produce materials at a comparable or lower cost, while maintaining or improving the material properties. The reinforcement of polymers with filler is also common in composite production. Recently, interest has grown in the use of nanoscale fillers because of their distinctive advantages, such as dramatic improvement in mechanical properties with low filler content, to produce new value-added products. Recently, polymer nanocomposites have attracted an increased attention, where nanotechnology is applied to produce materials with remarkable improvements in properties and performance. The most popular approach to produce this new family of composite materials is to introduce nanoscale particles into a polymer matrix to produce polymer/nanoparticle composites. Examples of such nanoparticles include layered silicates, layered titanates, carbon nanotubes (CNTs), gold, silver, and maghemite nanoparticles, and fluorine mica . Nanosilicates are the most commonly used nanoparticle reinforcements for polymer nanocomposites. Different types of nanoclays, such as Cloisite Na, Cloisite 30B, and Cloisite 20A, have been used for PLA-based composite films . Various approaches have been successfully developed to fabricate PLA/clay nanocomposites, namely, in situ polymerization intercalation, melt intercalation and solution intercalation, and film casting techniques . The inclusion of well-dispersed nanosilicates in polymers has led to a vast array of changes in properties, including increased storage modulus, increased tensile and flexural properties, heat deflection temperature (HDT), gas barrier property, and decreased permeability and flammability. X-ray diffraction studies have revealed that a good affinity between the organo modified clay and the PLA matrix exists in an intercalated nanocomposite. The rate of biodegradation of neat PLA can also increase significantly after nanocomposite preparation . Owing to the potential of

significant property improvement, a lot of researches have now been dedicated toward development of PLA nanocomposite to exploit the benefits of biodegradable PLA and nanolayered silicates . The crystallization behavior of PLA/clay nanocomposites indicates that the dispersed silicate nanoparticles act as nucleating agents for PLA crystallization. The degree of clay miscibility with the matrix and the clay dispersion state in the PLA matrix both significantly influence the crystallization behavior and final morphology of the nanocomposites. Besides layered silicates, other nanoparticles, including carbon nanotubes , and nanoscale magnetites , have been used to make PLA nanocomposites. Recently, carbon nanotubes have been the subject of considerable attention due to their unique and remarkable physical and mechanical properties. These unique properties have led to a significant amount of research on utilizing CNTs as new reinforcement in polymer composites. Purified multiwalled carbon nanotube (MWCNT) is a chemical vapor deposition material with outside diameter of 10–20 nm, inside diameter of 5–10 nm, and length of 10–30 mm. Its surface area is higher than 200m_2/g. Both the dispersion state and the surface functionalization of MWCNTs are very important for nanocomposite production. PLA nanocomposites containing various functionalized MWCNTs have been prepared directly by melt compounding or extrusion through a twin-screw extruder (with a high shear rate configuration) followed by injection molding. Fe_3O_4 magnetic nanoparticles have also been used as filler with a PLA matrix for potential applications in drug controlled release systems and tumor hyperthermia treatments. It is expected that more suitable nanoparticles will be discovered that will allow PLA nanocomposites to be prepared with more outstanding properties[8].

In recent years, the nanoscale, and the associated excitement surrounding nanoscience and technology, affords unique opportunities to create revolutionary material combinations. These new materials promise to enable the circumvention of classical material performance trade-offs by accessing new properties and exploiting unique synergisms between constituents that occur only when the length scale of the morphology and the critical length associated with the fundamental physics of a given property coincide. Nanostructured materials or nanocomposites based on polymers have been an area of intense industrial and academic research over the past one-and-a-half decades . In principle, nanocomposites are an extreme case of composite materials in which interface interactions between two phases are maximized. In the literature, the term nanocomposite is generally used for polymers with sub-micrometer dispersions. In polymer-based nanocomposites, nanometer sized particles of inorganic or organic materials are homogeneously dispersed as separate particles in a

polymer matrix. This is one way of characterizing this type of material. There is, in fact, a wide variety of nanoparticles and a way to differentiate them and to classify them by the number of nanoscale dimensions they possess. Their shape varies and includes:

(i) one-dimensional needle- or tube-like structures, for example, inorganic nanotubes, carbon nanotubes, sepiolites, and;
(ii) two-dimensional platelet structures, for example, layered silicates; and spheres
(iii) three-dimensional structures, for example, silica, zinc oxide, and so on.

The main objective of this chapter is to provide a snapshot of the rapidly developing nanocomposite materials based on PLA. To date, various types of nano-reinforcements such as nanoclay, cellulose nanowhiskers, ultrafine layered titanate, nanoalumina, carbon nanotubes , and so on have been used for the preparation of PLA nanocomposites. For each particular system, progress is discussed chronologically, beginning with the pioneering work. Various physicochemical characterization and improved mechanical properties are summarized. Ongoing developments and promises are also discussed[8].

2.7.7.1 POLY(LACTIC ACID)NANOCOMPOSITES

Ogata et al. first reported the preparation of PLA–organoclay blends by dissolving the PLA in hot chloroform in the presence of dimethyl distearyl ammonium-modified MMT (2C18MMT). In the case of PLA/MMT composites, wide angle X-ray diffraction (WXRD) and small-angle X-ray scattering (SAXS) showed that the layered silicate could not be intercalated in the PLA/MMT blends when prepared by the solvent cast method. In other words, the clay existed in the form of tactoids, consisting of several stacked silicate monolayers. These tactoids are responsible for the formation of particular geometrical structures in the blends, which leads to the formation of superstructures in the thickness of the blended film. This kind of structural feature increases the Young's modulus of the hybrid. Bandyopadhyay et al. reported the preparation of intercalated PLA–organoclay nanocomposites with much improved mechanical and thermal properties. Two different kinds of clay, fluorohectorite (FH) and MMT, both modified with dioctadecyl trimethyl ammonium cation, were used for the preparation of nanocomposites with PLA. Sinha Ray et al. used the same melt intercalation technique for the preparation of intercalated PLA–organoclay nanocomposites. WXRD patterns and TEM observations clearly established that the silicate layers of the clay were intercalated, and randomly distributed in the PLA matrix . Incorporation of a very small amount of o-PCL as a compatibilizer in the nanocomposites led to a better parallel stacking of the silicate layers, and also to much stronger flocculation due to the hydroxylated edge–edge interaction of the

silicate layers. Owing to the interaction between clay platelets and the PLA matrix in the presence of a very small amount of o-PCL, the strength of the disk–disk interaction plays an important role in determining the stability of the clay particles, and hence the enhancement of mechanical properties of such nanocomposites. Maiti et al. prepared a series of PLA-based nanostructured materials with three different types of pristine clays, saponite, MMT, and synthetic mica (SM), and each was modified with alkyl phosphonium salts having different chain lengths. In their work, they first tried to determine the effect of varying the chain length of the alkyl phosphonium modifier on the properties of the organoclay, and how the various clays behaved differently with the same organic modifier. They also studied the effects of dispersion, intercalation, and the aspect ratio of the clay on the properties of PLA. Paul et al. used an in situ intercalative method for the preparation of exfoliated PLA–clay nanocomposites. They used two different kinds of organoclays (C30B and C25A, Southern Clay Products) for the preparation of nanocomposites with PLA. In a typical synthetic procedure, the clay was first dried overnight at 70°C in a ventilated oven, and then, at the same temperature under reduced pressure, directly in the flame-dried polymerization vial for 3.5 h. A 0.025M solution of L-lactide in dried tetrahydrofuran (THF) was then transferred under nitrogen to the polymerization vial and the solvent was eliminated under reduced pressure. Polymerizations were conducted in bulk at 120°C for 48 h, after 1 h of clay swelling in the monomer melt. When C30B was used, the polymerization was co-initiated by a molar equivalent of $AlEt_3$, with respect to the hydroxyl groups borne by the ammonium cations of the filler, in order to form aluminum alkoxide active species, and was added before the L,L-lactide. $Sn(Oct)_2$ (monomer/$Sn(Oct)_2$¼300) was used to catalyze the polymerization of L,L-lactide in the presence of C25A. The same group also reported the preparation of plasticized PLA/MMT nanocomposites by a melt intercalation technique. The organoclay used was MMT modified with bis-(2-hydroxyethyl) methyl (hydrogenated tallow alkyl) ammonium cations. X-ray diffraction (XRD) analyses confirmed the formation of intercalated nanocomposites. Chang et al. reported the preparation of PLA based nanocomposites with three different kinds of organoclays (such as Cloisite®20A, Cloisite®25A, and Cloisite®30B) via a solution intercalation method. They used N,N_0- dimethylacetamide (DMA) for the preparation of nanocomposites. XRD patterns indicated the formation of intercalated nanocomposites for all the three organoclays tested. TEM images proved that most of the clay layers were dispersed homogeneously in the PLA matrix, although some clusters or agglomerated particles were also detected.

Moon et al. prepared PLA/MWCNT nanocomposites by solvent casting. For the synthesis of nanocomposites, they used two different methods. In the first method, a 10 wt% solution of PLA in chloroform was prepared, which was then combined with previously dispersed MWCNTs in chloroform, and the whole mixture was sonicated for 6 h. Subsequently, the mixture was poured into Teflon dishes and dried at room temperature for 1 week, and then the sample was vacuum dried at 80°C for 8 h. In the second method, the as-cast composite films from the first method were folded and broken into pieces of 0.5–1.0 cm^2 and stacked between two metal plates. This stack was then hot pressed at 200°C and 150 kgf/cm^2 for 15 min. As a result 100–200 mm thick films were obtained. TEM analysis shows uniform dispersion of MWCNTs in the PLA matrix. This uniform dispersion of MWCNTs changes the physical properties of the pure polymer. Chen et al. synthesized PLA/CNT nanocomposites using a ''grafting to'' technique. To understand the effect of molecular weight on the properties of the final nanocomposites, they used PLA of three different molecular weights. They first oxidized MWCNTs by acid treatment. In a typical procedure, a 500mL flask charged with 2.5 g of the crude MWCNTs and 200mL of 60% HNO_3 aqueous solution was sonicated in a bath (28 kHz) for 30 min. The mixture was then stirred for 12 h under reflux. After the solution was cooled to room temperature, it was diluted with 400mL of deionized water and vacuum filtered through a 0.22 mm polycarbonate membrane. The solid was washed with deionized water until the pH of the filtrate reached approximately 7. The solid was then dried under vacuum for 12 h at 60°C to yield 1.5 g of the carboxylic acid-functionalized MWCNT (MWCNT-COOH)[8].

Hiroi et al. prepared PLA/organically modified layered titanate (OHTO) nanocomposites by a melt extrusion method. For nanocomposite preparation, the OHTO (dried at 120°C for 8 h) and PLA were first dry mixed by shaking them in a bag. The mixture was then melt extruded using a twin-screw extruder (KZW15-30TGN, Technovel Corp.) operated at 195°C (screwspeed¼300 rpm, feed rate¼22 g/min) to yield nanocomposite strands. XRD patterns and TEM observations showed the formation of intercalated structures. Recently, Nishida et al. reported the preparation of aluminum hydroxide ($Al(OH)_3$) based nanocomposites of PLA to achieve the chemical recycling of flame-resisting properties of PLA. For the preparation of PLLA/$Al(OH)_3$ hybrids, PLLA was first synthesized by the ring-opening polymerization of L-lactide catalyzed by Sn(2-ethylhexanoate)$_2$. The obtained PLLA was purified in a three-stage process, by first extracting the catalyst and residues from the PLLA/chloroform solution with a 1M HCl aqueous solution, then washing with distilled water until the aqueous phase became totally neutral, and finally precipitating the polymer with methanol before vacuum drying. The

purified PLLA was then mixed with $Al(OH)_3$ in a prescribed weight ratio in a chloroform solution and vigorously stirred for 1 h to disperse the inorganic particles uniformly. The mixture was then cast on glass Petri dishes in order to fabricate poly (lactic acid) composites[8]. Research works in the area of poly (lactic acid) and poly (lactic acid) composites are many, selected references whose work are considered while structuring the idea of the thesis are:
[11][12][13][14][15][16][17][18][19][20][21][22][23][24][25][26][27][28][29][30][31][32][33][34][35][36][37][38][39][40][41][42][43][44][45][46][47][48][49][50][51][52][53][54][55][56][57][58][59][60][61][62][63][64][65][66][67][68][69][70][71][72][73][74][75][76][77][78][79][80][81][82][83][84][85][86][87][88][89][90][91][92][93][94][95][96][97][98][99][100][101][102][103][104][105][106][107][108][109][110][111][112][113][114][115][116][117][118][119][120][121].

2.7.7.2 MECHANICAL PROPERTIES

Modern engineering practice makes continual demands upon the material and many of the time-honored approximations made by designers cease to be valid as operating conditions extend beyond those hitherto encountered. Since the properties of interest depend, in the last analysis, upon the structure (both at the atomic and microscopic levels), the object of the present volume is twofold. Firstly, to relate properties and structure, secondly (and possibly more important), to provide a theoretical basis upon which to extrapolate when conditions or materials outside previous experience arise[122].
When an engineer specifies the use of a particular material for a given application, he does so from a consideration of the properties of the substance. This statement must be examined further. Firstly, the term "properties" is a very wide one and may have a particular meaning to a particular group of people. Thus a mechanical or structural engineer is primarily interested in the load carrying capacity and in such characteristics as machineability, weldability. On the other hand, an electrical engineer requires some knowledge of conductivity, magnetic permeability, dielectric constants—and while strength is still significant it is often of secondary importance[122].
Mechanical properties of a composite are not governed by reinforcement alone but by a synergy between the reinforcement and the matrix. Along with several other factors, the mechanical performance of a composite is expected to depend on the following factors:

- wettability and interfacial bonding,
- volume fraction of the fillers,
- thermal stability,

- .aspect ratio of the reinforcements,
- .dispersion of the fillers in the matrix,
- .fiber orientation,
- .crystallinity of the matrix.

Reinforced PLA composites generally possess good stiffness and tensile characteristics. In general, tensile and flexural modulus results are improved by increasing the content of cellulose or cellulose-based reinforcements in PLA-based composites, whereas tensile and flexural strengths remain practically unchanged or are worsened. This stems from the fact that tensile or flexural modulus is only measured at very small strain when simple physical contact of components is sufficient to transfer the stress, whereas tensile and flexural strengths are very sensitive to the filler/matrix interfacial adhesion and interface plays a crucial role in transferring the stress from the matrix to the dispersed phase. Mechanical properties are widely reported for engineering materials[8]. This is especially true for particulate composites. Elastic properties are measured nondestructively. Strength, fatigue, impact, and toughness tests are destructive. An array of material attributes arises from these tests as used in evaluating structural materials. The main properties are generated via uniaxial loading in tensile and bending tests, supplemented by fatigue and fracture tests. It is possible to adapt the test for elevated temperatures or corrosive environments, or other environmental conditions to ensure the test is relevant to the application[123][124][125][126].

2.7.8 CONCLUSION

By above information on poly (lactic acid) and poly (lactic acid) composites, it was clear that its application well suits the fabrication of biomedical devices. Structural applications for poly (lactic acid) and poly (lactic acid) composites were not considered due to its inability to deform under stress. Hence through our research study we propose a technique, wherein processing and shape of fillers are considered.

Further **Chapter 3** discusses in detail the materials, methods and the processing techniques adopted in this study to fabricate singly poly (lactic acid) composites and hybrid filler poly (lactic acid) composites.

3 MATERIALS AND METHODS

The research focuses on the effective shape factor of particulate fillers on structural and mechanical properties of poly (lactic acid) composites in line with morphological evidences .In this study carbon black, multiwalled carbon nanotubes, cellulose nanofibers, carbon black + multiwalled carbon nanotubes, carbon black + cellulose nanofibers were used to fabricate poly (lactic acid) composites and hybrid filler poly (lactic acid) composites. Quantitative research design and experimental research approach used in this study are described in this chapter. The study is divided into preliminary, pilot and finally the main study. Preliminary study relates to the extraction of cellulose nanofibers from raw kenaf fibers and selection of a process [DD – Dissolution dispersion, MMCM – Melt mixing compression molding] and optimized concentration of filler for fabrication of poly (lactic acid) composites. Pilot study examines the selected process,[i.e. DD] and a modification in the process with respect to its interface characteristics [i.e. OD – Oligomeric dispersion] was performed. Ultraviolet Visible spectroscopy was used as a tool to determine the interface modification. This provided a guidance for the main study, subsequently the main study describes and examines the poly (lactic acid) composites and hybrid composites prepared via oligomeric dispersion. Structural, mechanical and morphological evidence are presented in **Chapter 5, 6, 8** and **7** respectively. The basis for carrying out this study was observation and deductive reasoning from the available literature related to poly (lactic acid) composites and hybrid composites. Poly (lactic acid) is a brittle thermoplastic, with little plastic deformation and toughness limiting its application in structural components. Many researchers have tried to enhance toughness of poly (lactic acid) by filling them with fillers, oligomer and/or biopolymers with possible sacrifice in strength. It can therefore be inferred that oligomeric dispersion could be useful to enhance toughness without sacrificing strength of poly (lactic acid) composites and hybrid composites.

The research study in this thesis is an quantitative research, wherein collection of numerical measured data are statistically analyzed to explain and predict the outcomes, provided the data should be tangible, reliable and able to confirmed. According to statistical researchers experimental designs are divided into after only, before – and – after, experimental, control group, double control, comparative, matched control experimental, placebo designs. The main study of this research used the control group design. As the name “Control group” its experimental group is intervened and not the control group. Assigning variables to the research subjects and manipulating other factors is one of the experimental approach in research design and establishes relation or effect between variables and subjects.

3.1 MATERIALS AND METHODS FOR EXTRACTION OF CELLULOSE NANOFIBERS

Extraction of cellulose nanofibers from raw kenaf fibers was a preliminary study, involving extraction of particulate fillers for fabrication of poly (lactic acid) composites and hybrid composites.

3.1.1 MATERIALS FOR EXTRACTION OF CELLULOSE NANOFIBERS

Raw kenaf fibers, sodium hydroxide, pressure vessel, acetic acid, water, sodium hypochlorite, oxalic acid were the chemicals used for extraction of cellulose nanofibers from raw kenaf fibers. All the chemicals were procured from a local supplier and were used as received.

3.1.2 METHOD ADOPTED FOR EXTRACTION OF CELLULOSE NANOFIBERS

Extraction of cellulose nanofibers from raw kenaf fibers involved physical, mechanical and chemical techniques. Raw kenaf fibers were grounded finely and weighed for further process. Fine grounded kenaf fibers were then treated with 5% of sodium hydroxide, i.e. alkali treatment for 60minutes. Repetition of alkali treatment was done when necessary changes (change in texture color, i.e. from dark brown to pale yellow) did not occur. Alkali treated fibers were then washed with water to ensure the removal of sodium hydroxide. Steam explosion on washed alkali treated fibers using a pressure vessel was carried out. Alkali treated fibers were then bleached in a bleaching solution. Bleaching solution is a combination of two solutions combined in 1:1 ratio. Solution 1 consist of 26g of sodium hydroxide + 74ml of acetic acid + 900ml of water ~ 1000ml. Solution 2 was prepared using 250ml sodium hypochlorite +750ml water. Bleached fibers were neutralized by washing them with water. Finally the bleached fibers were treated with 10% oxalic acid until the fiber turned white. The suspension must be further freeze dried to change the physical form of cellulose nanofibers, i.e. from liquid suspension to solid powder[127].

3.2 MATERIALS AND METHODS FOR PREPRATION OF POLY (LACTIC ACID) COMPOSITES

3.2.1 MATERIALS FOR POLY (LACTIC ACID) COMPOSITES

Poly (lactic acid) [PLA] and Lactic acid [LA], Glycolic acid [GA] were the polymers and monomers used; carbon black [CB], multiwalled carbon nanotubes [MWCNT], cellulose nanofibers [CNF] were the particulate fillers; chloroform was the solvent used in our study.

Poly (lactic acid) – IngeoTM Biopolymer 3100HP, with specific gravity, melt index, relative viscosity of 1.24, 24g/10min, 3.1 respectively (1.0 g/dL in chloroform at 30°C) a medium viscosity grade and semi-crystalline polymer, procured from Nature works, USA was used in this study. DL - Lactic acid syrup [Product no: L1250] and glycolic acid solution [Product no: 420603] used in our study were procured from Sigma Aldrich. CB – N220, with surface area, DBP number, density of 100 to 120m^2/g, 113cm^3/100 g, 1.7g/cm^3 in kind, from CABOT Ltd; MWCNT – NC7000TM, with specific gravity, surface area, average length, an average diameter of 1.4, 250 to 300m^2/g, 1.5µm, 9.5nm respectively from NANOCYL and CNF [extracted in our laboratory with an aspect ratio of 80 – 160] was used. Chloroform was procured from Merck Life Sciences Pvt Ltd. All materials were used as obtained.

Poly (lactic acid) composites using DD, MMCM and OD were prepared. In preliminary study selection of process [between DD and MMCM] / optimization of filler concentration was carried out. In pilot study a comparative study with respect to DD and OD were done to determine the state of dispersion and interphase characteristics. To minimize the loss of solvents for maximizing effective dispersion, a water condenser was used. In main study poly (lactic acid) composites and hybrid composites were prepared using OD and tested for structural, mechanical and morphological properties. Detailed process conditions to prepare poly(lactic acid) composites and hybrid composites are described below.

3.2.2 METHODS ADOPTED FOR FABRICATION OF POLY (LACTIC ACID) COMPOSITES

3.2.2.1 DISSOLUTION DISPERSION [DD][128][129]

For DD, polymer dissolution was prepared by immersing poly (lactic acid) granules [20g] in chloroform [50ml] undisturbed overnight [**Figure 3.1**]. Filler dispersion was prepared using chloroform [50ml] and filler at 50℃ for 80min [**Figure 3.2**].

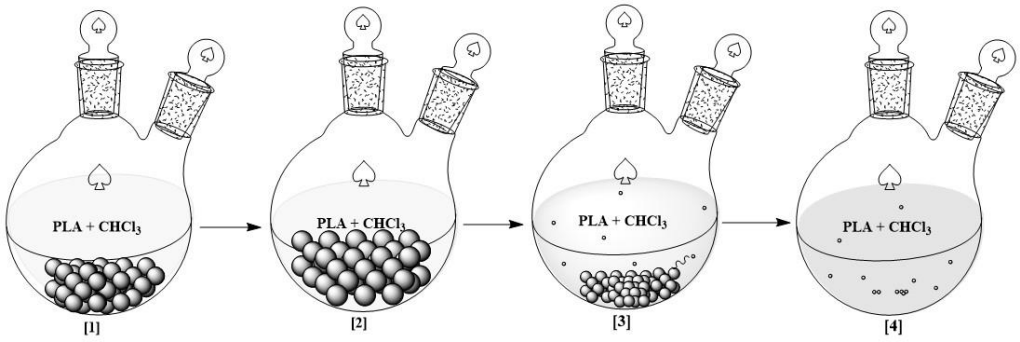

Figure 3.1: Poly(lactic acid) dissolution stages

Poly (lactic acid) dissolution was heated to reduce the viscosity enhancing dispersion of fillers [**Figure 3.3**]. Finally, poly (lactic acid) dissolution and filler dispersions were heated at 80℃

for 80min on a high-velocity magnetic stirrer [**Figure 3.3**]. The prepared suspension of filler in poly (lactic acid) dissolution was then cast on Teflon plate and vacuum dried in oven at 65℃.

3.2.2.2 OLIGOMRIC DISPERSION [OD][128][129]

OD was carried out in steps, which include preparation of a poly (lactic acid) dissolution [using the same method as used in DD], preparation of oligomeric dispersion and finally preparing a “ready to pour mixture”. All the steps in OD were accompanied by a water condenser to maintain a constant viscosity in the reactor [OD is modification of DD].

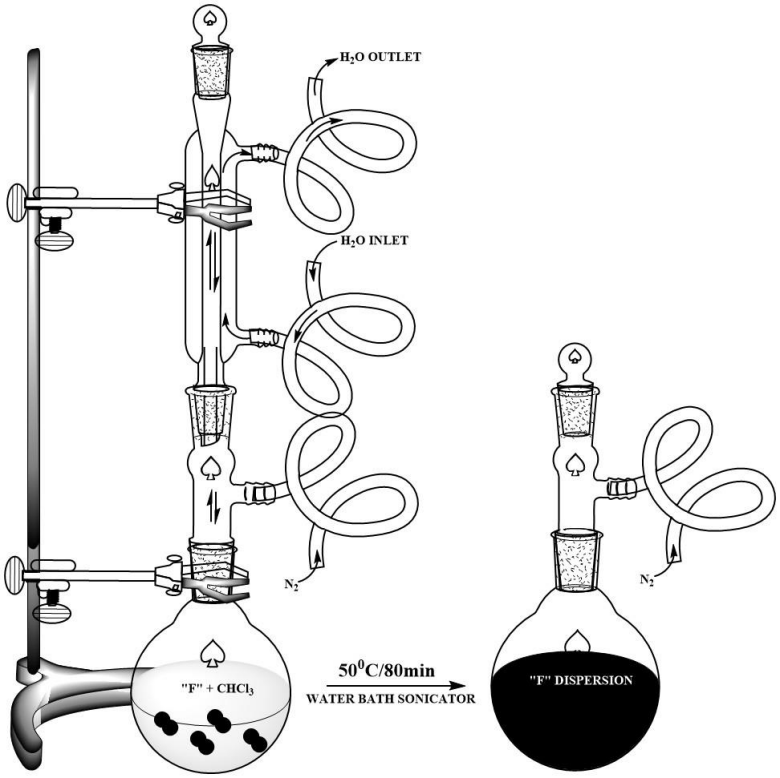

Figure 3.2: Preparation of Filler Dispersion

By minimizing the evaporation of solvents and maximizing dispersion of particulate fillers during ultra-sonication and high-velocity mixing. Sufficient time, and the temperature was maintained during ultra-sonics and high velocity mixing to avoid regions of high or low particulate filler concentration during macromixing. The energy in the form of ultrasonic and high-velocity mixing was required to reduce the size of particulate filler aggregate with respect to the viscosity of the dispersion medium. The viscosity of the dispersion medium is an important factor before selecting a process of dispersion. Experiments related to OD, sonication was only used for preparing filler dispersion and lastly to prepare “ready to pour mixture” [RTPM].

Sonication was observed not to be suitable for high viscosity liquids [polymer melts] and hence to overcome this limitation high velocity mixing using a magnetic stirrer was carried out. Poly (lactic acid) dissolution was prepared using poly (lactic acid) granules [20g] and chloroform [50ml] undisturbed overnight [**Figure 3.1**]. For poly (lactic acid) composites involving single filler, dispersions were prepared in chloroform [50ml] using half quantity of filler at 50℃ for 80min using a water bath sonicator.

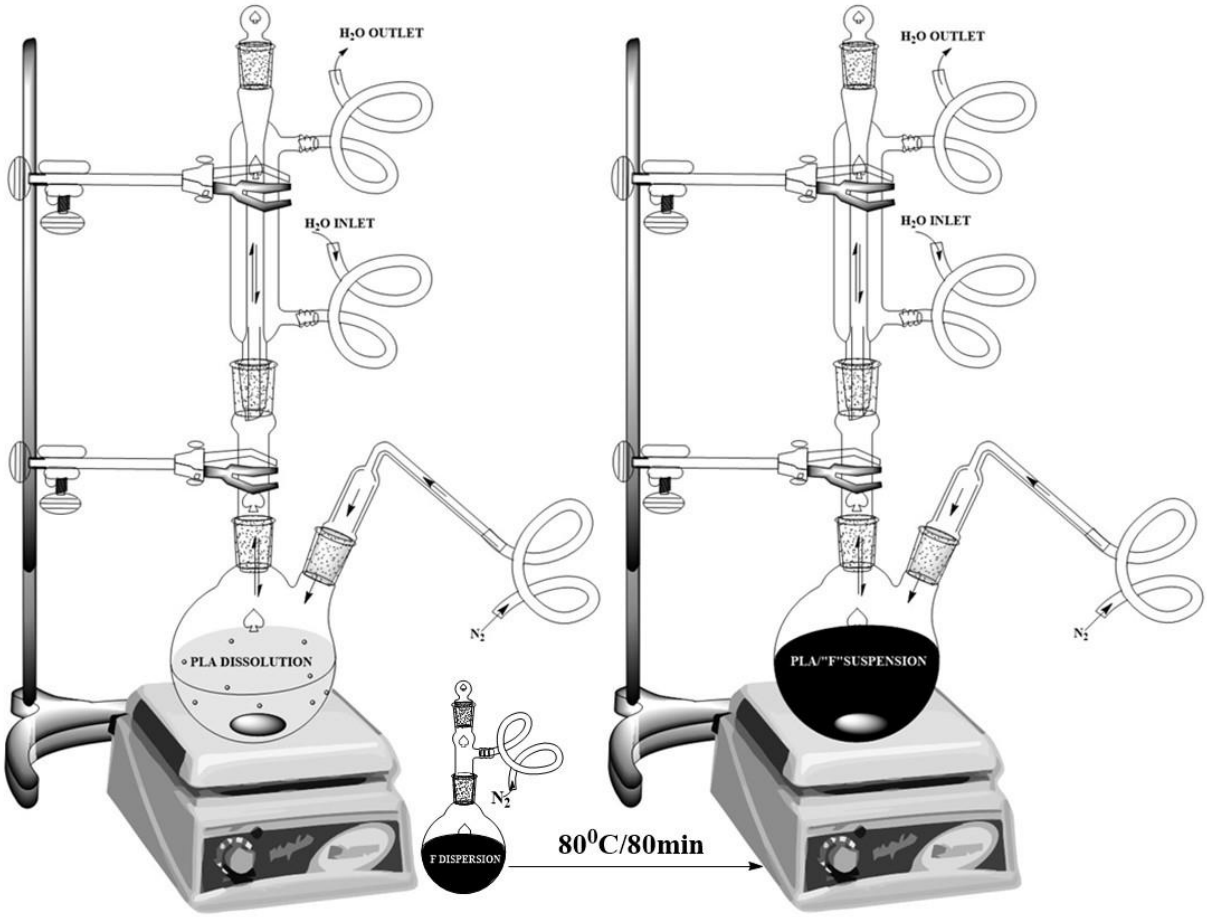

Figure 3.3: Preparation of PLA - filler Suspension

Poly (lactic acid) dissolution and filler dispersion were heated to 80℃ for 80min on a high-velocity magnetic stirrer to form a stable suspension of filler in poly (lactic acid) [figure 3.3]. Oligomeric dispersion using remaining half filler, DL – lactic acid [50ml] and glycolic acid [50ml] were prepared at 150℃ for 100min in chloroform media using a high-velocity magnetic stirrer [**Figure 3.4**]. Oligomeric dispersion was mixed with a stable suspension of filler in poly (lactic acid) at 80℃ for 40min to form a poly (lactic acid) mixture in chloroform media on a high-velocity magnetic stirrer [**Figure 3.5**]. Further, the poly (lactic acid) mixture was warmed at 50℃ for 20min using a water bath sonicator to prepare an RTPM. The RTPM was poured

on a Teflon plate and kept in a vacuum oven at 65℃ to make solid films which were used for characterization. To study the hybrid effect, via DD, filler dispersion of both the fillers were prepared in chloroform at 50℃ for 80min and further heated with poly (lactic acid) dissolution at 80℃ for 80min. For OD, filler dispersions of filler in major quantity (carbon black in this study) was mixed with poly (lactic acid) dissolution and filler in minor quantity was added while preparation of oligomeric dispersion. The conditions and steps to prepare a suspension of filler in poly (lactic acid); oligomeric dispersion and finally hybrid poly (lactic acid) composites remain similar as mentioned above.

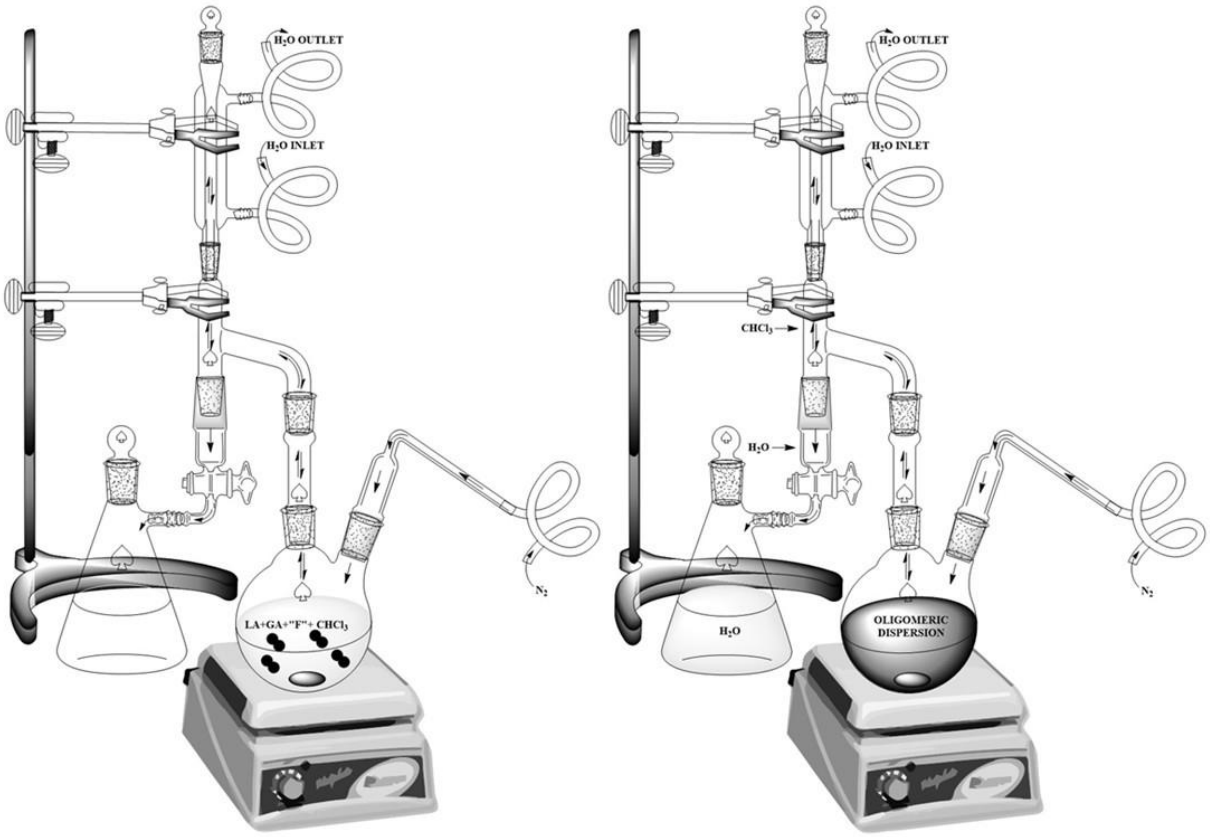

Figure 3.4: Preparation of oligomeric dispersion

3.2.2.3 MELT MIXING COMPRESSION MOLDING [MMCM][128]

Poly (lactic acid) granules were dried in hot air oven to remove moisture. Oven-dried poly (lactic acid) was processed on a pre-heated laboratory Haake mixer at melt temperature of poly (lactic acid) granules i.e. 190 ± 5°C following a mixing cycle of 15 minutes, 160 rotations per minute, in line with specific quantity of filler. The poly (lactic acid)/filler melt was then collected on a polyester film. Poly (lactic acid)/ filler melt solidifies and forms lump. The lump was then pressed with a pressure of 150kg/cm^2 in between cold compression molding press

to deform the lump into thick sheet of 5mm. The prepared thick sheet was then worked on a two-roll mill to ensure orientation of poly (lactic acid) chains, distribution, and dispersion of filler on a minute scale. Flash type mold was used in compressing poly (lactic acid) composites, wherein metal picture frame was placed in between two thin metal plates. The use of flat mold types squeezed out excess molding materials and did not exert pressure on the molding material during cooling, reducing internal stresses in the molded sheet.

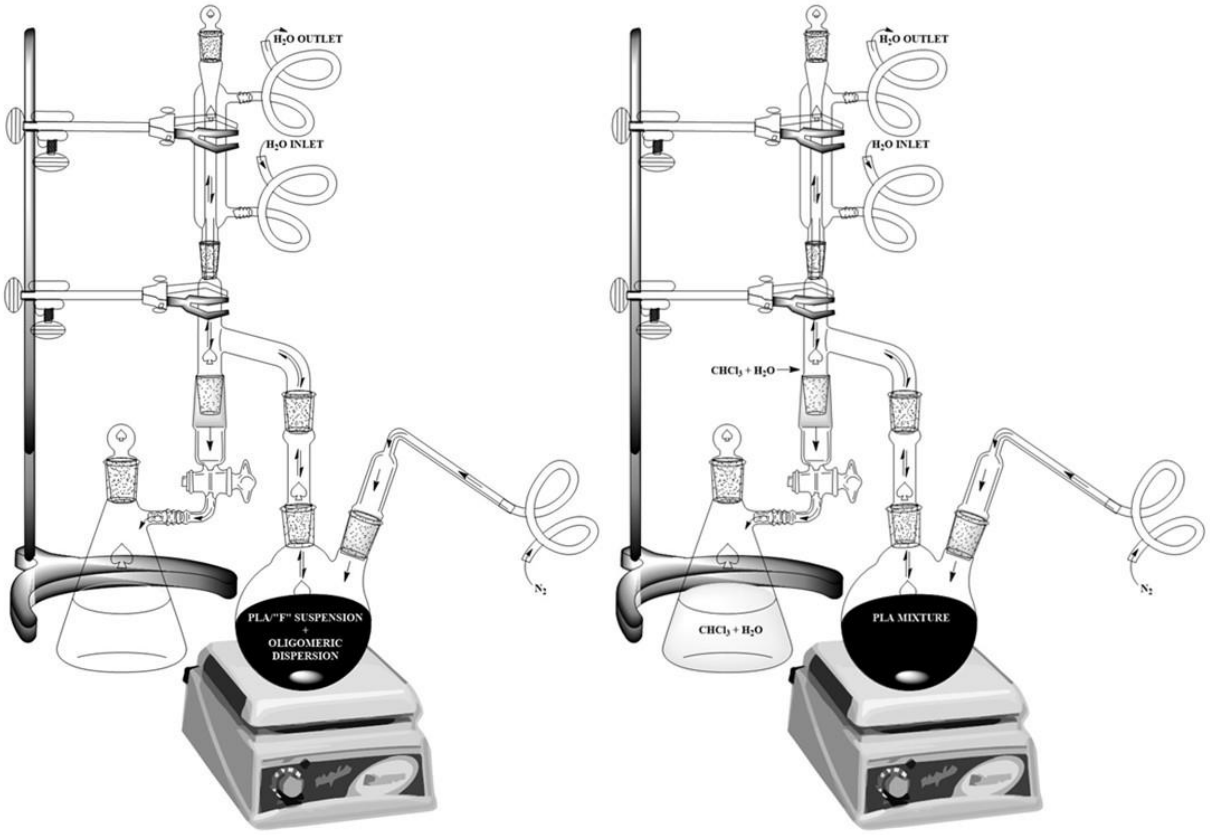

Figure 3.5: Preparation of PLA mixture

The thick sheet of poly (lactic acid) composites was passed through two roll mill and placed in a flash type mold with a metal plate frame and compressed in a single daylight press, pre-heated at 160°C, to melt and further cooled to mold. Mold temperature is an important parameter in molding operation, mold temperature was checked for as per the ASTM Practice 957. The compression molding assembly was also equipped with a cooling fixture to cool the flash type mold to fabricate a sheet with homogenous and isotropic nature in the form of a smooth sheet of uniform thickness. Weighed quantity of material (including 10% flash) for proper filling in the mold, in case of poly (lactic acid) granules even distribution on mold surface should be considered and for thick sheet in case of poly(lactic acid) composites, weight and the center position in mold cavity of the thick sheet is of prime importance.

Closure of the molding press and preheating by applying contact pressure for a minimum 5 minutes, thereafter, apply full pressure for 2 minutes. Preheating time, molding time, molding temperature, demolding temperature, and cooling rate were monitored while performing compression molding of poly (lactic acid) and poly (lactic acid) composites.

3.3 CHARACTERIZATIONS

3.3.1 CHARACTERIZATIONS FOR TESTING CELLULOSE NANOFIBERS

3.3.1.1 FOURIER TRANSFORM INFRARED SPECTROSCOPY – ATTENUATED TOTAL REFLECTANCE [FTIR – ATR]

3.3.1.2 DYNAMIC LIGHT SCATTERING

3.3.1.3 X RAY DIFFRACTION

3.3.1.4 THERMAL GRAVIMETRIC ANALYSIS

3.3.1.5 SCANNING ELECTRON MICROSCOPY

Tests listed for cellulose nanofibers were done to determine the quality of cellulose nanofibers synthesized using the materials and method mentioned in **Section 3.1.1 and 3.1.2**.

3.3.2 CHARACTERIZATIONS FOR TESTING POLY (LACTIC ACID) COMPOSITES

3.3.2.1 STRUCTURAL CHARACTERIZATION

3.3.2.1.1 ULTRAVIOLET – VISIBLE SPECTROSCOPY [UV – VIS]

Ultraviolet – Visible spectroscopy [UV – VIS] was part of pilot study. Wavelength range of 800nm to 250nm on UV-Visible Spectrophotometer (LAMBDA 650, Perkin Elmer) was used to characterize neat poly (lactic acid), fillers and filled poly (lactic acid) composites, to determine the dispersion and interphase characteristics of filled poly (lactic acid) composites. Ultra – Violet spectroscopy was performed on poly (lactic acid) composites and hybrid composites prepared by DD and OD, to understand the interphase characteristics, based on the absorbance. The test confirmed the process to be used for the main study.

3.3.2.1.2 FOURIER TRANSFORM INFRARED SPECTROSCOPY – ATTENUATED TOTAL REFLECTANCE [FTIR – ATR]

Infrared Spectroscopy helps in investigating the relationship existing between the structure of polymer composites and their structure sensitive properties by determining molecular interactions. Attenuated total reflectance Fourier transform infrared spectra were obtained using Shimadzu; IR Prestige 21 – ATR/FTIR [4000-500cm^{-1}] and were collected with a

resolution of 4cm^{-1} by co-addition of scans for each spectrum at room temperature. The IRsolution Agent software complied with FDA 21 CFR Part 11 regulation for Windows was used to manage the ATR/FTIR instrument. Results from preliminary study related to structural analysis was published in “Materials Performance and Characterization 8,no. 1 (2019): pp617–625. ASTM International Publishers”

3.3.2.2 PHYSICAL AND MECHANICAL CHARACTERIZATION

Physical and mechanical characterization were an integral part of the pilot study and the main study to determine the physical and mechanical aspects of poly (lactic acid) and hybrid composites. Results from preliminary study related to process selection are published in “Strength of Materials 51, no. 3 (2019): pp476 – 489. Springer”

3.3.2.2.1 RELATIVE DENSITY

Relative density for poly (lactic acid) sheets and poly (lactic acid) composites were characterized as per ASTMD 792 on 7 specimen on Shimadzu AUW220D, SMK 401. Relative density was used for the identification of polymers, tracking physical changes in polymer samples/ filled and reinforced composites. Theoretical density was calculated using **Equation 1**

$$dp, p = \frac{dc - dmf * Vmf}{1 - Vmf} \qquad Equation\ 1$$

where: *dp, p* is the density of the polymer, *dc* is the density of composite, *dmf* density of filler, *Vmf* volume fraction of filler

3.3.2.2.2 HARDNESS

Hardness measurements were performed on 5 specimen using Durometer Shore D, following ASTM D2240 using a GSE, SHR MARK III.

3.3.2.2.3 TENSILE TEST

Tensile yield strength and Tensile strength was performed on 10 specimen as per ASTM D638; with a strain rate of 50mm/min on a Type I specimen on Tinius Olsen, H25KL.

Elongation at Break was a derived result, obtained while performing tensile yield strength as per ASTM D638, on Type I specimen.

Theoretical values of Modulus (Young’s and Flexural) were calculated using [Einstein Equation] **Equation 2** and [Guth and Gold Equation] **Equation 3**

$$Ec = Ep\ (1 + 2.5Vmf) \qquad Equation\ 2$$

$$Ec = Ep\ (1 + 2.5Vmf + 14.1Vmf^2) \qquad Equation\ 3$$

where *Ec* is Modulus of composites, *Ep* is Modulus of polymer and *Vmf* is volume fraction of filler.

3.3.2.2.4 IMPACT TEST

Notch Izod impact was carried out on 10 specimen as per ASTM D256 on Hounsfield Impact Tester.

3.3.2.2.5 FLEXURAL TEST

Flexural strength and Flexural Modulus of poly (lactic acid) and poly (lactic acid) composites on 10 specimen were performed as per ASTMD 790 (Method 1, Procedure B), using MTS Criterion, 143.

3.3.2.2.6 HEAT DEFLECTION TEST

Heat deflection tests were performed on 5 test specimen as per ASTM D 648. The results obtained was compared to those applications that depict analogy similar to test conditions on Analogue 2 station VSP/HDT Apparatus – International Equipment.

3.3.2.3 MORPHOLOGICAL CHARACTERIZATION

Morphological characterizations are an integral part of the pilot study and main study which helped in corroborating the results of mechanical strength of poly (lactic acid) and hybrid composites. Results from preliminary study related to morphology was published in “Surfaces and Interfaces, 18 (2020) 100451 Elsevier”

Morphological characterizations were performed using microscopic instruments (using Optical Microscope, Scanning Electron Microscope, Transmission Electron Microscope, and Atomic Force Microscope).

Optical Microscopy [Polarized optical microscope of LEICA DMLP] and Scanning Electronic Microscopy [TESCAN VEGA 3SBH, at 30kV, with gold-palladium alloy coating with Quorum SC7620.] were performed on tensile fractured specimens in order to determine the microstructural features affecting mechanical properties.

Transmission Electron Microscopy [High-resolution transmission electron microscope of JEOL, JEM 2100] and Atomic Force Microscopy [APER-A-100 SPM] were performed to

evaluate effect of processing techniques on dispersion of carbon black, multiwalled carbon nanotubes, cellulose nanofibers carbon black + multiwalled carbon nanotubes and carbon black + cellulose nanofibers reinforcement in poly (lactic acid).

3.3.2.4 THERMAL CHARACTERIZATION

Thermal gravimetric analysis [TGA] was used to determine the thermal stability and decomposition characteristics of extracted nanocellulose fibers, i.e. decomposition temperature and residue. TGA was performed from 30℃ to 500℃, with a heating rate of 10℃/minute. Thermal characterizations forms part of main study.

3.3.2.5 ESTIMATION OF CONSTRAINED REGION

Estimation of constrained region forms a part of main study. Perkin Elmer DMA 8000 was used to characterize viscoelastic properties of poly (lactic acid) composites. Tan∂ curve obtained from dynamic mechanical analysis was used to determine the constrained regions. The viscoelastic measurements were carried out in temperature range of -50℃ to 75℃ in nitrogen atmosphere.

The constrained length in each sample can be estimated from the height of the tan delta peak.

Constrained region was calculated using **Equation 4, 5 and 6**:

$$W = \frac{\pi tan\delta}{\pi tan\delta + 1} \qquad Equation\ 4$$

$$W = \frac{(1 - Cv)W_0}{(1 - C_0)} \qquad Equation\ 5$$

$$Cv = 1 - \frac{(1 - C_0)W}{W_0} \qquad Equation\ 6$$

Where **Equation 4**, states the relationship between energy loss fraction (W) and tanδ, **Equation 5** is an expression for energy loss fraction (W) at the tanδ, is also known as "dynamic viscoelastic equation", Cv – volume fraction of constrained region, W_0 – energy fraction loss of the constrained region for neat poly (lactic acid), C_0 – volume fraction of the constrained region for neat poly (lactic acid).

3.3.2.6 STATISTICAL ANALYSIS OF MECHANICAL TEST

Numerical values of mechanical test were analyzed for descriptive and inferential statistics , particularly using the one way analysis of variance [ANOVA] on Origin 8.5. Multi-variate test was done to examine the pair wise differences in the various sample groups.

3.3.2.6.1 VALIDITY AND RELIABILITY

Effectiveness of any research depends on its ability of “not to” mislead its users. Features such as tools, methods and procedures of data collection, analysis and conclusion drawn accounts to the credibility of the research which is an important factor for validity of quantitative research design and experimental research strategy Internal validity was used to ensure accurate analysis of data, as internal validity allows precise conclusions and cause, and effect relationships within data. Therefore in this research study we have used ASTM standards and calibrated equipment for testing of specimens was used. Degree of reproducibility and repeatability was important. Similar numerical values of the mechanical strength within the study confirmed the repeatability of test.

Overall this chapter has detailed the research paradigm and experimental procedures adopted in this study. The subsequent chapters explain the results and discussions of the study, while highlighting the recommendations and directions of future research.

3.3.2.6.2 GRAPHICAL REPRESENTATIONS

All graphical representations in thesis are made using Origin 8.5. The mean value of the numerical data are used to represent the hardness, tensile test, flexural test, impact test, heat distortion test for poly (lactic acid) composites and hybrid composites.

3.3.2.6.3 SCHEMATIC REPRESENTATIONS

All schematic representation in thesis are made using Adobe Photoshop & Adobe Image Ready and Autodesk 3DS MAX 2017.

This chapter discussed the materials, processing techniques and characterizations involved with raw materials and poly (lactic acid) composites. Further **Chapter 4** discusses the pilot study carried out. Pilot study was conducted to confirm a processing technique for fabrication of poly (lactic acid) composites along with extraction technique of nanocellulose from kenaf fibers (which was later used in main study to fabricate nanocellulose filled poly (lactic acid) composites and hybrid filler poly (lactic acid) composites).

4 PROCESS TECHNIQUE SELECTION & EXTRACTION OF CELLULOSE NANOFIBERS

Process Technique Selection (section 4.1) of this chapter is published in “Strength of Materials 51, no. 3 (2019): pp476 – 489. Springer” and “Surfaces and Interfaces, 18 (2020) 100451 Elsevier”

4.1 PROCESS TECHNIQUE SELECTION

4.1.1 PHYSICAL AND MECHANICAL PROPERTIES AND MORPHOLOGICAL PROPERTIES

4.1.1.1 PHYSICAL AND MECHANICAL PROPERTIES

4.1.1.1.1 ABSTRACT

Carbon black filled poly (lactic acid) composites, has attracted significant interest in recent past due to their superior structural and functional applications. Properties of carbon black filled poly (lactic acid) composites depend on physical and chemical interactions within composites. Here, interactions within carbon black (N220) filled poly (lactic acid) composites as a function of processing method, filler concentration and its effect on mechanical properties were studied via physical, mechanical tests. Strong intermolecular interaction at an intermediate concentration of 2.5wt% carbon black with poly (lactic acid) was confirmed through the mechanical test. 2.5wt% of carbon black formed a connected network within poly (lactic acid) composites, these networks created resistance to fracture path in weaker phase thereby increasing mechanical properties. Beyond 2.5wt%, the linked skeletal grid was formed leading to easy fracture path in weaker phase and declined mechanical properties. Experimental results were compared with the theoretical model for density and modulus. This chapter gives an understanding of interactions emphasizing probable improvement and decrease in physical and mechanical property related to processing techniques and weight percent of carbon black in poly (lactic acid) composites.

4.1.1.1.2 DENSITY

Relative density for poly (lactic acid) sheets and carbon black filled poly (lactic acid) composites were characterized as per ASTMD 792. 7 specimens were tested, and the values were represented in **Figure 4.1**, with statistical significance of 95%. Relative density was used in the identification of polymers, tracking physical changes in polymer samples/ filled and reinforced composites and assuring product quality to suppliers and processors. Additive

curve differentiates theoretical and experimental density. The density of carbon black used was 1.7g/cm^3.

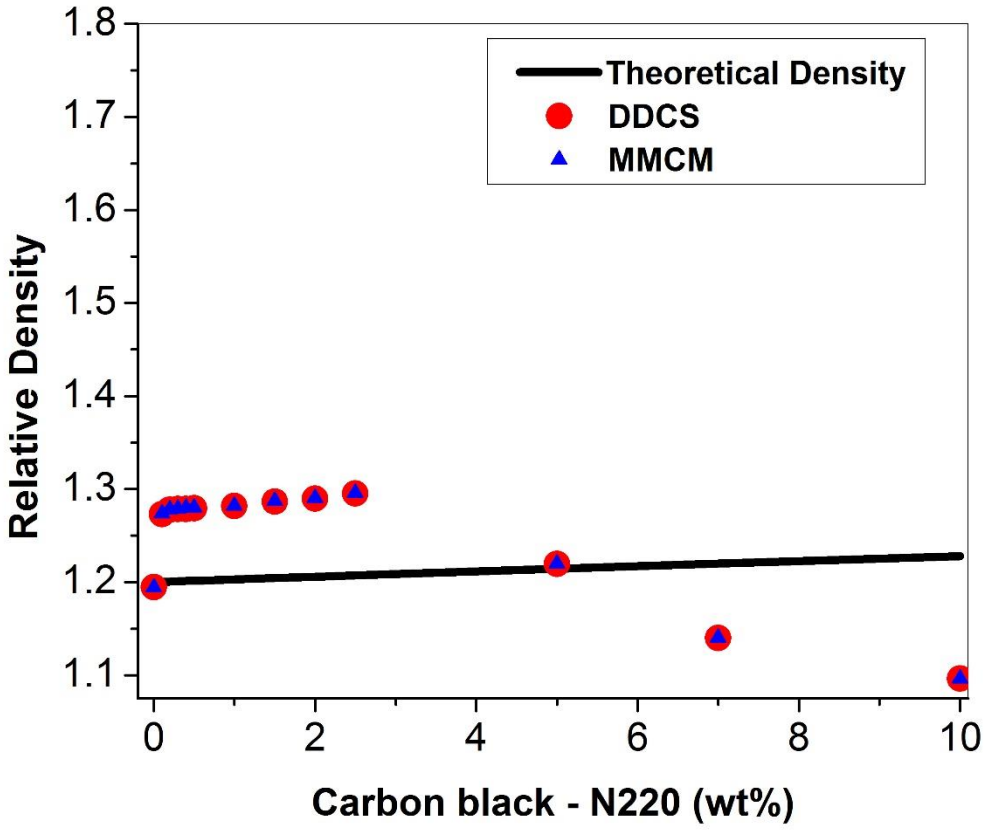

Figure 4.1: Effect of carbon black on the relative density of carbon black filled poly (lactic acid) composites (unit of measurement – g/cm^3)

For lower loading (till 2.5wt%) of carbon black in poly (lactic acid) matrix, experimental values were greater than theoretical values, indicating physical and chemical interaction between poly (lactic acid) chains and carbon black in poly (lactic acid) composites, thereby increasing density of the poly (lactic acid) filled carbon black composites. At 5wt% loading, theoretical value was almost similar to experimental value, following additive rule and above 5wt% experimental values are below additive curve, which confirms processing defects like voids and irregular dispersion of carbon black in poly (lactic acid) matrix, also carbon black particle-particle interaction affects maximum packing in poly (lactic acid) matrix which are factors responsible for the decrease in relative density values. Firstly uneven distribution of fillers and reinforcement/ filler and reinforcement's content in filled and reinforced polymer composites respectively varied the density of the composite. Secondly, air voids in polymer composites

also was a reason for variation in density which can related to the mixing method followed to incorporate fillers in the polymer matrix.

From the data in **Figure 4.1**, carbon black filled composites fabricated via melt mixing followed by compression molding (MMCM) showed slight increase in density compared to carbon black filled composites fabricated through dissolution dispersion method followed by casting sheet (DDCS). The slight increase in density for MMCM carbon black filled composites attributes to increase in poly (lactic acid) chains – carbon black aggregate chemical interaction, which reduces physical interaction between carbon black particles. In addition, size reduction of air voids due to hydraulic pressure of compression molding. The density of carbon black filled composites increases up to 2.5 weight percent (wt %) of carbon black, after which density decreases readily. The increase in density of carbon black filled composites (for MMCM and DDCS) up to 2.5wt% of carbon black can be related to void spaces of carbon black; void spaces are the areas between and around primary aggregates of carbon black. The carbon black used in the current work is N220, which is a low structure carbon black and hence possess less number of void spaces in comparison to high structure carbon blacks. Poly (lactic acid) chains migrate into the void spaces of carbon black, increasing adhesion between the phases [poly (lactic acid) and carbon black] and forms an interphase layer [surface of carbon black bears reactive functional groups which reacts with poly (lactic acid) chains to form an interphase layer], increase in wt%, of carbon black in poly (lactic acid) increases the number of interphase layers in the carbon filled composites, which in turn leads to an increase in density of carbon black filled poly (lactic acid) composites till 2.5wt% of carbon black loading. The decrease in density of carbon black filled composites (for MMCM and DDCS) at and after 5wt%, may be accounted to deficiency of poly (lactic acid) chains to cover void spaces in between carbon black during mixing process, (or in other words poly (lactic acid) chains becomes tightly bound) which increases the free volume (of filler) and on contrary decreases the density. It should be noted that poly (lactic acid) granules fabricated via dissolution show increase in density value, as compared to poly (lactic acid) granules fabricated via compression molding, this can be attributed to uneven distribution of poly (lactic acid) granules in the mold cavity, which gives rise to small size air voids [air entrapment between poly (lactic acid) granules in vicinity], throughout the surface of the molded sheet, leading to slight decrease in density of compression molded poly (lactic acid) sheet.[130][131]

4.1.1.1.3 HARDNESS

Hardness measurements were performed using Durometer Shore D, for 5 specimens following ASTM D2240. From the graph in **Figure 4.2,** it is clear that addition of carbon black at increasing weight percentages does not have any significant effect (but a slight effect) on the hardness of carbon black filled poly (lactic acid) composites. A slight increase in hardness for MMCM composites was observed which can be attributed to the formation of an interlayer i.e. interphase, as discussed in relative density.

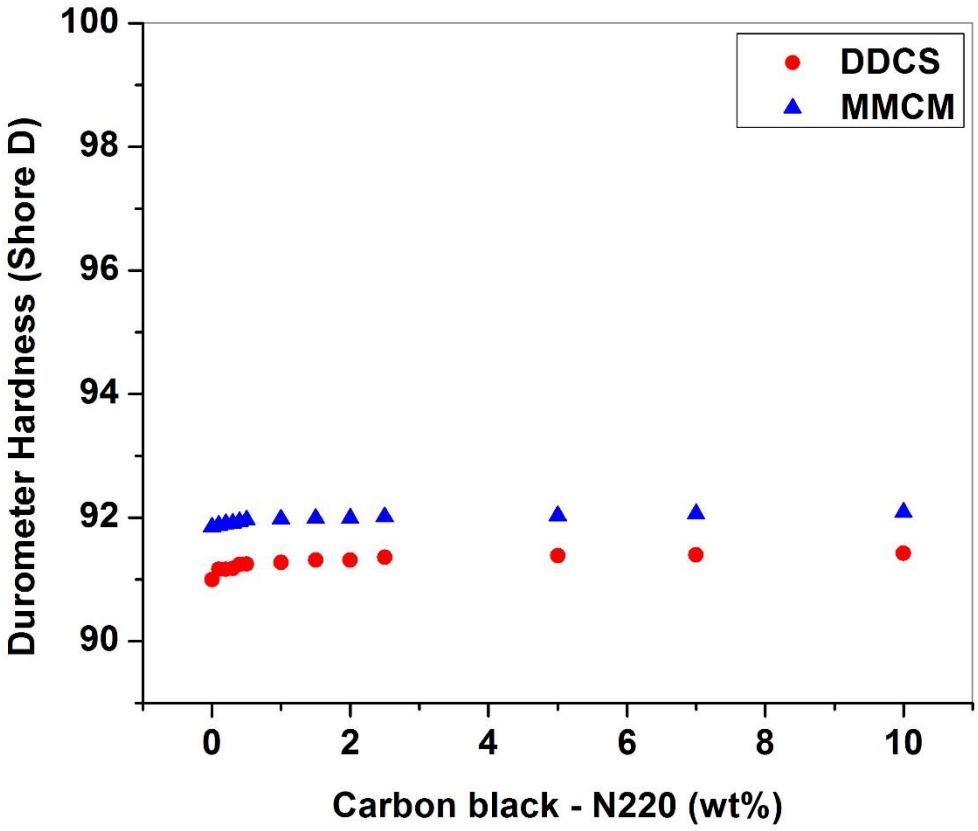

Figure 4.2: Effect of carbon black on the hardness of carbon black filled poly (lactic acid) composites

Secondly, in MMCM, a small increase in hardness value shall be due to the formation of physical crosslink's at an early stage during cooling, as physical crosslinks are responsible for reinforcement through crystallization, hence, in turn, increases the hardness of carbon black filled poly (lactic acid) composites fabricated via MMCM[131].

4.1.1.1.4 TENSILE TEST

4.1.1.1.4.1 STRESS STRAIN CURVES

Stress-Strain curves are extremely important graphical measures of materials mechanical properties i.e. the relation between stress and strain, material displays. **Figure 4.3 and 4.4** displays the comparison between stresses applied to the corresponding strain for MMCM and DDCS poly (lactic acid) composites. To have a brief insight into the material property we have compared neat PLA and PLA filled with 0.5wt%, 2.5wt% and 5.0wt% of carbon black in both cases, i.e. MMCM and DDCS. Stress-Strain curves may vary depending on the test condition and specimens.

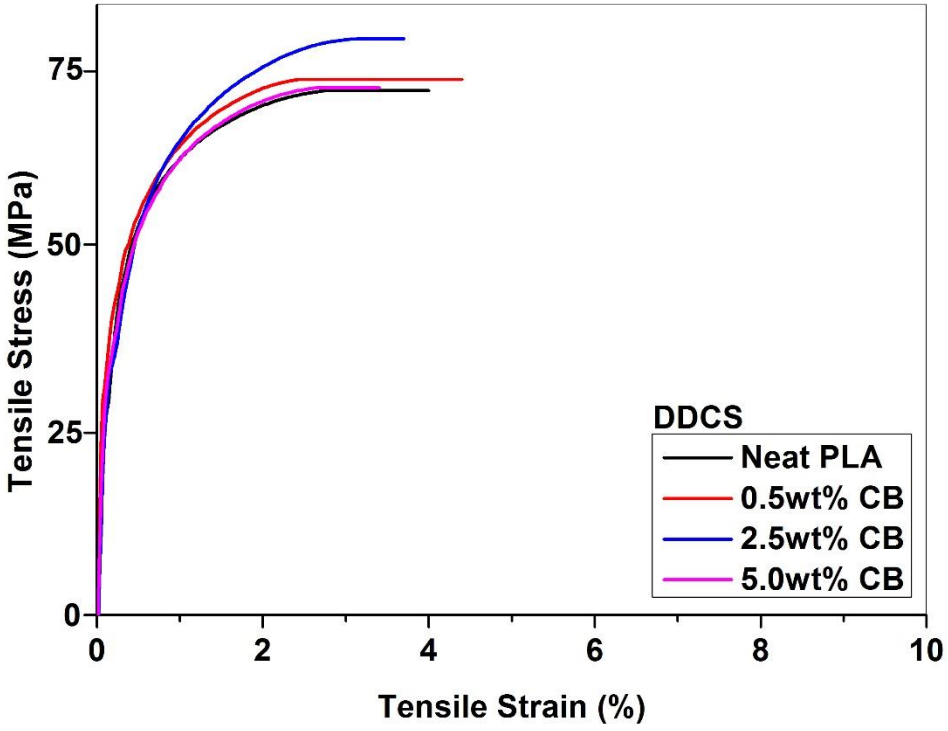

Figure 4.3: Stress-Strain Curve for DDCS poly (lactic acid) composites

From, the stress-strain curves **Figure 4.3** and **Figure 4.4**, for neat poly (lactic acid) and its composites via MMCM and DDCS, we confirm that poly (lactic acid) composites fabricated are of high strength in comparison to neat poly (lactic acid). It also confirms that composites fabricated via MMCM are of higher strength than that of DDCS. Stress-Strain curves also confirm the brittle character of the neat poly (lactic acid) and its composites, due to its inability to deform to a large extent under low stresses. In addition to its brittle nature poly (lactic acid)

and its carbon black filled composites also exhibits a slight deformation at high-stress levels, which confirms ductile behavior in poly (lactic acid) and its composites. This slight ductility shall be attributed to mechanics of a semi-crystalline polymer, which is discussed in tensile yield strength. Stress, deforming poly (lactic acid) and its composites are almost similar in MMCM and DDCS, the only difference is the shape of the curve on the stress-strain curve. The curve for MMCM looks more like inverted “L” whereas for DDCS is “C” shaped from the point of deformation. From stress-strain curve for DDCS and MMCM, at initial portions, mobility is locked due to microstructures that block dislocation motions and hence linearity is observed, but at high stresses, these mobility is unlocked, and dislocation motions rise due to which strain increases.

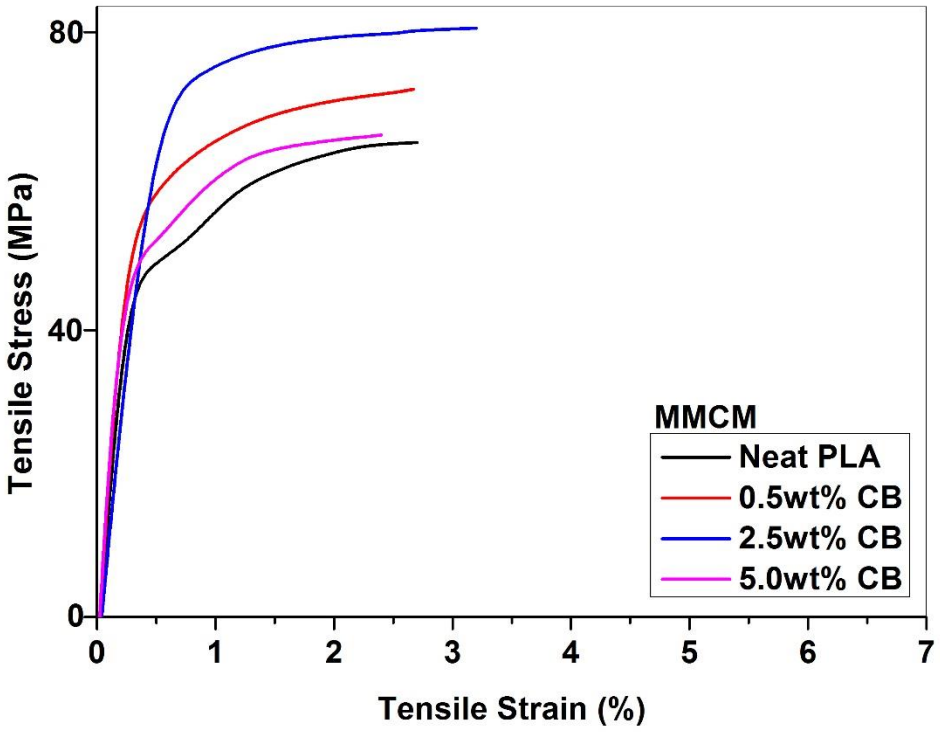

Figure 4.4: Stress-Strain Curve for MMCM poly (lactic acid) composites

The difference in shape for the stress-strain curve is due to the rate at which the material undergoes rearrangement from its initial molecular structure in which atoms are being moved to a new equilibrium position. For MMCM, the rate at which these rearrangements take place is slow, whereas rearrangement in case of DDCS is comparatively fast.

4.1.1.1.4.2 TENSILE YIELD STRENGTH

Tensile yield strength was performed as per ASTM D638; with a strain rate of 50mm/min on a Type I specimen for 10nos, and are represented in **Figure 4.5**. Tensile yield strength of the poly (lactic acid) composites discussed has the statistical significance of 95%. Poly (lactic acid) used in our study is semi-crystalline in nature, i.e. having both crystalline forms and amorphous regions in its bulk matrix.

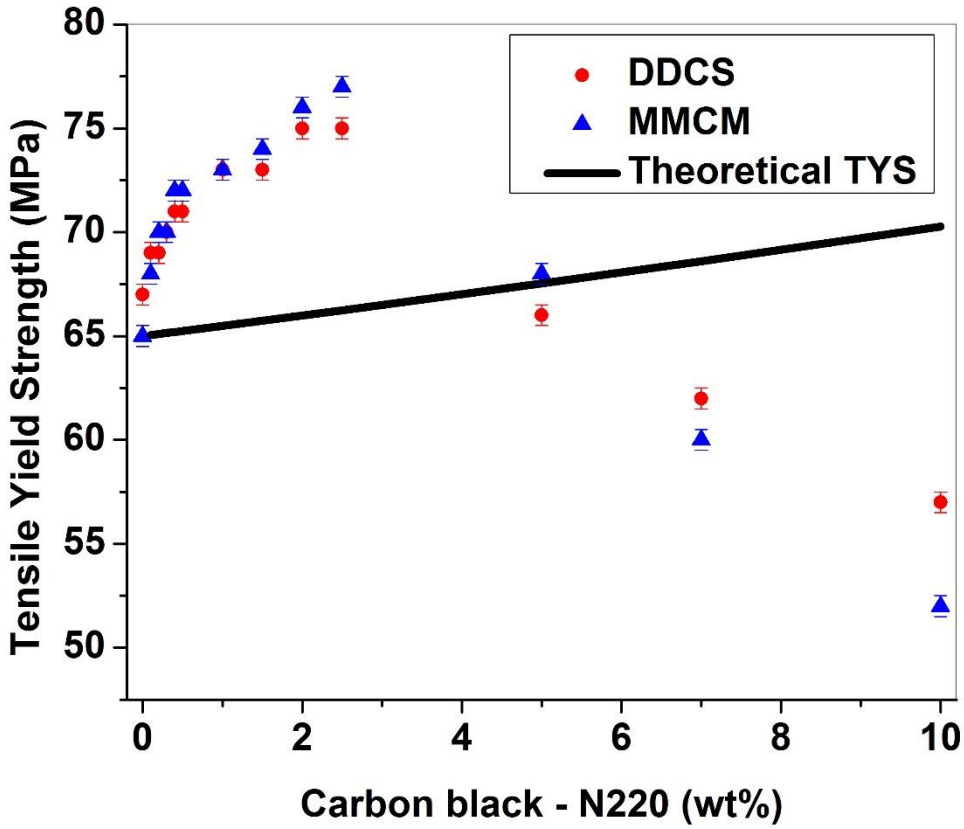

Figure 4.5: Effect of wt% of carbon black on the tensile yield strength of carbon black filled poly (lactic acid) composites

Rough estimation of cross-links through relative density measurements, is indicated in the section of "Relative Density", wherein changes in density of a specimen may be due to formation of interphase layers between carbon black surface and poly (lactic acid) chains, thereby inducing changes in crystallinity, i.e. as crystallinity in a material raises, density increases**.** Nature of carbon black, i.e. particle size, particle shape, interaction with poly (lactic acid), concentration, cohesion between poly (lactic acid) chains, carbon black aggregates, adhesion between poly (lactic acid) chains and carbon black aggregates are the parameters

which contributes to the increase or decrease in the tensile yield strength of the carbon black filled poly (lactic acid) composites. A primary particle of filler is the smallest structure of any filler, but in case of carbon black preformed aggregates are considered as primary structure. Physical and mechanical properties for carbon black filled polymer composites depends on the size of particles, aggregates and their distribution in the polymer matrix. Semi-crystalline thermoplastics like poly (lactic acid) exhibits different stages during its tensile deformation include lengthening of amorphous regions, rearrangement of crystalline regions, separation into blocks, lastly formation of microfibers. **Figure 4.5** indicates the comparison of tensile yield strength obtained theoretically and experimentally, it is well observed that experimental data points for carbon black loading (till 2.5wt %) are above the theoretical line indicating good physical force and chemical interaction between poly (lactic acid) chains and carbon black, in presence of mechanical interlocking of poly (lactic acid) chains. On contrary experimental data points for loading above 5wt% are below the theoretical line which indicates decrement in the tensile yield strength, which can be due to decrease in adhesive forces between poly (lactic acid) chains and carbon black surface, due to which an increase in carbon black physical network takes place, replacing the mechanical interlocking between poly (lactic acid) chains thus decreasing the tensile yield strength. Further, it is recorded that tensile yield strength for poly (lactic acid) granules fabricated by dissolution shows increased value as compared to poly (lactic acid) granules fabricated by compression molding. Increase in tensile yield strength may be due to “orientation crystallization” induced due to loose mechanical interlocking induced in poly (lactic acid) sheet fabricated by poly (lactic acid) dissolution; while in poly (lactic acid) compression molded sheet, poly (lactic acid) chains freeze or set at a relatively faster rate (cooling) due to which the molecules are unable to form loose interlocks, on contrary they form tight mechanical interlocks, i.e. induced crystallinity. Some of the poly (lactic acid) chains during cooling stage do not form entanglements, i.e. mechanical interlocking; so they pass through each other during stretching in tensile testing, leading to decrease in tensile yield strength for neat poly (lactic acid).

Air voids in the compression molded sheet may be due to uneven distribution of poly (lactic acid) granules in the cavity of the mold and might be a possible reason for the decrease in tensile yield strength. For carbon black filled poly (lactic acid) composites, at different carbon black loading, a change in an interaction mechanism is likely to occur. Interphase in poly (lactic acid) composites is responsible for changes in mechanical and physical properties of carbon black filled poly (lactic acid) composites, which contributes to improvement in mechanical reinforcement. Tensile yield strength for 0.1wt% carbon black filled poly (lactic

acid) composites fabricated via DDCS showed a slight increase compared to MMCM, which can be attributed to the similar reason as mentioned for neat poly (lactic acid) sheet fabricated via poly (lactic acid) dissolution and compression molding. A sharp increase in tensile yield strength for 0.1wt% carbon black was observed in carbon black filled poly (lactic acid) composites fabricated by DDCS and MMCM, is indicative of physical force and chemical interactions initiated by carbon black's surface groups with poly (lactic acid) matrix and within individual phases (i.e. crystallinity induced by carbon black). Tensile yield strength of carbon black filled poly (lactic acid) composites from 0.1wt% to 2.5wt% depicted an increasing trend for DDCS and MMCM fabricated poly (lactic acid) composites; the increase is due to interaction between poly (lactic acid) chains and carbon black aggregates, which is combination of a physical force and chemical interaction, contributing to reinforcement in carbon black filled poly (lactic acid) composites. Carbon black is para crystalline filler and its surface acts as a template for interface formation and enhances chemical interaction of surface groups with poly (lactic acid) chains, due to which strong interactions are formed between surface groups on carbon black and poly (lactic acid) chains. As, wt% of carbon black in poly (lactic acid) increases till 2.5wt%, chemical interaction in filled composite increases and composites materials improves much of their mechanical properties, as chemical interactions require higher energy to disrupt. In **Figure 4.5**, we observe that tensile yield strength remains similar at certain weight percentages which indicate that small increments of carbon black as filler in the poly (lactic acid) matrix, does not contribute much to the structural changes in interface and interphases within the poly (lactic acid) matrix in bulk. Further tensile yield strength for 0.2wt% to 5.0wt% carbon black filled poly (lactic acid) composites fabricated via MMCM showed slight increase in values compared to DDCS, this shall be attributed to migration of poly (lactic acid) chains into voids and pores of carbon black during melt mixing (at high shear rate), which increased the adhesion between poly (lactic acid) chains and carbon black surface groups, i.e. formation of chemical links via chemical interactions. For both the types of carbon black filled poly (lactic acid) composites (DDCS and MMCM) increase in tensile yield strength was recorded until 2.5wt% carbon black. For concentration 5.0wt% and above, a decrease in tensile yield strength value was observed due to insufficient mass of poly (lactic acid) chains to interact with carbon black's surface (groups and void space), due to which a continuous physically bonded filler network is formed which reduces the reinforcing effect of the carbon black in carbon black filled poly (lactic acid) composites[131][132][133].

4.1.1.1.4.3 ELONGATION AT BREAK

Elongation at Break is a derived result, obtained while performing tensile yield strength as per ASTM D638, on Type I specimen for 10nos, represented in **Figure 4.6**, elongation at break results discussed here have statistical significance similar to the tensile yield strength, i.e. 95%. It is usually a trend that, increases in tensile strength decreases elongation at break.

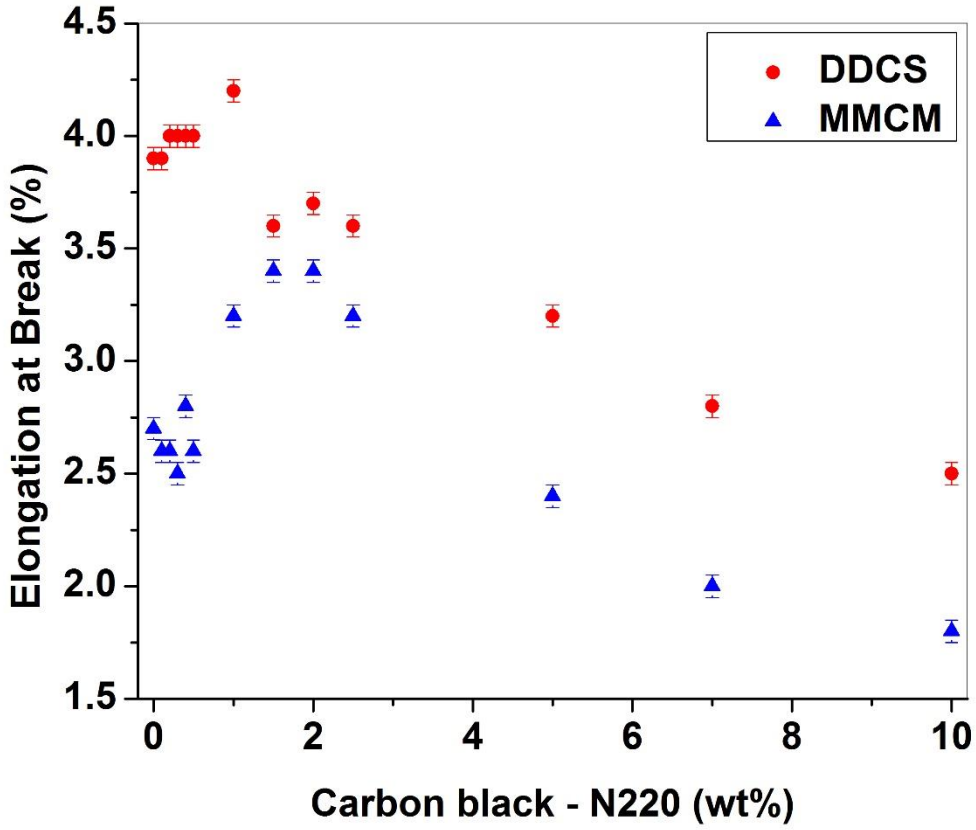

Figure 4.6: Effect of wt% of carbon black on elongation at break of carbon black filled poly (lactic acid) composites

Figure 4.6 represents elongation at break data for poly (lactic acid) and carbon black filled poly (lactic acid) composites. Chain mobility; responsible for elongation during tensile mode is controlled by the concentration of filler and their network forming ability, within the polymer matrix. Tensile elongation represents uncoiling and slippage between polymer chains and fillers. Lower values of elongation at break were observed for MMCM poly (lactic acid) composites, compared to DDCS, due to the fact that during cooling of the poly (lactic acid) melt, thermal energy associated with poly (lactic acid) chains decreases and molecular mobility of the poly (lactic acid) chains are arrested (i.e. crystallization of poly (lactic acid)

chains). Adhered layers of poly (lactic acid) chains with carbon black particles and aggregates behave differently from poly (lactic acid) in crystalline form due to the crystallization of poly (lactic acid) chains, which leads to alteration in tensile yield strength as well as elongation at break. Tensile elongation for poly (lactic acid) specimen and DDCS/MMCM poly (lactic acid) composites filled with 0.1wt% carbon black were similar. In DDCS poly (lactic acid) carbon black filled composites, an increase in elongation at break is observed until 1.0wt% of carbon black, after which a decreasing trend was observed. In MMCM poly (lactic acid) carbon black filled composites, an increase in tensile elongation was observed until 2.0wt% (although the numerical values were less as compared to DDCS). The increase in elongation at break can be attributed to the presence of very small carbon black particles that can act as local stress concentrates. The decrease in elongation at break can be due to the presence of large aggregates and strongly bonded clusters in poly (lactic acid) composites filled with a higher weight percentage of carbon black. The decrease in elongation at higher weight percentages of carbon black can also be attributed to rapid rupture of filler network in high loaded poly (lactic acid) solution. For DDCS composites, tensile elongation remains constant until 0.5wt% of carbon black and increases for 1.0wt%, further for 1.5wt% to 2.5wt% of carbon black; values of tensile elongation almost remains similar, in spite of increase in tensile yield strength which can be related with carbon black particles forming entanglement with poly (lactic acid) chains, and absorption of poly (lactic acid) chains on carbon black surface in composites. Considering the increasing trend for tensile yield strength for MMCM, with values of elongation at break, a resemblance of physical cross-linking is observed even if tensile elongation values are numerically lower than DDCS[131][133].

4.1.1.1.4.4 YOUNGS MODULUS

Young's modulus is a measure of stiffness in the initial part of tensile deformation. From, **Figure 4.7** we can observe that MMCM poly (lactic acid) composites possess an increase in stiffness. Also in both the cases for DDCM and MMCM poly (lactic acid) composites, as the weight percentage of carbon black increases, the rise in stiffness is observed. The reason behind the increase in stiffness of the poly (lactic acid) composites at higher loading of carbon black is the increase of density of polymer material along with a surface layer at filler-matrix interface, as molecular mobility of poly (lactic acid) chains and segments are reduced at such surface layers, i.e. harder layers. The formation of hard layers in MMCM poly (lactic acid) composites contributes to increased stiffness. Nanocellulose whiskers, reinforced poly (lactic

acid) matrix possessed Young's modulus of 427.27±19.32 Mpa at 2.5wt% [134] whereas in our present work at 2.5wt% of carbon black in poly (lactic acid) matrix possessed the value of 3825 and 4510 Mpa for DDCS and MMCM fabricated composites. The Einstein Equation fits well to experimental values as compared to Guth Equation (**see Figure 4.7**), where no experimental points meet theoretical line – possibly due to fact that Guth Equation is an expansion of Einstein Equation to account for the inter-particle interaction at higher filler loading whereas Einstein Equation is suitable for systems having spherical particles. For Einstein equation too, some of the experimental data points are above the theoretical line, which indicates increased reinforcement action in comparison to theoretical Einstein equation, this difference is due to the real contact surface between the two phases, as contact surface is greater than the predicted from a theoretical model[135][134].

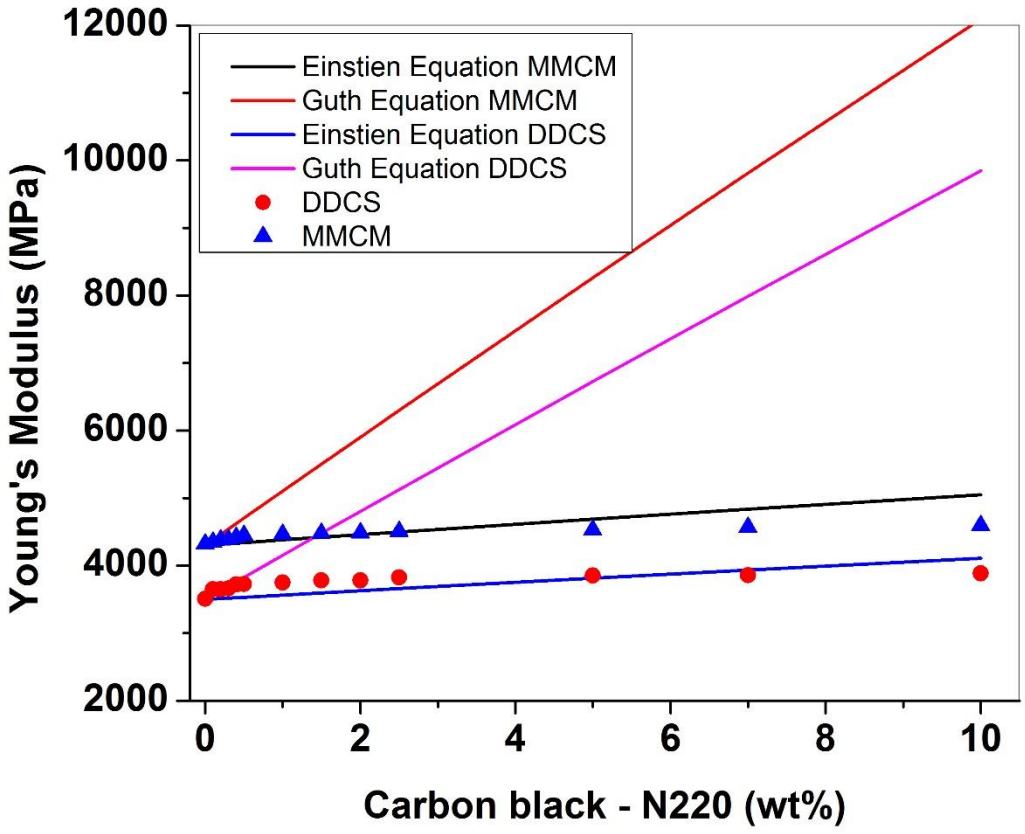

Figure 4.7: Effect of carbon black on Young Modulus of carbon black filled poly (lactic acid) composites and theoretical modeling for Young Modulus

4.1.1.1.5 NOTCHED IZOD IMPACT

Notch Izod impact was carried out as per ASTM D256, for 10nos, represented in **Figure 4.8**. Notched Izod impact values of the poly (lactic acid) composites discussed have the statistical significance of 95%. As mentioned in relative density, the increase in relative density can be directly related to the presence of interphase layers i.e. crystalline components in composites which confirms MMCM composites are slightly more crystalline than DDCS composites. **Figure 4.8** depicts MMCM composites to have high notched Izod impact values in comparison with DDCS composites, which confirm that a slight change in relative density (formation of interphase layers, i.e. crystalline component) in composites can have a huge difference in notched Izod impact values.

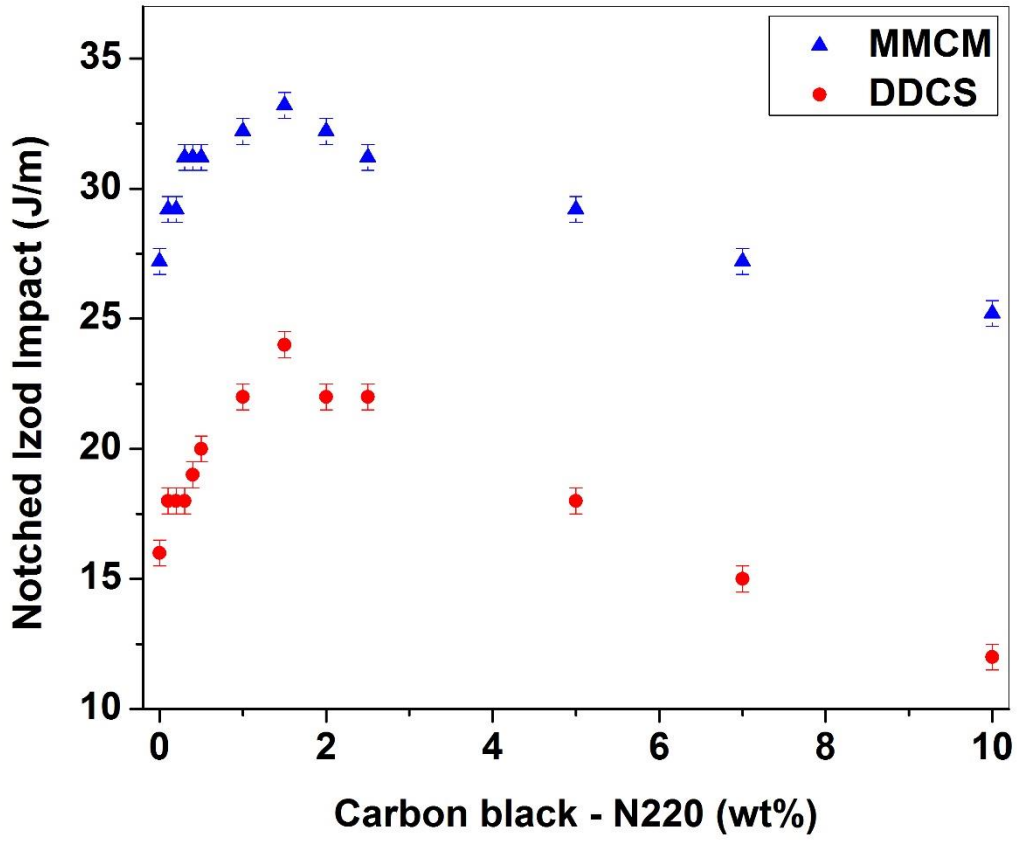

Figure 4.8: Effect of carbon black on notched Izod impact of carbon black filled poly (lactic acid) composites

Crystallinity via heterogeneous nucleation in MMCM composites can be introduced into poly (lactic acid) composites via carbon blacks and/or during the solidifying process on compression molding. Loading of carbon black as active filler till 1.5wt%, for MMCM and

DDCS composites increases notched Izod impact energy, for composites after 1.5wt% requires less energy to break the specimen. The reason for decrease in notched Izod impact energy after 1.5wt% attributes to optimum adhesion between poly (lactic acid) matrix and carbon black which constrains the poly (lactic acid) matrix at a greater extent and causes embrittlement in poly (lactic acid) composites; also particle bridging increases with high concentration of carbon black, which can be easily collapsed via impact forces. The increase in notched Izod impact for poly (lactic acid) composites till 1.5wt% of carbon black can be attributed to control over inter-particle distances, formation of agglomerates, and nucleation of carbon blacks (at low concentration) in poly (lactic acid) composites leading to increase in number of crystalline components in poly (lactic acid) matrix, which further contributes to increasing in notched Izod impact values[131][134][136].

4.1.1.1.6 FLEXURAL TEST

4.1.1.1.6.1 FLEXURAL STRENGTH

Flexural strength and Flexural Modulus of poly (lactic acid) and carbon black filled poly (lactic acid) composites were performed as per ASTMD 790 (Method 1, Procedure B) on 10nos and reported in **Figure 4.9 and 4.10** respectively. Flexural strength and Flexural Modulus of the poly (lactic acid) and carbon black filled composites discussed are considering statistical significance of 95%. Flexural strength, here is the ability of the poly (lactic acid) sheet and carbon black filled poly (lactic acid) composites to withstand bending forces applied perpendicular to its longitudinal axis. In work carried out by Jizhe wherein higher loading of $Bi_{0.5}$ $S_{4.5}$ Te_3 from 35.8 to 87.5wt%, gradually decreases flexural strength to 13.4 MPa from 50.1 Mpa, which corresponds to data reported herein, where a decrease in flexural strength is recorded beyond 2.5wt%.Carbon black in DDCS and MMCM composites contribute to stiffness in poly (lactic acid) composites as indicated by data in **Figure 4.9 and 4.10**. Flexural stiffness indicates resistance to bending during the flexural test. In the data represented in **Figure 4.9**, MMCM composites possess a lower value of flexural strength as compared to DDCS composites (exceptional to poly (lactic acid) composites with 10 weight percent of carbon black). The increase in flexural strength for DDCS composites contributes to “loose mechanical interlock chains of poly (lactic acid) chains” and few numbers of functional groups of carbon black forming chemical linkages with poly (lactic acid) chains and with functional group of carbon black in vicinity due to less energy in form of heat available while forming a sheet, wherein for MMCM energy during melt mixing as well as compression molding is sufficient enough to form chemical linkages between poly (lactic acid) chains and functional

groups of carbon black as well as between carbon black aggregates in vicinity and forms “tight mechanical interlocks within poly (lactic acid) chains”. Flexural strength increases as the weight percentage of carbon black in the poly (lactic acid) composites increases till 2.5wt%, for DDCS and MMCM composites, this increase in flexural strength values can be related to the probability of chemical linkages formed between surfaces of carbon black with poly (lactic acid) chains and between surfaces of carbon black in vicinity, also bridging between poly (lactic acid) chains and carbon black on a wide surface area contributes to increase. A decrease in flexural strength value is observed for DDCS and MMCM composites, at and after 5wt% which shall be due to unavailability of free poly (lactic acid) chains in composites, absence of mechanical interlocking between poly (lactic acid) chains, dissipation of local stresses by carbon black aggregates, leading to debonding between carbon black aggregates[133][137].

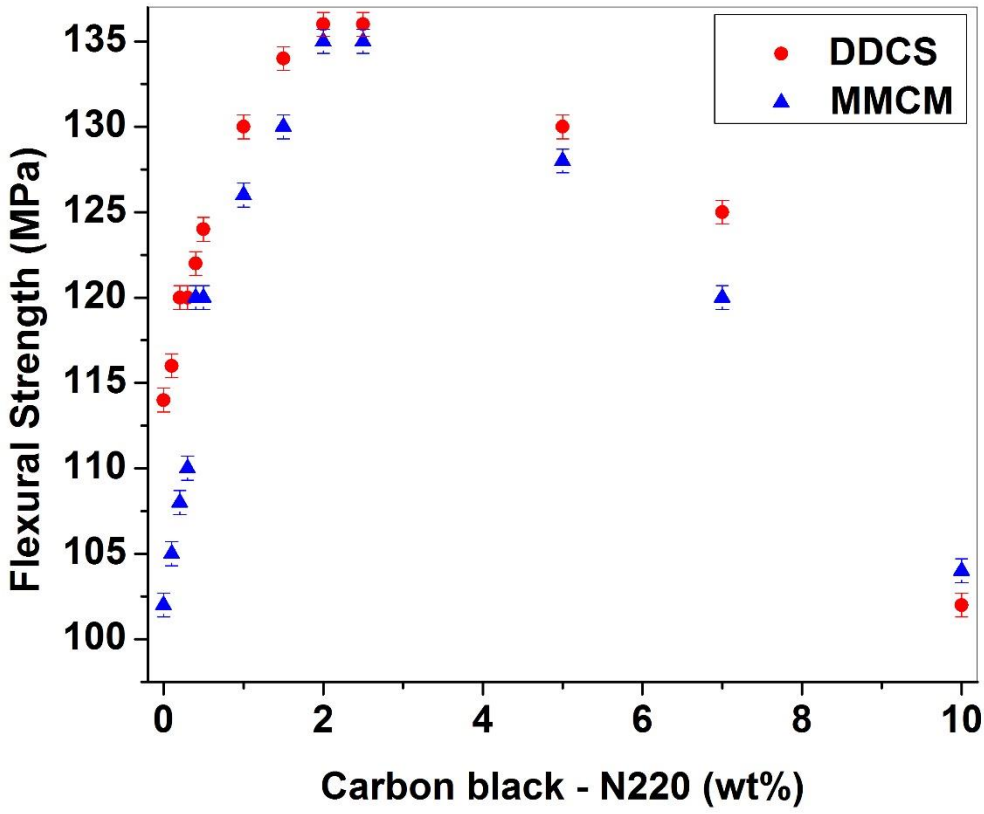

Figure 4.9: Effect of carbon black on Flexural strength of carbon black filled poly (lactic acid) composites

4.1.1.1.6.2 FLEXURAL MODULUS

Flexural modulus of the poly (lactic acid) and carbon black filled composites discussed are considering statistical significance of 95%. Flexural modulus, here is the measure of stiffness, during the initial part of the bending process in a flexural test. As mentioned in flexural strength, carbon black contributes to the stiffness of poly (lactic acid) composites. Unlike results for flexural strength (decrease at/after 5.0wt %), flexural modulus for DDCS and MMCM composites shows an increase in values as weight percentage of carbon black increases, which is in line with work carried out by Jizhe[138], in which as loading of $Bi_{0.5}$ $S_{4.5}$ Te_3 increases from 35.8 to 87.5wt%, flexural modulus gradually increases to 4379.8 MPa from 1684Mpa, which corresponds to data reported herein, where increase in flexural modulus is recorded as carbon black loading increases.

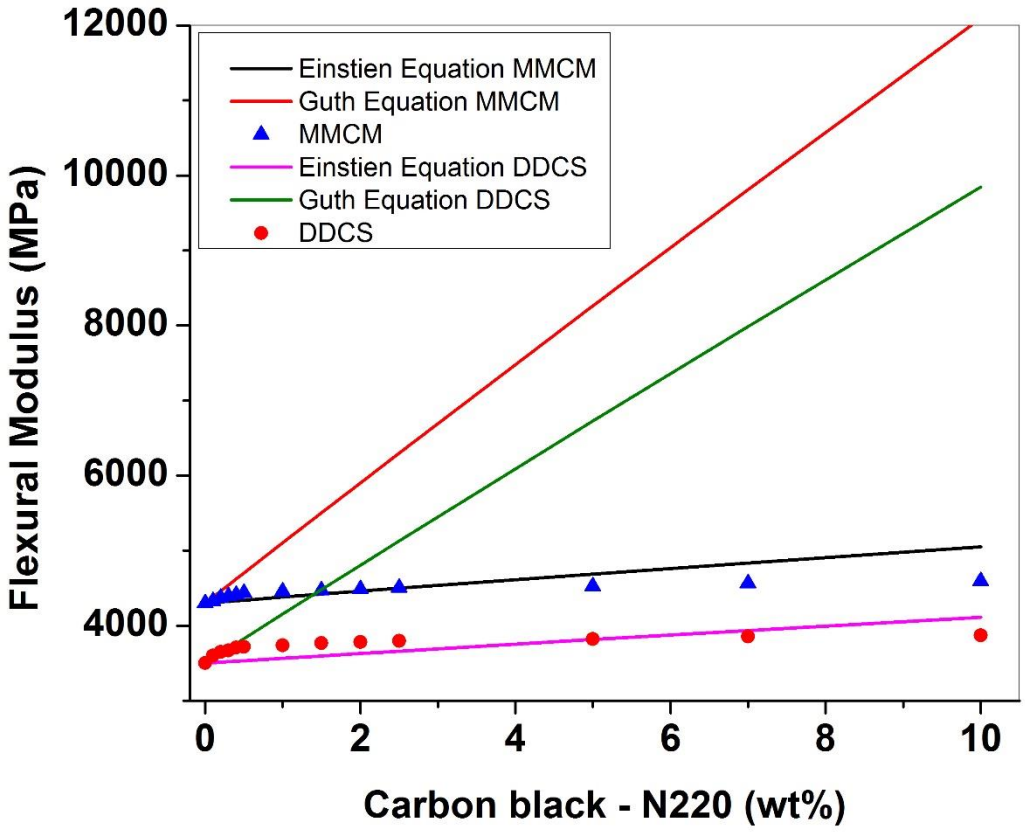

Figure 4.10: Effect of carbon black on Flexural Modulus of carbon black filled poly (lactic acid) composites and theoretical modeling for Flexural Modulus

Flexural modulus is result of combined properties of poly (lactic acid) chains network, poly (lactic acid) chains – carbon black interaction and carbon black – carbon black interaction

within poly (lactic acid) composites. At lower levels of carbon black, the interaction between poly (lactic acid) chains and carbon black are dominant and responsible for the rise in flexural modulus. At higher levels of carbon black, its carbon black – carbon black interaction, is dominant and contributes to the rise in flexural modulus. A carbon black aggregate forms a three-dimensional network, on carbon black – carbon black interaction and is a reason for reinforcement in poly (lactic acid) MMCM composites. The three-dimensional network formed is broken down during the flexural test, three-dimensional networks are enhanced in MMCM composites, hence at initial stages of bending, strength level increases and contribute to increased flexural modulus for MMCM composites. One may also observe that, the increase in flexural modulus for DDCS (numerical value lesser than MMCM) and MMCM composites as the weight percentage of carbon black raises, this can be attributed to similar facts of "poly (lactic acid) chains – carbon black interaction at lower levels of carbon black" and "formation of three dimensional networks and its breakage at higher levels of carbon black". As the percentage of carbon black increases probability of chemical interaction between the poly (lactic acid) chain and carbon black increases at lower levels of carbon black and formation of three-dimensional networks in poly (lactic acid) composites increases at a higher level of carbon black and in turn increases flexural modulus. Carbon black networks in poly (lactic acid) matrix contribute to strain energy due to which the increase in flexural modulus is observed. From theoretical modeling using Einstein Equation and Guth Equation the flexural modulus matches with Einstein Equation, for which reason has been already mentioned in the Tensile Test section[133][134][137].

4.1.1.1.7 HEAT DEFLECTION TEST

Heat deflection tests were performed on 5nos of test specimen as per ASTM D 648, reported in **Figure 4.11**. Heat deflection test is short term thermal test and their result should not be considered for selection of a material for a particular application. The results obtained can be compared to only those applications that depict analogy similar to test conditions. Thermal properties of plastics are equally important as mechanical properties, as plastics are extremely sensitive to change in temperature. Crystallinity (interphase layers) has a number of effects on the thermal properties of plastics. Intermolecular bonding between constituents of composite has an effect on thermal properties. Looking back at the data for "Relative density" we can conclude that interphase layers (i.e. crystalline components) in poly (lactic acid) matrix increases as wt%, for carbon black increases till 2.5wt%, also an increase in interphase layers (i.e. crystalline component) can be related to compression molding

technique. From **Figure 4.11**, it is clear that heat distortion temperature for MMCM poly (lactic acid) composites show increasing thermal stability as compared to DDCS poly (lactic acid) composites. This increase in thermal stability value for MMCM poly (lactic acid) composites can be attributed to tight mechanical interlocked poly (lactic acid) chains, as described in the tensile yield strength section. The tight mechanical interlocks between the poly (lactic acid) chains and chemical interactions of functional groups on carbon black surface with poly (lactic acid) chains as well as with other functional group on other carbon black at higher temperature during compression molding, contributes to formation of crystallites, via heterogeneous nucleation, within the poly (lactic acid) matrix and contributes to increase in thermal stability as compared to DDCS poly (lactic acid) composites.

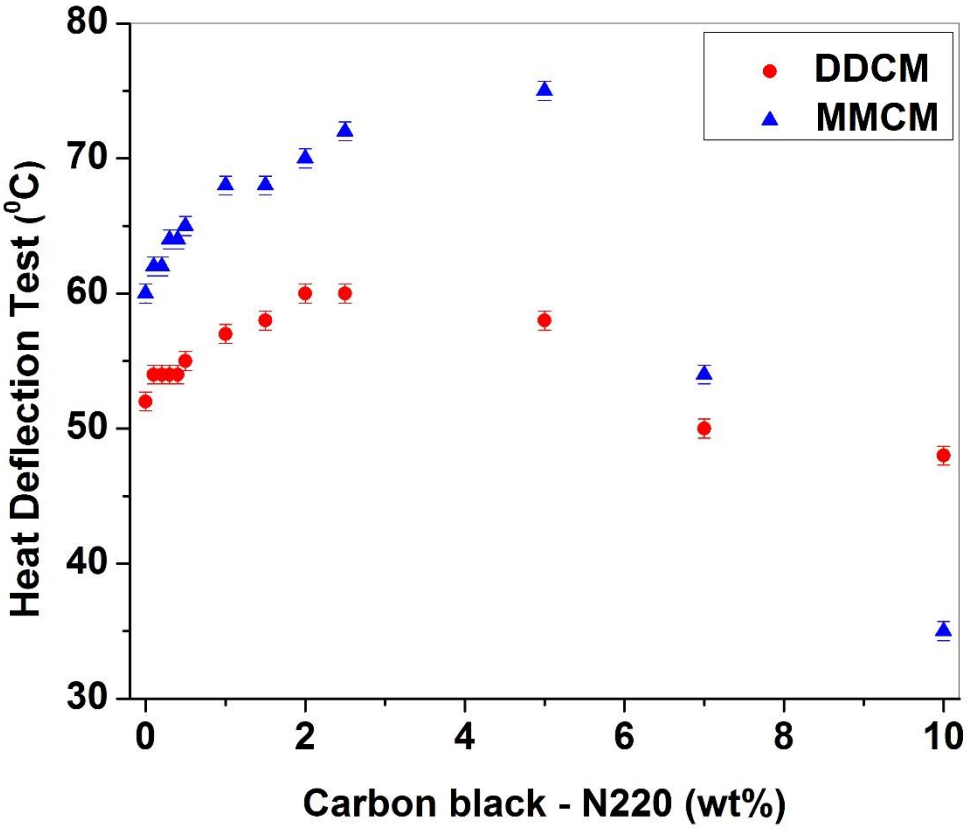

Figure 4.11: Effect of carbon black on heat deflection of carbon black filled poly (lactic acid) composites

The decrease in heat distortion temperature for DDCS poly (lactic acid) composites can be due to the presence of loosely interlocked chains, which tend to lose and segregate their loose mechanical networks due to heat-induced, a possible reason might also be due to physical reaction between carbon black and poly (lactic chains) due to insufficient heat

energy during mixing and curing. This weak physical interaction shall be overcome when a poly (lactic acid) composite absorbs heat from its surrounding media and leads to a decrease in heat distortion temperature for DDCS poly (lactic acid) composites. You shall also observe that as a weight percentage of carbon black increases to 2.5wt% in poly (lactic acid), there is an increase in heat deflection temperature. This can be related to thermal conductivity, thermal conductivity measured via heat deflection test for poly (lactic acid) is 52°C for solution cast and 60°C for compression molded sheet. The loading of carbon black in gradual amount increases the thermal conductivity of the poly (lactic acid) till 2.5wt% due to the network formed by carbon black as well as due to molecular restrictions of poly (lactic acid) chains in the vicinity of carbon black aggregate, after which decrease in value is observed. This decrease in heat deflection temperature after 2.5wt% i.e. at and after 5wt% of carbon black, can be due to distribution of thermal energy absorbed by carbon black within the poly (lactic acid) matrix, which distorts the specimen at an early temperature as compared to formulations, where carbon black loading is below 5wt%, other possible reason can be dissipation of local stresses due to indentor, which is carried out by carbon black aggregates, due to unavailability of free poly (lactic acid) chains and leading to debonding between carbon black aggregates[139][140].

4.1.1.2 CONCLUSION

Distribution and Dispersion can be monitored and controlled by identifying the right processing method for a specified set of properties. In current work, MMCM processed poly (lactic acid) composites possessed slightly higher values of mechanical strength in comparison to DDCS processed poly (lactic acid) composites. Almost all mechanical properties, including relative density (a physical property) for DDCS and MMCM poly (lactic acid) composites, decreased at 5wt% and beyond, exceptionally only hardness, Young's modulus, and flexural modulus increased as weight percentage of carbon black loading increased in poly (lactic acid) matrix (numerical value for MMCM composites were high). Tensile yield strength values for DDCS and MMCM were similar, while elongation at break for MMCM decreased due to chain immobility. Theoretical prediction for modulus using the Einstein equation gave a fit with experimental values. Notched Izod impact values were higher for MMCM composites. Flexural strength for DDCDS and MMCM poly (lactic acid) composites for all weight percentages of carbon black were almost similar. 2.5wt% of carbon black forms connected network within poly (lactic acid) composites and creates resistance to fracture path in weaker phase thereby increasing mechanical strength. Carbon black beyond

2.5wt%, forms linked skeletal grid facilitating fracture path in weaker phase and decreasing mechanical strength.

4.1.1.3 MORPHOLOGICAL PROPERTIES

4.1.1.3.1 ABSTRACT

The interrelation between microstructure and macroscopic behavior is important information, which is used to characterize generally inhomogeneity, orientations, distributions; ultimately its structure relationship with specific properties. Carbon black (N220) filled poly (lactic acid) composites were processed by using melt mixing (i.e. **MMCM** – **M**elt **M**ixing followed by **C**ompression **M**olding) and solution mixing technique (i.e. **DDCS** – **D**issolution **D**ispersion followed by **C**asting **S**heet.

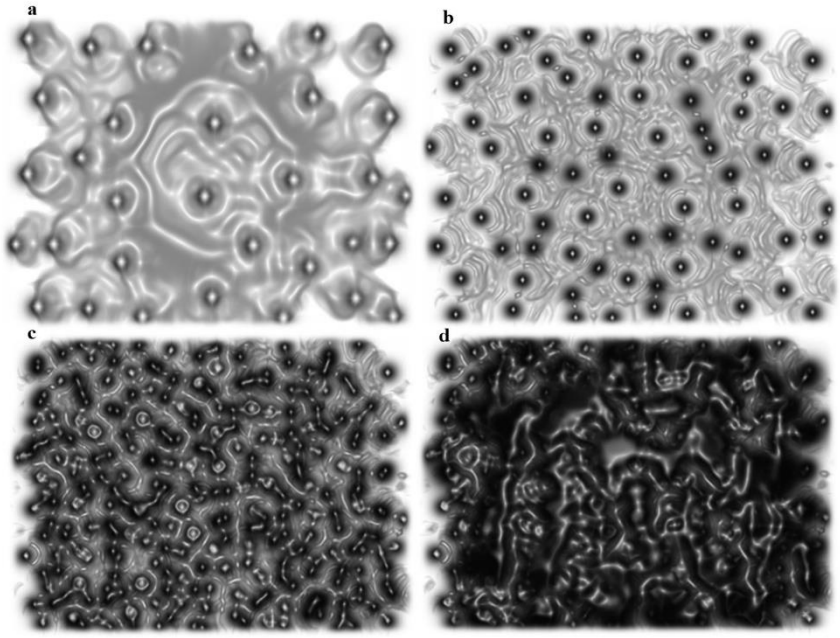

Figure 4.12: Carbon black particles dispersed in poly (lactic acid) matrix at (a) 0.5wt% (b) 1.5wt% (c) 2.5wt% and (d) 10.0wt% (black color indicates carbon black particles and rest as poly (lactic acid) matrix)

Carbon black filled poly (lactic acid) composites were characterized for microscopic – structural analysis and compared with mechanical properties. Microstructural analysis on tensile fractured specimens by optical microscope and scanning electron microscope was done in order to determine the microstructural features affecting mechanical properties; transmission electron microscopy and atomic force microscopy were performed to evaluate the effect of processing techniques on the dispersion of carbon black nanoparticles reinforcement in poly (lactic acid). The analysis of the mechanical properties showed an

increase up to the loading of 2-3 weight percent of carbon black followed by a decrease in mechanical properties at 5 weight percent and above due to microstructural changes induced by low structure carbon black in the poly (lactic acid) matrix. The dominance of filler-filler interaction beyond 2.5wt% was clearly visible in optical, electron and atomic force microscopic studies. The appearance of smooth and rough surfaces in optical and scanning electron microscopic images, presence of agglomerated carbon black in transmission electron microscopic images and the decrease in average roughness analyzed via atomic force microscopic images indicates microstructural changes in poly (lactic acid) after addition of carbon black. The filler-filler interaction as imaged and recorded from the transmission electron images and atomic force microscopic roughness values was the cause for a decrease in mechanical properties of carbon black filled poly (lactic acid) composites at 5.0wt% and beyond.

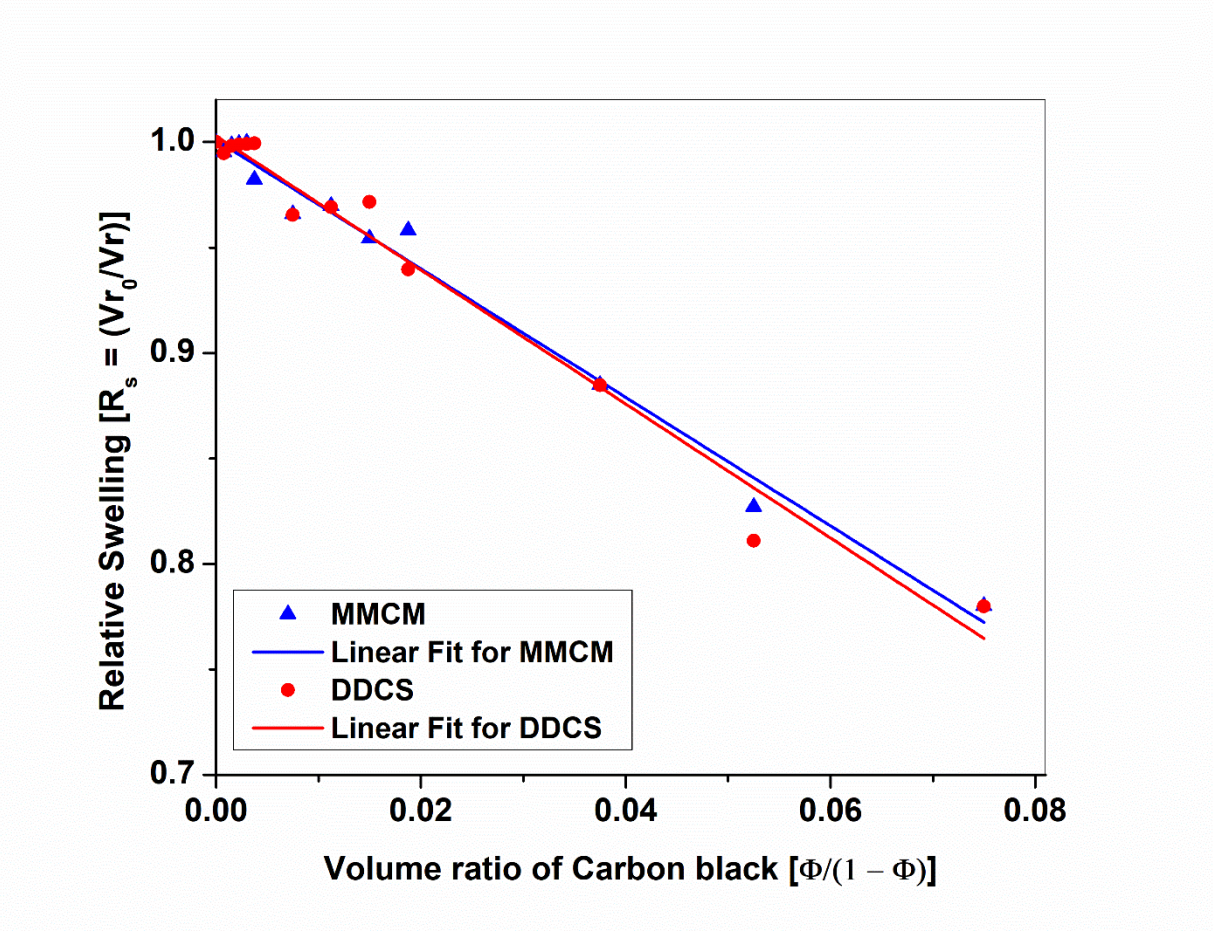

Figure 4.13: Relative Swelling – Kraus Plot

4.1.1.3.2 OPTIMIZING ACTIVE FILLER CONCENTRATION FOR CARBON BLACK IN POLY (LACTIC ACID)

To be sure about the interactions (i.e. physical and chemical) within carbon black filled poly (lactic acid) composites, a minor but an informative study, i.e. to determine active filler concentration in poly (lactic acid) matrix was carried out considering chemistry of alkaline hydrolysis of ester bonds in poly (lactic acid). The experiment was performed on a 2mm thick sheet at room temperature for a period of 15 days. The neat poly (lactic acid) and carbon black filled poly (lactic acid) were dipped in 5wt% sodium hydroxide aqueous solution and change in the physical appearance of specimen and their weights were monitored for a period of 15 days. Neat poly (lactic acid) started to disintegrate after a week's time, which can be attributed to alkaline hydrolysis of the ester bonds in poly (lactic acid), whereas carbon black filled poly (lactic acid) composites (filled with 2.5wt% of carbon black) remained stable (without any disintegration) till the end of experiment. For carbon black loading 5wt% and above; the carbon black started to leach out of the filled composites, which shall be attributed to weak physical interaction within carbon black aggregates also carbon black loosely bonded with poly (lactic acid) chains. Cracks and pieces were observed and till end of experiment. Hence through this experiment, determination of active filler loading (i.e. 2.5wt %) could be estimated.

Figure 4.12a, 4.12b, 4.12c, and 4.12d represents the proposed microstructure of carbon black and poly (lactic acid) at 0.5, 1.5, 2.5 and 10.0wt% of carbon black respectively. One can observe that carbon black aggregates are well dispersed at lower concentration of 0.5 and 1.5wt% with enough space in poly (lactic acid) matrix which are not subjected to interactions with filler (**Figure 4.12a and 4.12b**), while at 2.5wt% a network structure of carbon black with poly (lactic acid) matrix leads to increase in mechanical properties (**Figure 4.12c**). At 10wt% (**Figure 4.12d**) of carbon black in poly (lactic acid) matrix – interaction between poly (lactic acid) chains and carbon black aggregates decreases and physical network between carbon black aggregates increases and dominates within the composites system, due to which decrease in mechanical properties takes place[1].

4.1.1.3.3 UNDERSTANDING POLY (LACTIC ACID) CARBON BLACK INTERACTIONS VIA THE CONCEPT OF BOUND PLA – SWELLING CHARACTERISTICS

The concept of bound poly (lactic acid) here signifies the amount of carbon black which is not extracted by alkali solution from a carbon black filled poly (lactic acid) composites. This experiment was performed on a 5mm thick sheet at room temperature and was monitored for

48 hours. The test results can be considered as measure of poly (lactic acid) reinforcement by carbon black as well as of carbon black activity towards poly (lactic acid) which determines the mechanical strength of the poly (lactic acid) composites with varied concentration of carbon black. To be more precise, about interactions between carbon black and poly (lactic acid) at various loadings in DDCS and MMCM, relative swelling versus volume ratio was calculated and represented in **Figure 4.13**. The decrease in relative swelling was observed, as filler loading increased, this falling trend can be attributed to decrease in free poly (lactic acid) chains in carbon black filled composites. The extent of physical and chemical interactions within neat poly (lactic acid) and poly (lactic acid) composites [carbon black – carbon black, poly (lactic acid) and carbon black, poly (lactic acid) – poly (lactic acid)] can be correlated with values of relative swelling. Kraus plot in **Figure 4.13** confirms a strong physical force and chemical interaction between poly (lactic acid) chains and carbon black till 2.5wt% concentration both in MMCM and DDCS due to which relative swelling decreases; and can be attributed to strong interfacial adhesion, i.e. formation of strong adsorption layers between poly (lactic acid) chains and surface of carbon black which further contributes to increment in mechanical strength. A further decrease in relative swelling beyond 2.5wt% should not be attributed to strong interfacial adhesion between poly (lactic acid) chains and carbon black but can be attributed to the formation of weak interactions between poly (lactic acid) chains and carbon black and thus forms physical network of carbon black chains (weak bonds) which dominates over poly (lactic acid) – carbon black interaction, due to which solvent absorption decreases due to inability of carbon black network to absorb alkali solution; weak interactions between poly (lactic acid) chains and carbon black along with low strengthened network of carbon black within poly (lactic acid) composites decreases the mechanical strength[1][141].

4.1.1.3.4 DISPERSION CHARACTERISTICS

4.1.1.3.5 TRANSMISSION ELECTRON MICROSCOPY

Transmission electron microscopy on ultra-microtomed specimens for both types of poly (lactic acid) sheets (compression molded, and dissolution cast granules) and carbon black filled poly (lactic acid) (i.e. for DDCS and MMCM) were observed, to determine basic data on dispersion characteristics of carbon black within poly (lactic acid) matrix in poly (lactic acid)/ carbon black composites (**Figure 4.14**). It is clearly observed from the TEM images, that dispersion of carbon black is close to homogenous for MMCM poly (lactic acid) composites but large-scale extent of distribution is seen in DDCS poly (lactic acid) composites for loading

5wt% and 10wt%(i.e. for high loadings). For low loadings of carbon black, i.e. 2.5wt%, 1.5wt%, and 0.2wt% dispersion and extent of distribution for MMCM and DDCS are almost similar, but it is close to homogenous in 2.5wt%, which contributes to rising in mechanical properties.

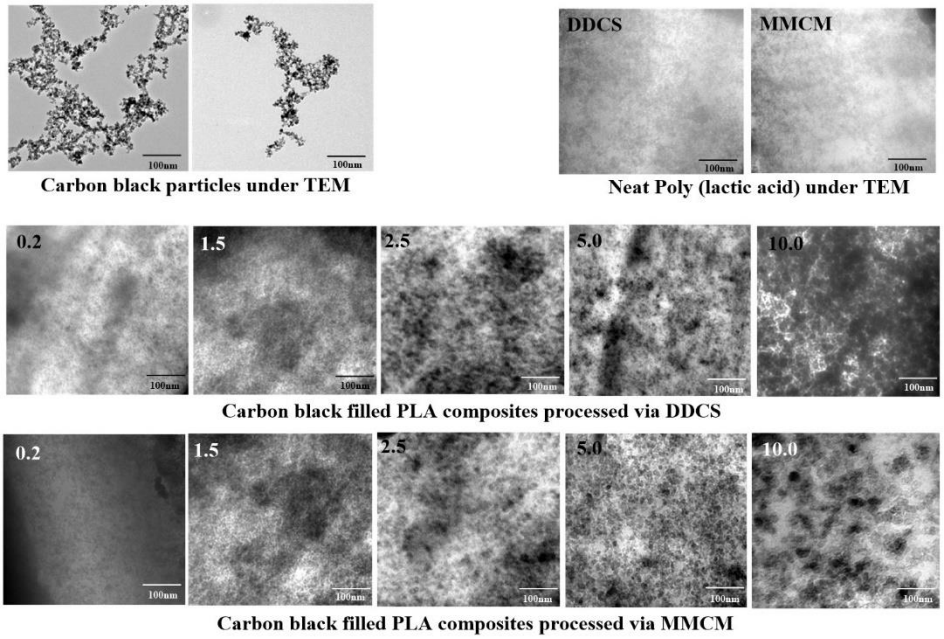

Figure 4.14: Transmission electron microscopic images for carbon black, ultra-microtomed specimens of poly (lactic acid) and carbon black filled poly (lactic acid) composites

Higher loading of carbon black in poly (lactic acid) disturbs the distribution of carbon black within poly (lactic acid) matrix and hence leads to formation of carbon black agglomerates in poly (lactic acid) matrix and acts as a point of high stress concentration which further leads to decrease in mechanical properties of carbon black filled poly (lactic acid). The purpose of imaging neat poly (lactic acid) sheets and carbon black dispersion was done to have a brief comparison and understanding of structures within carbon black filled poly (lactic acid) composites, has networked structures are observed for carbon black particles, these networks forming ability of carbon black along with poly (lactic acid) matrix increases the mechanical strength of carbon black filled poly (lactic acid) composites till 2.5wt%. From **Figure 4.14**, it is clear that as weight percentage of carbon black in poly (lactic acid) increases, agglomeration of carbon aggregates and particles increases correlate to observation by X.Wen et al[142].

Figure 4.15 describes the dependence of particle size with respect to concentration of carbon black in poly (lactic acid) composites. After careful observation from **Figure 4.15**, it is confirmed that melt mixing due to its high shear is capable of reducing the carbon black

agglomerate in comparison to dissolution dispersion solution casting, owing to which tensile yield strength increases till 5.0wt% of carbon black. Tensile yield strength for DDCS poly (lactic acid) composites increases in comparison to MMCM poly (lactic acid) composites at carbon black concentration above 5.0wt%, which can be attributed to large scale extent of distribution, and should not be confused with dispersion.

The agglomeration of carbon black in poly (lactic acid) composites at higher weight percentages (in MMCM and DDCS) shall be due to dominance of particle-particle interaction overcoming particle – polymer interaction due to which mechanical strength decreases[1][142].

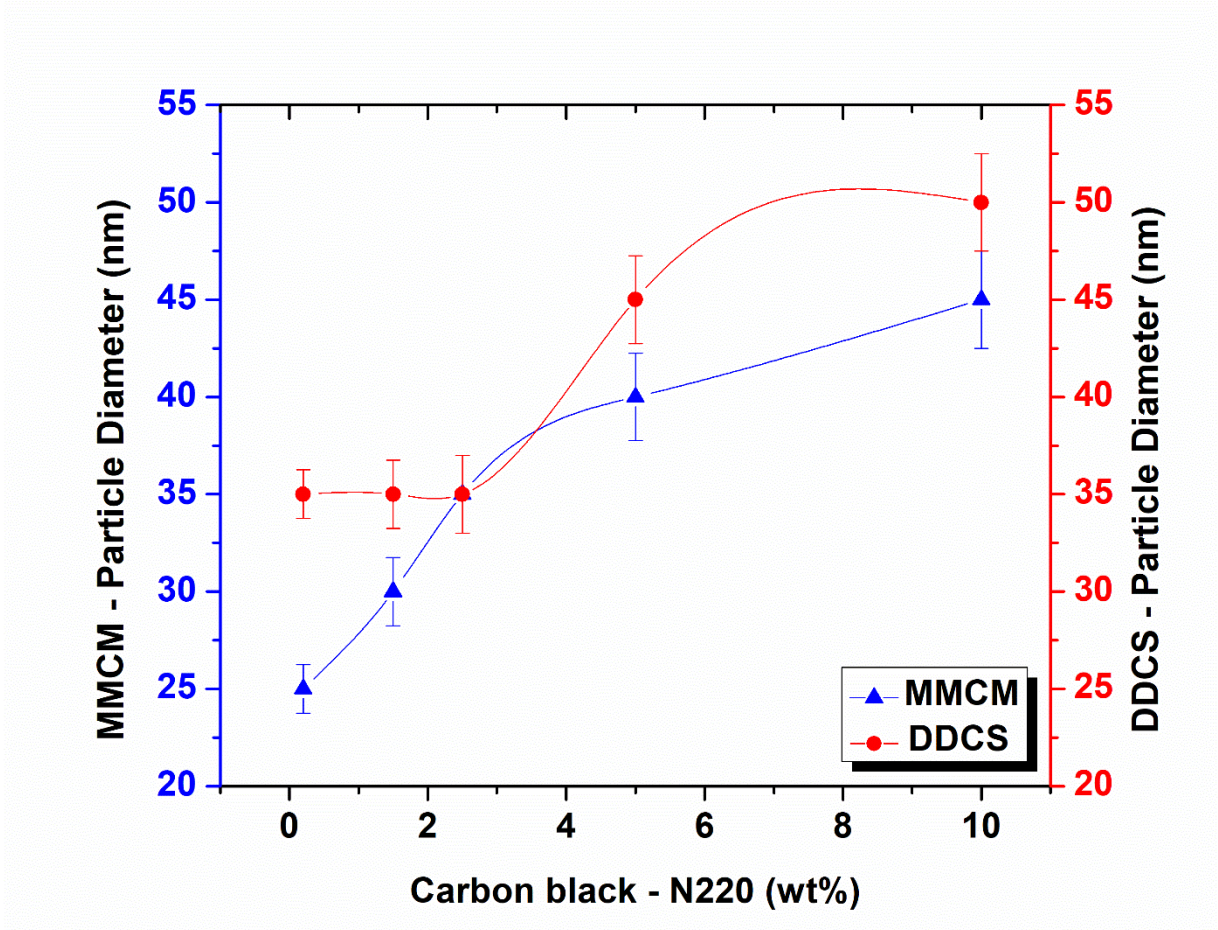

Figure 4.15: : Particle size distribution in transmission electron microscopic images for carbon black filled poly (lactic acid) composites. (0.2 wt %, 1.5 wt %, 2.5 wt %, 5.0 wt % and 10.0wt %) (Particle size was determined using ImageJ Software)

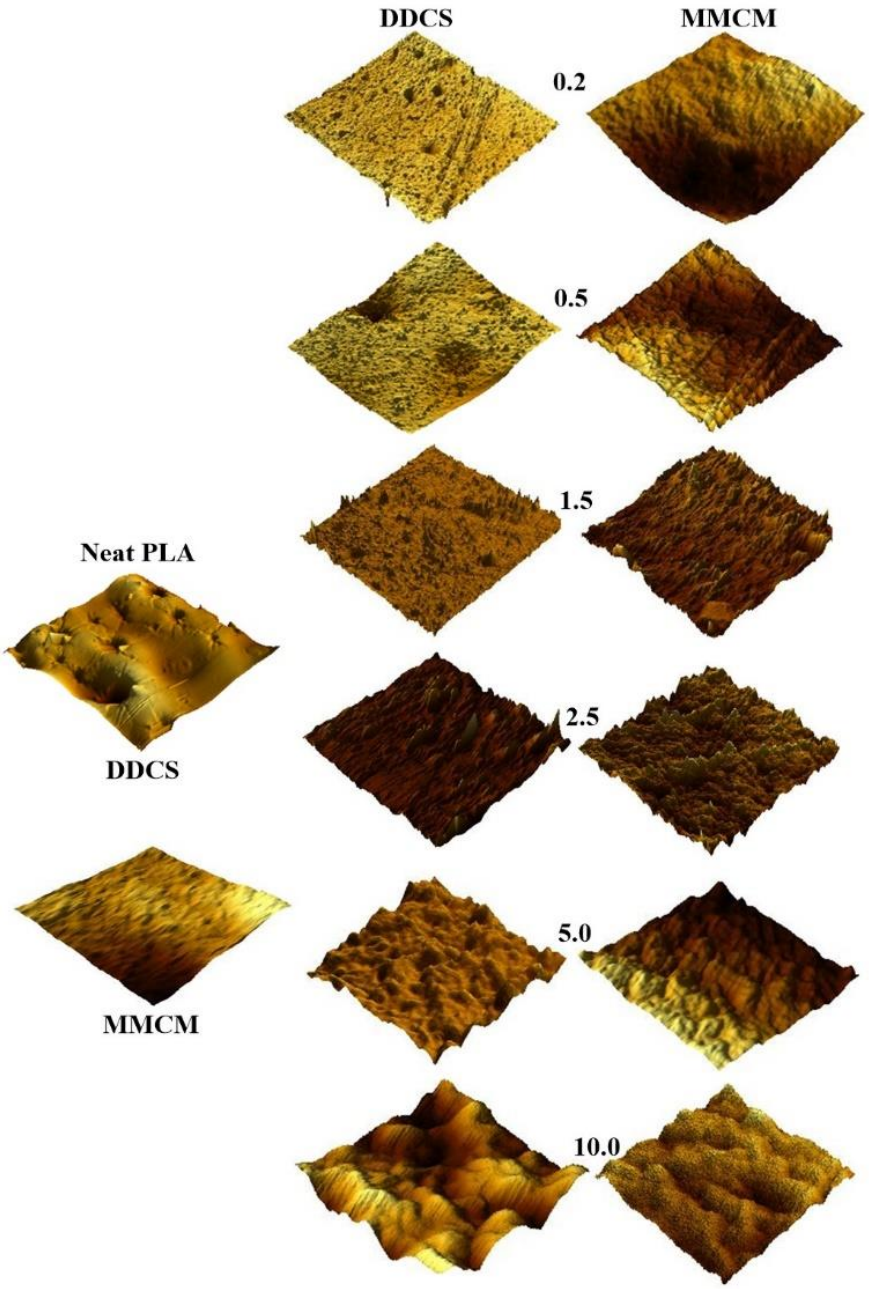

Figure 4.16: Atomic force microscopic images for microtomed specimens of poly (lactic acid) and carbon black filled poly (lactic acid) composites.

4.1.1.3.6 ATOMIC FORCE MICROSCOPY

Atomic force microscopy on microtomed specimens for both types of poly (lactic acid) sheets (compression molded, and dissolution cast granules) and carbon black filled poly (lactic acid) (i.e. for DDCS and MMCM) were observed under an atomic force microscope to determine basic data on surface characteristics with help of a statistical quantity in terms of roughness, which is not obtained in scanning electron microscopy. Tip – Sample interactions on selected

area vary due to difference in Vander Waal's forces between tip and specimen, also due to difference in stiffness for selected area on a specimen, which lead to change in phase contrast and simultaneously change in image contrast imaged via atomic force microscope.

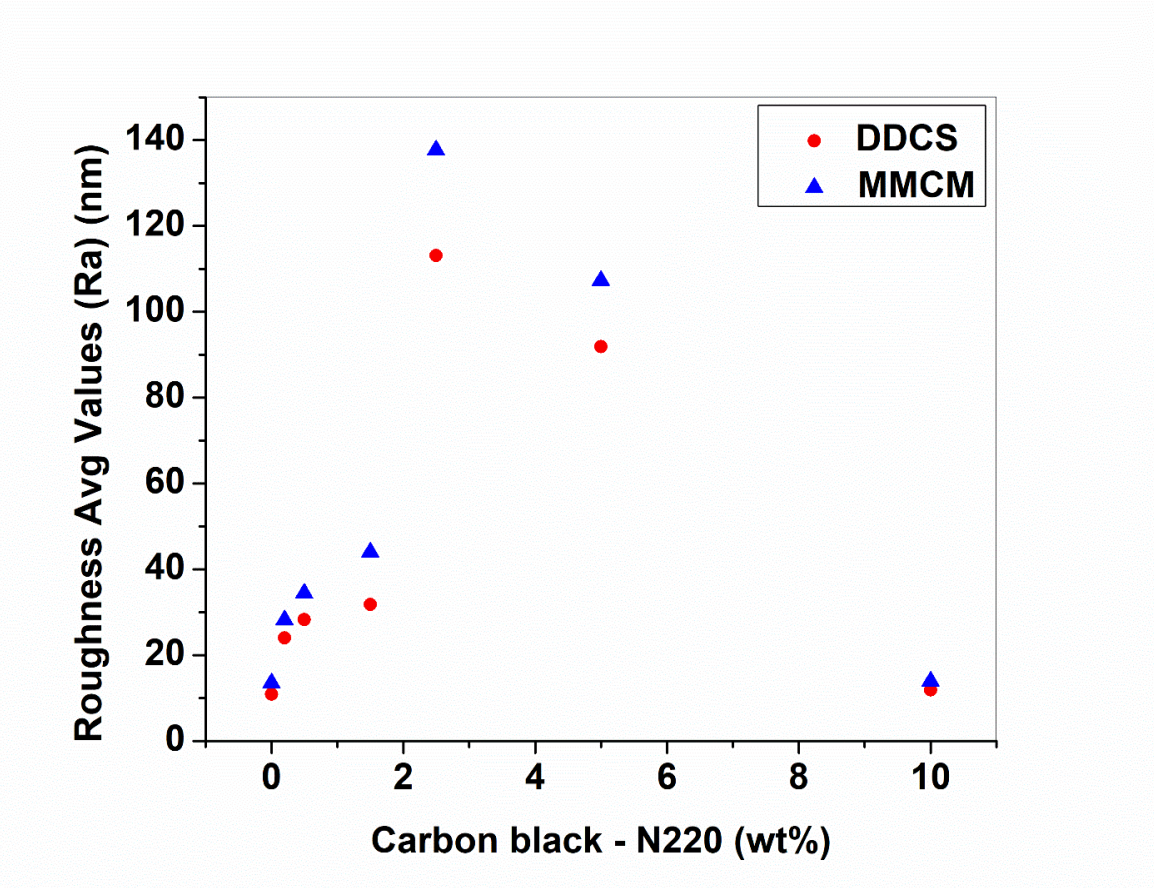

Figure 4.17: Roughness Average Values in Atomic Force Microscopic images for carbon black filled poly (lactic acid) composites (0.2 wt %, 0.5 wt %, 1.5 wt %, 2.5 wt %, 5.0 wt % and 10.0wt %)

Here we shall discuss roughness and compare calculated surface roughness i.e. "roughness average (Ra)" (**see Figure 4.17**) with imaged surface roughness (**Figure 4.16**) symbolizing interaction between poly (lactic acid) chains and carbon black surface. Through the images presented in **Figure 4.16**, it is well obvious that surface roughness increases as the loading of carbon black in poly (lactic acid) matrix increases, but it is not always true, as at very low concentrations of carbon black, interaction between poly (lactic acid) chains and carbon black is well confined and does not contribute much to surface roughness. One can observe that surface of the neat poly (lactic acid) sheets are less rough as compared to poly (lactic acid) matrix filled with 10wt% of carbon black, which depicts a rough surface with more valleys and peaks. For poly (lactic acid) sheets, we observe some pores on surface of specimen prepared via dissolution, which are absent on surface of specimen prepared via compression

molding - these pores arise due to evaporation of chloroform. The peaks and valleys in 10wt%, carbon black filled poly (lactic acid) composites are broad in shape, representing decreasing interactions between poly (lactic acid) chains to carbon black surface; where poly (lactic acid) chains are insufficient to occupy free volume of carbon black and hence interaction between carbon black and poly (lactic acid) chains decreases and carbon black – carbon black increases, therefore decreases the surface roughness measured via atomic force microscopy.

A similar observation regarding size of peaks can be made in poly (lactic acid) composites filled with 5wt% of carbon black, but the size of peaks is less broad as compared to size of peaks for 10wt% carbon black filled composites. Hence the surface morphology imaged for 10wt% composites, through atomic force microscope with broad peaks and valleys points to decrease in tensile yield strength, tensile elongation, notched Izod impact, flexural strength of poly (lactic acid) composites filled with carbon black above 5wt%. Moving on to atomic force microscopic images of 0.2wt%, 0.5wt%, 1.5wt% and 2.5wt% carbon black filled poly (lactic acid) composites, roughness average increases for 1.5wt% and 2.5wt% of carbon black filled composites, which indicates participation of physical force and chemical interaction between carbon black and poly (lactic acid) chains during composite fabrication. Further peaks in poly (lactic acid) composites with 1.5wt% and 2.5wt% carbon black are narrow structured, in comparison to 5.0wt% and 10.0wt% composites which are broad. Hence narrow peak morphology imaged via atomic force microscope, indicates physical and chemical interactions between carbon black and poly (lactic acid) chains and correlates to optimized value of mechanical properties, compared to other carbon black filled counterparts with broad peaks (i.e. 5.0wt% and 10.0wt%). In 0.2wt% and 0.5wt% carbon black filled poly (lactic acid) composites, the imaging of surface roughness for dissolution casted composites exhibit almost similar surface topography in comparison to compression molded specimens as shown in **Figure 4.16** but values of surface roughness differ, i.e. roughness average increases for compression-molded specimens, MMCM. Atomic Force Microscopic images in **Figure 4.16,** where the surface roughness of carbon black filled poly (lactic acid) composites prepared by MMCM shows increase in surface roughness when compared to DDCS composites. This increase in surface roughness (Ra) is due to migration of poly (lactic acid) chains into pores of carbon black, surface adsorption of poly (lactic acid) chains on carbon black rough surface, increasing the probability of interfaces and interphases between the phases, and thus indicates strong adhesion of poly (lactic acid) chains with carbon black surface[1][143].

4.1.1.3.7 FRACTURE STUDIES

4.1.1.3.7.1 OPTICAL MICROSCOPY

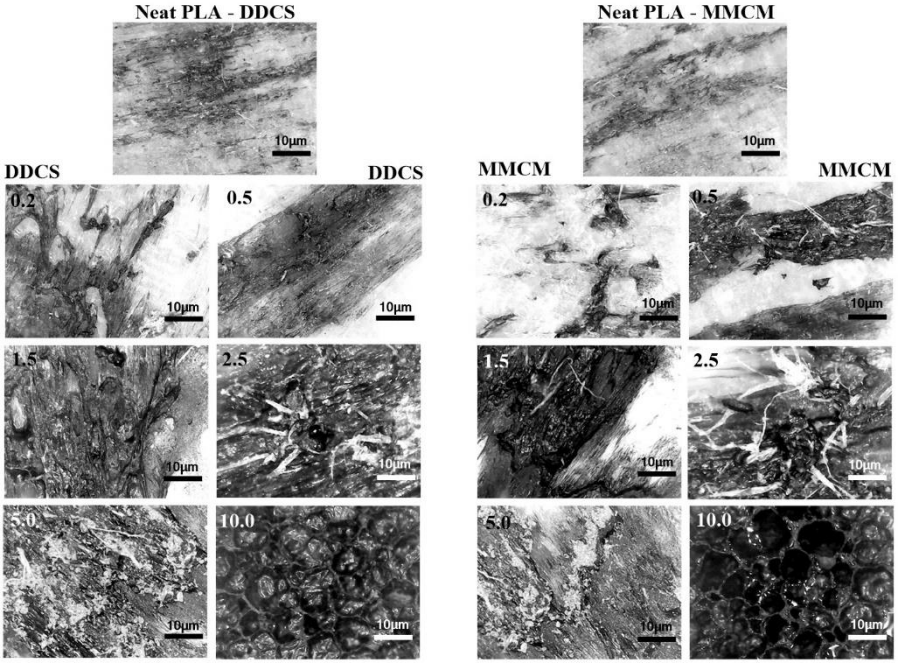

Figure 4.18: Optical microscopic images for tensile fractured specimens of poly (lactic acid) specimen and carbon black filled poly (lactic acid) composites (at X200 magnification))

Morphological analyses on tensile fractured specimens of neat poly (lactic acid) and carbon black filled poly (lactic acid) were performed to determine the nature of fracture occurred, during tensile deformation. One can observe as the loading of carbon black in poly (lactic acid) composites increases, tensile fractured surface of poly (lactic acid) composites specimens appears rough in optical microscopic images. Here, roughness indicates any change in surface texture in comparison to the poly (lactic acid) specimen without carbon black (**see Figure 4.18**). Let us first compare the two extremes (**refer Figure 4.18**), poly (lactic acid) in both cases (i.e. melt mixed/compression molded and dissolution /casted) without carbon black has smooth surface in comparison to poly (lactic acid) filled with 10wt% of carbon black, where voids are observed in the tensile fractured samples (a greater number of voids in DDCS are closed and voids in MMCM are open). These voids are result of breaking up of connection between poly (lactic acid) chains and carbon black filler, during tensile deformation. These closed voids in DDCS carbon black filled poly (lactic acid) composites, can be a possible reason to resist tensile deformation and possess tensile yield strength values higher than MMCM, carbon black filled poly (lactic acid) composites. Tensile fractured surface of poly (lactic acid) melt mixed/compression molded specimen appears to be less rough under an optical microscope in comparison to poly (lactic acid) dissolution

/cast. This roughness indicates the extent of deformation undergone by the test specimen to rupture, hence DDCS poly (lactic acid) specimen possess higher value of tensile yield strength as compared to MMCM poly (lactic acid) specimen.

Optical images for 2.5wt% of carbon black filled poly (lactic acid) composites (DDCS and MMCM) shows fiber-like structures along with its rough surface, the fiber-like structure shall be attributed to increasing resistance to rupture due to effective physical and chemical interaction between carbon black and poly (lactic acid) chains in composites, due to which it possesses tensile yield strength higher than its counterparts. Optical microscopic images for 0.2wt%, 0.5wt%, and 1.5wt% show rough surface, which indicates good physical and chemical attraction between poly (lactic acid) chains and carbon black aggregates, which is evident by a steady rise in tensile yield strength values. 5.0wt% filled carbon black/ poly (lactic acid) composite shows a tensile deformation near to brittle failure with slightly rough surface indicating less resistance before tensile fracture[1].

(**Note:** Visual Roughness indicated in optical microscopy should not be confused with roughness values obtained in Atomic Force Microscopy as; visual roughness in optical microscope is in terms of tensile deformation of respective specimen, which can't be compared to roughness values obtained from Atomic Force Microscope wherein a specimen is microtomed to study surface characteristics which arise due to interaction between poly (lactic acid) chains and carbon black.)

4.1.1.3.7.2 SCANNING ELECTRON MICROSCOPY

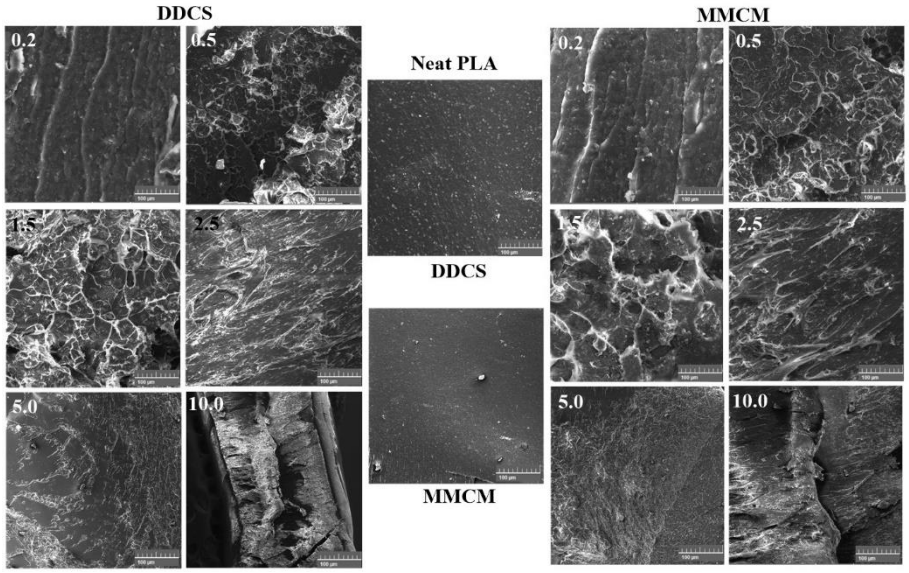

Figure 4.19: Scanning electron microscopic images for tensile fractured specimens of poly (lactic acid) specimen and carbon black filled poly (lactic acid) composites (at X1000 magnification))

To get further insight into the morphology of tensile fractured samples at higher magnification of x1000, scanning electron microscope was equipped. Findings from scanning electron microscopy give rise to similar discussion as mentioned in optical microscopic analysis but with clearer images, in comparison to optical microscope images. Scanning electron microscopic images (**see Figure 4.19**) of MMCM based poly (lactic acid) composites show slightly rough surface morphology in comparison to DDCS for 0.2wt%, 0.5wt%, 1.5wt%, 2.5wt% and 5.0wt% indicating resistance to tensile deformation. Imaging of surface roughness via scanning electron microscope can be very well explained from **Figure 4.19** – firstly neat poly (lactic acid) shows a smooth surface morphology, indicating brittle failure, secondly poly (lactic acid) filled with 5.0wt% and 10.0wt% of carbon black presents images with a smaller number of rough surfaces, which again can be stated as brittle failure. A decrease in tensile yield strength values supports the morphological characterizations. For 10wt% loading we can observe few cracks, which can be due to unavailability of poly (lactic acid) chains for carbon black interaction, which leads to decrease in mechanical properties. Poly (lactic acid) filled with 0.2wt% shows a slight change in morphology which indicates that 0.2wt% of carbon black is enough to have a prominent effect on microstructure of poly (lactic acid). Further 0.5wt%, 1.5wt%, 2.5wt%, 5.0 wt% and 10.0wt% of carbon black too have a significant effect on surface morphology of poly (lactic acid) composites (**see Figure 4.19**). Observing morphology of poly (lactic acid) composites with 2.5wt% carbon black, fibrillar structures are observed which agree with optical microscopic images; these fibrillar structures contribute to increase in tensile yield strength with a small decrease in tensile elongation values. Slightly similar morphologies were obtained for DDCS and MMCM poly (lactic acid) composites; which supports the data on mechanical properties, as no much difference is observed in mechanical properties of poly (lactic acid) composites with similar concentration of carbon black, irrespective of the processing technique used i.e., DDCS or MMCM[1].

4.1.1.4 CONCLUSION

Optical microscopic images and scanning electron microscopic images of tensile fractured specimens for neat poly (lactic acid) showed a brittle failure, whilst for carbon black filled poly (lactic acid) composites till 2.5wt% indicated rough surface morphology and a slight fiber-like morphology indicating the high deformation level, i.e. resistance, during the tensile test. Transmission electron microscopic images could clearly indicate close to homogenous dispersion of carbon black in carbon black filled poly (lactic acid) composites, with few secondary aggregates as the amount of carbon black loading increased. Atomic force

microscopic topographical images were self-explanatory in determining the surface characteristics, i.e. interaction between poly (lactic acid) chains and carbon black in fabricated carbon black filled poly (lactic acid) composites, owing to the size, shape, and number of valleys and peak structures.

4.1.2 FINAL CONCLUSION

Considering the conclusions from the physical and mechanical properties (**Section 4.1.1.2**) in comparison to morphological evidences (**Section 4.1.1.4**) dissolution dispersion solution casting was selected with a slight modification to fabricate the poly (lactic acid) composites.

4.2 EXTRACTION OF CELLULOSE FIBERS AND CONFIRMING ITS NANOFORM

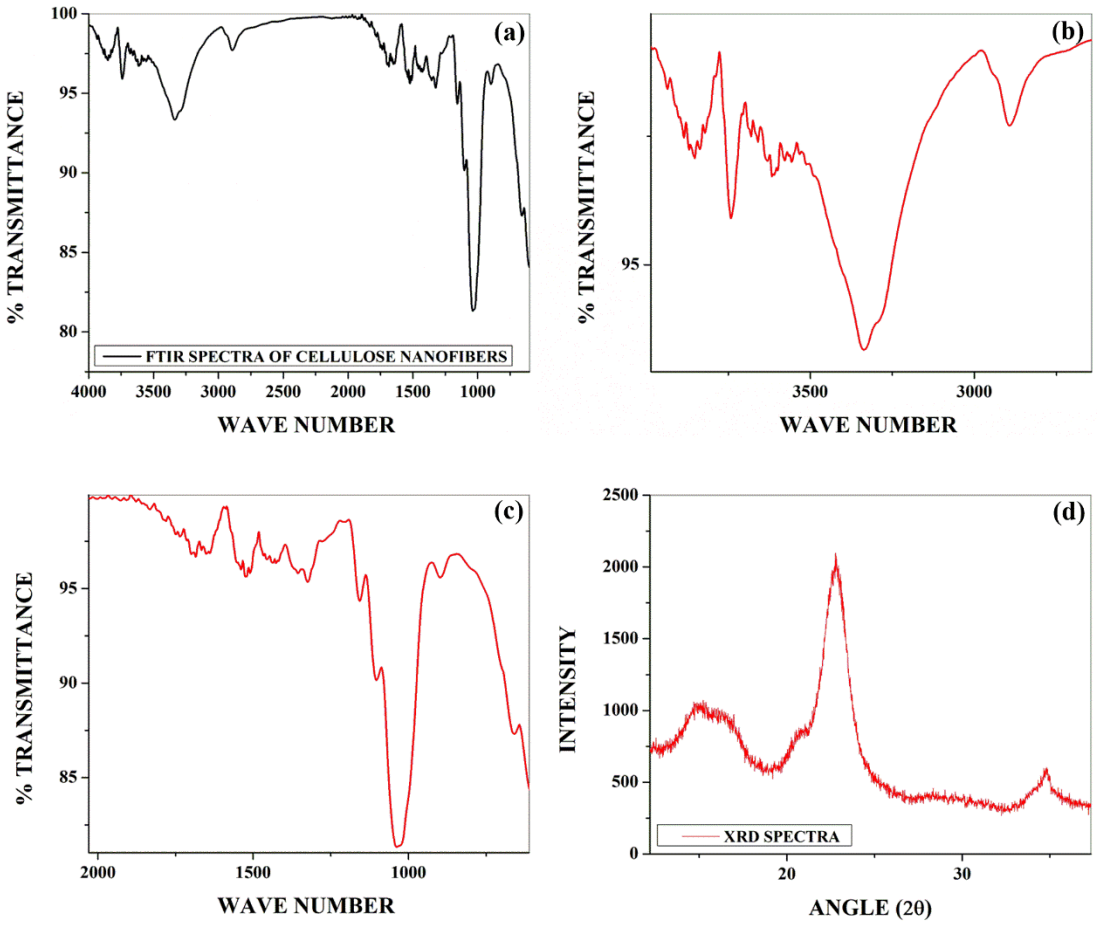

Figure 4.20: Structural Characterization by Infrared Spectroscopy(ATR - FTIR) and X Ray Diffraction (XRD) – of cellulose nanofibers (a) (b) (c) ATR - FTIR spectra and (d) XRD spectra

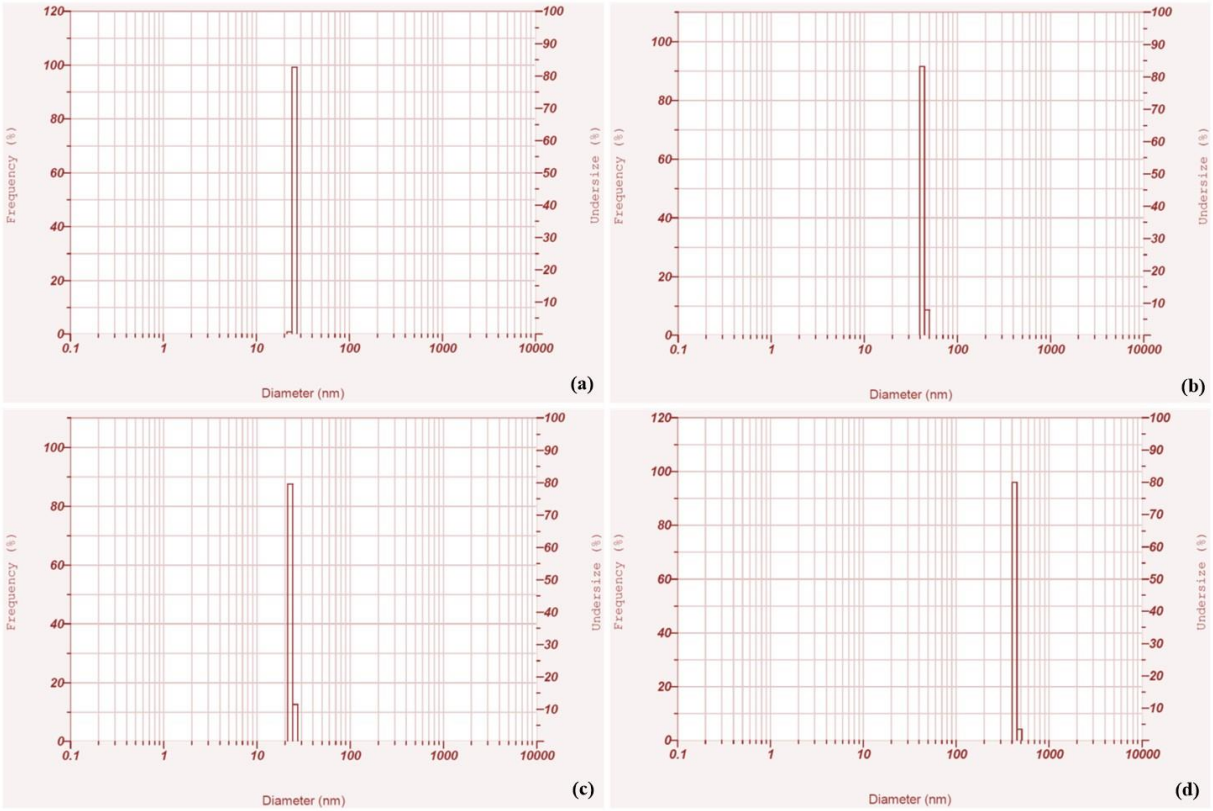

Figure 4.21: Particle size analysis of cellulose nanofibers by Dynamic Light Scattering (DLS)

4.2.1 CHEMICAL COMPOSITION AND NATURE [ATR – FTIR AND XRD]

Extraction of cellulose fibers was carried out as per the method mentioned in **Section 3.1.2**.Technically extracted cellulose fibers were characterized for chemical composition and form (structure and form) by infrared spectroscopy and x ray diffraction. Particle size and surface charge determination by dynamic light scattering analysis. Thermal gravimetric analysis was done to determine technical quality. Scanning electron microscopy was done to confirm the shape of the cellulose fibers extracted from raw kenaf fibers. **Figure 4.20 (a)** is a result of ATR – FTIR on cellulose fibers. **Figure 4.20(b)** and **4.20(c)** magnifies the major peaks of cellulose. It can be observed that in all 26 peaks were visible on ATR - FTIR spectra, out of which few characteristics peaks like 657cm^{-1}, 1037cm^{-1}, 1103cm^{-1} and 1157cm^{-1} , 1417 cm^{-1} and 1435 cm^{-1}, 2893 cm^{-1}, 3336 cm^{-1}, assigned to ‘s’ C – H bend, ‘s’ C – O stretch, ‘s’ C – O stretch, ‘m’ C – C stretch, ‘s’ CH stretch, ‘s’ RCO – OH respectively, confirms the chemical composition of cellulose fibers. **Figure 4.20 (d)** confirms the semi – crystalline form of cellulose fibers. A hump between 2θ value 13 to 18 confirms the amorphous region, a long and short sharp peak at 2θ = 22.8 and 34.8 confirms the

crystalline form. Hence over all conclusion from **Figure 4.20** confirms the chemical composition and semi – crystalline form of extracted cellulose fibers[127].

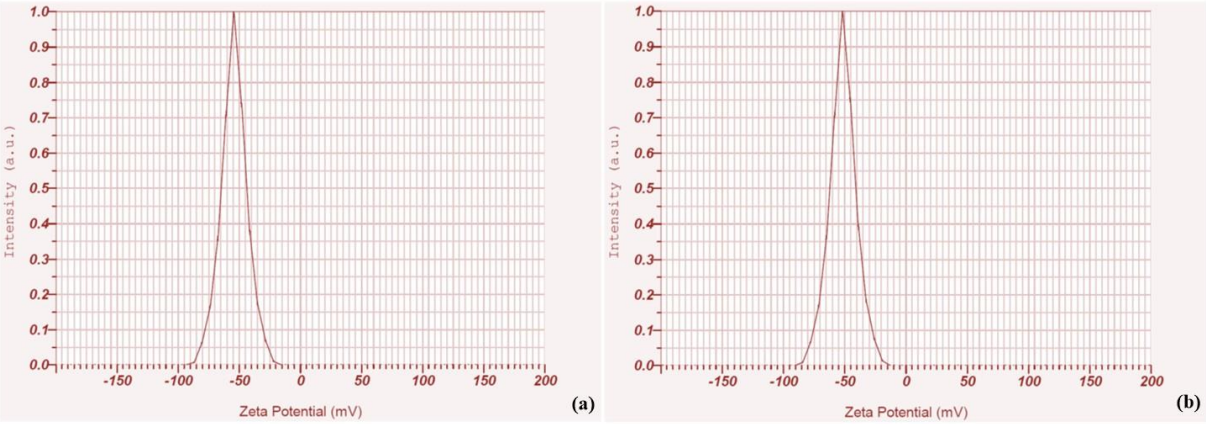

Figure 4.22: Surface charge determination on cellulose nanofibers by Zeta Potential

4.2.2 PARTICLE SIZE ANALYSIS AND SURFACE CHARGE DETERMINATION [DYNAMIC LIGHT SCATTERING]

Figure 4.21 confirms the particle size of the cellulose fibers. 25.8nm, 42.5nm, 23.2nm and 430nm were the sizes obtained from dynamic light scattering experiments. Hence it was confirmed that the cellulose fibers extracted were nanosized.

Determining stability, i.e. aggregation characteristics of nanocellulose fibers in suspension is of prime importance. **Figure 4.22** confirms the existence of negative zeta potential and confirms the stability of cellulose nanofibers in suspension form.

Above analysis through ATR – FTIR, XRD and DLS confirms the extracted cellulose fibers to be “nanocellulose fibers” and can be addressed as nanocellulose fibers in further discussions[127].

4.2.3 THERMAL ANALYSIS [THERMAL GRAVIMETRIC ANALYSIS]

Determining the technical quality of cellulose nanofibers is of utmost importance for which percent weight change with respect to temperature was determined, which gives an idea on molecular restriction (i.e. amorphous regions or crystalline forms). Extracted cellulose nanofibers were thermally stable up to 318℃ with a weight loss of 4%, this weight loss can be attributed to moisture (see **Figure 4.23**). From the graph in **Figure 4.23** it is confirmed that cellulose nanofibers extracted from raw kenaf fibers have both amorphous regions and crystalline forms, owing to which thermograph shows the down shift at 110℃ which attributes to transition in amorphous regions of cellulose nanofibers; a more down shift of 150℃ can be

attributed to transition of crystalline forms. A steep decrement from 318℃ to 338℃ confirms the degradation of amorphous regions and crystalline forms of cellulose nanofibers. One can also observe 2 percent residue , which confirms the complete degradation of the organic content of cellulose nanofibers (i.e., C H O)[127].

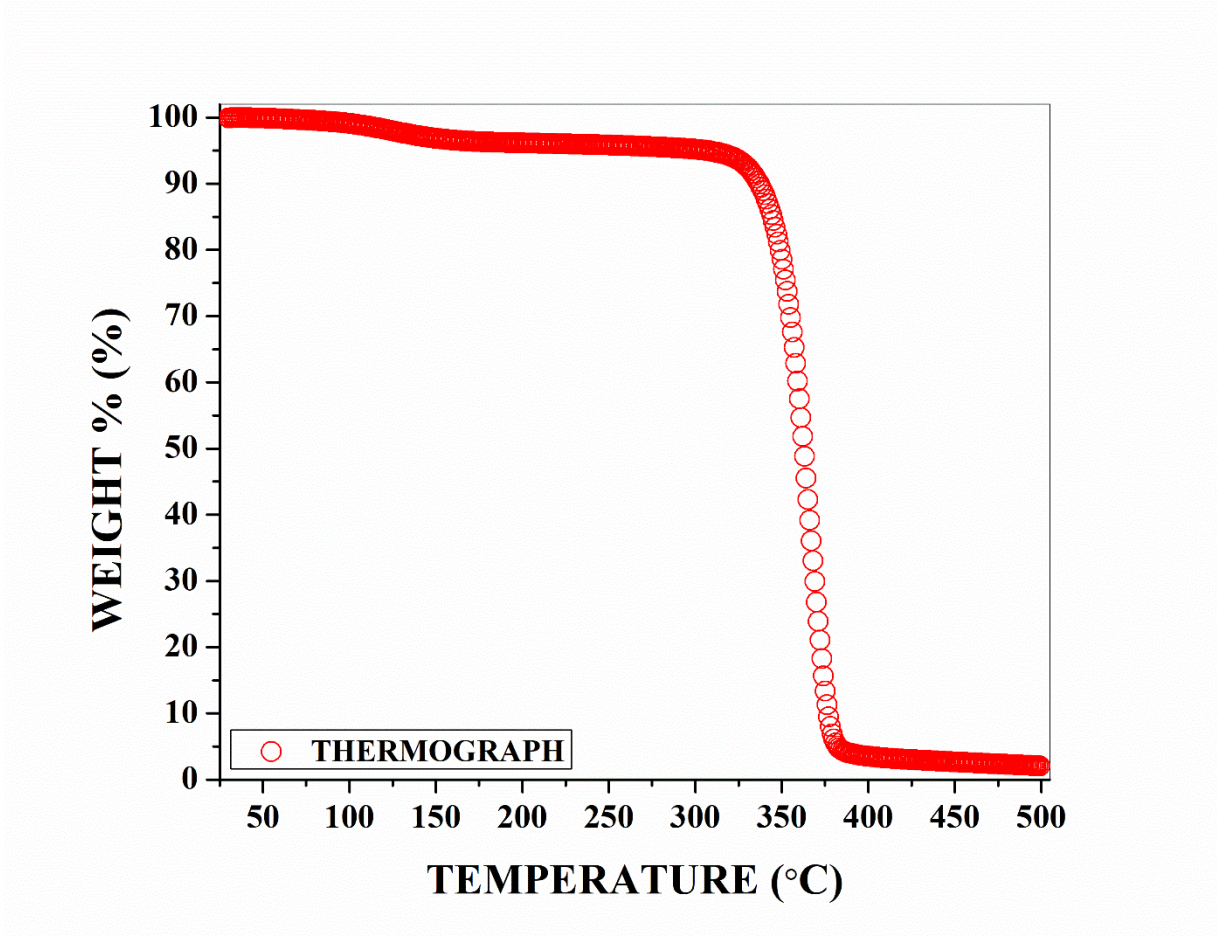

Figure 4.23: Thermal Gravimetric Thermograph for cellulose nanofibers

4.2.4 MORPHOLOGICAL ANALYSIS [SCANNING ELECTRON MICROSCOPY]

Scanning electron microscope pictographs as evidenced in **Figure 4.24 (a) 4.24(b), 4.24(c)** and **4.24(d)** confirms the fibrillar nature of the cellulose nanofibers, but it does not clearly state the nano – size of the cellulose nanofibers as evident from the dynamic light scattering. These “woolen balls like structures” are due to bundling of cellulose nanofibers. Aggregation rate of nanoparticles is faster in solid form than in liquid form. Hence cellulose nanofibers appear as “woolen ball like structures” in the scanning electron microscope images owing to aggregative nature of cellulose nanofibers. These “woolen ball like structures” when sonicated are separated into their nano – size (evident from particle size analysis through

dynamic light scattering). Further in this thesis dispersion analysis, i.e., details on the extent and level of dispersion of fillers within poly (lactic acid) is detailed.

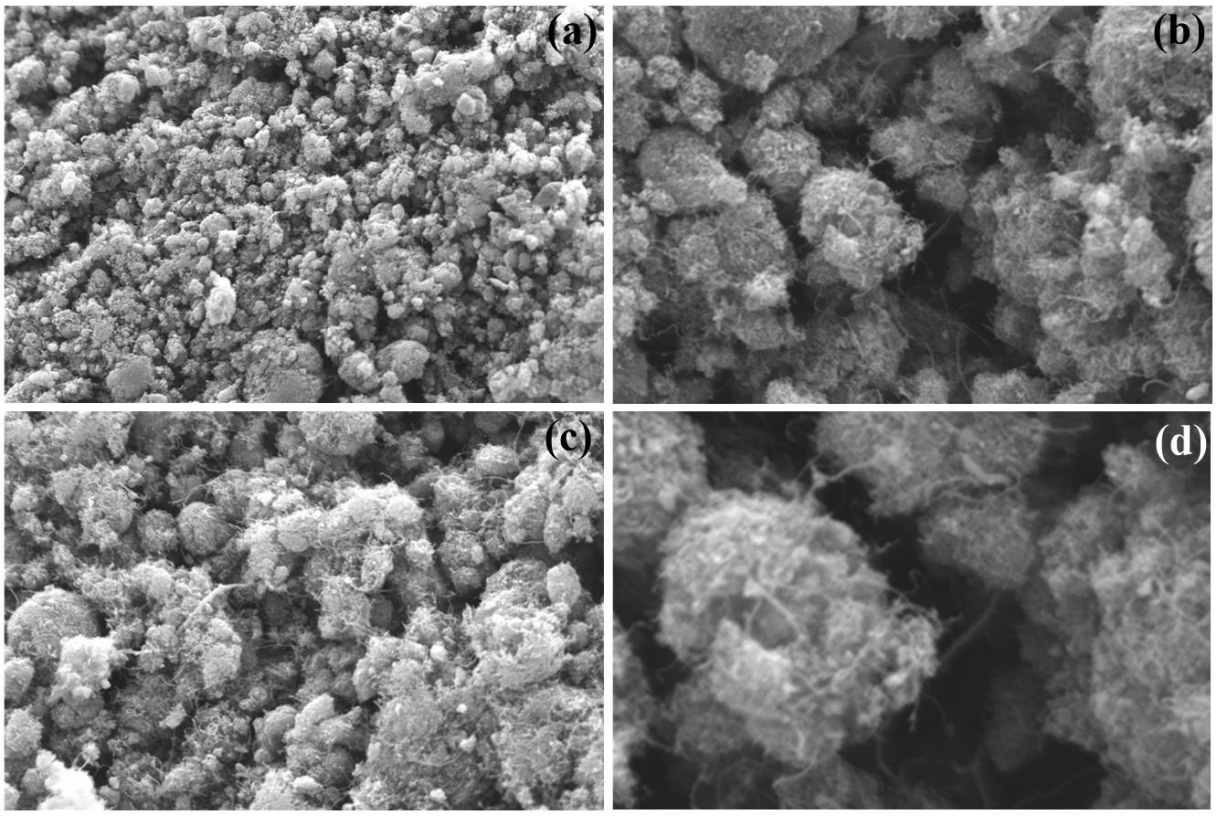

Figure 4.24: Scanning electron microscopic images of cellulose nanofibers (x1000)

4.2.5 CONCLUSION

Structural analysis confirms the synthesized material as cellulose. Particle size analysis confirms it to be in nano range. Surface charge determination confirmed the presence of negative charge. Thermal analysis confirms it to be in fiber form with both amorphous and crystalline regions. Morphological characterization using scanning electron microscope was unable to confirm the nanostructure due to aggregative property of nanocellulose in its solid form. Hence synthesis of cellulose nanofibers out of kenaf fibers was confirmed.

Further **Chapter 5** describes ultraviolet – visible spectroscopy as a tool to determine the interphase characteristics for carbon based composites (single and hybrid). Absorbance limitation of cellulose nanofibers filled poly (lactic acid) composites limited its interphase characterization by ultraviolet – visible spectroscopy.

5 CHARACTERIZING INTERPHASE MODIFICATION

5.1 ULTRAVIOLET – VISIBLE SPECTROSCOPY

5.1.1 INTRODUCTION

Properties of polymer composites depend to a large extent on the characteristics of dispersion and interphase layers.

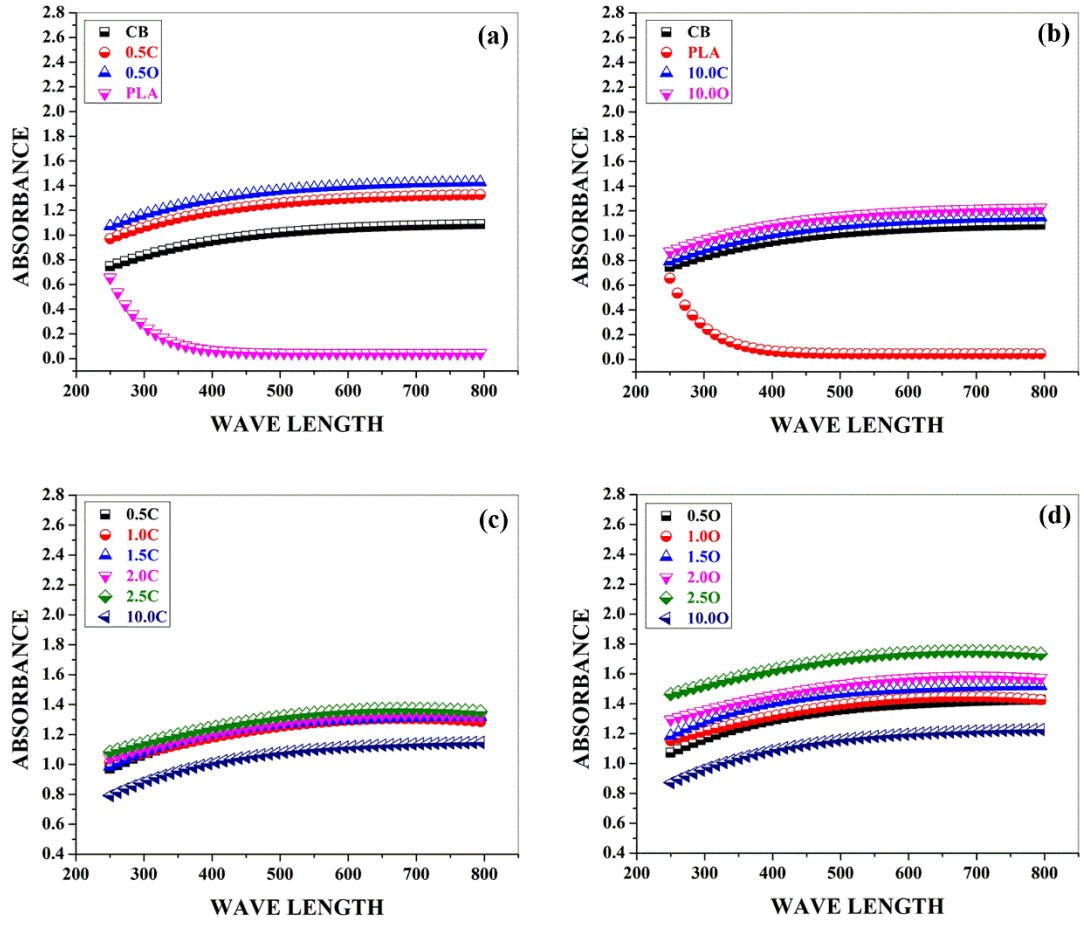

Figure 5.1: Comparison of UV-VIS absorption spectra for carbon black filled poly (lactic acid) composites (a) PLA/CB/0.5C/0.5O (b) PLA/CB/10.0C/10.0O (c) DD poly(lactic acid) composites with 0.5, 1.0, 1.5, 2.0, 2.5 and 10.0wt% of carbon black and (d) OD poly(lactic acid) composites with 0.5,1.0, 1.5, 2.0, 2.5 and 10.0wt% of carbon black ("C" represents DD and "O" represent DD)

In this work, poly (lactic acid) composites [PLAC] were prepared by via dissolution – dispersion method [DD] and oligomeric – dispersion method [OD]. Ultraviolet-Visible spectroscopy [UV – VIS] was used to determine the dispersion and interphase characteristics within the PLAC.

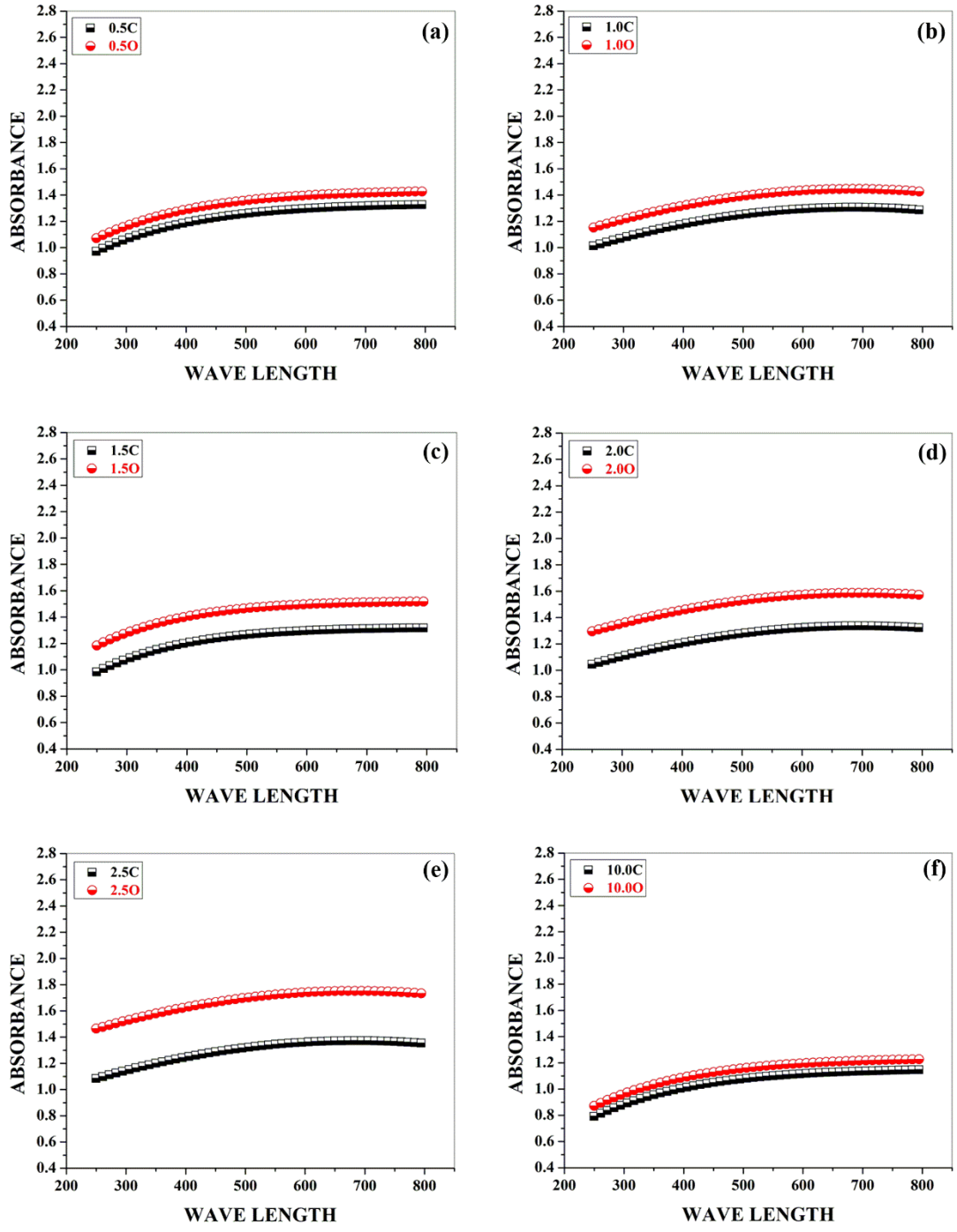

Figure 5.2: Comparison of UV-VIS absorption spectra for carbon black filled poly (lactic acid) composites (a) 0.5 (b) 1.0 (c) 1.5 (d) 2.0 (e) 2.5 and (f) 10wt% prepared via DD and OD ("C" represents DD and "O" for OD)

An increase in absorbance at higher wavelength within the absorbance spectra was observed for PLAC prepared by DD and OD, which may be attributed to formation of strong adlayers as

well as “near to homogenous dispersion” for carbon-based particulate filled composites. An increase in absorbance was observed for PLAC prepared by OD in comparison to DD and can be attributed to modifications occurring at interphase regions. PLAC using Carbon black, multiwalled carbon nanotubes in poly (lactic acid) were prepared via DD and OD, were further characterized by UV – VIS. To study the “hybrid effect”, composites with 2.5wt% of carbon black with varied concentration of multiwalled carbon nanotubes and nanocellulose fibers were prepared using DD and OD, further characterized for UV - VIS. This chapter portrays the role of UV – VIS to determine dispersion, as well as the interphase characteristics for poly (lactic acid), filled carbon composites.

5.1.1.1 PART I – SINGLE FILLER EFFECT

Figure 5.1 and **5.2** shows the comparative analysis of UV – VIS absorbance spectra for carbon black, neat poly (lactic acid) [PLA] and carbon black filled poly (lactic acid) prepared by DD and OD. One may observe from **Figure 5.1a** and **5.1b** that absorbance for neat poly (lactic acid) in range 800nm to 250nm is far below in comparison to the absorbance of carbon black in the same range. It is also observed from **Figure 5.1a** [0.5wt%] and **5.1b** [10wt%], that addition of carbon black to poly (lactic acid) increased the absorbance of poly (lactic acid) composites prepared by DD and OD [with maximum for OD] in comparison to absorbance of carbon black; this increase in absorbance for poly (lactic acid) composites can be attributed to the synergistic effect between poly (lactic acid) chains and surface of carbon black, i.e. adsorption pattern formed due to adsorption of poly (lactic acid) chains on the surface of carbon black which in turn forms the adsorption layers and increases the absorbance in poly (lactic acid) composites. Adsorption pattern is subjected to change in its structure of adsorption layers formed within poly (lactic acid) composites with a change in the processing technique, owing to which poly (lactic acid) composites prepared with OD shows an increase in absorbance over poly (lactic acid) composites prepared via DD.

To discuss in short, a corresponding increase in absorbance for poly (lactic acid) composites prepared by DD and OD is observed till 2.5wt%, after which a decrease in absorbance was observed at 10wt%. The corresponding increase in absorbance for poly (lactic acid) composites prepared by DD and OD till 2.5wt% of carbon black can be attributed to the free electrons of sp^2 carbon of carbon black which is capable of forming a conjugation with poly (lactic acid) chains [DD] and poly (lactic acid) chains – oligomer chains [OD], thereby increasing the absorbance [with maximum absorbance for 2.5wt% carbon black filled poly (lactic acid) prepared with OD]. At 10wt% of carbon black in poly (lactic acid) composites

prepared by DD and OD, most of the poly (lactic acid) chains [DD] and poly (lactic acid) chains – oligomer chains [OD] are adsorbed on the surface of the carbon black and hence very few poly (lactic acid) chains [DD] and poly (lactic acid) chains – oligomer chains [OD] are available to form a conjugation with remaining carbon black, due to which a decrease in absorbance is observed [with maximum absorbance for 10wt% carbon black filled poly (lactic acid) prepared with OD][4][1].

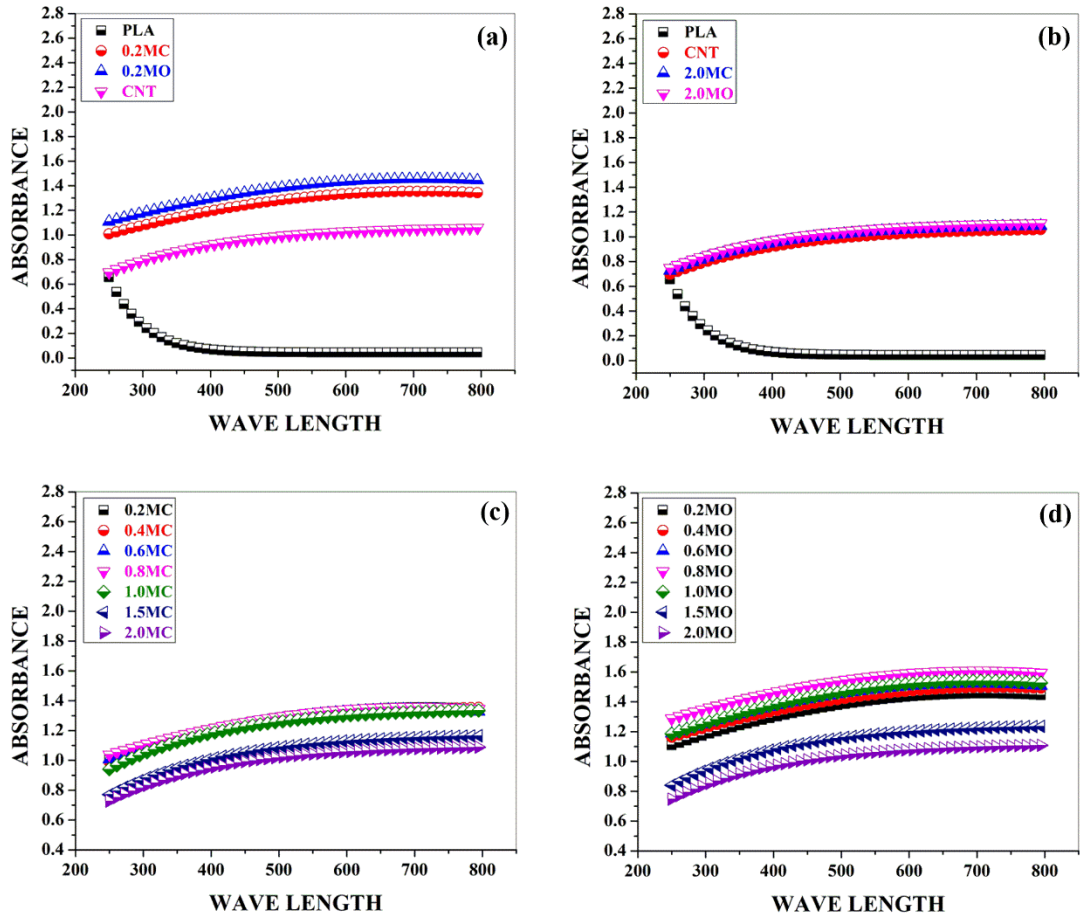

Figure 5.3: Comparison of UV-VIS absorption spectra for multiwalled carbon nanotubes filled poly (lactic acid) composites (a) PLA/MWCNT/0.2MC/0.2MO (b) PLA/MWCNT/2.0MC/2.0MO (c) DD poly(lactic acid) composites with 0.2, 0.4, 0.6, 0.8, 1.0,1.5 and 2.0wt% of multiwalled and (d) OD poly(lactic acid) composites with 0.2, 0.4, 0.6, 0.8, 1.0,1.5 and 2.0wt% of multiwalled carbon nanotubes ("C" represents DD, "O" for OD and "M" for multiwalled carbon nanotubes)

The detailed reason for the increase in absorbance for poly (lactic acid) composites prepared with OD will be discussed in the further sections of the thesis. Increase in the absorbance at higher wavelength for poly (lactic acid) composites till 2.5wt% of carbon black as observed in **Figure 5.1c** and **5.1d**, can be attributed to "near to homogenous state of dispersion" for

carbon black within poly (lactic acid) composites with strong adhesion within the layers (adlayers) at the interphase region of poly (lactic acid) and carbon black surface; decrease in absorbance at low wavelength can be attributed to weakening of bond strength within poly (lactic acid) composites.

Increase in absorbance at higher wavelength and a decrease in absorbance at lower wavelength for poly (lactic acid) composites filled with 10wt% carbon black can be attributed to the increase and decrease in strength of physical entanglements (where filler – filler interaction dominates polymer – filler entanglements) respectively.

Figure 5.2 shows a comparative UV – VIS absorbance spectra for poly (lactic acid) composites filled with 0.5, 1.0, 1.5, 2.0, 2.5 and 10.0wt% of carbon black prepared via DD and OD. One can observe that in each of the composition the absorbance for poly (lactic acid) composites prepared via OD shows an increase in comparison to poly (lactic acid) composites prepared by DD. The difference of absorbance in poly (lactic acid) composites prepared by OD and DD increases with a corresponding increase in carbon black till 2.5wt%, after which the difference of absorbance for 10wt% carbon black filled poly (lactic acid) composites prepared by OD and DD decreases. One should be aware of the fact that the formation of the adsorption sequence between polymer chains and the surface of filler determines the thickness of the adsorbed layers and these adsorbed layers further contribute to the interphase region. Adsorption of high molecular weight polymers on filler surface differs essentially from the adsorption process of low molecular weight oligomers on filler surface. Hence our attempt to increase the thickness of the interphase region with the formation of strong adlayers using the concept of adsorption of high and low molecular substances on filler surface was a successful attempt, which is evident from the UV – VIS absorbance spectra's reported in this manuscript. In preparing poly (lactic acid) composites via OD, use of carbon black filled suspension of high molecular weight poly (lactic acid) and low molecular weight carbon black oligomeric dispersions, induces phase separation, which resulted in a greater thickness of the adsorption layer (i.e. interphase region) with strong adlayers. With increasing concentration of carbon black in high molecular weight suspension of carbon black in poly (lactic acid) and oligomeric dispersion used in OD, indicates the formation of a bridged network between the carbon black particles connected either by polymer chains and/or oligomer chains. The formation of a bridge network (connected network) induces unsaturation and thus increases the difference of absorbance in UV – VIS spectra. Decrease in the absorbance in UV – VIS after a specific concentration of filler can be attributed to the

reduction in thickness of adsorption layers, which can be attributed to the minimization of phase separation in presence of fillers[4].

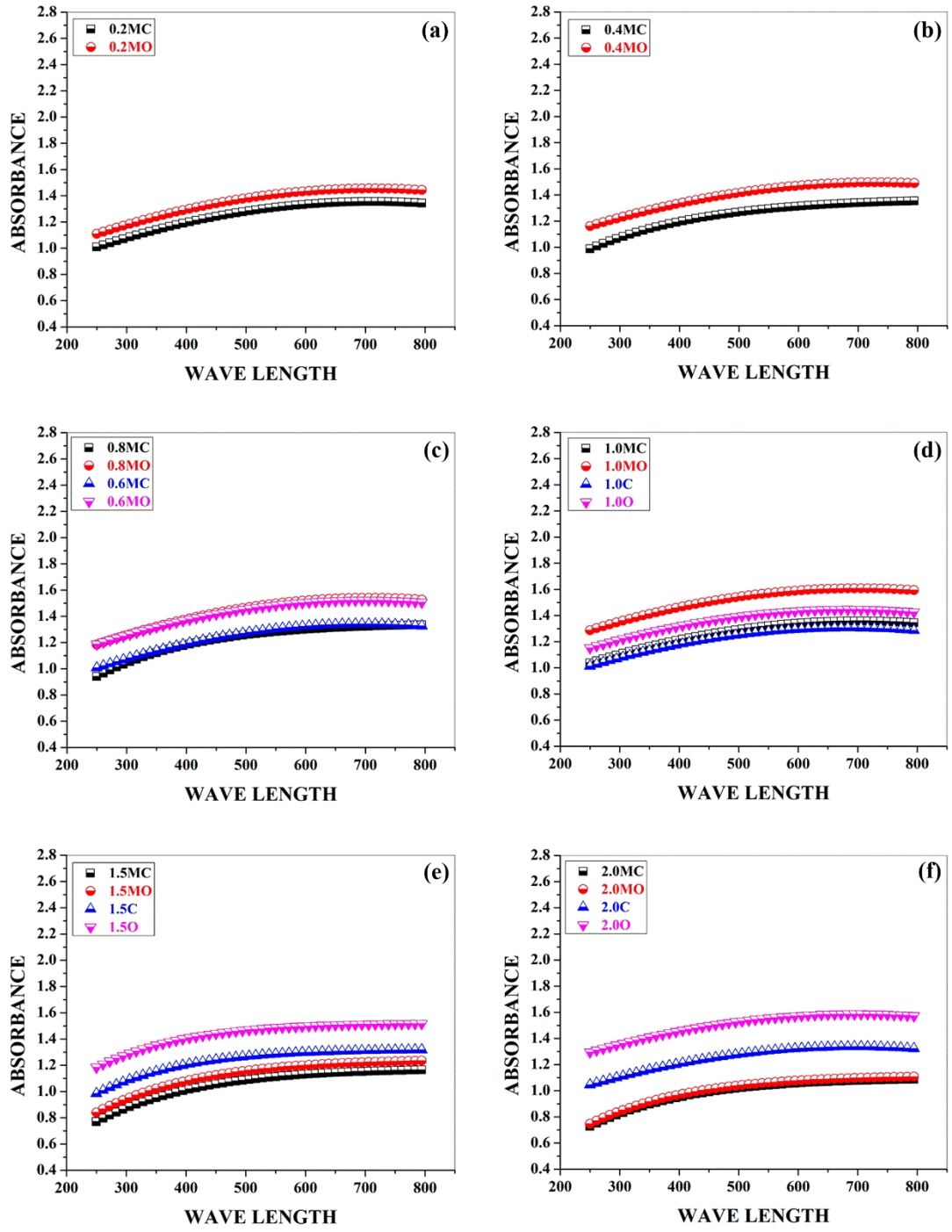

Figure 5.4: Comparison of UV-VIS absorption spectra for multiwalled carbon nanotubes filled poly (lactic acid) composites (a) 0.2 (b) 0.4 (c) 0.6 and 0.8 (d) 1.0 (e) 1.5 and (f) 2.0wt% in comparison to equally filled [for 1.0, 1.5 and 2.0wt% in (d), (e) and (f)] carbon black poly (lactic acid) composites prepared via DD and OD. ("C" represents DD, "O" for OD and "M" for multiwalled carbon nanotubes)

Although 10wt% of carbon black filled poly (lactic acid) composites prepared via OD shows an increase in absorbance in comparison to composites prepared via DD as seen in **Figure 5.2f**, a decrease within the batch as seen in **Figure 5.1d** and with a small difference of absorbance as seen in **Figure 5.2f** was observed.

This decrease within the batch with a minor difference in absorbance can be attributed to a decrease in thickness of adsorption layers due to the minimization of phase separation in the presence of carbon black. Relating to its microstructure this decrease in absorbance can also be due to decreased adsorption of poly (lactic acid) chains on surface of carbon black with formation of linked skeletal network i.e. physical network of entanglements which hinders and prevents transition of poly (lactic acid) chains [DD] and poly (lactic acid) chains – oligomer chains [OD] on the saturated surface of carbon black. It is important to mention that the adsorption process is specific and unique to an individual system with respect to its polymer-solvent and filler surface characteristics.

In this experimental study, poly (lactic acid) composites filled with MWCNT by using DD and OD. This study was carried out to have an understanding of the influence of filler shape on the absorbance characteristics via UV – VIS. **Figure 5.3** and **5.4** shows the comparative analysis of UV – VIS absorbance spectra for MWCNT, neat poly (lactic acid) [PLA] and MWCNT's filled poly (lactic acid) composites in comparison with carbon black filled poly (lactic acid) composites prepared by DD and OD respectively. Absorbance for neat poly (lactic acid) in the range 800nm to 250nm was lower as compared to absorbance for MWCNT, but on loading of MWCNT into poly (lactic acid) matrix increased the absorbance [in comparison to MWCNT as well as neat poly (lactic acid)] irrespective of its method of composite preparation (DD and OD) and concentration of MWCNT in poly (lactic acid). This increase in absorbance can be attributed to the synergism taking place between functional groups of poly (lactic acid) and the surface of MWCNT's.

An increase in absorbance was observed for poly (lactic acid) composites upto 0.8wt% of MWCNT after which decrease in absorbance irrespective of the method of preparation (i.e. DD and OD) was observed as graphed in **Figure 5.3c** and **Figure 5.3d**. An increase in absorbance till 0.8wt% of MWCNT can be attributed to well-aligned tubes within poly (lactic acid) matrix i.e. formation of a well-connected network structure (bridged network) with poly (lactic acid) chains.

MWCNT are long tubular structures and are curvy in nature at higher concentrations, unsaturated MWCNT has a woolen yarn structure, forming a physical network entanglement within poly (lactic acid) composites and are responsible for the decrease in absorbance.

Figure 5.4 represents the comparative absorbance for MWCNT's filled poly (lactic acid) composites prepared by DD and OD. Absorbance pattern for an equal amount of carbon black concentration is also shown for a better understanding of the influence of filler shape on absorbance. It may be observed that MWCNT's poly (lactic acid) composites prepared with OD have higher absorbance in comparison to MWCNT's poly (lactic acid) composites prepared using DD; irrespective of the concentration of MWCNT's. The increase in absorbance for poly (lactic acid) composites filled with MWCNT's prepared by OD can be attributed to the increase in the thickness of adsorbed layers [due to phase separation as discussed in the section of carbon black filled poly (lactic acid)]. An increase in absorbance till 0.8wt% of MWCNT's in poly (lactic acid) composites may be attributed to the formation of strong linked (i.e. connected network) between the poly (lactic acid) chain – oligomer chains. The decrease in absorbance after 0.8wt% of MWCNT's in poly (lactic acid) composites can be attributed to the decreased thickness of adsorbed layers [due to minimization of phase separation in fillers presence as discussed in the section of carbon black]. A decrease in absorbance can also be attributed to the inefficiency of MWCNT's in poly (lactic acid) dissolution and oligomeric dispersion to form a strongly network – bridged structure, which in turns forms a weak skeletal network. On comparing absorbance pattern of equal quantity of carbon black with MWCNT's, we confirm that absorbance for 1.0wt% MWCNT's filled poly (lactic acid) composites are higher irrespective of the method of preparation (OD and DD), but as the concentration of MWCNT's increases to 1.5wt% and 2.0wt%; absorbance pattern for equal quantity of carbon black filled poly (lactic acid) composites increases which can be attributed to the formation of strong bridged network within carbon black filled poly (lactic acid) composites, whereas weak skeletal networks are formed within poly (lactic acid) composites filled with MWCNT's. The increase in absorbance at higher wavelength and slight decrease in absorbance at lower wavelength for poly (lactic acid) composites filled till 0.8% MWCNT's can be attributed to "near to homogenous dispersion" with formation of strong adlayers between poly (lactic acid) chains/MWCNT's surface and weakening of bond strength respectively. Similarly increase in absorbance at higher wavelength and a decrease in absorbance at lower wavelength after 0.8wt% can be attributed to strength of physical entanglements which decreases at lower wavelength [filler – filler interactions dominates polymer – filler entanglements]. One can also observe (**see figure 5.4**) the increase in the difference of absorbance till 0.8wt%, between MWCNT's filled poly (lactic acid) prepared via OD and DD which is attributed to the formation of bridge network (connected network) inducing unsaturation; after which the decrease in difference of absorbance is recorded. This

decrease in difference of absorbance can be attributed to decreased adsorption of poly (lactic acid) chains on surface of MWCNT's with formation of linked skeletal network i.e. physical network of entanglements which hinders and prevents transition of poly (lactic acid) chains [DD] and poly (lactic acid) chains – oligomer chains [OD] on the saturated surface MWCNT's.

5.1.1.2 PART II – HYBRID FILLER EFFECT

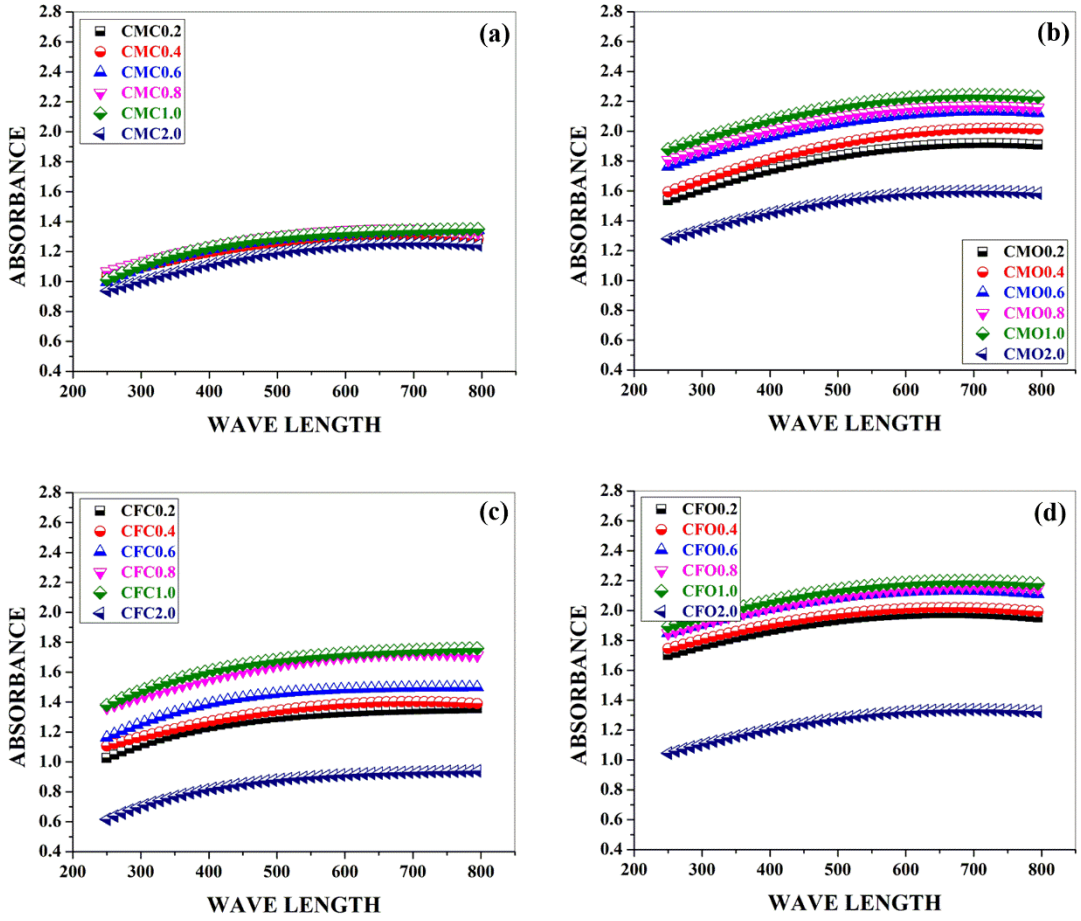

Figure 5.5: UV-VIS absorption spectra for hybrid poly (lactic acid) composites (a) DD and (b) OD 2.5wt% carbon black + (0.2, 0.4, 0.6, 0.8, 1.0 and 2.0wt%) of multiwalled carbon nanotubes filled poly (lactic acid) composites and (c) DD and (d) OD 2.5wt% carbon black + (0.2, 0.4, 0.6, 0.8, 1.0 and 2.0wt%) of cellulose nanofibers filled poly (lactic acid) composites (first "C" stands for 2.5wt% of carbon black, "M" for multiwalled carbon nanotubes, "F" for cellulose nanofibers and second "C" represents DD and "O" for OD)

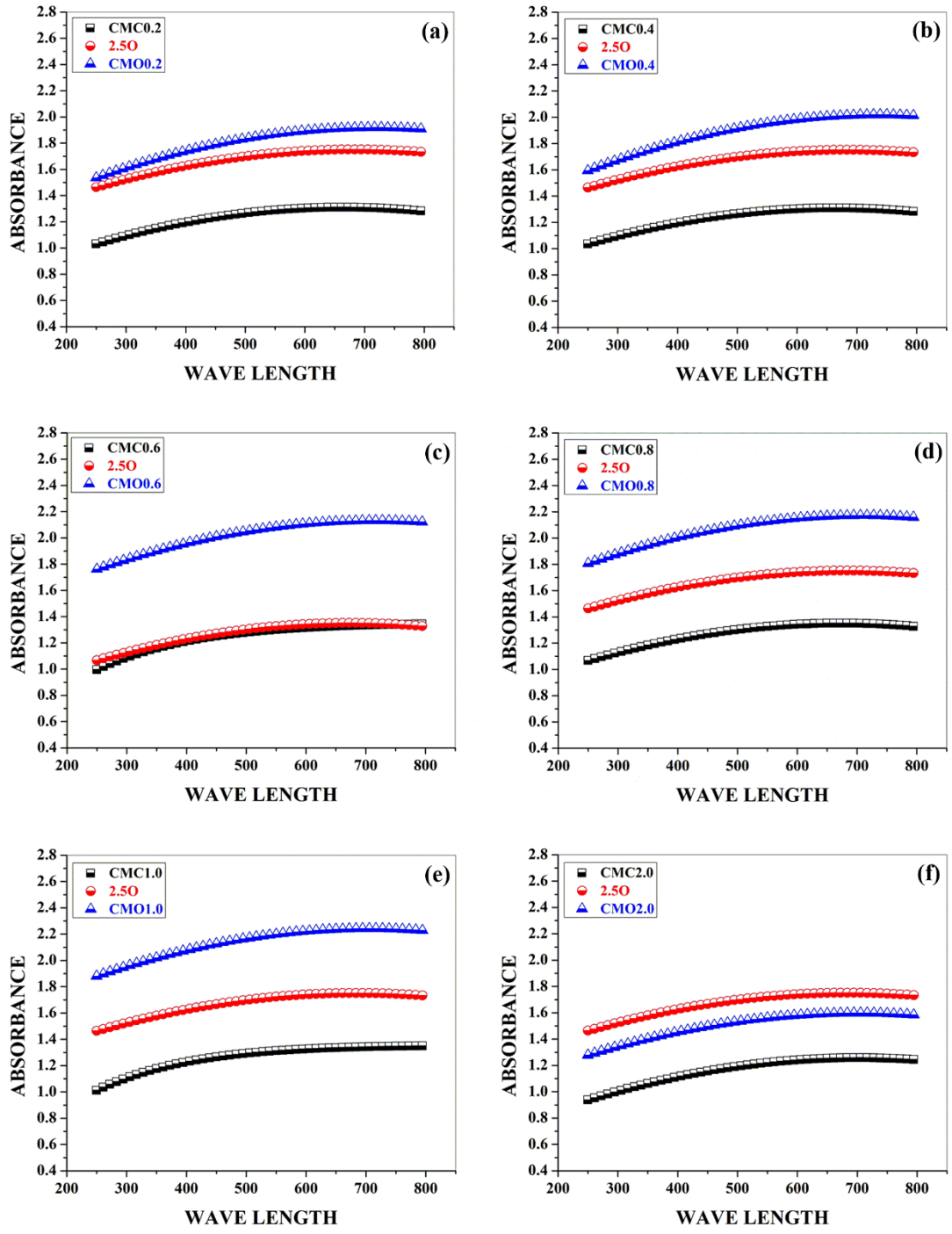

Figure 5.6: Comparison of UV-VIS absorption spectra for hybrid poly (lactic acid) composites, i.e., 2.5wt% carbon black with (a) 0.2 (b) 0.4 (c) 0.6 (d) 0.8 (e) 1.0 and (f) 2.0 multiwalled carbon nanotubes prepared via DD and OD in comparison to 2.5wt% filled poly (lactic acid) composites prepared via OD

Poly (lactic acid) composites with 2.5wt% of carbon black [OD] showed maximum absorbance in UV – VIS spectra and hence the concentration of 2.5wt% of carbon black were

selected for studying hybrid filler effect. Two batches of poly (lactic acid) composites with hybrid filler i.e. 2.5wt% of carbon black + 0.2, 0.4, 0.6, 0.8, 1.0 and 2.0wt% of MWCNT's and 2.5wt% of carbon black + 0.2, 0.4, 0.6, 0.8, 1.0 and 2.0wt% of CNF were prepared via DD and OD following the procedure mentioned in the method section.

From **Figure 5.5**, one can clearly observe that absorbance for hybrid filler poly (lactic acid) composites increased till 1.0wt% of a second filler, it be MWCNT's or CNF; after which a decrease is observed irrespective of the process used for preparing the hybrid filler poly (lactic acid) composites. Increase in absorbance till 1.0wt% of second filler can be attributed to bridged network formed between the fillers participating in the hybrid filler poly (lactic acid) composites and the decrease in absorbance can be attributed to agglomeration between the fillers participating in formation of hybrid filler poly (lactic acid) composites. One can observe that hybrid filler poly (lactic acid) composites prepared by OD showed maximum absorbance in UV – VIS spectra in comparison to hybrid filler poly (lactic acid) composites prepared by DD. Increase in absorbance for hybrid filler poly (lactic acid) composites prepared via OD can be attributed to increasing in the thickness of adsorbed layers due to difference in energy of interaction between poly (lactic acid) chains – oligomer chains which induces phases separation within the hybrid filler poly (lactic acid) composites[4].

The phase separation results in increased thickness of the adsorbed layers, due to the formation of bridge networks between the carbon black in high molecular weight poly (lactic acid) dissolution and second filler (it be MWCNT's and CNF) in oligomeric dispersion. These well-bridged structures in hybrid poly (lactic acid) composites form a connected network between the adsorbed layers at the interphase region and thereby increases the absorbance in UV – VIS. To have further information on shape factor and thickness of adsorption layers, the absorbance values of hybrid filler poly (lactic acid) composites prepared by using OD were compared with the absorbance of 2.5wt% carbon black filled poly (lactic acid) composites prepared using OD. On comparison made from **Figure 5.6** and **Figure 5.7** one can observe that absorbance of hybrid filler poly (lactic acid) composites shows maximum absorbance than 2.5wt% of carbon black filled poly (lactic acid) composites, till 1.0wt% of second filler (it be MWCNT's or CNF). At 2.0wt% of second filler (it be MWCNT's or CNF), a decrease in absorbance in comparison to 2.5wt% of carbon black filled poly (lactic acid) composites was observed. The increase in absorbance for hybrid filler poly (lactic acid) composites prepared using OD, till 1.0wt% of second filler (it be MWCNT's or CNF) can be attributed to the increased thickness of adsorbed layers formed at interphase regions within hybrid filler poly (lactic acid) composites. The decrease in absorbance for hybrid filler poly

(lactic acid) composites prepared using OD, at 2.0wt% of second filler (it be MWCNT's or CNF) is well attributed to the reduction in the size of adsorption layers.

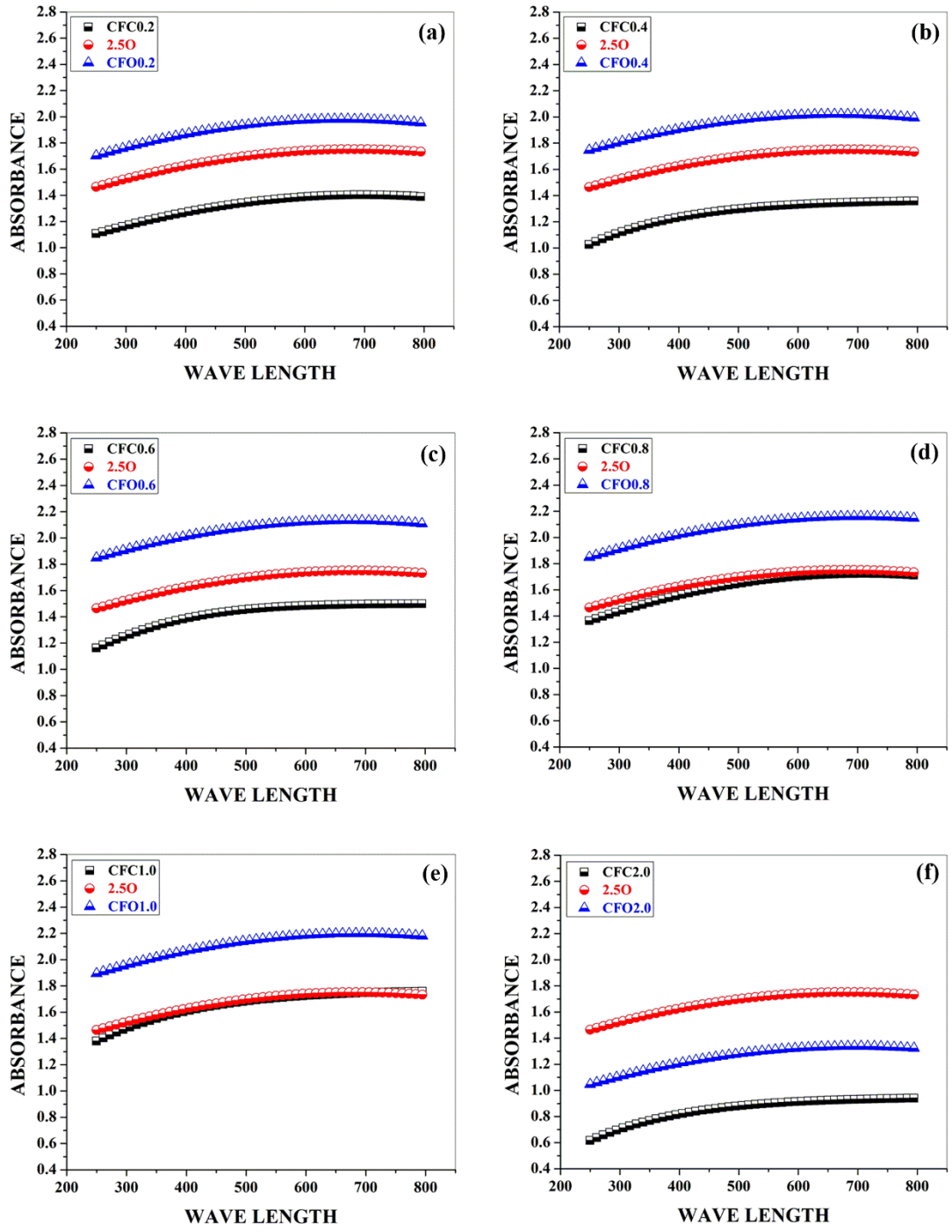

Figure 5.7: Comparison of UV-VIS absorption spectra for hybrid poly (lactic acid) composites, i.e., 2.5wt% carbon black with (a) 0.2 (b) 0.4 (c) 0.6 (d) 0.8 (e) 1.0 and (f) 2.0 cellulose nanofibers prepared via DD and OD in comparison to 2.5wt% filled poly (lactic acid) composites prepared via OD

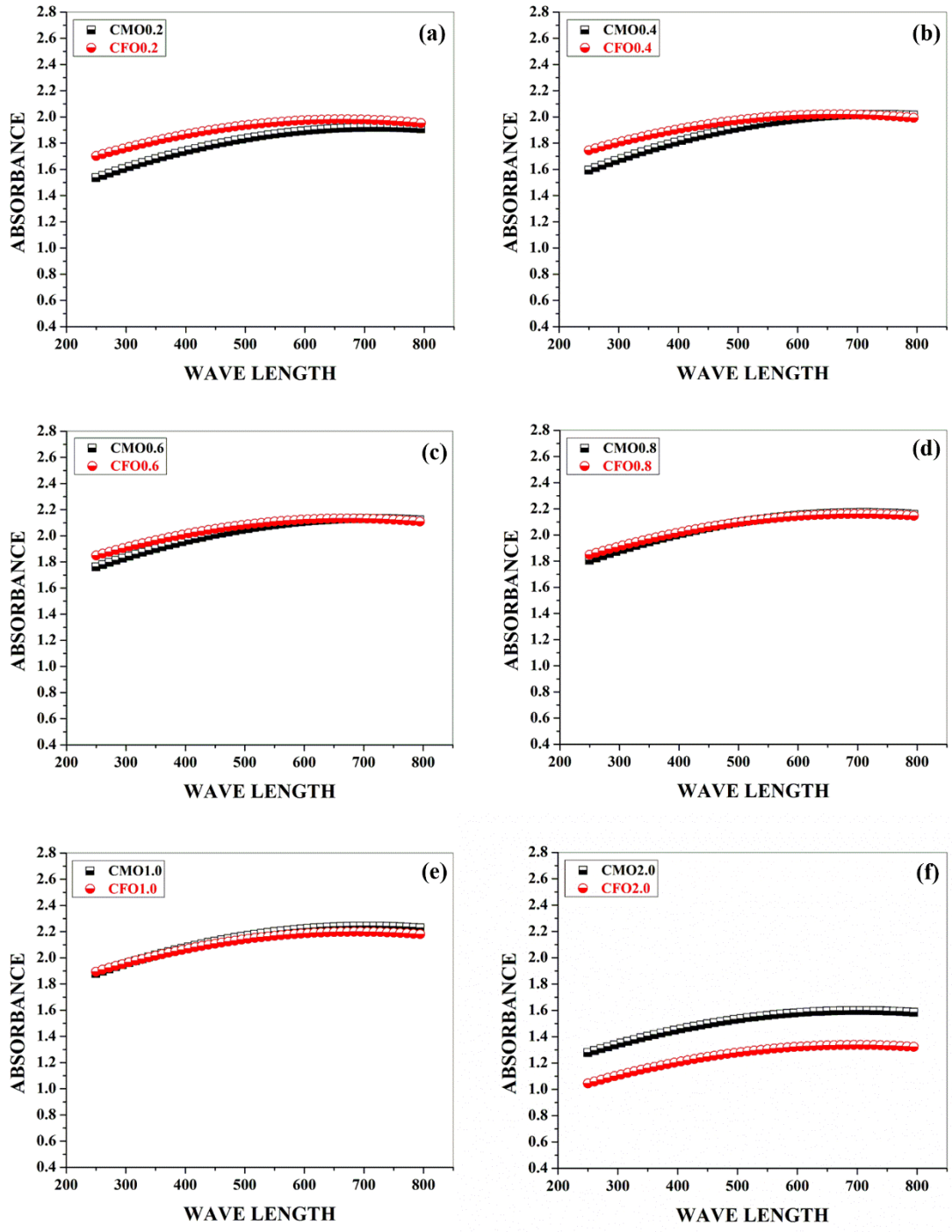

Figure 5.8: Comparison of UV-VIS absorption spectra for hybrid poly (lactic acid) composites with an equal concentration of second filler [MWCNT's and CNF] prepared using OD

The increase in absorbance can be correlated to phase separation with strong adlayers and the decrease can be related to minimization of phase separation owing to the presence of fillers with physical entanglements formed within hybrid filler poly (lactic acid) composites.

One shall observe an increase in the absorbance at higher wavelength; the absorbance pattern till 1.0wt% of second filler (it be MWCNT's or CNF) can be attributed to "near to homogenous dispersion" with strong adlayers formed within hybrid filler poly (lactic acid) composites.

Likewise, increase in absorbance at higher wavelength for hybrid filler poly (lactic acid) composites with 2.0wt% of second filler (it be MWCNT's or CNF) can be related to strength of the physical entanglements formed within hybrid filler poly (lactic acid) composites. Decrease in absorbance at lower wavelength can be attributed to the decrease in strength of adlayers as well as physical entanglements formed within hybrid filler poly (lactic acid) composites. Hybrid filler poly (lactic acid) composites prepared using DD with CNF and 2.5wt% of carbon black shows maximum absorbance range in comparison to the absorbance of hybrid filler poly (lactic acid) composites with MWCNT and 2.5wt% carbon black [see **Figure 5.5a** and **5.5c**]. On preparing the hybrid poly (lactic acid) using OD, near to close absorbance was observed, which is graphed in **Figure 5.8**. A minor increase in absorbance is seen for hybrid filler poly (lactic acid) composites with 0.2wt% and 0.4wt% CNF in comparison to hybrid filler poly (lactic acid) composites with 0.2wt% and 0.4wt% MWCNT's as seen in **Figure 5.8(a)** and **5.8(b)**. Absorbance for hybrid filler poly (lactic acid) composites with 0.6wt%. 0.8wt% and 1.0wt% of second filler (it be MWCNT's or CNF) remain almost similar as observed in **Figure 5.8(c), 5.8(d)** and **5.8(e)**. A decrease in absorbance was observed for hybrid filler poly (lactic acid) composites with 2.0wt% of CNF in comparison to hybrid filler poly (lactic acid) composites with 2.0wt% of MWCNT's. A slight increase in absorbance for hybrid filler poly (lactic acid) composites with 0.2wt% and 0.4wt% of CNF can be attributed to the ability of CNF to form bridge network in comparison to MWCNT's in hybrid filler poly (lactic acid) composites with 0.2wt% and 0.4wt% of MWCNT's.

This slight increase in absorbance can be related to the nature of hybrid effect of CNF at 0.2wt% and 0.4wt% with 2.5wt% carbon black favoring phase separation and thus increasing the thickness of the adsorbed layers in the interphase region. Whereas a decrease in absorbance for hybrid filler poly (lactic acid) composites with 2.0wt% of CNF can be attributed to hydroxyl functional groups on CNF interacting strongly with poly (lactic acid) chains and oligomeric chains; and are responsible for the decrease in thickness of the adsorption layers in interphase region of hybrid filler poly (lactic acid) composites. Close to absorbance in hybrid filler poly (lactic acid) composites filled with 0.6wt%, 0.8wt% and 1.0wt% of second filler (it be MWCNT's or CNF) indicates that there is no much difference in the thickness of adsorption layers but strength of adlayers may vary depending on the functional groups

present on the filler surface. A slight increase in the absorbance at higher wavelength attributes to the formation of strong adlayers and is observed for hybrid filler composites filled with MWCNT's; whereas a slight decrease in absorbance at higher wavelength is observed for hybrid filler composites filled with CNF which indicates a minor decrease in strength of adlayers. An increase in the thickness of adsorption layers using OD with strengthened adlayers helps in optimizing the structure for interphase of poly (lactic acid) composites with enhanced stiffness, strength and toughness[4][144].

5.1.2 CONCLUSION

Poly (lactic acid) composites prepared using OD showed an increase in UV – VIS absorbance in comparison to DD poly (lactic acid) composites. Phase separation occurring between high molecular poly (lactic acid) and oligomeric dispersion with the bridged network between the fillers is responsible for the increase in the thickness of the adsorption layers in interphase regions of the composites. A decrease in the absorbance at higher concentration of filler can be attributed to the formation of the weak skeletal network, i.e. physical entanglements; wherein filler – filler interaction increases with decrease in polymer – filler interaction and is a responsible factor for the decrease in the adsorption thickness in the interphase region of the composites. Increase and decrease in the absorbance at higher and lower wavelength respectively can be attributed to the increase and decrease in strength of adlayers and physical entanglements in the interphase region of poly (lactic acid) composites. Manuscript published in Materials Performance and Characterizations,9 (1), 2020, 518 - 530.

5.1.3 LIMITATION OF ULTRAVIOLET – VISIBLE SPECTROSCOPY

Ultraviolet Visible spectroscopy was unable to determine the interface modifications within cellulose nanofibers reinforced poly (lactic acid) composites, owing to inability of poly (lactic acid) and/or cellulose nanofibers to absorb ultraviolet – visible source. Hence density measurements were performed, and graphical representations can be observed in **Figure 5.9** and **5.10**

5.2 DENSITY

5.2.1 ABSTRACT

Density measurements are quick, efficient and crucial in determining the structure and quality of solid materials. For polymer composites, properties tend to increase and/or decrease with density.

5.2.1.1 PART I – SINGLE FILLER EFFECT

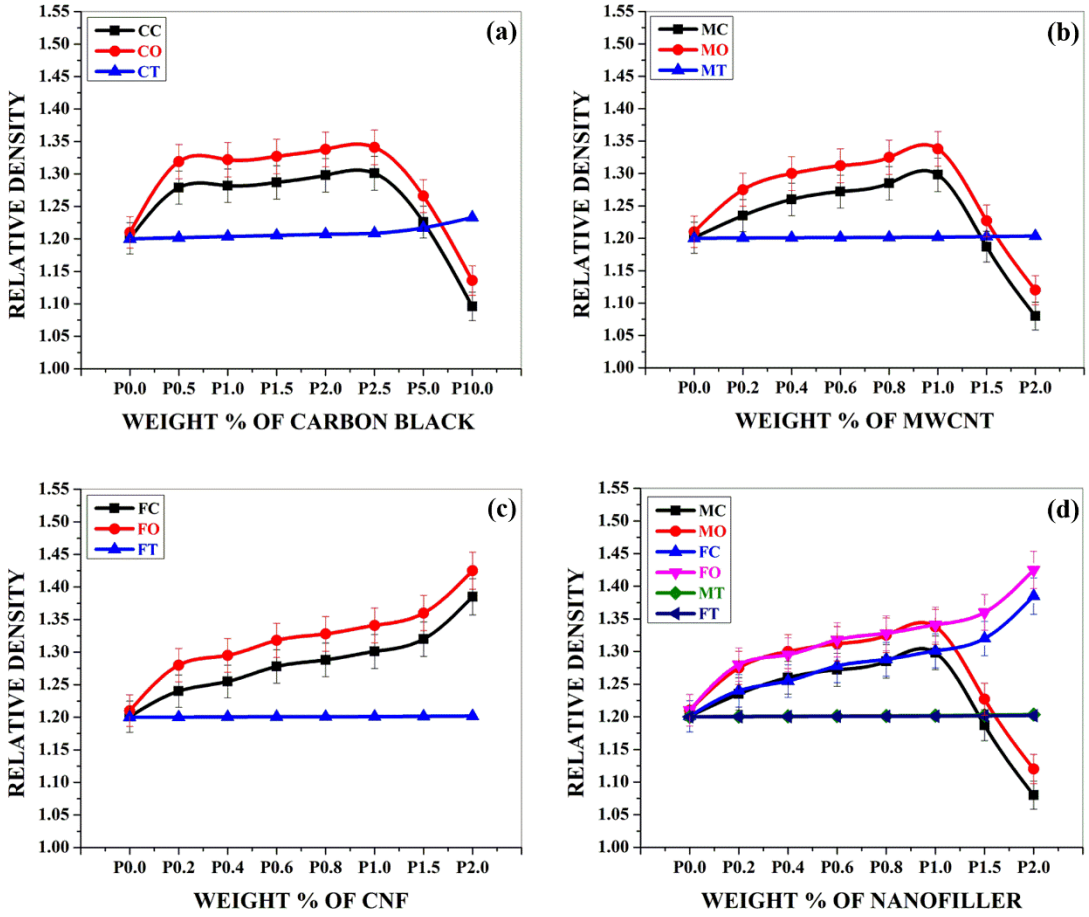

Figure 5.9: Comparison of density values for poly (lactic acid) composites prepared by dissolution dispersion [DD] and oligomeric dispersion [OD] ["C" represents DD, "O" for OD and "T" for Theoretical density] filled with (a) carbon black (C) (b) multiwalled carbon nanotubes (M) (c) cellulose nanofibers (F) (d) comparison between multiwalled carbon nanotubes and cellulose nanofibers

From the **Figure 5.9**, it can be observed that density of single filler filled poly (lactic acid) composites prepared by OD has numerical value of density higher than poly (lactic acid) composites prepared by DD. This increase in density for poly (lactic acid) composites prepared by OD can be attributed to formation of interconnected interphase layers between the poly (lactic acid) – filler surface – oligomer – filler surface (mechanical interlocking), increasing the thickness of the interphase region, due to phase separation and filler chain links. Theoretical density for single filler poly (lactic acid) composites were calculated; experimental density values were higher and lower than theoretical value. The increase in the experimental value with respect to theoretical value can be attributed to maximum filler surface – poly (lactic acid) chains adsorption and the decrease in the experimental value with

respect to theoretical value can be due to unavailability of poly (lactic acid) chains to cover the surface of filler which increases the free volume and decreases the value of density Similar observations were made for hybrid filler poly (lactic acid) composites (**see figure 5.10**) i.e., density of poly (lactic acid) composites prepared by OD >> density of poly (lactic acid) composites prepared by DD; and can be attributed to phase separation, filler poly (lactic acid) chain links between poly (lactic acid) – filler surface – oligomer – filler surface[131].

5.2.1.2 PART II – HYBRID FILLER EFFECT

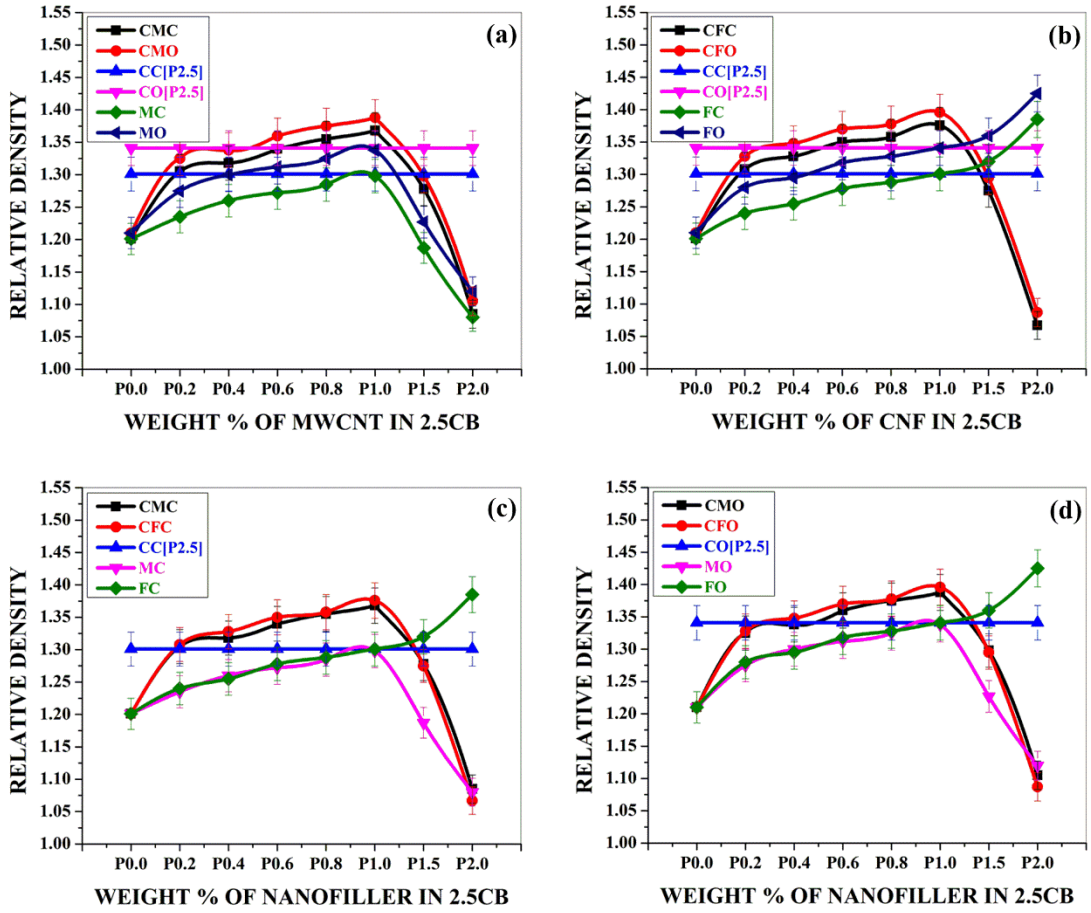

Figure 5.10: Comparison of density values for hybrid poly (lactic acid) composites prepared by dissolution dispersion [DD] and oligomeric dispersion [OD] filled with (a) 2.5wt% carbon black + multiwalled carbon nanotubes (0.2, 0.4, 0.6, 0.8, 1.0, 1.5 and 2.0wt%) (b) 2.5wt% carbon black + cellulose nanofibers (0.2, 0.4, 0.6, 0.8, 1.0, 1.5 and 2.0wt%) (c) comparison between hybrid poly (lactic acid) composites prepared by DD (d) comparison between hybrid poly (lactic acid) composites prepared by OD

At higher concentration of carbon black (5wt% and 10wt%) and multiwalled carbon nanotubes (1.5wt% and 2.0wt%) decrease in density is observed, which can be attributed to

unavailability of poly (lactic acid) chains to adsorb on filler surface due to which free volume increases and decreases density. On other hand density for poly (lactic acid) composites filled with cellulose nanofibers density increases in direct proportion to weight percent of cellulose nanofibers. This increase in magnitude of density can be attributed to strong and thick interphase region formed due to chemical activity of hydroxyl groups on cellulose nanofibers and carbonyl group of poly (lactic acid) chains. Addition of 0.2, 0.4, 0.6, 0.8, 1.0 and 1.5wt% of nanofillers (i.e., multiwalled carbon nanotubes and cellulose nanofibers) to 2.5wt% of carbon black increases the density of hybrid poly (lactic acid) composites. The increase in the density can be attributed to the increase in the thickness of adsorption layer i.e. interphase region. Addition of nanofillers to poly (lactic acid) composites occupies the free space between carbon black particles in poly (lactic acid) composites and increases the packing which increases the thickness of the interphase regions; and contributes to increase in magnitude of the density[131].

5.2.2 CONCLUSION

Poly (lactic acid) composites prepared with oligomeric dispersion [OD] shows increase in density values, which is attributed to the phase separation along with the filler chain links between the poly (lactic acid) – filler surface – oligomer – filler surface .Hybrid poly (lactic acid) composites shows increase in the density of the composites when compared with their single filled (it be carbon black, multiwalled carbon nanotubes and cellulose nanofibers) poly (lactic acid) composites. Decrease in the density is observed, which can be attributed to unavailability of poly (lactic acid) chains to cover the filler surface, due to which voids are formed within the poly (lactic acid) composites; these voids are responsible for decrement in the density of poly (lactic acid) composites.

5.3 FINAL CONCLUSION

Analysis made through conclusion in **Section 5.1.2** and **Section 5.2.2**, states that modification in interphase region took place when poly (lactic acid) composites were prepared by oligomeric dispersion. Modification in the interphase region is characterized through change in the absorbance in UV – Visible spectra and magnitude of density. Here modification in interphase region is accounted to the thickness and filler chain links within the poly (lactic acid) matrix. Structural analysis via ATR – FTIR as discussed in **Chapter 6** also proves to be an additional technique in determining the physical and chemical interactions in polymer composites irrespective of the filler used in polymer composites.

6 STRUCTURAL ANALYSIS

Measurements through ultraviolet – visible spectroscopy (**Section 5.1**) and density (**Section 5.2**), confirmed oligomeric dispersion as the best method with thick interphase region and hence confirms itself as a method to process and design a poly (lactic acid) composites and hybrid poly (lactic acid) composites. Hence further testing and characterizations would focus on understanding the structural, morphological and mechanical properties of poly (lactic acid) composites and hybrid poly (lactic acid) composites fabricated by oligomeric dispersion. The role of ATR – FTIR in analyzing poly (lactic acid), composites and hybrid composites is discussed in this chapter.

A manuscript including a part of this chapter was published in “Materials Performance and Characterization 8,no. 1 (2019): pp617–625. ASTM International”

In this chapter, structural aspects of carbon black filled poly (lactic acid) composites are discussed. Numerical data on spectral parameters for poly (lactic acid) composites filled with multiwalled carbon nanotubes, cellulose nanofibers, carbon black + multiwalled carbon nanotubes, carbon black + cellulose nanofibers are tabulated and inclined to discussions made for carbon black filled poly (lactic acid) composites.

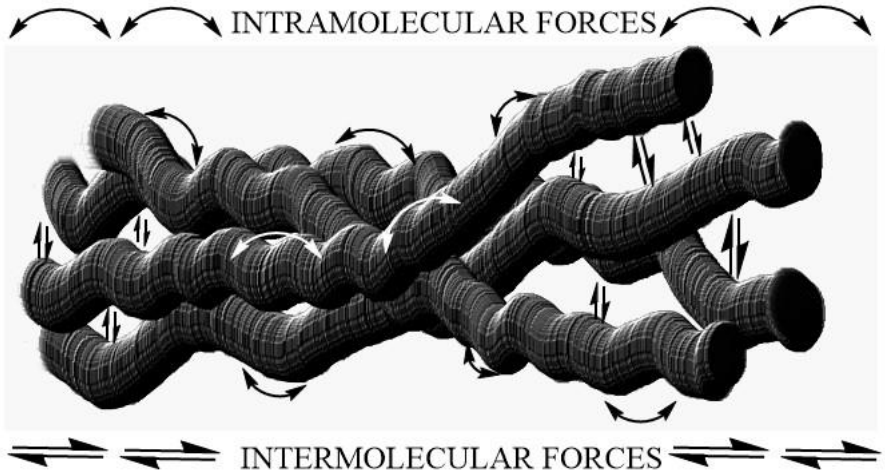

Figure 6.1: Intramolecular and Intermolecular forces of attraction existing within polymer composites

6.1 CARBON BLACK

6.1.1 ROLE OF ATR – FTIR SPECTROSCOPY

Structural analysis through infrared spectroscopy is presented in this chapter. Infrared Spectroscopy helps in investigating the relationship between the structure of polymer composites and their structure sensitive properties by molecular interactions. Neat poly (lactic

acid) and filled poly (lactic acid) composites were fabricated via oligomeric dispersion and characterized for structural analysis. Composites filled with specific wt% of specific filler showed increased mechanical properties in tensile mode, were compared with neat and other filled poly (lactic acid) composites. Hence an interest to analyze the structure – property dependence via Attenuated Total Reflectance Fourier Transform Infrared Spectroscopy [ATR – FTIR] for neat poly (lactic acid) and filled poly (lactic acid) composites was felt. Analyzing ATR – FTIR spectrographs for neat poly (lactic acid) and filled poly (lactic acid) composites confirmed strong interactions on addition of specific quantity and shape of filler. Displacement [i.e. shift], % transmittance and area of absorption peaks in infrared spectra, confirmed the strength of molecular interaction in poly (lactic acid) composites and are corroborated with the numerical values of the mechanical properties in tensile mode.

6.1.2 INTRODUCTION

Due to a wide range of applications of polymeric materials, there has been a growing interest in polymer composites where fillers of micro and nano dimension impart specific structural and functional properties to the final product. Molecular level interactions are tailored to achieve required performance. Short time quality measurements are utmost important in predicting the performance of a composite material – hence, infrared spectroscopy was used to determine the structural properties and functional features of polymer composites. Incorporating optimized quantity of particulate filler of high aspect ratio and large surface area in a polymer matrix. These properties tends to form strong intermolecular interactions between filler particles and polymer, leading to polymer composites with required modulus and stiffness. Nature and dimension of filler, concentration, polymer type, filler dispersion, filler-polymer compatibility are vital tools which make polymer composites applicable in engineering applications. Properties of all materials arise from their structure, owing to which studies correlating structure and properties of the materials should be given standing position and practiced. Many of the properties of materials are best-understood in-terms of the structure of the atom and the ways in which atoms join to form molecules, crystals, and macro-units of matters. The atom can be seen as consisting of two main parts, the heavy nucleus and the surrounding highly structured configuration of electrons; both are equally important in the explanation of the properties of engineering materials. It is of prime importance to note that the electrons particularly those in the outer most orbitals, the valence electrons determine many engineering properties of materials such as physical & chemical reactivity, binding patterns established with other atoms and thus strength characteristics,

electrical properties and optical characteristics. Out of several characterizations techniques to determine intermolecular interactions infrared spectroscopy is best suited for polymers, fillers and their composites[131][2][145][146][147][148][149][150][151].

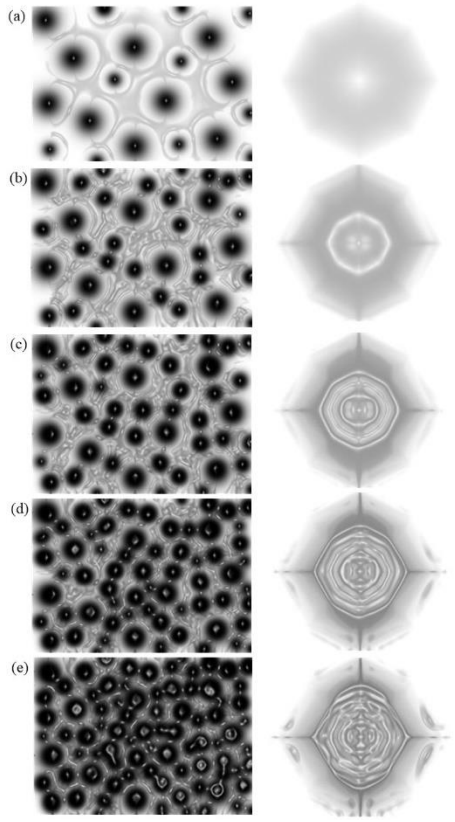

Figure 6.2: Schematic representation of Carbon black filled poly (lactic acid) at 0.5, 1.0, 1.5, 2.0 and 2.5wt%

Infrared spectroscopy measures the behavior of polymer composites in the presence of electromagnetic radiations analyzing the extent of interaction of fillers with polymers building a bridge between molecular level information and mechanical properties of polymer composites. Furthermore, Attenuated Total Reflectance Fourier Transform Infrared Spectroscopy [ATR – FTIR] is a technique providing sensitive, relatively quick, non-destructive test in determining molecular interactions in polymer composites. Acrylonitrile/palm fibres, polystyrene/ block copolymer of poly(styrene-butadiene), epoxy resin/ carbon fibres, poly (vinyl chloride)/hardwood and wood polymers, poly (lactic acid)/ epoxidized palm oil, polyester resin/clay, poly (vinylene difluoride)/ multiwalled carbon nanotubes, poly (vinyl acetate)/coir fibres have been studied. Determining molecular interactions within nanocomposites to understand its properties for material development is a need. Considering its need and growing interest in revealing molecular-level information on polymers, fillers, and composites – spectroscopic techniques are required. Mechanical

properties are also used to study polymer composites; in general, a polymer composite with strong intermolecular interactions has enhanced mechanical strength. In spite of previous studies, greater clarity is still needed on the reinforcing effects of fillers in poly (lactic acid). In this study, neat poly (lactic acid) sheet and filled poly (lactic acid) sheets are prepared with different weight percent of fillers by oligomeric dispersion method for structural analysis through ATR – FTIR. Characteristics absorption peaks of neat poly (lactic acid) are compared with absorption peaks of carbon black filled poly (lactic acid) composites to detect molecular interactions, with respect to displacement, % transmittance and area of absorption peaks. A comparative study of filled poly (lactic acid) composites with neat poly (lactic acid) is of interest to determine the reinforcement efficiency of fillers within poly (lactic acid) composites.

6.1.3 RESULTS AND DISCUSSION

6.1.3.1 RESULTS

6.1.3.1.1 ABSORPTION BANDS OF POLY (LACTIC ACID)

Absorption bands in ATR – FTIR spectra ($600cm^{-1}$ – $4000cm^{-1}$) for neat poly (lactic acid) elucidates $603.72cm^{-1}$, $669.3cm^{-1}$ for strong C-H bend; 704.02 cm^{-1}, 754.17 cm^{-1}, 866.04 cm^{-1} for strong C-COO stretch; $1045.42cm^{-1}$, $1082.07cm^{-1}$, $1128.36cm^{-1}$, $1182.36cm^{-1}$, 1267.23 cm^{-1}, $1315.45cm^{-1}$ for strong C-O stretch; 1359.82 cm^{-1} for medium C-H rocking; 1381.03 cm^{-1} for weak $-CH_3$; $1452.4cm^{-1}$ for strong $-CH_3$; $1749.44cm^{-1}$ for strong C=O stretch; 2943.37 cm^{-1}, $2995.45cm^{-1}$ for strong $-CH_2$ stretch. Out of the absorption peaks for neat poly (lactic acid) we shall observe the effect of carbon black particles on the characteristics peaks, those are $1749.44cm^{-1}$ -C=O stretching peak of poly (lactic acid); C-O- bond stretching in -CH-O- at $1182.36cm^{-1}$; and characteristics peaks ascribed to -C-O- stretching vibration in -O-C=O group at $1128.36cm^{-1}$, $1082.07cm^{-1}$ and $1045.42cm^{-1}$.

6.1.3.1.2 ABSORPTION BANDS OF CARBON BLACK

Absorption spectra for carbon black portraits $613.36cm^{-1}$, $638.44cm^{-1}$, $669.3cm^{-1}$ for strong C-H bend; $719.45cm^{-1}$,$738.74cm^{-1}$ for medium C-H out of plane; $966.34cm^{-1}$ for strong =C-H out of plane; $1020.34cm^{-1}$, 1178.51 cm^{-1}, $1228.66cm^{-1}$, $1313.52cm^{-1}$ for strong C-O stretch; $1338.6cm^{-1}$ for strong S=O, sulfone; $1359.82cm^{-1}$, $1396.46cm^{-1}$ for strong S=O, sulphate; $1417.68cm^{-1}$, $1454.33cm^{-1}$, $1490.97cm^{-1}$ for medium C-C in ring stretch; $1519.91cm^{-1}$ for medium N-O;$1539.2cm^{-1}$ for NH out of plane; $1597.06cm^{-1}$, $1647.21cm^{-1}$ represents strong conjugated dienes; $1770.65cm^{-1}$, 1793.8 cm^{-1} for strong C=O stretch, 1888.31 cm^{-1}could not be traced; $1942.32cm^{-1}$ for tricarbonyl; $2013.68cm^{-1}$ for N=C in R-N=C=S; $2912.51cm^{-1}$ for

strong C-H stretch; 3685.97cm^{-1} represents isolated hydroxyls; 3745.76cm^{-1} represents silanol band in amorphous materials and acts as adsorption sites for surface hydrolysis and source of hydroxyl radicals; 3799.77cm^{-1} represents free OH stretching.

Characteristics absorption bands for neat poly (lactic acid) and carbon black are in line with the work carried out by Elisabeta et al and Rositani et al respectively[152][153]. Detailed representation of all the absorption peaks (characteristics peaks, shifts in absorption peaks and new absorption peaks) for neat poly (lactic acid) and carbon black filled poly (lactic acid) composites are well presented in **Table 6.1**. Intensity and Area of characteristics peaks for neat poly (lactic acid) and their shifts in wave number are represented in **Table 6.2**.

6.1.3.2 DISCUSSION

6.1.3.2.1 ABSORPTION BANDS

Many factors influence the precise wavenumber of molecular vibration, and it was impossible to isolate one effect from another. Here we shall discuss the change in % transmittance and area, which are brought about by structural changes in the molecule, due to change in polarity (change in % transmittance) and hydrogen bonding (change in the area). Intramolecular hydrogen bonding is within the same chain; hence it is not affected by a change in intermolecular distances, thus intramolecular hydrogen bonds of poly (lactic acid) are least affected by the addition of carbon black (**see Figure.6.1**) and hence does not play much role in polymer composites. Hence intermolecular interactions are considered important in imparting required properties to polymer composites.

Poly (lactic acid) composites with low concentration of carbon black forms few numbers of strong hydrogen bonds depending on the dispersion of carbon black in poly (lactic acid) matrix, but as the concentration of carbon black increases a greater number of intermolecular hydrogen bonds are formed due to increase in probability of molecular contact between poly (lactic acid) and carbon black (**see Figure.6.2**). Thus, intermolecular hydrogen bonding is concentration dependent. Firstly 1749.44 cm^{-1}, represent characteristics stretching peak of strong C=O in neat poly (lactic acid). Stretching vibration usually cause peaks of high % transmittance. For absorption peak at 1749.44cm^{-1}, one may observe a decrease in % transmittance for carbon black filled poly (lactic acid) composites in comparison to % transmittance for neat poly (lactic acid) (**see Table 6.2**). A sharp decrease in % transmittance is observed till 1.0wt% of carbon black which can be attributed to decrease in stretching vibration of C=O bond, due to intermolecular interactions induced by addition of carbon black. Further, an increase in % transmittance [lower than neat poly (lactic acid)] was observed for

1.5wt% to 2.5wt% with a decreasing trend [lower than the neat poly (lactic acid)], confirmed the formation of strong polar interactions between C=O of poly (lactic acid) and surface functional groups present on carbon black. On contrary area of the absorption peak for filled composites increases in comparison with area of absorption peak for neat poly (lactic acid). Area of the absorption peak for 1749.44cm^{-1} increased up to 1.5wt% of carbon black and further decreases till 2.5wt% of carbon black [higher than neat poly (lactic acid)]. Increase in area attributes to strong hydrogen bonds and broadens the absorption peak. C=O is the characteristics group of neat poly (lactic acid) which is inclined to physical and chemical interactions with surface functional groups of carbon black. Coupling vibrations, hydrogen bonding, and inductive effect between poly (lactic acid) and carbon black within carbon black filled poly (lactic acid) composites might be a possible reason for the decrease in % transmittance and increase in the area of carbon black filled poly (lactic acid) composites. The absorption peak at 1182.36cm^{-1} represents C-O- bond stretching in -CH-COO- in the neat poly (lactic acid) matrix. The % transmittance of 1182.36cm^{-1} decreases as the percentage of carbon black increases when compared with neat poly (lactic acid). Within the batches, decrease in % transmittance values is observed for all batches [compared to neat poly (lactic acid)] as seen in **Table 6.2**. Shifts to higher positions are relative to bond strength, i.e. stiffness which is due to strong bonds. Shift to 1184.29cm^{-1} was observed for 0.5wt%, 1.5wt% and 2.0wt%. The shift in wavenumber can be attributed to structural changes in the poly (lactic acid) composites, i.e., by the intermolecular interaction between functional groups on surface of carbon black and C-O- of poly (lactic acid) within carbon black filled poly (lactic acid) composites. In spite of a shift at higher position, % transmittance for 0.5wt%, 1.5wt%, and 2.0wt% lies below the % transmittance as observed for neat poly (lactic acid), which confirms strong interaction between carbon black and poly (lactic acid) in composites. For poly (lactic acid) composites with 2.5wt% of carbon black, there is no shift in wavenumber but a decrease in % transmittance and increase in area is observed. The decrease in % transmittance can be attributed to a decrease in stretching vibrations of C-O- bond stretching in -CH-COO- in the poly (lactic acid) matrix due to the addition of carbon black. As noted in **Table 6.2**, area increases as the carbon black content increases in poly (lactic acid) composites; which can be attributed to formation of strong hydrogen bonds within the carbon black filled composites.

Absorption peaks at 1045.42cm^{-1}, 1082.07$cm^{-1,}$ and 1128.36cm^{-1} are assigned to stretching vibrations of -C-O- in -O-C=O. Observing the data in **Table 6.2**, we conclude that similar observation as made for 1749.44 cm^{-1} and 1182.36 cm^{-1}, wherein the % transmittance of

peaks decreases, and area increases in comparison to the % transmittance and area of neat poly (lactic acid)[154].

Table 6.1: Absorption peaks in neat poly (lactic acid) and its carbon black filled poly (lactic acid) composites

Neat PLA	0.5wt%	1.0wt%	1.5wt%	2.0wt%	2.5wt%
603.72	✗	✗	✗	✗	✗
669.3	✗	✗	✗	✓	✗
704.02	✗	✓	✓	✗	✓
754.17	✓	✓	✗	✓	✗
866.04	✗	✗	✗	✗	✓
1045.42	✓	✓	✓	✓	✓
1082.07	✓	✓	✓	✗	✓
1128.36	✓	✓	✗	✗	✓
1182.36	✗	✓	✗	✗	✓
1267.23	✓	✓	✓	✓	✓
1315.45	✗	✓	✓	✓	✗
1359.82	✓	✓	✓	✓	✓
1381.03	✓	✓	✗	✗	✓
1452.4	✓	✓	✓	✓	✓
1749.44	✓	✓	✓	✓	✓
2943.37	✗	✗	✗	✗	✗
2995.45	✓	✓	✓	✓	✓
Shifts	0.5wt%	1.0wt%	1.5wt%	2.0wt%	2.5wt%
667.37	✓	✓	✓	✗	✓
702.09	✗	✗	✗	✓	✗
705.95	✓	✗	✗	✗	✗
752.24	✗	✗	✓	✗	✓
867.97	✓	✓	✓	✓	✗
1083.99	✗	✗	✗	✓	✗
1126.43	✗	✗	✓	✓	✗
1184.29	✓	✗	✓	✓	✗
1317.38	✓	✗	✗	✗	✓

1375.25	✗	✗	✓	✗	✗
2945.3	✓	✓	✓	✓	✓
New Bands	0.5wt%	1.0wt%	1.5wt%	2.0wt%	2.5wt%
613.36	✗	✗	✗	✗	✓
617.22	✓	✗	✗	✗	✗
896.9	✗	✗	✗	✗	✓
898.83	✓	✓	✗	✗	✗
902.69	✗	✗	✗	✓	✗
904.61	✗	✗	✓	✗	✗
952.84	✗	✓	✓	✓	✗
954.76	✓	✗	✗	✗	✗
956.69	✗	✗	✗	✗	✓
1624.06	✗	✗	✓	✗	✗
1629.85	✓	✗	✗	✗	✗
2428.38	✗	✗	✗	✗	✓
2438.02	✗	✗	✗	✓	✗

Note: ✗ = absence of absorption band; ✓ = presence of absorption band; **Neat PLA** = neat poly (lactic acid); **Shifts**: shifting of the absorption bands on a spectra; **New Bands**: newly formed absorption bands on a spectra; **0.5wt%** = 0.5wt% of carbon black in poly (lactic acid); **1.0wt%** = 1.0wt% of carbon black in poly (lactic acid); **1.5wt%** = 1.5wt% of carbon black in poly (lactic acid); **2.0wt%** = 2.0wt% of carbon black in poly (lactic acid); **2.5wt%** = 2.5wt% of carbon black in poly (lactic acid).

The decrease in % transmittance of absorption peaks for carbon black filled poly (lactic acid) composites may be attributed to decrease in stretching vibration of -C-O- in -O-C=O structure of poly (lactic acid) owing to the presence of carbon black in the poly (lactic acid) matrix. One may observe that 1128.36 cm^{-1} shifts to 1126.43 cm^{-1} for 1.5wt% and 2.0wt% of carbon black filled poly (lactic acid) composites. 1082.07 cm^{-1} shifts to 1083.99 cm^{-1} for 2.0wt% filled poly (lactic acid) composites. The shift in 1128.36 cm^{-1} and 1082.07 cm^{-1} can be attributed to strong intermolecular interactions reducing the bond length within filled poly (lactic acid) which contributes to an increase in bond strength of the filled composites (**see Figure.6.1** and **Figure.6.2**). Although there is a shift in wavenumbers, the % transmittance is lower and the increase in area is observed. Area values for 1045.42 cm^{-1}, 1082.07 cm^{-1} and 1128.36 cm^{-1} show higher value in comparison with the neat poly (lactic acid). Higher area values can be due to the formation of strong hydrogen bonds, i.e., intermolecular interaction between poly

(lactic acid) and carbon black at varied concentration within carbon black filled poly (lactic acid) composites.

Table 6.2: %Transmittance and Area for characteristics peaks of neat poly (lactic acid) and its shifts in carbon black filled poly (lactic acid) composites

Wave number (cm^{-1})	Neat poly(lactic acid)		0.5wt% of carbon black		1.0wt% of carbon black	
	%T	**A**	**%T**	**A**	**%T**	**A**
1749.44	55.59	9.855	46.811	12.146	43.743	13.176
1182.36→**1184.29**	58.243	10.011	**50.027**	**12.606**	47.63	13.496
1082.07	44.355	13.288	34.491	16.577	31.842	17.776
1045.42	67.864	6.073	61.64	7.561	59.553	7.93
1128.36	69.58	4.164	63.106	5.226	60.96	5.949
866.04→**867.97**	89.016	1.654	**86.831**	**1.891**	**85.816**	**2.118**
754.17	76.736	4.193	64.776	6.4	60.988	7.577

Wave number (cm^{-1})	1.5wt% of carbon black		2.0wt% of carbon black		2.5wt% of carbon black	
	%T	**A**	**%T**	**A**	**%T**	**A**
1749.44	54.572	10.319	51.514	11.075	50.983	10.596
1182.36→**1184.29**	**56.615**	**10.971**	**55.146**	**11.406**	52.06	11.325
1082.07→**1083.99**	40.665	14.995	**39.193**	**15.366**	39.56	14.592
1045.42	63.609	7.982	64.359	7.067	64.218	7.257
1128.36→**1126.43**	**67.419**	**4.606**	**66.779**	**4.703**	65.773	4.583
866.04→**867.97**	**85.695**	**2.795**	**87.895**	**2.012**	87.277	1.959
754.17→**752.24**	**66.27**	**7.192**	66.873	6.432	**65.917**	**6.309**

Note: **%T** = Percent transmittance; **A** = Area under absorption peak; → indicates shift in absorption band; Bold digits in table indicates the numerical value of %transmittance and area under absorption peak for shifted absorption band.

The absorption peak at 754.17 cm^{-1} and 866.04 cm^{-1} signifies strong C-COO stretch in the neat poly (lactic acid) matrix. The decrease in % transmittance values and increase in area values for carbon black filled poly (lactic acid) composites in comparison to neat poly (lactic acid) are observed; which may be attributed to decrease in polarity and formation of strong hydrogen bonds respectively; owing to intermolecular interaction between C-COO of poly (lactic acid) and functional groups on surface of carbon black. Shifts in absorption peaks are

observed for 0.5wt%, 1.0wt%. 1.5wt% and 2.0wt% from 866.04 cm^{-1} to 867.97 cm^{-1}; for 1.5wt% and 2.5wt% from 754.17 cm^{-1} to 752.24 cm^{-1}. The shift at higher position is due to increase in bond strength or decrease in reduced mass of the bonded atoms. Absorption area increases with increase in weight percent of carbon black, irrespective of the shift; which is due to the presence of strong hydrogen bonds within the carbon black filled poly (lactic acid) composites. Refer **Table 6.2** for numerical data on increase of area and decrease in % transmittance with respect to neat poly (lactic acid). Few new absorption bands are observed in carbon black filled poly (lactic acid) composites, which are not present in absorption spectra of neat poly (lactic acid). Their presence in the composites with their respective wavenumbers is mentioned systematically in **Table 6.1**. The absorption peak at 613.36cm^{-1}, 617.22cm^{-1} represents strong C-H bend; 896.9cm^{-1}, 898.83cm^{-1} for strong S-OR esters; 902.69cm^{-1}, 904.61cm^{-1} for strong P-OR ester; 952.84cm^{-1}, 954.76cm^{-1} and 956.69cm^{-1} for weak P-H bending; 1624.06cm^{-1} and 1629.85cm^{-1} represents aromatic – CH = CHR; 2428.38cm^{-1} and 2438.02cm^{-1} for medium P-H phosphine. These new absorption bands in carbon black filled poly (lactic acid) composites may be due to the combined effect of randomly joining segments of pre-existing chains; random copolymerization or end linking functionally terminated chain ends and steric effect of the functional groups present on the surface of carbon black with poly (lactic acid), i.e. chemical interactions within polymer composites.

6.1.3.2.2 CORRABORATION WITH MECHANICAL PROPERTIES

Tensile test determines the strength of intermolecular interactions. Tensile yield strength as reported in **Section 4.1.1** for neat poly (lactic acid) is 65MPa. Schematic representation in **Figure.6.2** shows us the probable arrangement of carbon black at different loading in neat poly (lactic acid). One can observe that at lower concentration of carbon black, mobility of poly (lactic acid) chains was possible due to the availability of free space in its surrounding, with less network formation; but as the concentration of carbon black increases free space around the poly (lactic acid) decreases due to which mobility is declined and a network of carbon black with poly (lactic acid) chains are formed, owing to which a strong network is built within the composites and increase in tensile yield strength is observed. Adding 0.5wt%, 1.0wt%, 1.5wt%, 2.0wt% and 2.5wt% of carbon black in poly (lactic acid) via dissolution dispersion process increases the tensile yield strength to 72MPa, 73MPa, 74MPa, 75MPa, and 77MPa due to effective molecular contact and homogenization of carbon black into the poly (lactic acid) matrix. One may observe that there is a steep rise in tensile yield strength

with respect to the concentration of carbon black, which can be attributed to physical and chemical interactions, i.e. intermolecular interactions within carbon black filled poly (lactic acid) composites[1].

6.1.4 CONCLUSION

As per the observation from the ATR-FTIR absorption spectra of neat poly (lactic acid) and filled composites, it can be concluded that % transmittance values represent the strength of zone boundaries [i.e. interface and interphase], absorption area to hydrogen bonds formed within polymer composites, peak position [i.e. shift] to bond strength and presence of new absorption bands to chemical interactions within polymer composites. Existence of entanglements in polymer chains, absorption of polymer chains on fillers surface, the formation of crystallites, coalescence of ionic centers or of glassy blocks and randomly joining segments of pre-existing chains; random copolymerization or end linking functionally terminated chain ends along with steric effect of the functional groups present on the surface of carbon black with poly (lactic acid) contributes to physical and chemical interactions within polymer composites respectively. Physical interactions can be attributed to those absorption bands wherein decrease in % transmittance is observed at matched, higher or lower positions in absorption spectra. New bands formed on absorption spectra can be attributed to chemical interactions within polymer composites. These physical and chemical interactions are portrayed via absorption peaks in ATR-FTIR spectra. ATR – FTIR spectra for poly (lactic acid) composites with 2.5 wt% showed decrease in % transmittance and increase in absorption area without change in peak position confirming strong and stable bonds within poly (lactic acid) composites. Hence ATR – FTIR proved itself as a technique providing sensitive, relatively quick and a non-destructive test to determine intermolecular interactions within polymer composites.

6.2 MULTIWALLED CARBON NANOTUBES

6.2.1 ABSORTION BANDS OF MULTIWALLED CARBON NANOTUBES AND POLY (LACTIC ACID) COMPOSITES FILLED WITH MULTIWALLED CARBON NANOTUBES

6.2.1.1 MULTIWALLED CARBON NANOTUBES

Absorption spectra of multiwalled carbon nanotubes, shows a list of absorption peaks, assignments for which along with their wavenumber are; absorption at 682.8 cm^{-1} corresponds to medium C – H out of plane in aromatics; 1022.27 cm^{-1} for strong C – O

stretch in RCO – OH; absorption peaks at 1184.29 cm^{-1}, 1303.88 cm^{-1}, 1367.53 cm^{-1} and 1388.75 cm^{-1} for strong S = O in form of sulfonyl chlorides, sulfone and sulfate respectively; 1234.44 cm^{-1} for strong P = O in phosphonate; 1404.18 cm^{-1} for medium strength bonds C – C stretch in aromatic C – C rings;1460.11 cm^{-1} indicates strong bonds between alkanes CH2 and CH3; 1514.12 cm^{-1} for medium or strong N – O in aromatic nitro compounds; 1541.12 cm^{-1} for medium strength NH out of plane in amides; 1608.63 cm^{-1} for weak C – C stretch in 5 ring alkene; 1699.29 cm^{-1} for strong C = O stretch in 5 ring amide structure; 1973.18 cm^{-1} for strong CO stretch bands; 2748.56 cm^{-1} for CH stretch or CHO out of plane in RCHO; 2845 cm^{-1}, 2914.44 cm^{-1} and 2991.59 cm^{-1} for strong CH stretch in alkanes; 3242.34 cm^{-1}, 3614.6 cm^{-1} and 3738.05 cm^{-1} for strong and sharp aromatic OH bonds.

6.2.1.2 MULTIWALLED CARBON NANOTUBES FILLED POLY (LACTIC ACID) COMPOSITES

Table 6.3: Absorption peaks in neat poly (lactic acid) and its multiwalled carbon nanotubes filled poly (lactic acid) composites

Neat PLA	0.2wt%	0.4wt%	0.6wt%	0.8wt%	1.0wt%
603.72	✗	✗	✗	✗	✗
669.3	✓	✗	✗	✗	✗
704.02	✓	✗	✗	✓	✗
754.17	✓	✗	✓	✗	✗
866.04	✗	✓	✓	✓	✓
1045.42	✓	✓	✓	✓	✓
1082.07	✗	✓	✓	✓	✓
1128.36	✗	✓	✓	✓	✓
1182.36	✗	✓	✓	✓	✓
1267.23	✓	✓	✓	✓	✓
1315.45	✓	✗	✗	✗	✗
1359.82	✓	✓	✗	✗	✗
1381.03	✗	✓	✓	✓	✓
1452.4	✓	✓	✓	✓	✓
1749.44	✓	✓	✓	✗	✓
2943.37	✗	✓	✗	✗	✗
2995.45	✓	✓	✓	✗	✓
Shifts	0.2wt%	0.4wt%	0.6wt%	0.8wt%	1.0wt%
667.37	✗	✓	✓	✓	✓

702.09	✗	✓	✓	✗	✓
752.24	✗	✓	✗	✓	✓
867.97	✓	✗	✗	✗	✗
1083.99	✓	✗	✗	✗	✗
1126.43	✓	✗	✗	✗	✗
1184.29	✓	✗	✗	✗	✗
1317.38	✗	✓	✓	✓	✓
1361.74	✗	✗	✓	✓	✓
1373.32	✓	✗	✗	✗	✗
1747.51	✗	✗	✗	✓	✗
2945.3	✓	✗	✓	✓	✓
2993.52	✗	✗	✗	✓	✗
New Bands	0.2wt%	0.4wt%	0.6wt%	0.8wt%	1.0wt%
613.36	✗	✓	✗	✗	✗
632.65	✗	✗	✗	✗	✓
636.51	✗	✗	✗	✓	✗
688.59	✗	✗	✗	✓	✗
894.97	✗	✗	✓	✗	✓
896.9	✗	✓	✗	✗	✗
902.69	✓	✗	✗	✗	✗
952.84	✓	✗	✗	✗	✗
956.69	✗	✗	✓	✓	✓
1616.35	✓	✗	✗	✗	✗
1620.21	✗	✗	✗	✗	✓
2430.31	✗	✗	✓	✗	✗
2461.17	✗	✗	✗	✓	✗

Table 6.4: %Transmittance and Area for characteristics peaks of neat poly (lactic acid) and its shifts in multiwalled carbon nanotubes filled poly (lactic acid) composites

Wave number (cm^{-1})	P0.0		P0.2		P0.4	
	%T	**A**	**%T**	**A**	**%T**	**A**
754.17→**752.24**	76.736	4.193	71.376	5.427	**72.009**	**5.166**
866.04→**867.97**	89.016	1.654	**88.654**	**1.844**	88.113	1.865

1045.42	67.864	6.073	67.322	6.37	66.563	6.851
1082.07→**1083.99**	44.355	13.288	**43.731**	**13.641**	43.412	13.211
1128.36→**1126.43**	69.58	4.164	**69.738**	**4.186**	68.464	4.132
1182.36→**1184.29**	58.243	10.011	**59.29**	**10.048**	55.633	10.127
1749.44→**1747.51**	55.59	9.855	57.101	9.407	55.299	9.263

Wave number (cm^{-1})	P0.6		P0.8		P1.0	
	%T	**A**	**%T**	**A**	**%T**	**A**
754.17→**752.24**	70.551	5.012	**66.801**	**6.189**	**70.419**	**5.347**
866.04→**867.97**	88.283	1.494	86.655	2.104	88.274	1.819
1045.42	64.173	6.859	62.881	7.654	66.597	6.754
1082.07→**1083.99**	38.013	15.016	37.353	15.351	43.136	13.258
1128.36→**1126.43**	65.469	4.685	64.677	4.718	68.532	4.099
1182.36→**1184.29**	51.192	11.32	50.145	11.69	55.621	10.073
1749.44→**1747.51**	49.71	10.786	**49.265**	**10.966**	55.452	9.136

6.3 CELLULOSE NANOFIBERS

6.3.1 ABSORPTION BANDS OF CELLULOSE NANOFIBERS AND POLY (LACTIC ACID) COMPOSITES FILLED WITH CELLULOSE NANOFIBERS

6.3.1.1 CELLULOSE NANOFIBERS

Absorption characteristics peaks like 657cm^{-1}, 1037cm^{-1}, 1103cm^{-1} and 1157cm^{-1} , 1417 cm^{-1} and 1435 cm^{-1}, 2893 cm^{-1}, 3336 cm^{-1}, assigned to ‘s’ C – H bend, ‘s’ C – O stretch, ‘s’ C – O stretch, ‘m’ C – C stretch, ‘s’ CH stretch, ‘s’ RCO – OH respectively, confirms the chemical composition of cellulose fibers.

6.3.1.2 CELLULOSE NANOFIBERS FILLED POLY (LACTIC ACID) COMPOSITES

Table 6.5: Absorption peaks in neat poly (lactic acid) and its cellulose nanofibers filled poly (lactic acid) composites

Neat PLA	0.2wt%	0.4wt%	0.6wt%	0.8wt%	1.0wt%
603.72	✗	✗	✗	✗	✗
669.3	✓	✓	✗	✗	✗
704.02	✗	✗	✗	✗	✗

754.17	✓	✓	✗	✗	✗
866.04	✗	✗	✗	✓	✗
1045.42	✓	✓	✓	✓	✓
1082.07	✓	✓	✗	✗	✗
1128.36	✓	✓	✓	✗	✓
1182.36	✓	✓	✗	✗	✗
1267.23	✗	✗	✓	✗	✓
1315.45	✗	✗	✗	✗	✗
1359.82	✓	✗	✓	✗	✓
1381.03	✗	✓	✗	✗	✗
1452.4	✓	✗	✓	✓	✓
1749.44	✓	✓	✗	✗	✗
2943.37	✗	✗	✗	✗	✗
2995.45	✓	✓	✗	✗	✗
Shifts	0.2wt%	0.4wt%	0.6wt%	0.8wt%	1.0wt%
702.09	✓	✓	✗	✗	✗
750.31	✗	✗	✗	✓	✗
752.24	✗	✗	✓	✗	✓
867.97	✓	✓	✓	✗	✓
1083.99	✗	✗	✓	✓	✓
1124.5	✗	✗	✗	✓	✗
1184.29	✗	✗	✗	✗	✓
1186.22	✗	✗	✓	✓	✗
1265.3	✗	✗	✗	✓	✗
1269.16	✓	✓	✗	✗	✗
1311.59	✗	✗	✗	✓	✗
1313.52	✗	✗	✓	✗	✓
1317.38	✓	✓	✗	✗	✗
1361.74	✗	✓	✗	✗	✗
1365.6	✗	✗	✗	✓	✗
1382.96	✓	✗	✗	✗	✗
1454.33	✗	✓	✗	✗	✗
1751.36	✗	✗	✓	✓	✓

2945.3	✓	✓	✗	✗	✗
2947.23	✗	✗	✓	✗	✓
2997.38	✗	✗	✓	✓	✓
New Bands	0.2wt%	0.4wt%	0.6wt%	0.8wt%	1.0wt%
609.51	✗	✗	✗	✗	✓
623.01	✗	✗	✗	✗	✓
613.36	✗	✓	✗	✗	✗
694.37	✗	✗	✗	✗	✓
696.3	✗	✗	✗	✓	✗
700.16	✗	✗	✓	✗	✗
738.74	✓	✓	✗	✗	✗
894.97	✗	✓	✗	✗	✗
902.69	✗	✗	✓	✗	✓
908.47	✗	✗	✗	✓	✗
956.69	✗	✗	✗	✗	✓
1514.12	✗	✗	✗	✗	✓
1625.99	✗	✗	✗	✗	✓
1714.72	✓	✓	✓	✗	✓
2412.95	✗	✗	✗	✓	✗
3518.16	✗	✗	✗	✓	✗
3739.97	✗	✗	✗	✗	✓

Table 6.6: Transmittance and Area for characteristics peaks of neat poly (lactic acid) and its shifts in cellulose nanofibers filled poly (lactic acid) composites

Wavenumber (cm^{-1})	P0.0		P0.2		P0.4	
	%T	**A**	**%T**	**A**	**%T**	**A**
754.17	76.736	4.193	81.112	2.432	84.68	1.898
866.04→**867.97**	89.016	1.654	**88.024**	**1.465**	**89.388**	**1.389**
1045.42	67.864	6.073	63.27	6.671	67.284	6.409
1082.07	44.355	13.288	37.085	15.495	44.241	12.674
1128.36	69.58	4.164	62.379	5.201	68.036	4.234
1182.36	58.243	10.011	48.143	12.421	54.922	10.159

1749.44	55.59	9.855	46.884	10.737	54.257	8.789

Wavenumber (cm^{-1})	P0.6		P0.8		P1.0	
	%T	**A**	**%T**	**A**	**%T**	**A**
754.17→**752.24**→750.31	**82.755**	**3.588**	89.798	2.402	**86.05**	**3.01**
866.04→**867.97**	**89.691**	**1.444**	93.238	1.294	**90.046**	**1.538**
1045.42	67.338	5.706	79.745	3.852	69.298	5.961
1082.07→**1083.99**	**42.066**	**14.198**	64.592	8.188	**49.107**	**12.02**
1128.36→**1124.5**	66.482	4.823	80.914	2.611	70.346	4.107
1182.36→**1186.22**→1184.29	**54.786**	**11.262**	**73.923**	**6.187**	60.129	9.469
1749.44→**1751.36**	**51.773**	**9.834**	**72.363**	**6.248**	**57.937**	**8.075**

6.4 CARBON BLACK + MULTIWALLED CARBON NANOTUBES

6.4.1 ABSORPTION BANDS OF CARBON BLACK + MULTIWALLED CARBON NANOTUBES FILLED POLY (LACTIC ACID) COMPOSITES

6.4.1.1 CARBON BLACK + MULTIWALLED CARBON NANOTUBES FILLED POLY (LACTIC ACID) COMPOSITES

Table 6.7: Absorption peaks in neat poly (lactic acid) and its carbon black + multiwalled carbon nanotubes filled poly (lactic acid) composites

Neat PLA	0.2wt% MWCNT	0.4wt% MWCNT	0.6wt% MWCNT	0.8wt% MWCNT	1.0wt% MWCNT
603.72	✕	✕	✕	✕	✕
669.3	✕	✕	✕	✓	✕
704.02	✕	✕	✕	✕	✕
754.17	✕	✕	✕	✕	✕
866.04	✕	✕	✕	✕	✕
1045.42	✕	✕	✕	✕	✕
1082.07	✕	✕	✕	✕	✕
1128.36	✕	✕	✕	✕	✕
1182.36	✕	✕	✕	✕	✕
1267.23	✕	✕	✕	✕	✕
1315.45	✕	✕	✕	✕	✕

1359.82	✗	✗	✗	✗	✗
1381.03	✗	✗	✗	✗	✗
1452.4	✗	✗	✓	✓	✓
1749.44	✓	✓	✓	✗	✓
2943.37	✗	✓	✗	✗	✓
2995.45	✗	✓	✗	✗	✓
Shifts	0.2wt%	0.4wt%	0.6wt%	0.8wt%	1.0wt%
601.79	✗	✗	✗	✗	✓
750.31	✗	✗	✗	✓	✓
752.24	✓	✓	✓	✗	✗
864.11	✓	✓	✓	✓	✓
1043.49	✓	✓	✗	✓	✓
1083.99	✓	✓	✓	✓	✓
1122.57	✓	✓	✗	✗	✗
1184.29	✗	✓	✗	✗	✗
1186.22	✓	✗	✓	✓	✓
1263.37	✗	✗	✓	✓	✓
1265.3	✓	✓	✗	✗	✗
1313.52	✓	✓	✗	✗	✗
1450.47	✓	✓	✗	✗	✗
1751.36	✗	✗	✗	✓	✗
2945.30	✓	✗	✗	✗	✗
2997.38	✓	✗	✓	✗	✗
New Bands	0.2wt%	0.4wt%	0.6wt%	0.8wt%	1.0wt%
636.51	✗	✗	✗	✓	✗
673.16	✓	✓	✗	✗	✗
675.09	✗	✗	✓	✗	✓
696.3	✓	✓	✗	✗	✗
698.23	✗	✗	✓	✗	✗
796.6	✓	✗	✗	✗	✗
906.54	✓	✓	✗	✗	✗
908.47	✗	✗	✓	✗	✓
910.4	✗	✗	✗	✓	✗

941.26	✗	✗	✓	✗	✗
943.19	✗	✗	✗	✗	✓
945.12	✗	✓	✗	✗	✗
947.05	✗	✗	✗	✓	✗
1367.53	✓	✓	✗	✗	✗
1369.46	✗	✗	✓	✓	✓
1510.26	✗	✗	✓	✓	✓
1514.12	✓	✓	✗	✗	✗
1525.69	✗	✗	✓	✓	✓
1539.2	✗	✗	✓	✓	✓
1548.84	✓	✓	✗	✗	✗
1620.21	✗	✓	✗	✗	✗
1622.13	✓	✗	✗	✗	✗
1639.49	✗	✗	✓	✓	✓
1643.35	✓	✓	✗	✗	✗
1685.79	✗	✗	✗	✓	✗
1703.14	✗	✗	✗	✓	✓
1705.07	✗	✗	✓	✗	✗
2247.07	✗	✓	✗	✗	✗
2264.43	✓	✓	✗	✗	✗
2630.91	✗	✗	✗	✗	✗
3739.97	✓	✓	✗	✗	✗
3741.9	✗	✗	✓	✓	✓
3851.85	✗	✗	✗	✗	✓

Table 6.8: Transmittance and Area for characteristics peaks of neat poly (lactic acid) and its shifts in carbon black + multiwalled carbon nanotubes filled poly (lactic acid) composites

Wavenumber (cm^{-1})	P0.0 MWCNT		P0.2 MWCNT		P0.4 MWCNT	
	%T	**A**	**%T**	**A**	**%T**	**A**
754.17→**752.24**	76.736	4.193	**82.326**	**3.926**	**77.05**	**5.09**
866.04→**864.11**	89.016	1.654	**89.904**	**2.88**	**87.489**	**3.656**
1045.42→**1043.49**	67.864	6.073	**77.574**	**5.362**	**71.51**	**6.789**

1082.07→**1083.99**	44.355	13.288	**64.317**	**8.841**	**54.977**	**11.599**
1128.36→**1122.57**	69.58	4.164	**81.805**	**2.257**	**76.494**	**3.214**
1182.36→**1186.22**→1184.29	58.243	10.011	**75.373**	**6.123**	68.533	8.012
1749.44	55.59	9.855	74.076	6.418	66.62	8.464

Wavenumber (cm^{-1})	P0.6 MWCNT		P0.8 MWCNT		P1.0 MWCNT	
	%T	**A**	**%T**	**A**	**%T**	**A**
754.17→**752.24**→750.31	**77.246**	**5.343**	79.612	4.819	77.015	5.647
866.04→**864.11**	**87.954**	**3.803**	**88.824**	**3.681**	**86.879**	**4.572**
1045.42→**1043.49**			**73.954**	**5.012**	**71.337**	**6.098**
1082.07→**1083.99**	**52.905**	**23.261**	**57.515**	**15.108**	**54.658**	**16.498**
1128.36						
1182.36→**1186.22**	**67.407**	**8.702**	**70.906**	**7.627**	**68.826**	**8.231**
1749.44→**1751.36**	63.943	8.384	**67.517**	**7.43**	65.489	8.09

6.5 CARBON BLACK + CELLULOSE NANOFIBERS

6.5.1 ABSORPTION BANDS OF CARBON BLACK + NANOCELLULOSE FILLED POLY (LACTIC ACID) COMPOSITES

6.5.1.1 CARBON BLACK + NANOCELLULOSE FIBERS FILLED POLY (LACTIC ACID) COMPOSITES

Table 6.9: Absorption peaks in neat poly (lactic acid) and its carbon black + cellulose nanofibers filled poly (lactic acid) composites

Neat PLA	0.2wt% CNF	0.4wt% CNF	0.6wt% CNF	0.8wt% CNF	1.0wt% CNF
603.72	✕	✕	✕	✕	✕
669.3	✕	✕	✕	✕	✕
704.02	✕	✕	✕	✕	✕
754.17	✕	✕	✕	✕	✕
866.04	✕	✕	✕	✕	✕
1045.42	✕	✕	✕	✕	✕
1082.07	✕	✕	✕	✕	✓
1128.36	✕	✕	✕	✕	✕

1182.36	✗	✗	✗	✗	✗
1267.23	✗	✗	✗	✗	✗
1315.45	✗	✗	✗	✗	✗
1359.82	✗	✗	✗	✗	✗
1381.03	✗	✗	✗	✗	✗
1452.4	✓	✓	✓	✓	✓
1749.44	✗	✗	✗	✗	✗
2943.37	✗	✗	✗	✗	✗
2995.45	✗	✗	✗	✗	✓
Shifts	0.2wt%	0.4wt%	0.6wt%	0.8wt%	1.0wt%
750.31	✓	✓	✓	✓	✗
862.18	✓	✗	✗	✗	✓
864.11	✗	✓	✓	✓	✗
1083.99	✓	✓	✓	✓	✗
1188.15	✗	✗	✗	✗	✓
1261.45	✓	✓	✓	✓	✓
1751.36	✓	✓	✓	✓	✓
2941.44	✓	✓	✓	✓	✓
2997.38	✓	✓	✓	✓	✗
New Bands	0.2wt%	0.4wt%	0.6wt%	0.8wt%	1.0wt%
632.65	✗	✗	✗	✓	✗
678.94	✗	✗	✗	✗	✓
680.87	✗	✗	✗	✓	✗
682.8	✓	✓	✓	✗	✗
748.38	✗	✗	✗	✗	✓
912.33	✗	✗	✗	✗	✓
914.26	✓	✓	✓	✓	✗
933.55	✗	✗	✓	✗	✗
935.48	✓	✓	✗	✗	✗
1190.08	✓	✓	✓	✓	✗
1367.53	✓	✓	✓	✓	✗
1369.46	✗	✗	✗	✗	✓
1523.76	✓	✓	✓	✓	✓

1543.05	✗	✓	✗	✗	✗
1558.48	✗	✗	✗	✓	✗
1562.34	✗	✗	✗	✗	✓
1633.71	✓	✓	✗	✗	✗
1645.28	✗	✗	✓	✗	✗
1697.36	✓	✓	✗	✓	✓
3738.05	✓	✓	✓	✓	✓
3844.13	✗	✓	✗	✓	✗
3857.63	✗	✗	✓	✗	✓

Table 6.10: Transmittance and Area for characteristics peaks of neat poly (lactic acid) and its shifts in carbon black + cellulose nanofibers filled poly (lactic acid) composites

Wavenumber (cm^{-1})	P0.0		P0.2 CNF		P0.4 CNF	
	%T	**A**	**%T**	**A**	**%T**	**A**
754.17→**750.31**	76.736	4.193	**79.275**	**5.376**	**79.246**	**5.298**
866.04→**864.11**	89.016	1.654	**88.842**	**3.938**	**89.216**	**3.558**
1045.42	67.864	6.073	**-**	**-**	**-**	**-**
1082.07→**1083.99**	44.355	13.288	**59.012**	**21.23**	**56.388**	**22.113**
1128.36	69.58	4.164	**-**	**-**	**-**	**-**
1182.36→**1190.08**	58.243	10.011	**71.993**	**7.741**	**69.981**	**8.316**
1749.44→**1751.36**	55.59	9.855	**69.938**	**7.551**	**67.346**	**8.221**

Wavenumber (cm^{-1})	P0.6 CNF		P0.8 CNF		P1.0 CNF	
	%T	**A**	**%T**	**A**	**%T**	**A**
754.17→**750.31**→748.38	**74.973**	**6.634**	**72.331**	**7.433**	75.486	7.598
866.04→**864.11**→862.18	**87.335**	**4.311**	**86.924**	**4.463**	86.587	4.34
1045.42	**-**	**-**	**-**	**-**	-	-
1082.07→**1083.99**	**52.443**	**25.327**	**50.518**	**26.195**	57.322	22.635
1128.36	**-**	**-**	**-**	**-**	-	-
1182.36→**1190.08**→1188.15	**66.969**	**9.356**	**64.763**	**9.966**	71.035	8.009
1749.44→**1751.36**	**64.623**	**9.053**	**62.865**	**9.368**	**70.054**	**7.425**

6.6 FINAL CONCLUSION

A slight change in any of the parameters related to material or process (i.e. manufacturing) in fabrication of polymer composites alters the mechanism of interaction, further these interactions influences the properties of polymer composites. This chapter was an attempt to study intermolecular interactions within poly (lactic acid) composites in comparison to neat poly (lactic acid) considering the concentration of filler used to fill poly (lactic acid). **Table 6.3** and **Table 6.5** gives information on absorption bands of poly (lactic acid) filled with multiwalled carbon nanotubes and poly (lactic acid) filled with cellulose nanofibers respectively, in comparison with absorption bands of neat poly (lactic acid), shifts in absorption bands (in comparison to neat poly (lactic acid) and new absorption bands. **Table 6.4** and **Table 6.6** presents the % transmittance and absorption area of poly (lactic acid) filled with multiwalled carbon nanotubes and poly (lactic acid) filled with cellulose nanofibers respectively; in comparison to absorption intensity and absorption area of neat poly (lactic acid). Trend for % transmittance and absorption area in absorption spectra for carbon black are very close to the absorption spectra for multiwalled carbon nanotubes and hence discussions and conclusion made for carbon black filled poly (lactic acid) can be corelated to multiwalled carbon nanotubes filled poly (lactic acid) composites. For carbon black and multiwalled carbon nanotubes filled poly (lactic acid) composites % transmittance decreases (with or without shift) with increase in absorption area. On other hand for cellulose nanofibers filled poly (lactic acid) % transmittance increases and absorption area decreases; this can be accounted to strong hydrogen bonds due to adsorption between hydroxyl groups of cellulose nanofibers and poly (lactic acid) chains.

Shape of filler particles determined the pattern of their packing within polymer composites. Different sizes of particulate fillers are loaded to reach the minimum unoccupied volume; in which larger particulate fillers determines the total volume and smaller particulates fills the voids between the larger particulates. **Table 6.7** and **Table 6.9** gives information on absorption bands of poly (lactic acid) filled with carbon black + multiwalled carbon nanotubes and poly (lactic acid) filled with carbon black + cellulose nanofibers respectively, in comparison with absorption bands of neat poly (lactic acid) and poly (lactic acid) composites filled with 2.5wt% of carbon black. **Table 6.8** and **Table 6.10** presents the % transmittance and absorption area of poly (lactic acid) filled with carbon black + multiwalled carbon nanotubes and poly (lactic acid) filled with carbon black + cellulose nanofibers respectively; in comparison to % transmittance and absorption area of neat poly (lactic acid) and poly (lactic

acid) composites filled with 2.5wt% of carbon black. On comparison with neat poly (lactic acid) and poly (lactic acid) composites filled with 2.5wt% of carbon black, it can be noted that % transmittance increases, and absorption area decreases, which confirms the formation of strong adhesion and bond strength at interphase region within hybrid poly (lactic acid) composites. Large size particulates assumes a flat coverage over the surface; hence forms a thinner interphase; while the curvature of surface for smaller particulates does not allow for flat coverage; forming a thick interphase. (shape and size of filler determines the confirmation of the surrounding polymer matrix and hence determines the interphase characteristics). Hence, the change in the %transmittance and absorption area for above poly (lactic acid) composites can be attributed to interphase phenomena, i.e. total surface of the phase border between the phases (i.e. particle size and geometrical shape) .

Structural analysis of singly filled poly (lactic acid) composites and hybrid filler poly (lactic acid) composites using the basic principles of ATR – FTIR spectroscopy (% Transmittance and Area) was a successful attempt. Further **Chapter 7** describes morphological analysis considering the dispersion characteristics (through Transmission electron microscopy and Atomic force microscopy) and failure analysis (through Optical microscopy and Scanning electron microscopy).

7 MORPHOLOGICAL ANALYSIS

Part (Section 7.1) of this chapter is published in “Surfaces and Interfaces, 18 (2020) 100451 Elsevier

7.1 INTRODUCTION

The internal structure of a material, simply called the structure can be studied at various levels of observation. The degree of magnification required to study them by various methods is a measure of the level of observation. The details that are revealed or disclosed at a certain level of magnification are generally different from details disclosed at some other level of magnification. Macrostructure is the structure of a material as seen by the naked eye or low power magnification. Microstructure generally refers to the structure as observed under a microscope at magnification from X75 to X1500. Macrostructure and Microstructure are two words relating to the same general type of phenomena and differ only in the degree of magnification required to study them. Substructure refers to structure obtained by using a microscope with such high magnification. Various materials respond differently to the same stimuli and constraints; the “quality” of the response to imposed stimuli and constraints is determined by the nature of the material and termed as “material property”. In engineering, it is not enough to know “how a material responds?” to imposed stimuli and constraints but also “how much it responds?” and it depends only on the nature of the material itself. So, in recent years, there has been a growing awareness of the need to study the relationship between structure and properties of the materials, as the appreciation of their possible improvements does not come solely from the composition, treatment, properties, and uses of the materials. The fact that the properties of all materials arise from their structure, i.e. from the manner in which their atoms aggregate to form molecules or crystals or disordered amorphous structures. Moreover, the properties of bulk matter, depend strongly on the nature and distribution of imperfections, either chemical or architectural in the main order. Most of the properties observed and exploited in materials are cooperative properties of the aggregate rather than of constituent’s atoms and molecules. Properties of materials are directly related to the structures found within the materials and to the conditions under which the materials are used. Emphasizing research work in microscopic characterization of carbon black filled polymer composites. S. Zhao et al confirmed distribution of filler, localization of carbon black at interfaces between polypropylene particles is an important parameter for enhancement in liquid sensing capacity of conductive polymer composites. X. Wen et al emphasized-on

dispersion of nanofiller within polymer matrix and interfacial interaction between polymer matrix and nanoparticle as two important properties determining properties of polymer nanocomposites. Particulate filler particles are spherical, curvy, short fibers etc.; and its dispersion in polymer matrix depends on many factors out of which processing of polymer composites and filler concentration plays an important role. Filler particles were uniformly distributed within polypropylene matrix with diameter range 40nm-70nm as carbon black loading increased from 2.5wt% to 10wt%. Aggregates were present, amount and size of aggregates depended on the quantity of carbon black in polypropylene matrix. Poly (lactic acid) and its carbon black filled composites undergo elevated temperature, pressure, and shear during processing for variable period of time. Shearing depends on processing methodology used and their viscoelastic properties. Processing methodology relates morphology because of crystallization from melt and orientation during the process and stress formed after processing. Hence morphological evidence in this chapter (images generated by optical microscope, scanning electron microscope and transmission electron microscope, atomic force microscope) describes the macro, micro, and substructure of poly (lactic acid) composites. Particulates filled poly (lactic acid) has a heterogeneous morphology under an optical microscope and scanning electron microscope. Close to homogenous morphology is observed in atomic force microscope and a transmission electron microscope. In short, imaging is dependent and is analyzed here in correlation with information required, based on level of magnification. To have a correlation between morphological characterizations and mechanical properties, **Chapter 8** on mechanical properties of particulate filled poly (lactic acid) composites shall be referred, wherein insights on interactions controlling physical and mechanical properties related to processing techniques and weight percentage of particulate filler in poly (lactic acid) was discussed[1][2][155][142][156][157][158][159][160][161].

In this chapter, we discuss the microstructural and sub microstructural features affecting mechanical properties of particulates filled poly (lactic acid) composites, processed using oligomeric dispersion. Morphological analysis on tensile fractured specimens by optical microscope and scanning electron microscope was done in order to determine the microstructural features affecting mechanical properties; transmission electron microscopy and atomic force microscopy were performed on ultramicrotome specimens to evaluate effect of processing techniques on dispersion of particulate filler/s in poly (lactic acid). Dispersion studies and fracture studies on carbon black filled poly (lactic acid) prepared via oligomeric dispersion was compared with the carbon black filled poly (lactic acid) composites prepared by DDCS and MMCM, mentioned in **Section 4.1.1.3**.

7.2 DISPERSION CHARACTERISTICS [SUBMICROSTRUCTURE]

7.2.1 TRANSMISSION ELECTRON MICROSCOPY

7.2.1.1 CARBON BLACK FILLED POLY (LACTIC ACID) COMPOSITES

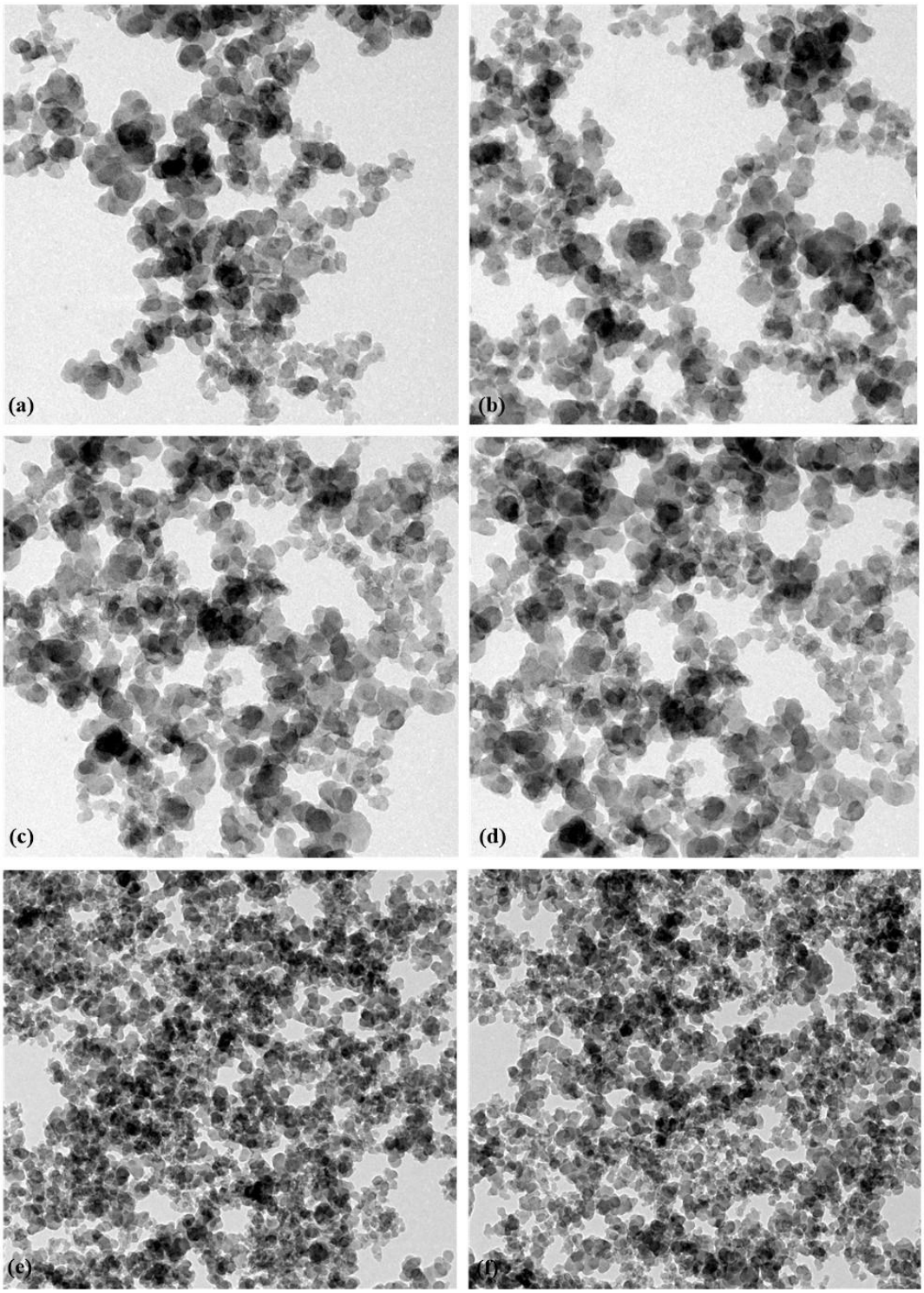

Figure 7.1: PLA Composites with (a) 0.5 (b) 1.5 (c) 2.0 (d) 2.5 (e) 5.0 (f) 10.0 of carbon black (X1000)

7.2.1.2 MULTIWALLED CARBON NANOTUBES FILLED POLY (LACTIC ACID) COMPOSITES

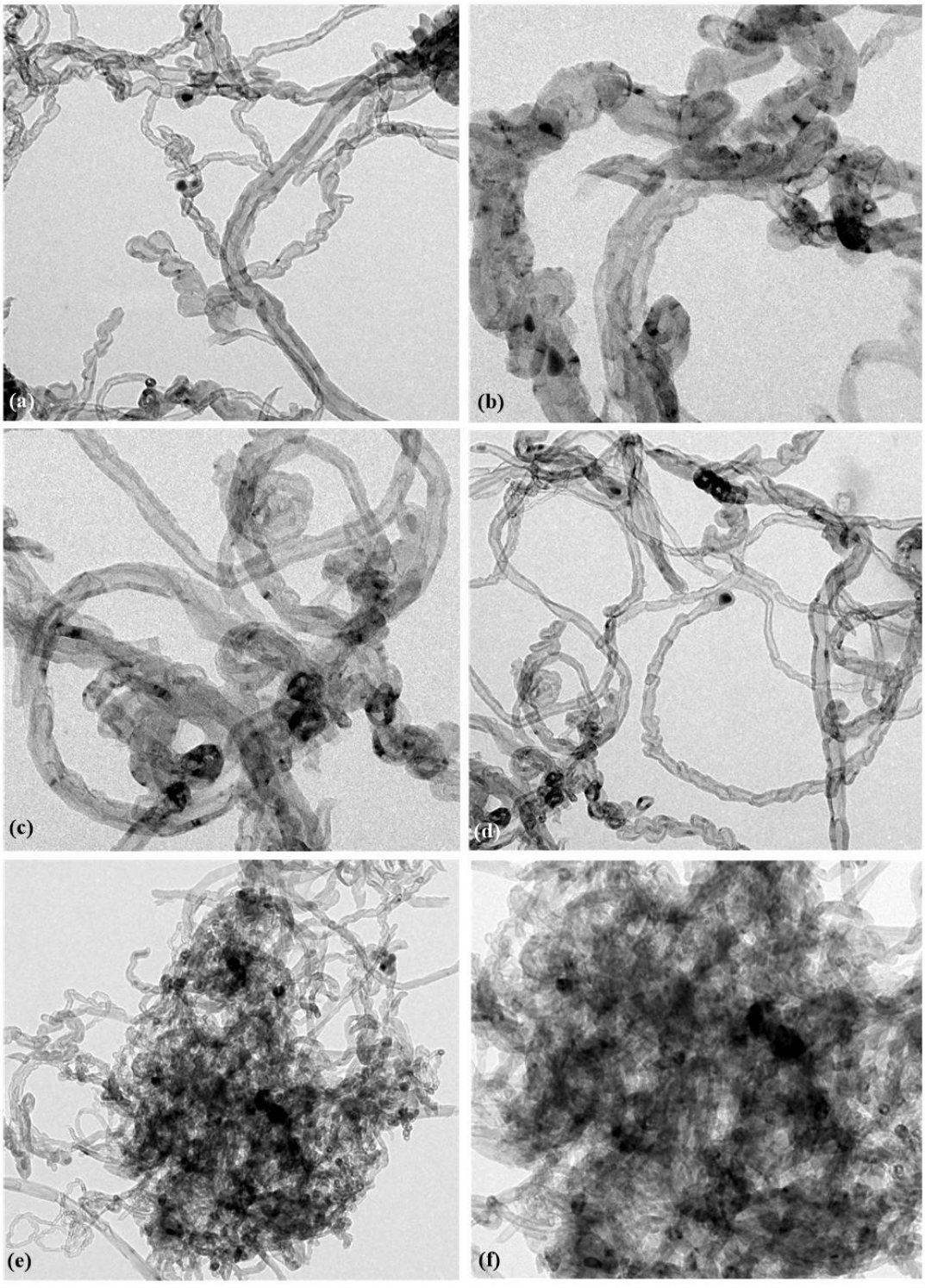

Figure 7.2: PLA Composites with (a) 0.2 (b) 0.4 (c) 0.6 (d) 0.8 (e) 1.5 (f) 2.0 of multiwalled carbon nanotubes (X1000)

Figure 7.1, **Figure 7.2** and **Figure 7.3** represents (TEM) transmission electron microscope images for single filler poly (lactic acid) composites filled with CB, MWCNT and CNF.

7.2.1.3 CELLULOSE NANOFIBERS FILLED POLY (LACTIC ACID) COMPOSITES

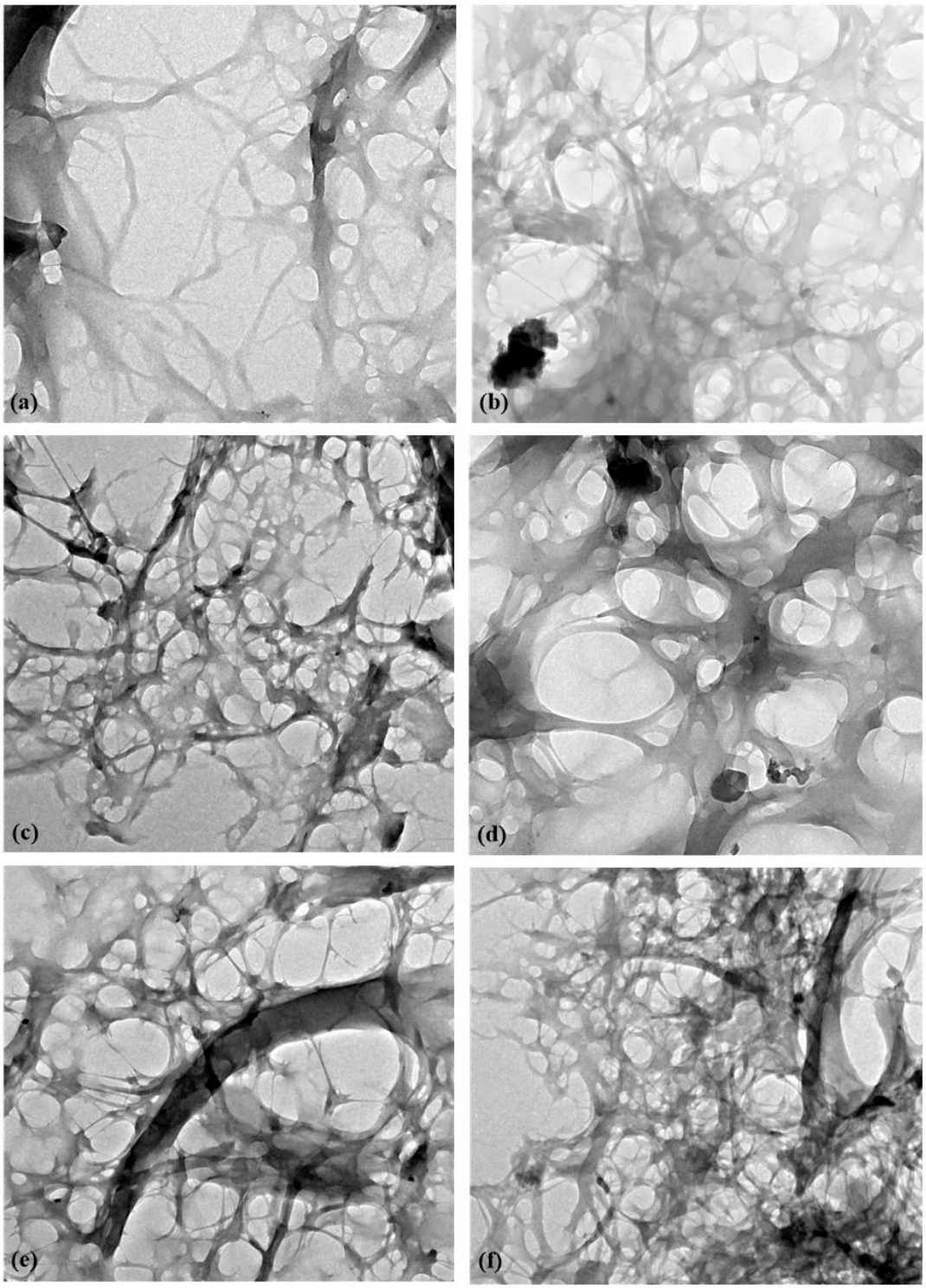

Figure 7.3: PLAC with (a) 0.2 (b) 0.4 (c) 0.6 (d) 0.8 (e) 1.5 (f) 2.0 of cellulose nanofibers (X1000)

Figure 7.4 and **Figure 7.5** represents (TEM) transmission electron microscope images for hybrid filler poly (lactic acid) composites filled with CB + MWCNT and CB + CNF.

7.2.1.4 CARBON BLACK + MULTIWALLED CARBON NANOTUBES FILLED POLY (LACTIC ACID) COMPOSITES

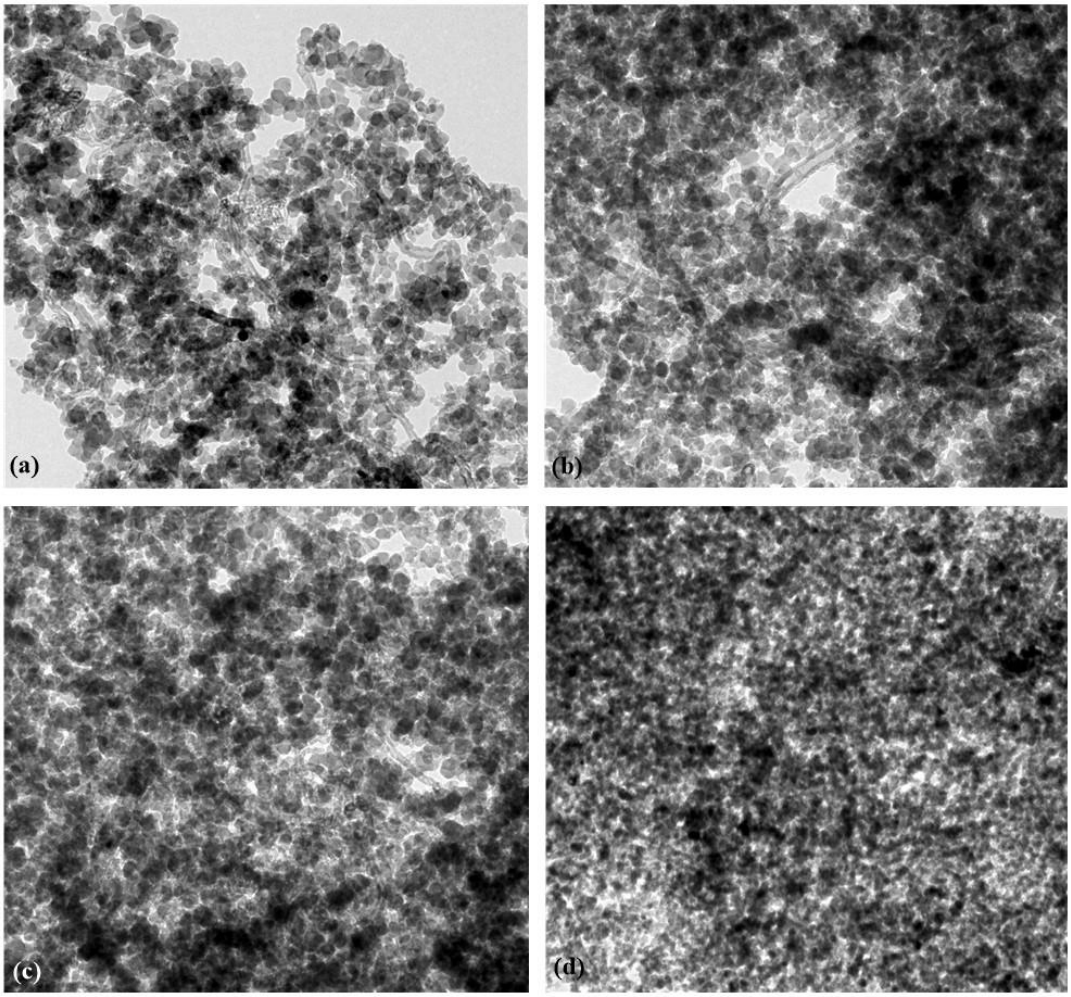

Figure 7.4: PLAC with 2.5CB + (a) 0.2MWCNT (b) 1.0MWCNT (c) 1.5MWCNT (d) 2.0MWCNT (X1000)

Transmission electron microscopy on ultra-microtomed specimens for poly (lactic acid) composites were observed, to determine basic data on dispersion characteristics of particulate fillers (carbon black, multiwalled carbon nanotubes and cellulose nanofibers) within poly (lactic acid) matrix in poly (lactic acid) composites and hybrid composites. For poly (lactic acid) composites with single filler (i.e. **Figure 7.1,7.2** and **7.3**), it was observed that at higher loading of particulate filler, agglomeration of particulate fillers takes place and these aggregates acts as stress concentration points thereby decreasing the mechanical properties of the poly (lactic acid) composites. Transmission electron microscopic images of poly (lactic acid) composites with low concentration of particulate fillers showed wide networking, thereby increasing the contact area between the filler surface and poly (lactic acid) chains; and increasing the strength of the poly (lactic acid) composites. 2.5wt%, 0.8wt% and 0.8wt% of

carbon black, multiwalled carbon nanotubes and cellulose nanofibers shows excellent and strong connectivity between the poly (lactic acid) chains and the filler surface, hence contributes to the mechanical strength of the poly (lactic acid) chains. Addition of multiwalled carbon nanotubes and cellulose nanofibers in increasing concentration of 0.2, 0.4, 0.6, 0.8, 1.5 and 2.0wt% to poly (lactic acid) composites with 2.5wt% of carbon black disturbs the existing microstructure of poly (lactic acid) composites (as evident from **Figure 7.4** and **7.5**). It can be observed that addition of multiwalled carbon nanotubes and cellulose nanofibers fills the voids between the spherical carbon black particles, involving more poly (lactic acid) chains to adsorb on the surface of multiwalled carbon nanotubes/ cellulose nanofibers. Although the TEM images within the batch show morphologically identical distribution of fillers, their mechanical properties were different[162][163][161].

7.2.1.5 CARBON BLACK + CELLULOSE NANOFIBERS FILLED POLY (LACTIC ACID) COMPOSITES

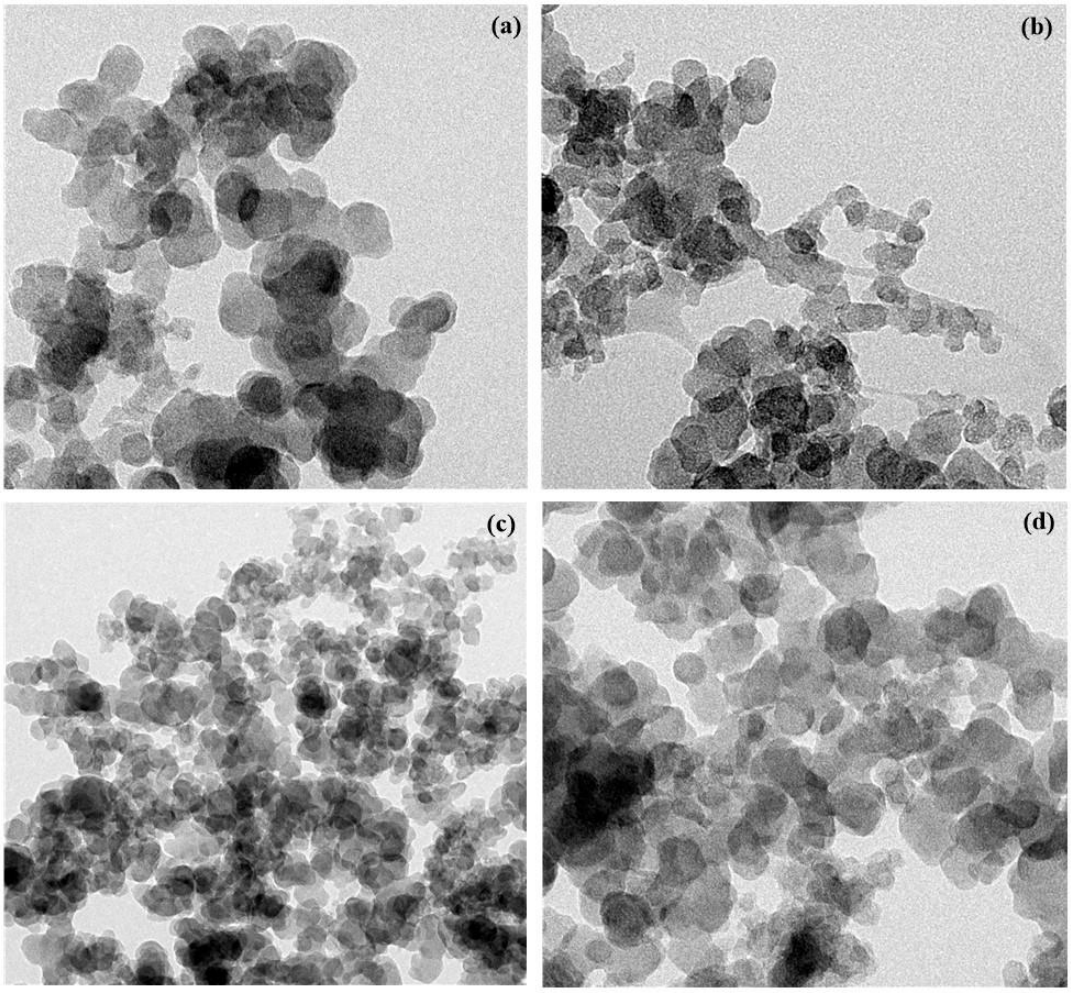

Figure 7.5: PLAC with 2.5CB + (a) 0.2CNF (b) 1.0CNF (c) 1.5CNF (d) 2.0CNF (X1000)

7.2.2 ATOMIC FORCE MICROSCOPY

7.2.2.1 CARBON BLACK FILLED POLY (LACTIC ACID) COMPOSITES

Figure 7.6: PLA Composites with (a) 0.5 (b) 1.5 (c) 2.0 (d) 2.5 (e) 5.0 (f) 10.0 of carbon black

Ultraviolet – Visible Spectroscopy and ATR – FTIR Spectroscopy indicated that difference in their mechanical behaviour was related to the interphase thickness and molecular interaction i.e., more precisely to molecular motion in poly (lactic acid) matrix. **Figure 7.6** to **Figure 7.11** are the atomic force microscopic images of single filler poly (lactic acid) composites and hybrid composites; giving more information on the interactions within poly (lactic acid)

composites. Images (**Figure 7.6** to **Figure 7.11**) in line with the average roughness values confirmed the interactions between fillers and poly (lactic acid) chains. It was observed that average roughness values increases up to a specific concentration, after which a fall in the average roughness values were observed. The increase in average roughness values can be attributed to interactions between the filler's surface and poly (lactic acid) chains. Increase in the roughness values can be attributed to increase in the adsorption sites between the filler surface and the poly (lactic acid) chains[164][161].

7.2.2.2 MULTIWALLED CARBON NANOTUBES FILLED POLY (LACTIC ACID) COMPOSITES

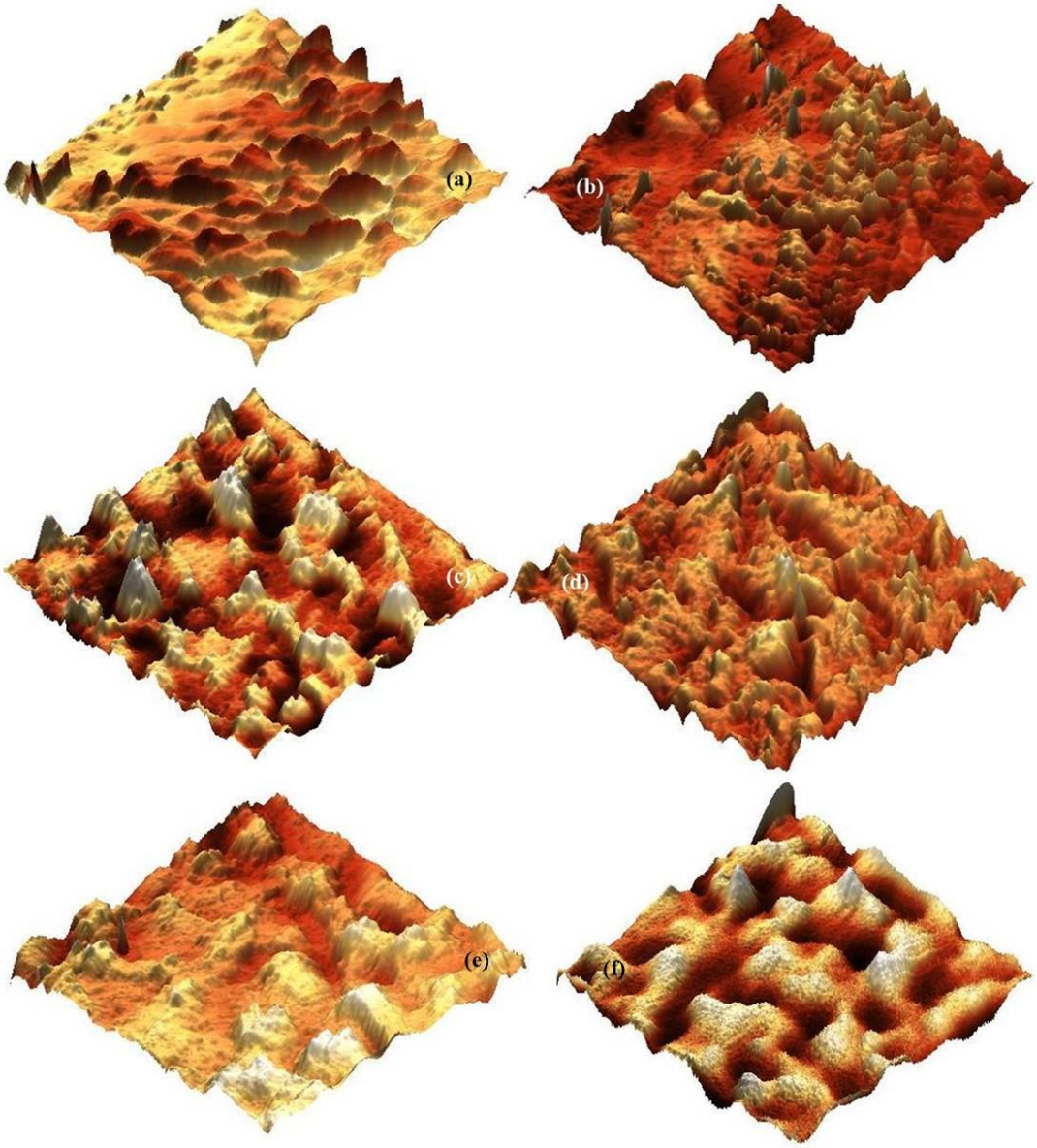

Figure 7.7: PLA Composites with (a) 0.2 (b) 0.4 (c) 0.6 (d) 0.8 (e) 1.5 (f) 2.0 of multiwalled carbon nanotubes

7.2.2.3 CELLULOSE NANOFIBERS FILLED POLY (LACTIC ACID) COMPOSITES

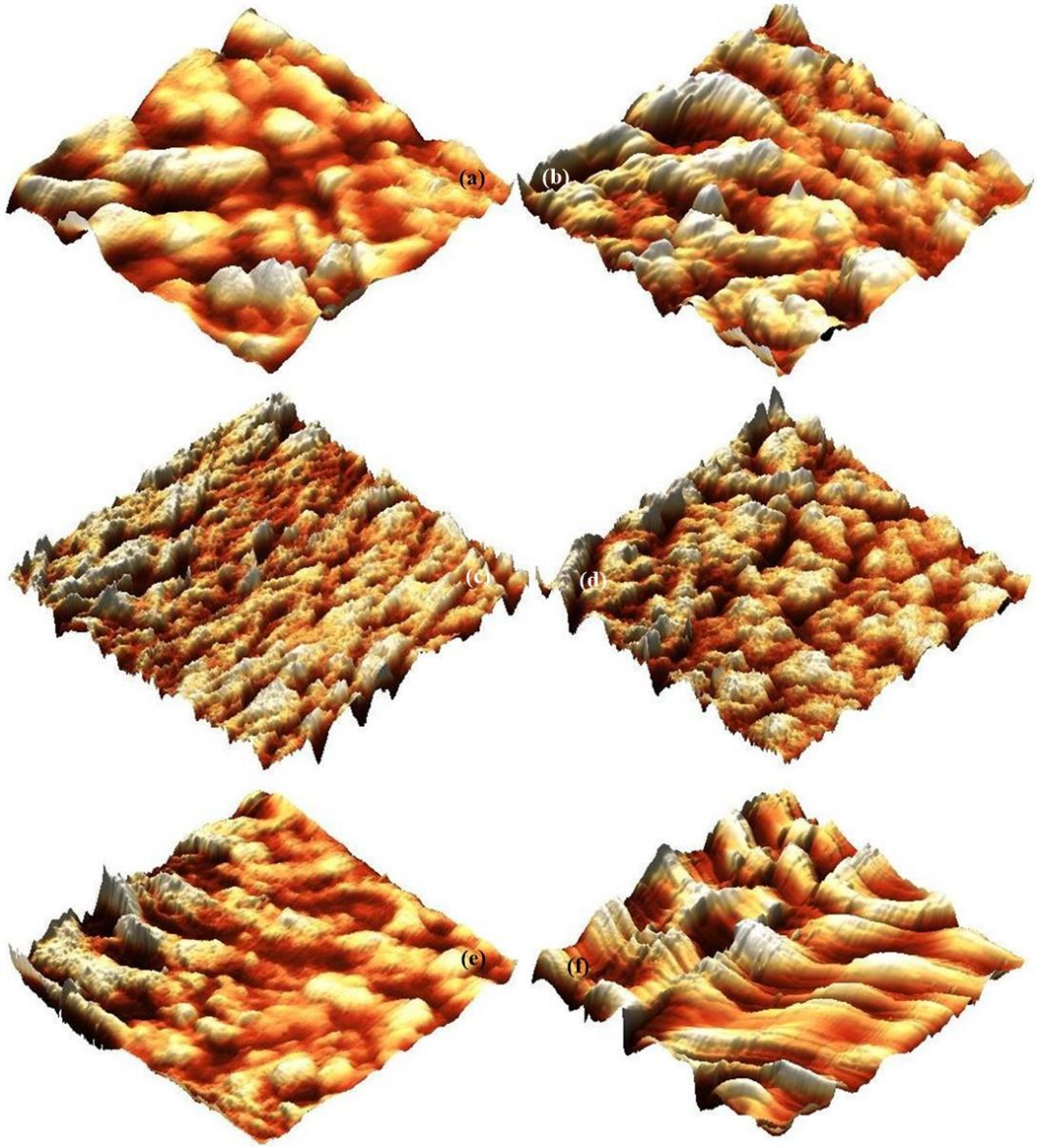

Figure 7.8: PLA Composites with (a) 0.2 (b) 0.4 (c) 0.6 (d) 0.8 (e) 1.5 (f) 2.0 of cellulose nanofibers

Hence, increasing the concentration (till specific conc) of particulate fillers in poly (lactic acid) matrix, increased the adsorption sites (anchoring sites) due to which interaction increases and so the average roughness values do. Decrease in average roughness values are observed at higher concentration of particulate fillers, which can be attributed to decrease in the interactions between the poly (lactic acid) matrix and filler's surface, whereby increasing the filler – filler interactions. These filler – filler interactions are responsible for the decrease of average roughness values in poly (lactic acid) composites at higher concentration. It can be --

7.2.2.4 CARBON BLACK + MULTIWALLED CARBON NANOTUBES FILLED POLY (LACTIC ACID) COMPOSITES

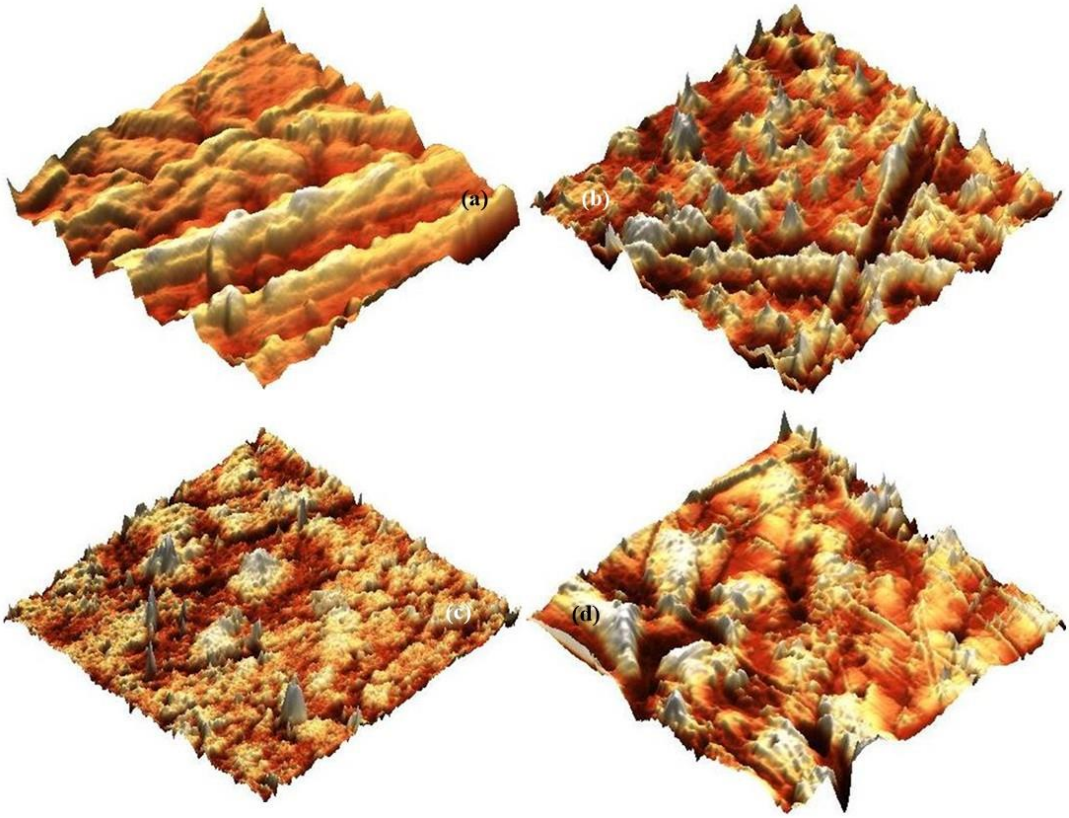

Figure 7.9: PLAC with 2.5CB + (a) 0.2MWCNT (b) 1.0MWCNT (c) 1.5MWCNT (d) 2.0MWCNT

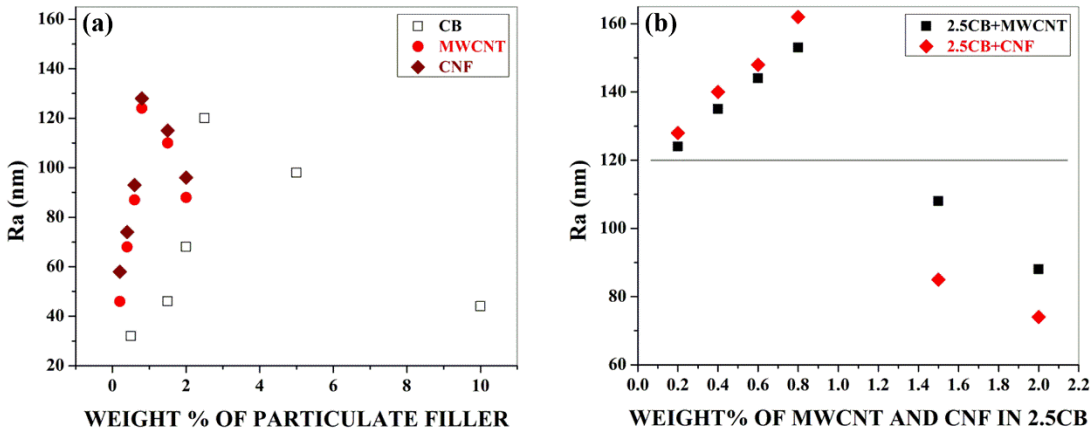

Figure 7.10: Roughness average value (Ra) for single filler poly (lactic acid) composites (a) and hybrid composites (b)

7.2.2.5 CARBON BLACK + CELLULOSE NANOFIBERS FILLED POLY (LACTIC ACID) COMPOSITES

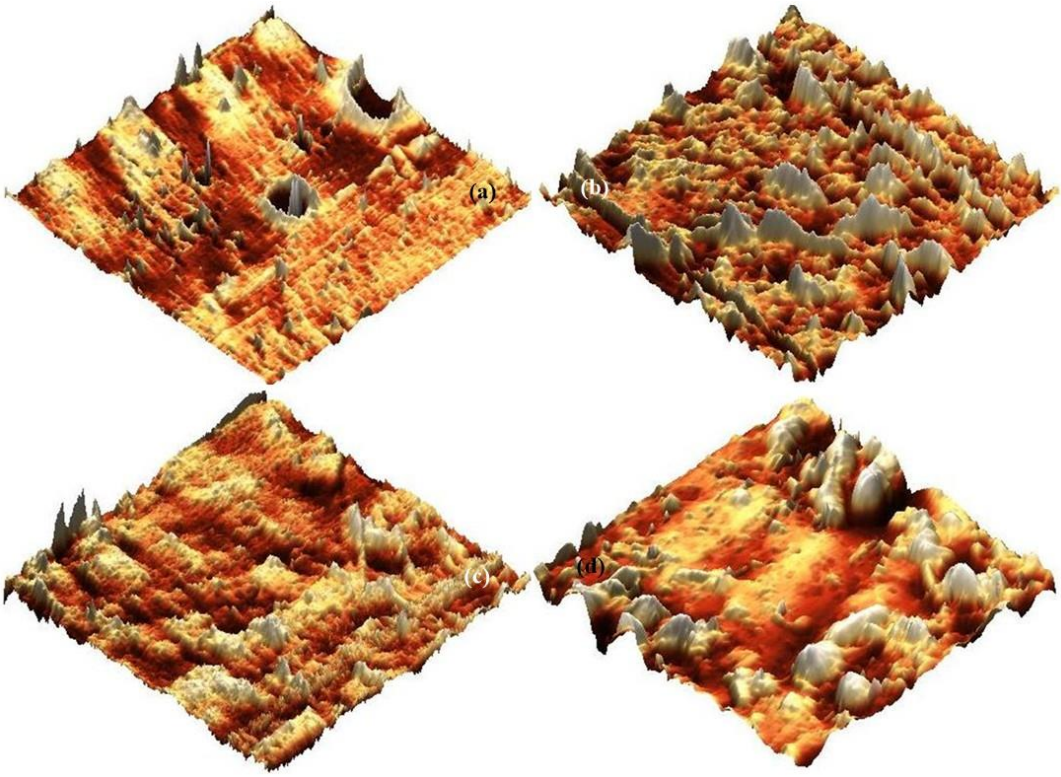

Figure 7.11: PLAC with 2.5CB + (a) 0.2CNF (b) 1.0CNF (c) 1.5CNF (d) 2.0CNF

--clearly differentiated from the atomic force microscopic images, that strong interactions between the filler's surface and the poly (lactic acid) chains are picturized with small and sharp peaks, whereas broad peaks denotes the weak interactions between the poly (lactic acid) chains and filler's surface. Roughness values in **Figure 7.10**, indicates that interactions of cellulose nanofibers with poly (lactic acid) chains are strong, thereby increasing the roughness value, and can be attributed to the hydroxyl groups with cellulose nanofibers with carbonyl group of poly (lactic acid) matrix. On comparing the roughness values of carbon black filled poly (lactic acid) composites and multiwalled carbon nanotubes filled poly (lactic acid) composites (even though the concentration of loading differs) – poly (lactic acid) composites filled with multiwalled carbon nanotubes possess higher magnitude of roughness values, which can be attributed to curvy nature of multiwalled carbon nanotubes in poly (lactic acid) matrix. Comparing the equal concentration of multiwalled carbon nanotubes filled poly (lactic acid) composites and carbon black filled poly (lactic acid) composites , poly (lactic acid) composites filled with multiwalled carbon nanotubes possess higher magnitude of roughness

value and can be attributed to the increasing number of interactions (physical and chemical interactions) due to curvy nature within poly (lactic acid) composites and functional groups on multiwalled carbon nanotubes. On detailed analysis, one can also observe that the atomic force microscopic images of poly (lactic acid) hybrid composites have smaller and sharper peaks as compared to 2.5wt% of carbon black poly (lactic acid) composite; thereby noting the strong interaction between the poly (lactic acid) chains and filler's surface, specifically between the unfilled spaces in 2.5wt% carbon black filled poly (lactic acid) composites and multiwalled carbon nanotubes / cellulose nanofibers. At concentration above 1.0wt% of multiwalled carbon nanotubes / cellulose nanofibers with 2.5wt% of carbon black in poly (lactic acid) matrix decreased the interactions between the poly (lactic acid) chains and fillers surface, owing to which broad peaks were formed. These interactions within poly (lactic acid) composites and hybrid composites can be corroborated with the results presented in **Chapter 6**, which characterizes poly (lactic acid) composites and hybrid composites for structural analysis using ATR – FTIR Spectroscopy considering the % transmittance, shifts in absorption bands, formation of new absorption bands and area of absorption bands.

7.3 FRACTURE STUDIES [MICROSTRUCTURE]

Fracture studies were done to have a brief understanding on failure mechanism in tensile mode. Optical microscopy (X100) and Scanning electron microscopy (X1000) are used to have a brief understanding of the failure mechanism with respect to the filler type and quantity in poly (lactic acid) composites and hybrid composites[161].

7.3.1 OPTICAL MICROSCOPY

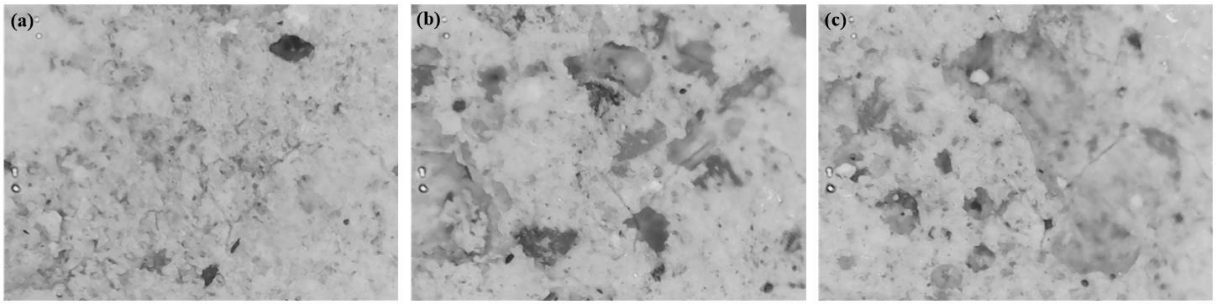

Figure 7.12:Poly (lactic acid) composites with (a) 0.5wt%, (b) 2.5wt% and (c) 10wt% of carbon black

Images in Figure 7.12, Figure 7.13 and Figure 7.14 are optical microscopic images for tensile fractured specimens of carbon black, cellulose nanofibers, multiwalled carbon nanotubes and 2.5wt% carbon black + multiwalled carbon nanotubes, 2.5wt% carbon black + cellulose nanofibers . At lower concentration of carbon black, least resistance is offered to deformation

in tensile mode owing to which minimum roughness is observed on the microscopic images; as the concentration of carbon black increases to 2.5wt% , resistance to tensile deformation increases due to which maximum roughness is observed . At concentration above 2.5wt% carbon black, i.e. 10wt% roughness due to resisting the tensile force is observed, in line with -

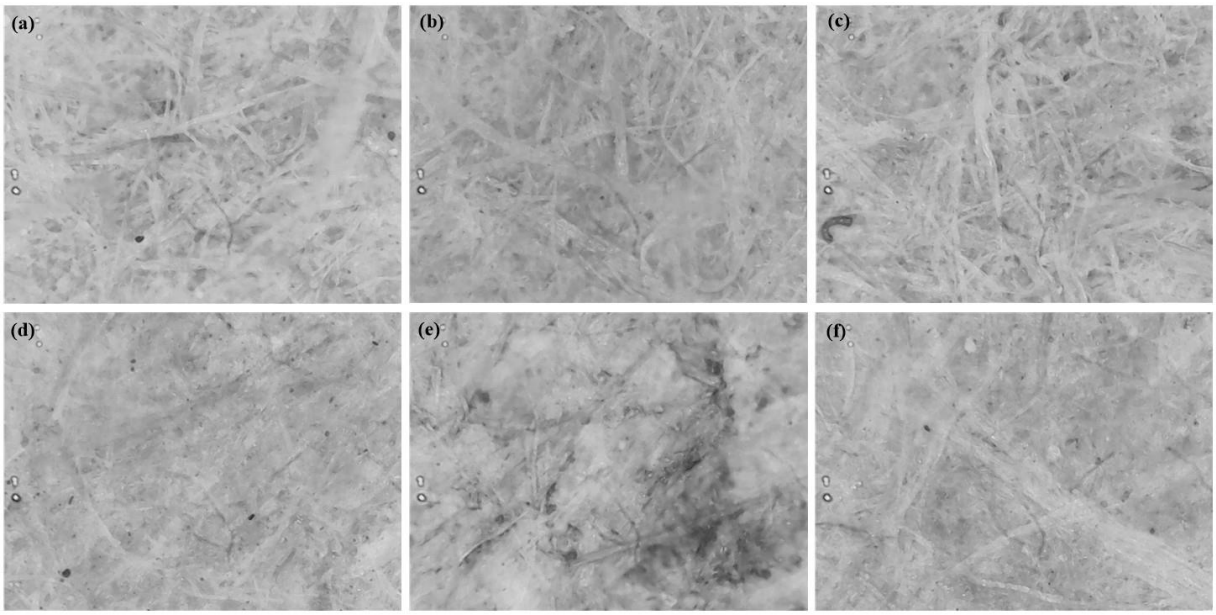

Figure 7.13: Poly (lactic acid) composites (a) 0.2wt% (b) 0.8wt% and (c) 2.0wt% of Cellulose nanofibers (d) 0.2wt%, (e) 0.8wt% and 2.0wt% of multiwalled carbon nanotubes (X100)

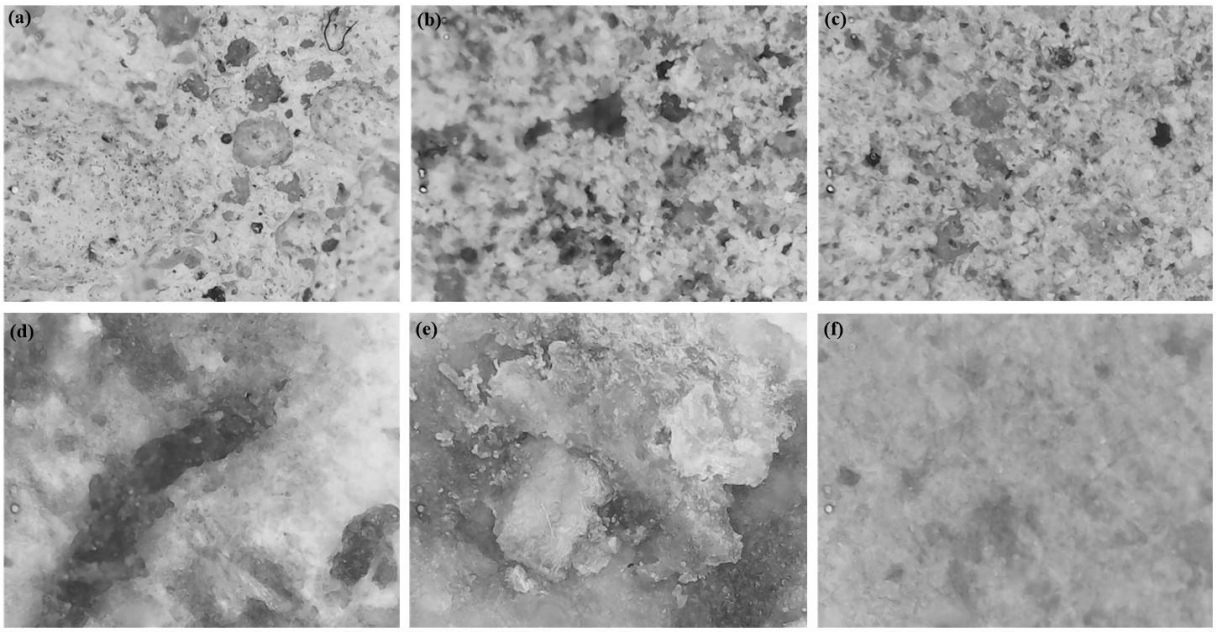

Figure 7.14: Poly (lactic acid) composites 2.5wt% Carbon black +[(a) 0.2wt% (b) 0.8wt% and (c) 2.0wt%] of Multiwalled carbon nanotubes 2.5wt% Carbon black + [(d) 0.2wt%, (e) 0.8wt% and 2.0wt%] of cellulose nanofibers (X100)

-smooth surfaces, which is in indicative of the brittle fracture of the carbon black filled poly (lactic acid) concentration at 10wt%. Similar conclusion can be made for poly (lactic acid) composites filled with cellulose nanofibers and multiwalled carbon nanotubes (collectively called nanofillers). Optical microscopic images for cellulose nanofibers and multiwalled carbon nanotubes filled poly (lactic acid) composites looks close to similar (**see Figure 7.13**), with no major difference in microstructure when observed through optical microscope; but when observed through scanning electron microscope difference in the microstructure is observed (**see Figure 7.16**) which confirmed the fact that morphological analysis was dependent on the level of magnification and the details needed by the observer. **Figure 7.14** are optical microscopic images for poly (lactic acid) hybrid filler composites of carbon black with multiwalled carbon nanotubes and carbon black with cellulose nanofibers. In the case of hybrid composites filled with carbon black and multiwalled carbon nanotubes maximum roughness texture was observed when compared to tensile fractured specimens of hybrid composites filled with carbon black and cellulose nanofibers. This increase in the roughness for hybrid composites filled with carbon black and multiwalled carbon nanotubes can be attributed to the increase in resistance to get apart from each other, which can be attributed to slight ductile behavior; whereas for hybrid composites filled with carbon black and cellulose nanofibers, smooth surfaces are observed and can be attributed to strong interactions between the hydroxyl groups of cellulose nanofibers and carbonyl group of poly (lactic acid), thereby making the hybrid composites brittle in nature. It can be concluded that poly (lactic acid) composites filled with carbon black and multiwalled carbon nanotubes possess the microstructure with maximum visible surface roughness , thereby leading to composites with optimized mechanical properties (in terms of strength and elongation).

7.3.2 SCANNING ELECTRON MICROSCOPY

To obtain detailed information on nature of fracture during tensile deformation was further analyzed using a scanning electron microscope [SEM]. **Figure 7.15**, **Figure 7.16** and **Figure 7.17** are the SEM images for tensile fractured surfaces of carbon black, multiwalled carbon nanotubes & cellulose nanofibers filled and hybrid fillers (CB + MWCNT) / (CB + CNF) respectively. Selected composites are viewed under the scanning electron microscope at x1000. **Figure 7.15** are images of carbon black filled poly (lactic acid) composites filled with 0.5wt%, 2.5wt% and 10.0wt% .One can observe that poly (lactic acid) composites filled with 2.5wt% of carbon black shows ductile deformation during tensile test; ductile deformation can be corelated to the rough surface; whereas tensile fractured surface for 0.5wt% and 10.0wt%

carbon black filled poly (lactic acid) composites appears smooth in comparison to 2.5wt% filled carbon black poly (lactic acid) composites.

7.3.2.1 CARBON BLACK FILLED POLY (LACTIC ACID) COMPOSITES

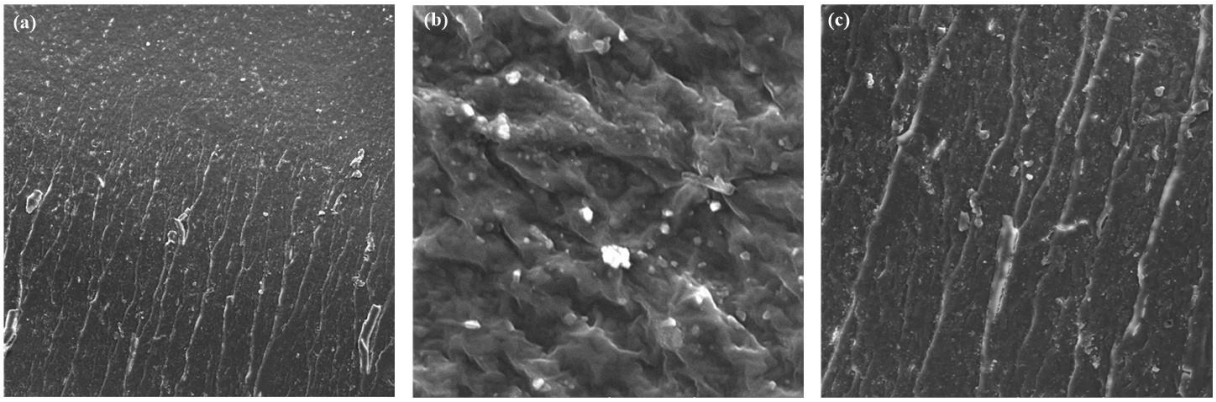

Figure 7.15: Poly (lactic acid) composites with (a) 0.5wt%, (b) 2.5wt% and (c) 10wt% of carbon black (X1000)

On comparison of the tensile fractured surface of 0.5wt% and 10.0wt% filled carbon black poly (lactic acid) composites, one can observe difference in the width of striations. Poly (lactic acid) composites with 0.5wt% carbon black have striations with narrow width in comparison to broad widths striations of 10.0wt% carbon black filled poly (lactic acid) composites. **Figure 7.16 (a)**, **7.16 (b)** and **7.16 (c)** represents poly (lactic acid) composites filled with 0.2wt%, 0.8wt% and 2.0wt% of multiwalled carbon nanotubes. One can observe that poly (lactic acid) composites filled with 2.0wt% of multiwalled carbon nanotubes shows smooth surfaces, compared with 0.2wt% and 0.8wt% multiwalled carbon nanotubes filled poly (lactic acid) composites which shows slight striations on tensile fractured surfaces; these slight striations indicates the occurrence of a ductile mechanism, which does not occur in poly (lactic acid) composites filled with 2.0wt% of multiwalled carbon nanotubes. Close to similar observations are observed in poly (lactic acid) composites filled with cellulose nanofibers at similar concentration with an exception to tensile fractured specimen filled with 2.0wt% cellulose nanofibers; wherein a minimum roughness is observed which can be attributed to strong interactions between hydroxyl groups of cellulose nanofibers and carbonyl group of poly (lactic acid). A maximum roughness is observed for poly (lactic acid) composites filled with 0.8wt% of cellulose nanofibers, which can be attributed to the maximum interaction between poly (lactic acid) matrix and hydroxyl groups of cellulose nanofibers. **Figure 7.17** represents SEM images of tensile fractured specimens of hybrid composites. On comparing the SEM image in **Figure 7.15(b)** for 2.5wt% carbon black filled poly (lactic acid) composites, one may

observe that microstructure of hybrid composites changes to a large extent which in way effects the mechanical properties of hybrid composites in comparison to poly (lactic acid) composites filled with 2.5wt% of carbon black[161].

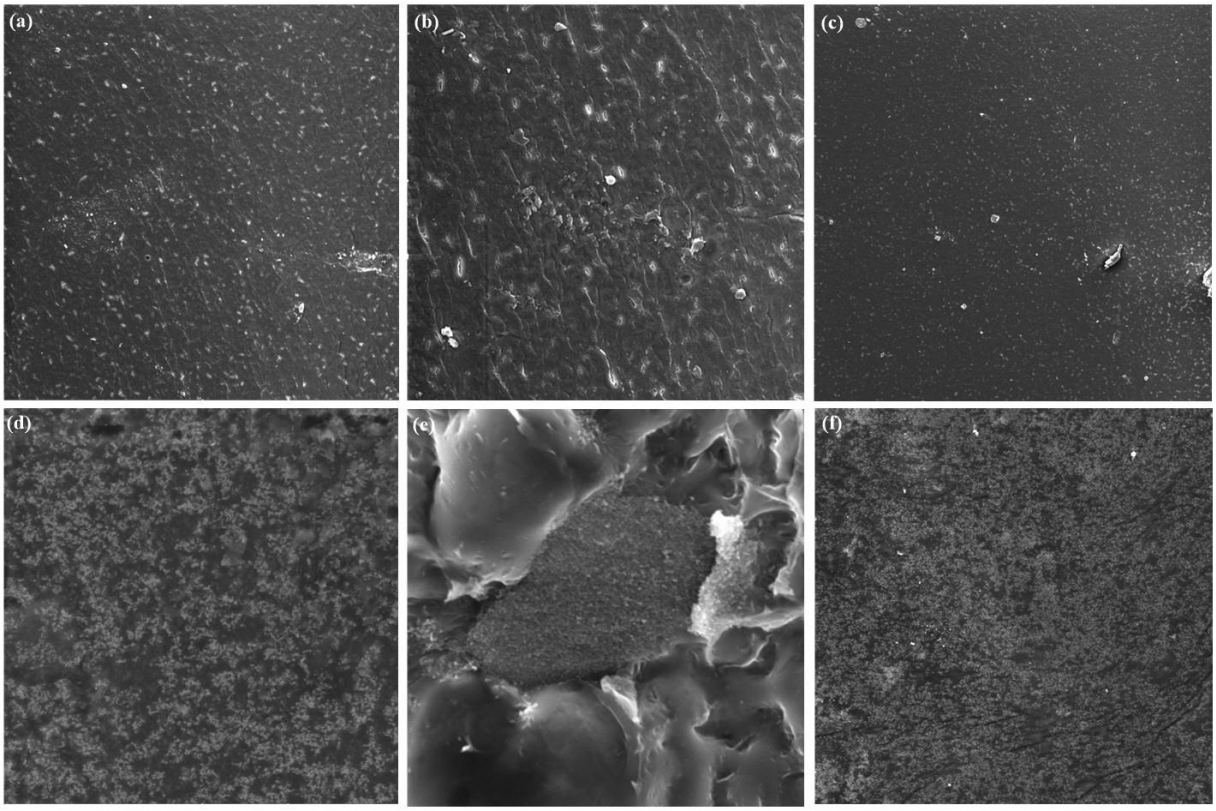

Figure 7.16: Poly (lactic acid) composites (a) 0.2wt% (b) 0.8wt% and (c) 2.0wt% of Multiwalled carbon nanotubes (d) 0.2wt%, (e) 0.8wt% and 2.0wt% of cellulose nanofibers (X1000)

Roughness observed on tensile fractured specimens indicates the resistance undergone by the specimen to break in tensile mode. Hence through **Figure 7.17 (c)**, **7.17 (d)** and **7.17 (e)** it is observed that maximum resistance is offered by 2.5wt% carbon black + nanocellulose fibers filled poly (lactic acid) composites in comparison to 2.5wt% carbon black + multiwalled carbon nanotubes, see **Figure 7.17 (a)**, **7.17 (b)** and **7.17 (c)**.Hence we can conclude that tensile fractured specimen with maximum roughness undergoes maximum resistance to rupture during its deformation. Tensile fractured specimens of hybrid composites depicts higher degree of deformation in comparison to their single filler poly (lactic acid) composites [see **Figure 7.15** and **Figure 7.16** for comparison]. The non – homogeneity of the structure for hybrid composites resembles its interaction with poly (lactic acid) matrix and its co-filler. The presence of co-filler make the microstructure more resistant to mechanical deformation and improves its mechanical properties[161].

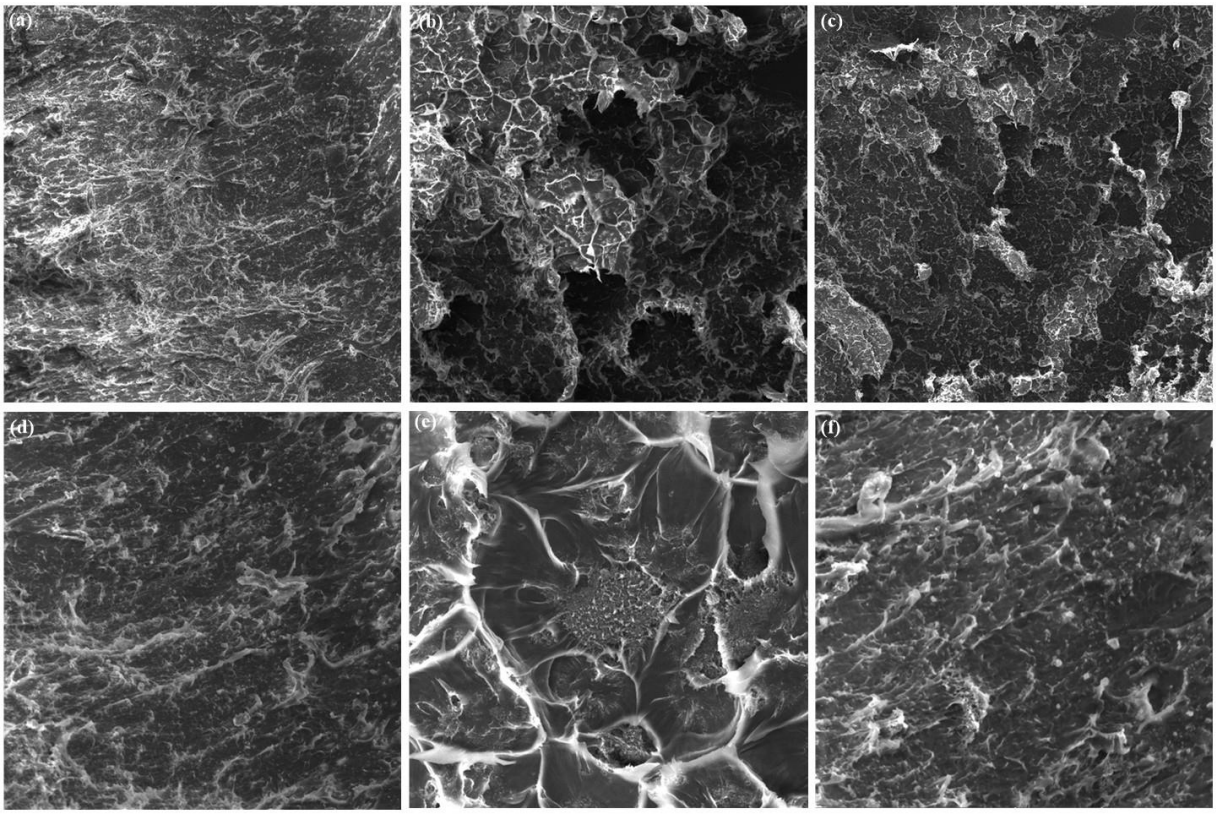

Figure 7.17: Poly (lactic acid) composites 2.5wt% Carbon black +[(a) 0.2wt% (b) 0.8wt% and (c) 2.0wt%] of Multiwalled carbon nanotubes 2.5wt% Carbon black + [(d) 0.2wt%, (e) 0.8wt% and 2.0wt%] of cellulose nanofibers (X1000)

7.4 FINAL CONCLUSION

Microstructural studies using morphological analysis through optical microscopy and scanning electron microscopy was done to study the deformation nature of poly (lactic acid) composites and hybrid composites. Sub microstructural studies using transmission electron microscopy and atomic force microscopy was done to study the dispersion characteristics of fillers in poly (lactic acid) composites and hybrid composites. Increasing concentration of filler in poly (lactic acid) composites and hybrid composites tend to deform poly (lactic acid) composites and hybrid composites in a brittle fashion; whereas poly (lactic acid) composites with optimized quantity of filler deformed the poly (lactic acid) composites and hybrid composites in a ductile manner. The ductile deformation in poly (lactic acid) composites and hybrid composites can be attributed to breakage of strong physical and chemical interactions within poly (lactic acid) composites and hybrid composites (i.e. strong connected network). Brittle deformation in neat poly (lactic acid) / poly (lactic acid) composites and hybrid composites can be attributed to weak physical interactions and connected network of fillers

themselves (i.e. weak linked skeletal network). Modification in the interphase region confirmed in **Chapter 5** and presence of intermolecular interactions [physical and chemical] in **Chapter 6** enhances the physio - mechanical strength of singly filled poly (lactic acid) composites and hybrid filler poly (lactic acid) composites and is presented in the next chapter, i.e. **Chapter 8**.

8 PHYSIO-MECHANICAL PROPERTIES

8.1 DENSITY

Results and relevant discussion for the change in density of poly (lactic acid) composites and hybrid composites is attributed to interphase modification, which is supported with results obtained from Ultraviolet – Visible spectroscopy and is well explained in **Section 5.2** and **Section 5.1** in **Chapter 5** respectively.

8.2 HARDNESS

Table 8.1. Descriptive Statistics of Hardness for Carbon black filled Poly (lactic acid) composites

Sample Code	Sample Size	Mean	Standard Dev	SE of mean
P0.0	10	89.62	0.5808	0.18367
P0.5	10	89.977	0.07846	0.02481
P1.0	10	90.355	0.07106	0.02247
P1.5	10	90.460	0.05831	0.01844
P2.0	10	90.565	0.01179	0.00373
P2.5	10	90.629	0.01853	0.00586
P5.0	10	90.784	0.05948	0.01881
P10.0	10	90.927	0.03529	0.01116

Table 8.2. Descriptive Statistics of Hardness for multiwalled carbon nanotubes filled Poly (lactic acid) composites

Sample Code	Sample Size	Mean	Standard Dev	SE of mean
P0.0	10	89.62	0.5808	0.18367
P0.2	10	90.316	0.08959	0.02833
P0.4	10	90.624	0.02319	0.00733
P0.6	10	90.638	0.03882	0.01227
P0.8	10	90.754	0.02914	0.00921
P1.0	10	90.853	0.01494	0.00473
P1.5	10	91.184	0.03534	0.01118
P2.0	10	91.625	0.06604	0.02088

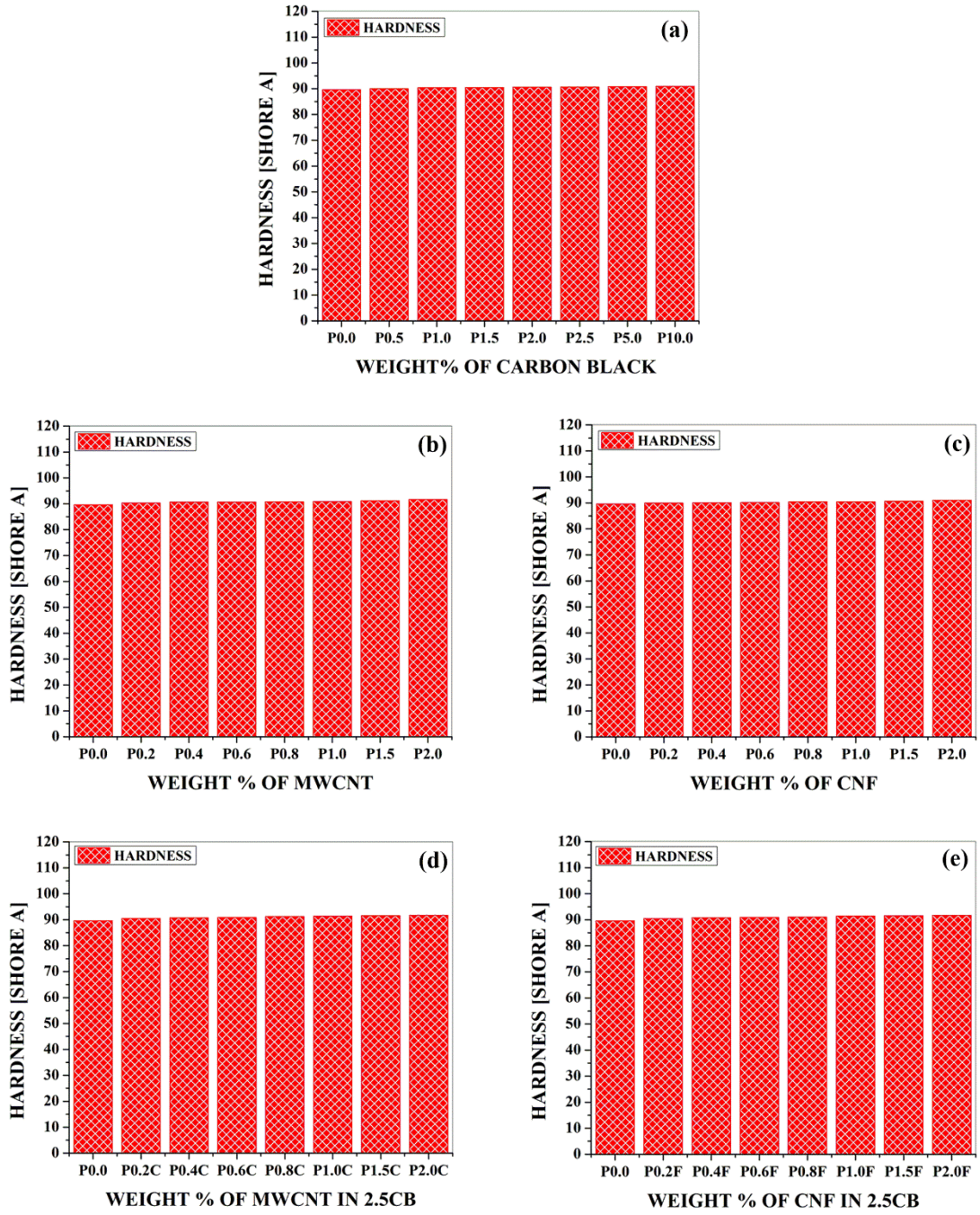

Figure 8.1. Hardness for poly (lactic acid) composites filled with (a) carbon black (b) multiwalled carbon nanotubes (c) cellulose nanofibers (d) multiwalled carbon nanotubes + 2.5carbon black (e) cellulose nanofibers + 2.5carbon black

Table 8.3. Descriptive Statistics of Hardness for cellulose nanofibers filled Poly (lactic acid) composites

Sample Code	Sample Size	Mean	Standard Dev	SE of mean
P0.0	10	89.62	0.5808	0.18367

P0.2	10	89.921	0.02923	0.00924
P0.4	10	90.056	0.01647	0.00521
P0.6	10	90.121	0.00994	0.00314
P0.8	10	90.422	0.01398	0.00442
P1.0	10	90.472	0.01619	0.00512
P1.5	10	90.620	0.13166	0.04163
P2.0	10	91.067	0.01059	0.00335

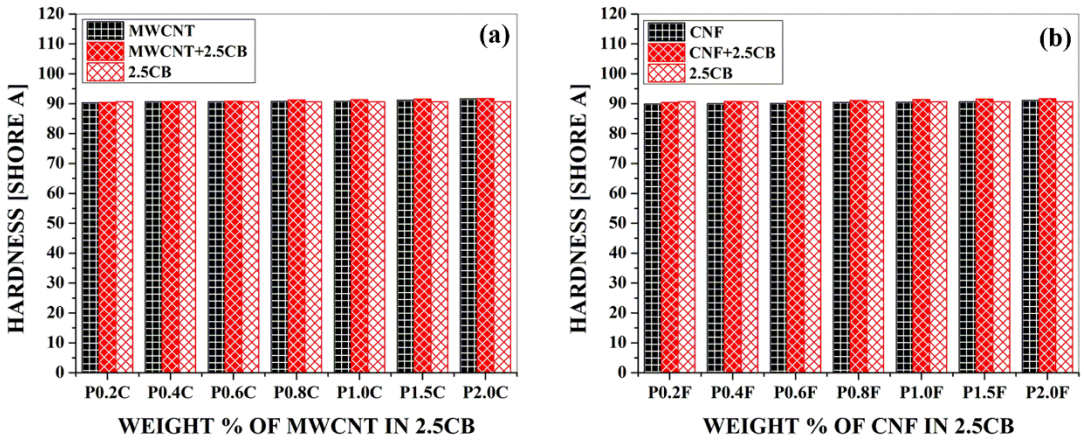

Figure 8.2. Comparative hardness for (a) multiwalled carbon nanotubes + 2.5 carbon black (b) cellulose nanofibers + 2.5 carbon black with 2.5carbon black poly (lactic acid) composites and specific nanofiller loaded poly (lactic acid) composites.

Table 8.4. Descriptive Statistics of Hardness for 2.5carbon black + multiwalled carbon nanotubes and 2.5carbon black + cellulose nanofibers filled Poly (lactic acid) composites

Sample Code	Sample Size	Mean	Standard Dev	SE of mean
P0.0	10	89.62	0.5808	0.18367
P0.2C	10	90.451	0.01853	0.00586
P0.4C	10	90.728	0.0253	0.008
P0.6C	10	90.841	0.01969	0.00623
P0.8C	10	91.266	0.0709	0.02242
P1.0C	10	91.372	0.02781	0.00879
P1.5C	10	91.552	0.02044	0.00646
P2.0C	10	91.719	0.01912	0.00605

P0.2F	10	90.446	0.01713	0.00542
P0.4F	10	90.771	0.01595	0.00504
P0.6F	10	90.877	0.00675	0.00213
P0.8F	10	91.067	0.00949	0.003
P1.0F	10	91.426	0.01955	0.00618
P1.5F	10	91.565	0.01509	0.00477
P2.0F	10	91.671	0.01197	0.00379

Table 8.5. Means Comparison of hardness by Bonferroni Test for carbon black filled poly (lactic acid) composites

Sample Code	Mean Diff	t Value	Alpha	Sigma
P0.5 P0.0	0.357	3.7778	0.05	1
P1.0 P0.0	0.735	7.77783	0.05	1
P1.0 P0.5	0.378	4.00002	0.05	1
P1.5 P0.0	0.84	8.88894	0.05	1
P1.5 P0.5	0.483	5.11114	0.05	1
P1.5 P1.0	0.105	1.11112	0.05	0
P2.0 P0.0	0.945	10.00006	0.05	1
P2.0 P0.5	0.588	6.22226	0.05	1
P2.0 P1.0	0.21	2.22224	0.05	0
P2.0 P1.5	0.105	1.11112	0.05	0
P2.5 P0.0	1.009	10.67732	0.05	1
P2.5 P0.5	0.652	6.89951	0.05	1
P2.5 P1.0	0.274	2.89949	0.05	0
P2.5 P1.5	0.169	1.78837	0.05	0
P2.5 P2.0	0.064	0.67725	0.05	0
P5.0 P0.0	1.164	12.31754	0.05	1
P5.0 P0.5	0.807	8.53974	0.05	1
P5.0 P1.0	0.429	4.53971	0.05	1
P5.0 P1.5	0.324	3.42859	0.05	1
P5.0 P2.0	0.219	2.31747	0.05	0
P5.0 P2.5	0.155	1.64022	0.05	0

P10.0 P0.0	1.307	13.83077	0.05	1
P10.0 P0.5	0.95	10.05297	0.05	1
P10.0 P1.0	0.572	6.05295	0.05	1
P10.0 P1.5	0.467	4.94183	0.05	1
P10.0 P2.0	0.362	3.83071	0.05	1
P10.0 P2.5	0.298	3.15346	0.05	0
P10.0 P5.0	0.143	1.51324	0.05	0

Table 8.6. Means Comparison of hardness by Bonferroni Test for multiwalled carbon nanotubes filled poly (lactic acid) composites

Sample Code	Mean Diff	t Value	Alpha	Sigma
P0.2 P0.0	0.696	7.39749	0.05	1
P0.4 P0.0	1.004	10.67109	0.05	1
P0.4 P0.2	0.308	3.2736	0.05	1
P0.6 P0.0	1.018	10.81989	0.05	1
P0.6 P0.2	0.322	3.4224	0.05	1
P0.6 P0.4	0.014	0.1488	0.05	0
P0.8 P0.0	1.134	12.05281	0.05	1
P0.8 P0.2	0.438	4.65532	0.05	1
P0.8 P0.4	0.13	1.38172	0.05	0
P0.8 P0.6	0.116	1.23292	0.05	0
P1.0 P0.0	1.233	13.10504	0.05	1
P1.0 P0.2	0.537	5.70755	0.05	1
P1.0 P0.4	0.229	2.43394	0.05	0
P1.0 P0.6	0.215	2.28514	0.05	0
P1.0 P0.8	0.099	1.05223	0.05	0
P1.5 P0.0	1.564	16.6231	0.05	1
P1.5 P0.2	0.868	9.22561	0.05	1
P1.5 P0.4	0.56	5.952	0.05	1
P1.5 P0.6	0.546	5.8032	0.05	1
P1.5 P0.8	0.43	4.57029	0.05	1
P1.5 P1.0	0.331	3.51806	0.05	1

P2.0 P0.0	2.005	21.3103	0.05	1
P2.0 P0.2	1.309	13.91281	0.05	1
P2.0 P0.4	1.001	10.63921	0.05	1
P2.0 P0.6	0.987	10.49041	0.05	1
P2.0 P0.8	0.871	9.25749	0.05	1
P2.0 P1.0	0.772	8.20526	0.05	1
P2.0 P1.5	0.441	4.6872	0.05	1

Table 8.7. Means Comparison of hardness by Bonferroni Test for cellulose nanofibers filled poly (lactic acid) composites

Sample Code	Mean Diff	t Value	Alpha	Sigma
P0.2 P0.0	0.301	3.18853	0.05	0
P0.4 P0.0	0.436	4.6186	0.05	1
P0.4 P0.2	0.135	1.43007	0.05	0
P0.6 P0.0	0.501	5.30715	0.05	1
P0.6 P0.2	0.2	2.11862	0.05	0
P0.6 P0.4	0.065	0.68855	0.05	0
P0.8 P0.0	0.802	8.49568	0.05	1
P0.8 P0.2	0.501	5.30715	0.05	1
P0.8 P0.4	0.366	3.87708	0.05	1
P0.8 P0.6	0.301	3.18853	0.05	0
P1.0 P0.0	0.852	9.02534	0.05	1
P1.0 P0.2	0.551	5.83681	0.05	1
P1.0 P0.4	0.416	4.40674	0.05	1
P1.0 P0.6	0.351	3.71819	0.05	1
P1.0 P0.8	0.05	0.52966	0.05	0
P1.5 P0.0	1	10.59312	0.05	1
P1.5 P0.2	0.699	7.40459	0.05	1
P1.5 P0.4	0.564	5.97452	0.05	1
P1.5 P0.6	0.499	5.28597	0.05	1
P1.5 P0.8	0.198	2.09744	0.05	0
P1.5 P1.0	0.148	1.56778	0.05	0

P2.0 P0.0	1.447	15.32825	0.05	1
P2.0 P0.2	1.146	12.13972	0.05	1
P2.0 P0.4	1.011	10.70964	0.05	1
P2.0 P0.6	0.946	10.02109	0.05	1
P2.0 P0.8	0.645	6.83256	0.05	1
P2.0 P1.0	0.595	6.30291	0.05	1
P2.0 P1.5	0.447	4.73512	0.05	1

Table 8.8. Means Comparison of hardness by Bonferroni Test for 2.5carbon black + multiwalled carbon nanotubes filled poly (lactic acid) composites

Sample Code	Mean Diff	t Value	Alpha	Sigma
P0.2C P0.0	0.831	8.94418	0.05	1
P0.4C P0.0	1.108	11.92557	0.05	1
P0.4C P0.2C	0.277	2.98139	0.05	0
P0.6C P0.0	1.221	13.14181	0.05	1
P0.6C P0.2C	0.39	4.19763	0.05	1
P0.6C P0.4C	0.113	1.21624	0.05	0
P0.8C P0.0	1.646	17.71614	0.05	1
P0.8C P0.2C	0.815	8.77197	0.05	1
P0.8C P0.4C	0.538	5.79057	0.05	1
P0.8C P0.6C	0.425	4.57434	0.05	1
P1.0C P0.0	1.752	18.85704	0.05	1
P1.0C P0.2C	0.921	9.91286	0.05	1
P1.0C P0.4C	0.644	6.93147	0.05	1
P1.0C P0.6C	0.531	5.71523	0.05	1
P1.0C P0.8C	0.106	1.14089	0.05	0
P1.5C P0.0	1.932	20.79441	0.05	1
P1.5C P0.2C	1.101	11.85023	0.05	1
P1.5C P0.4C	0.824	8.86884	0.05	1
P1.5C P0.6C	0.711	7.6526	0.05	1
P1.5C P0.8C	0.286	3.07826	0.05	0
P1.5C P1.0C	0.18	1.93737	0.05	0

P2.0C P0.0	2.099	22.59185	0.05	1
P2.0C P0.2C	1.268	13.64767	0.05	1
P2.0C P0.4C	0.991	10.66628	0.05	1
P2.0C P0.6C	0.878	9.45005	0.05	1
P2.0C P0.8C	0.453	4.87571	0.05	1
P2.0C P1.0C	0.347	3.73481	0.05	1
P2.0C P1.5C	0.167	1.79745	0.05	0

Table 8.9. Means Comparison of hardness by Bonferroni Test for 2.5carbon black + cellulose nanofibers filled poly (lactic acid) composites

Sample Code	Mean Diff	t Value	Alpha	Sigma
P0.2F P0.0	0.826	8.97548	0.05	1
P0.4F P0.0	1.151	12.50699	0.05	1
P0.4F P0.2F	0.325	3.53151	0.05	1
P0.6F P0.0	1.257	13.65881	0.05	1
P0.6F P0.2F	0.431	4.68333	0.05	1
P0.6F P0.4F	0.106	1.15182	0.05	0
P0.8F P0.0	1.447	15.72339	0.05	1
P0.8F P0.2F	0.621	6.74791	0.05	1
P0.8F P0.4F	0.296	3.21639	0.05	0
P0.8F P0.6F	0.19	2.06458	0.05	0
P1.0F P0.0	1.806	19.62435	0.05	1
P1.0F P0.2F	0.98	10.64887	0.05	1
P1.0F P0.4F	0.655	7.11736	0.05	1
P1.0F P0.6F	0.549	5.96554	0.05	1
P1.0F P0.8F	0.359	3.90096	0.05	1
P1.5F P0.0	1.945	21.13475	0.05	1
P1.5F P0.2F	1.119	12.15927	0.05	1
P1.5F P0.4F	0.794	8.62776	0.05	1
P1.5F P0.6F	0.688	7.47594	0.05	1
P1.5F P0.8F	0.498	5.41137	0.05	1
P1.5F P1.0F	0.139	1.5104	0.05	0

P2.0F P0.0	2.051	22.28657	0.05	1
P2.0F P0.2F	1.225	13.31109	0.05	1
P2.0F P0.4F	0.9	9.77958	0.05	1
P2.0F P0.6F	0.794	8.62776	0.05	1
P2.0F P0.8F	0.604	6.56318	0.05	1
P2.0F P1.0F	0.245	2.66222	0.05	0
P2.0F P1.5F	0.106	1.15182	0.05	0

Numerical data on hardness are represented **Table 8.1** to **Table 8.5** represents the descriptive statistics data and **Table 8.6** to **Table 8.9** represents means comparison for poly (lactic acid) composites filled with carbon black (CB), multiwalled carbon nanotubes (MWCNT), cellulose nanofibers (CNF), 2.5CB+MWCNT, 2.5CB+CNF respectively within batches. Graphical data on hardness are represented in **Figure 8.1** for poly (lactic acid) composites filled with carbon black (CB), multiwalled carbon nanotubes (MWCNT), cellulose nanofibers (CNF), 2.5CB+MWCNT, 2.5CB+CNF and **Figure 8.2** for comparative data between hybrid filler effect and single filler (2.5CB and MWCNT/CNF). Sigma value of “1” in means comparison indicates that the means difference is significant at 0.05 level; and “0” indicates that the difference is not significant at the 0.05 level. Slight increase in hardness values with increase in concentration of fillers is observed, irrespective of the filler used i.e. CB, MWCNT, CNF, 2.5CB + MWCNT and 2.5CB + CNF. Amongst single nanofillers i.e. MWCNT and CNF, MWCNT filled poly (lactic acid) showed slight increase in hardness, which can be attributed to the ability of MWCNT to form more number of interlayers due to its curvy nature with high surface area, owing to which hardness increases To study hybrid effect of nanofillers, poly (lactic acid) composites with 2.5CB was selected; further poly (lactic acid) composites with 2.5CB and 0.2, 0.4, 0.6, 0.8, 1.0, 1.5 and 2.0 wt% of nanofillers were fabricated and characterized for hardness measurements. One can observe that hardness values for hybrid filler poly (lactic acid) composites are slightly higher than single filler poly (lactic acid) composites. In order to study the hybrid filler effect, hardness values of hybrid filler poly (lactic acid) composites are compared with 2.5CB poly (lactic acid) composites. The slight increase in hardness for hybrid filler poly (lactic acid) composites can be attributed to filling up of spaces between spherical carbon black particles dispersed in poly (lactic acid) matrix with the nanofiller; as addition of nanofillers to CB filled poly (lactic acid) increases the surface area and increases the interlayers, and further contributing to increase in hardness. Generally addition of fillers contributes to the physical crosslinks within polymer matrix , which

further leads to crystallinity thereby increasing the hardness of the poly (lactic acid) composites irrespective of the filler used[131][165].

8.3 TENSILE TEST

Table 8.10. Descriptive Statistics of tensile modulus for Carbon black filled Poly (lactic acid) composites

Sample Code	Sample Size	Mean	Standard Dev	SE of mean
P0.0	10	2648.6	6.11374	1.93333
P0.5	10	2797.9	18.18699	5.75123
P1.0	10	3012	49.1709	15.54921
P1.5	10	3108.5	10.01388	3.16667
P2.0	10	3169.7	6.97695	2.2063
P2.5	10	3212	10.32796	3.26599
P5.0	10	3312.5	8.24958	2.60875
P10.0	10	3453	3.39935	1.07497

Table 8.11. Descriptive Statistics of yield strength for Carbon black filled Poly (lactic acid) composites

Sample Code	Sample Size	Mean	Standard Dev	SE of mean
P0.0	10	14.6	0.96609	0.30551
P0.5	10	8.44	0.1075	0.03399
P1.0	10	12.64	0.17127	0.05416
P1.5	10	11.2	0.17638	0.05578
P2.0	10	10.85	0.33082	0.10462
P2.5	10	10.88	0.15492	0.04899
P5.0	10	10.79	0.17288	0.05467
P10.0	10	8.48	0.11353	0.0359

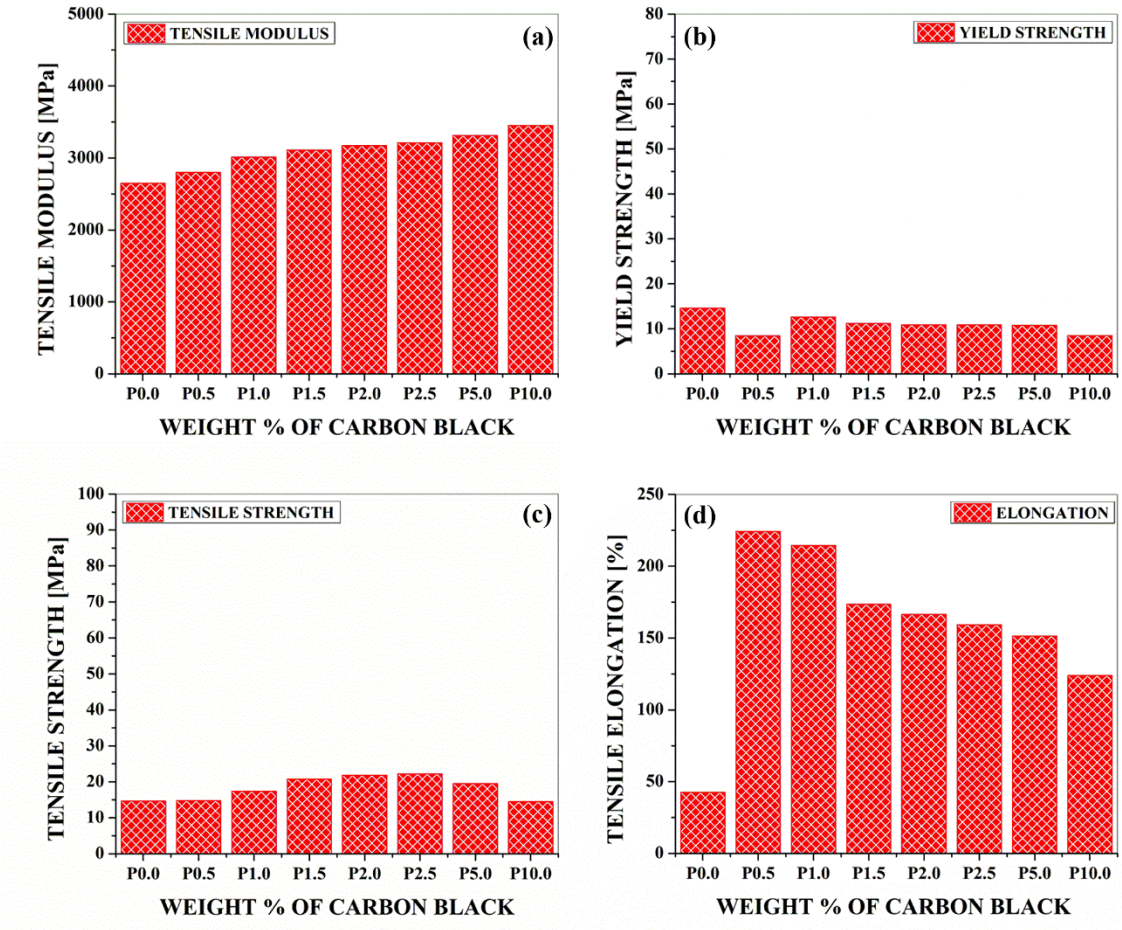

Figure 8.3. (a) Tensile Modulus (b) Yield Strength (c) Tensile Strength (d) Tensile Elongation of Carbon black filled poly (lactic acid) composites

Table 8.12. Descriptive Statistics of tensile strength for Carbon black filled Poly (lactic acid) composites

Sample Code	Sample Size	Mean	Standard Dev	SE of mean
P0.0	10	14.68	0.32931	0.10414
P0.5	10	14.71	0.07379	0.02333
P1.0	10	17.34	0.15776	0.04989
P1.5	10	20.77	0.13375	0.0423
P2.0	10	21.83	0.22632	0.07157
P2.5	10	22.2	0.35901	0.11353
P5.0	10	19.47	0.25408	0.08035
P10.0	10	14.49	0.2079	0.06574

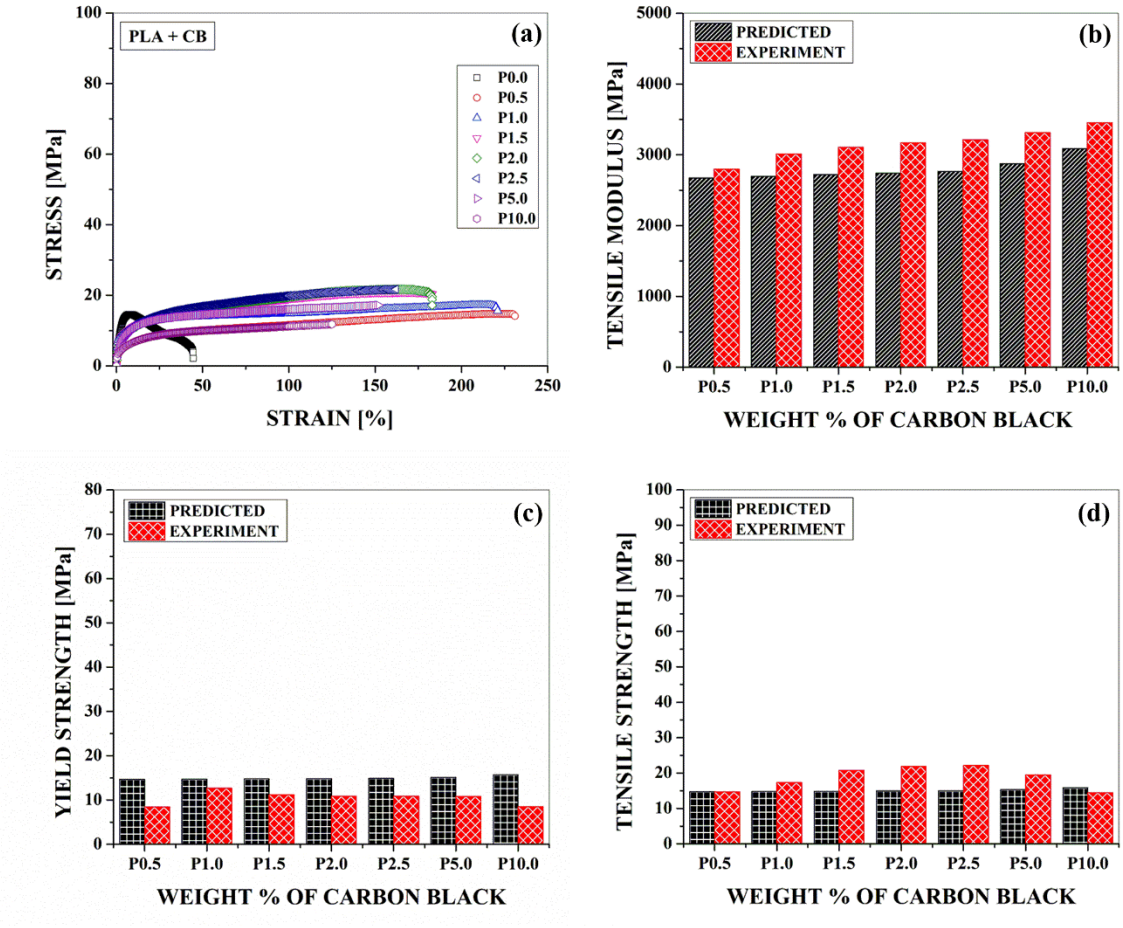

Figure 8.4. (a) Stress Strain Curves, Comparative properties of (b) Tensile Modulus (c) Yield Strength (d) Tensile Strength of carbon black filled poly (lactic acid) composites.

Table 8.13. Descriptive Statistics of tensile elongation for Carbon black filled Poly (lactic acid) composites

Sample Code	Sample Size	Mean	Standard Dev	SE of mean
P0.0	10	42.5	0.97183	0.30732
P0.5	10	224.3	1.82878	0.57831
P1.0	10	214.4	2.63312	0.83267
P1.5	10	173.5	7.09068	2.24227
P2.0	10	166.4	3.23866	1.02415
P2.5	10	159.3	2.31181	0.73106

P5.0	10	151.4	3.43835	1.0873
P10.0	10	123.9	3.69534	1.16857

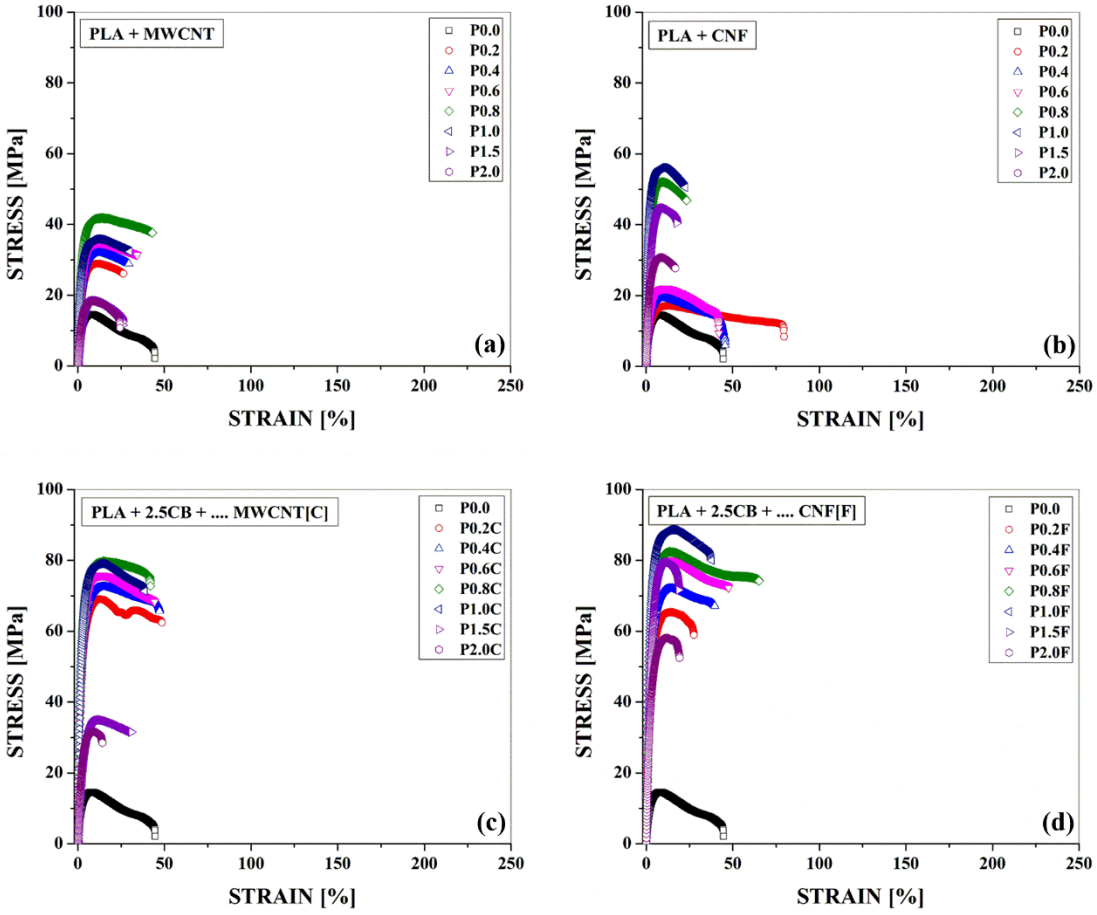

Figure 8.5. Stress Strain Curves for poly (lactic acid) composites filled with (a) multiwalled carbon nanotubes (b) cellulose nanofibers (c) multiwalled carbon nanotubes + 2.5carbon black (d) cellulose nanofibers + 2.5carbon black

Table 8.14. Descriptive Statistics of tensile modulus for multiwalled carbon nanotubes filled Poly (lactic acid) composites

Sample Code	Sample Size	Mean	Standard Dev	SE of mean
P0.0	10	2648.6	6.11374	1.93333
P0.2	10	2772.9	6.82235	2.15742
P0.4	10	2802.1	14.01943	4.43333
P0.6	10	2864.1	6.17252	1.95192

P0.8	10	2968	32.15587	10.16858
P1.0	10	3115	16.15893	5.1099
P1.5	10	3256.3	5.69698	1.80154
P2.0	10	3461.9	8.94986	2.83019

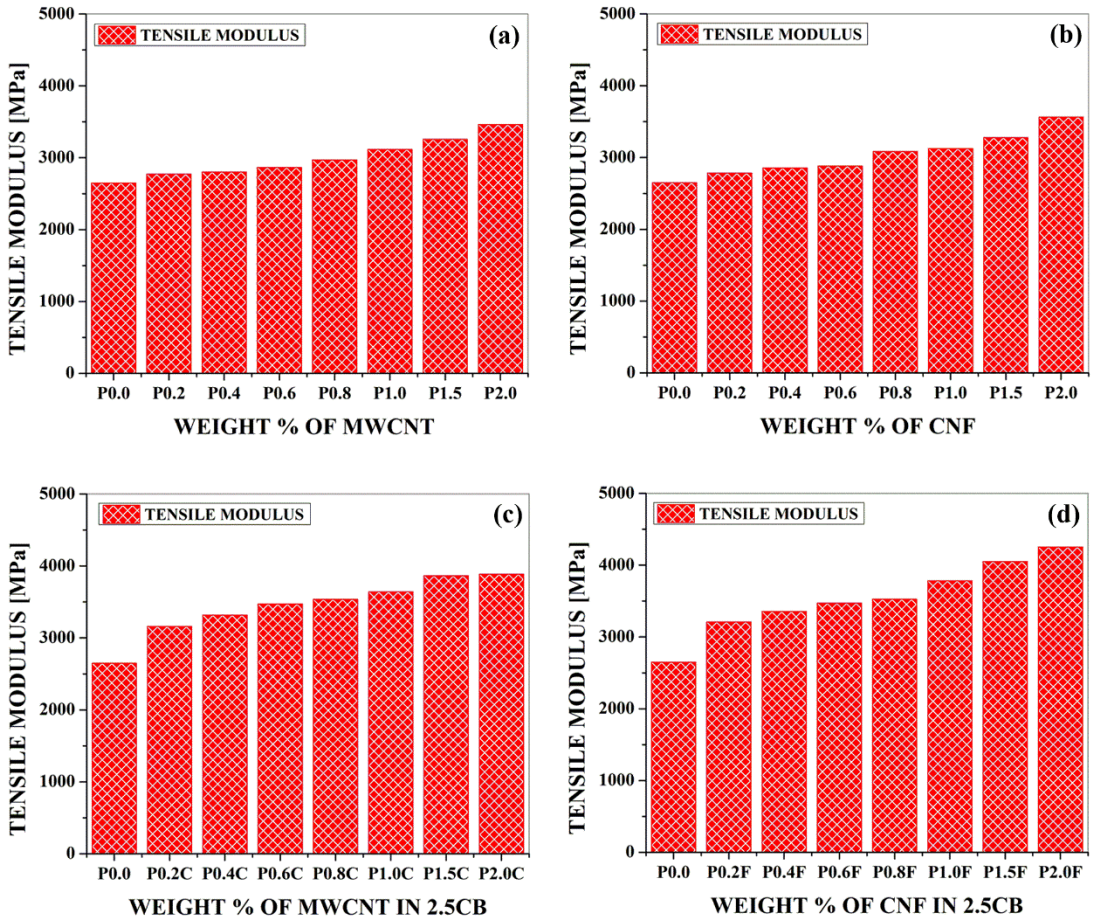

Figure 8.6. Tensile Modulus for poly (lactic acid) composites filled with (a) multiwalled carbon nanotubes (b) cellulose nanofibers (c) multiwalled carbon nanotubes + 2.5carbon black (d) cellulose nanofibers + 2.5carbon black

Table 8.15. Descriptive Statistics of tensile modulus for cellulose nanofibers filled Poly (lactic acid) composites

Sample Code	Sample Size	Mean	Standard Dev	SE of mean
P0.0	10	2648.6	6.11374	1.93333
P0.2	10	2781.9	4.04008	1.27758

P0.4	10	2854.2	3.55278	1.12349
P0.6	10	2881.4	3.40588	1.07703
P0.8	10	3082.6	2.41293	0.76303
P1.0	10	3123.7	2.79086	0.88255
P1.5	10	3277.6	3.40588	1.07703
P2.0	10	3564.2	4.51664	1.42829

Table 8.16. Descriptive Statistics of tensile modulus for 2.5carbon black + multiwalled carbon nanotubes and 2.5carbon black + cellulose nanofibers filled Poly (lactic acid) composites

Sample Code	Sample Size	Mean	Standard Dev	SE of mean
P0.0	10	2648.6	6.11374	1.93333
P0.2C	10	3158.5	49.78007	15.74184
P0.4C	10	3319	18.67857	5.90668
P0.6C	10	3472.3	7.71794	2.44063
P0.8C	10	3536.8	7.46548	2.36079
P1.0C	10	3639.3	31.1343	9.84553
P1.5C	10	3863.8	7.0993	2.24499
P2.0C	10	3885.3	27.07623	8.56226
P0.2F	10	3210	56.76462	17.95055
P0.4F	10	3353.1	4.35762	1.378
P0.6F	10	3470.1	8.29257	2.62234
P0.8F	10	3524.5	5.98609	1.89297
P1.0F	10	3783.7	4.32178	1.36667
P1.5F	10	4050.4	3.56526	1.12744
P2.0F	10	4253.3	2.83039	0.89505

Table 8.17. Descriptive Statistics of yield strength for multiwalled carbon nanotubes filled Poly (lactic acid) composites

Sample Code	Sample Size	Mean	Standard Dev	SE of mean
P0.0	10	14.6	0.96609	0.30551
P0.2	10	20.99	2.47045	0.78123
P0.4	10	27.217	0.50487	0.15965

P0.6	10	27.726	0.75159	0.23767
P0.8	10	29.467	0.28079	0.0888
P1.0	10	24.711	0.2456	0.07767
P1.5	10	13.235	0.54421	0.17209
P2.0	10	12.781	0.32313	0.10218

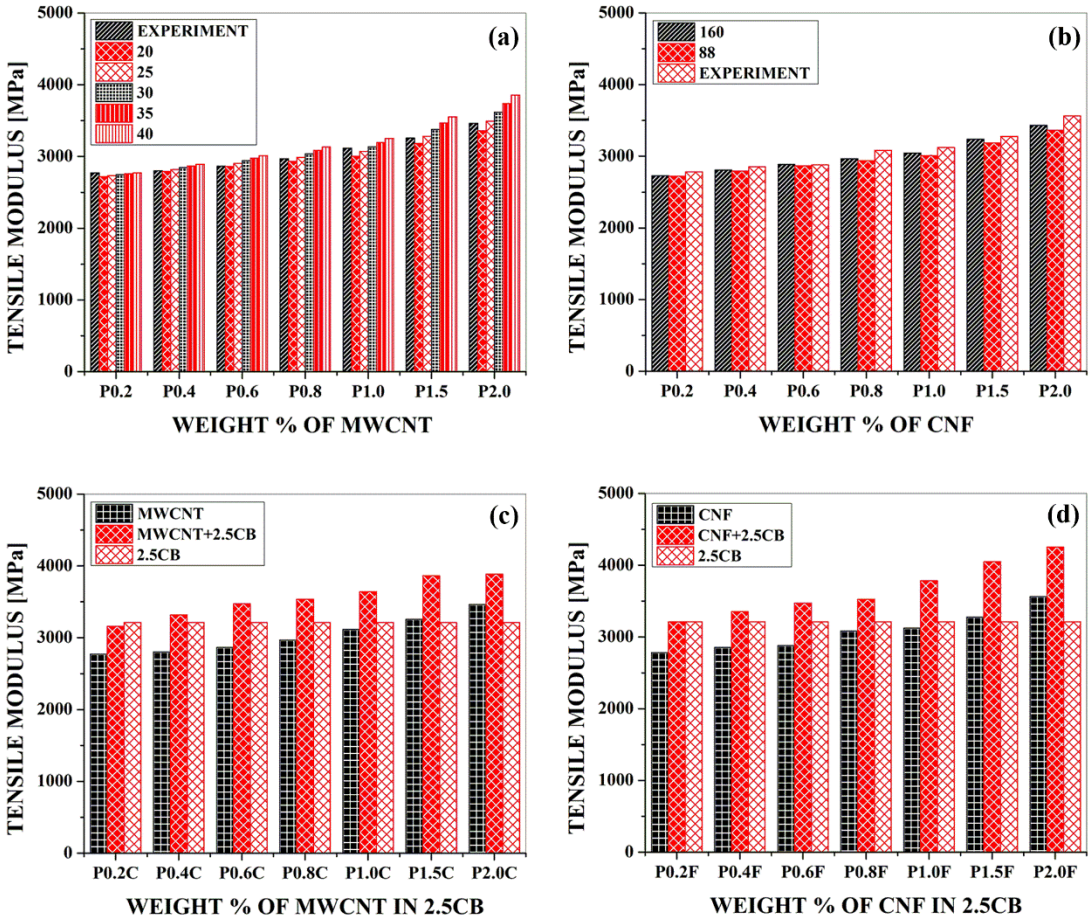

Figure 8.7. Comparative tensile modulus for (a) multiwalled carbon nanotubes (b) cellulose nanofibers (c) multiwalled carbon nanotubes + 2.5 carbon black (d) cellulose nanofibers + 2.5 carbon black with aspect ratio for multiwalled carbon nanotubes and cellulose nanofibers and 2.5carbon black poly (lactic acid) composites and specific nanofiller loaded poly (lactic acid) composites.

Table 8.18. Descriptive Statistics of yield strength for cellulose nanofibers filled Poly (lactic acid) composites

Sample Code	Sample Size	Mean	Standard Dev	SE of mean

P0.0	10	14.6	0.96609	0.30551
P0.2	10	12.9	0.73786	0.23333
P0.4	10	16.6	0.96609	0.30551
P0.6	10	18.4	0.96609	0.30551
P0.8	10	36.3	1.1595	0.36667
P1.0	10	40.8	1.31656	0.41633
P1.5	10	27.4	0.69921	0.22111
P2.0	10	19.3	1.25167	0.39581

Table 8.19. Descriptive Statistics of yield strength for 2.5carbon black + multiwalled carbon nanotubes and 2.5carbon black + cellulose nanofibers filled Poly (lactic acid) composites

Sample Code	Sample Size	Mean	Standard Dev	SE of mean
P0.0	10	14.6	0.96609	0.30551
P0.2C	10	57.2	2.14994	0.67987
P0.4C	10	60.3	2.35938	0.7461
P0.6C	10	61.3	2.71006	0.857
P0.8C	10	65	1.33333	0.42164
P1.0C	10	60	1.63299	0.5164
P1.5C	10	28.3	2.79086	0.88255
P2.0C	10	19.9	2.13177	0.67412
P0.2F	10	48.5	1.58114	0.5
P0.4F	10	52.7	1.88856	0.59722
P0.6F	10	62	2.26078	0.71492
P0.8F	10	73.7	1.1595	0.36667
P1.0F	10	71.6	2.1187	0.66999
P1.5F	10	56	1.88562	0.59628
P2.0F	10	42.2	2.74064	0.86667

Table 8.20. Descriptive Statistics of tensile strength for multiwalled carbon nanotubes filled Poly (lactic acid) composites

Sample Code	Sample Size	Mean	Standard Dev	SE of mean
P0.0	10	14.68	0.32931	0.10414

P0.2	10	29.228	0.65306	0.20651
P0.4	10	32.367	0.39967	0.12639
P0.6	10	34.83	0.37431	0.11837
P0.8	10	41.966	0.47143	0.14908
P1.0	10	35.864	0.37426	0.11835
P1.5	10	19.009	0.5673	0.1794
P2.0	10	18.21	0.1792	0.05667

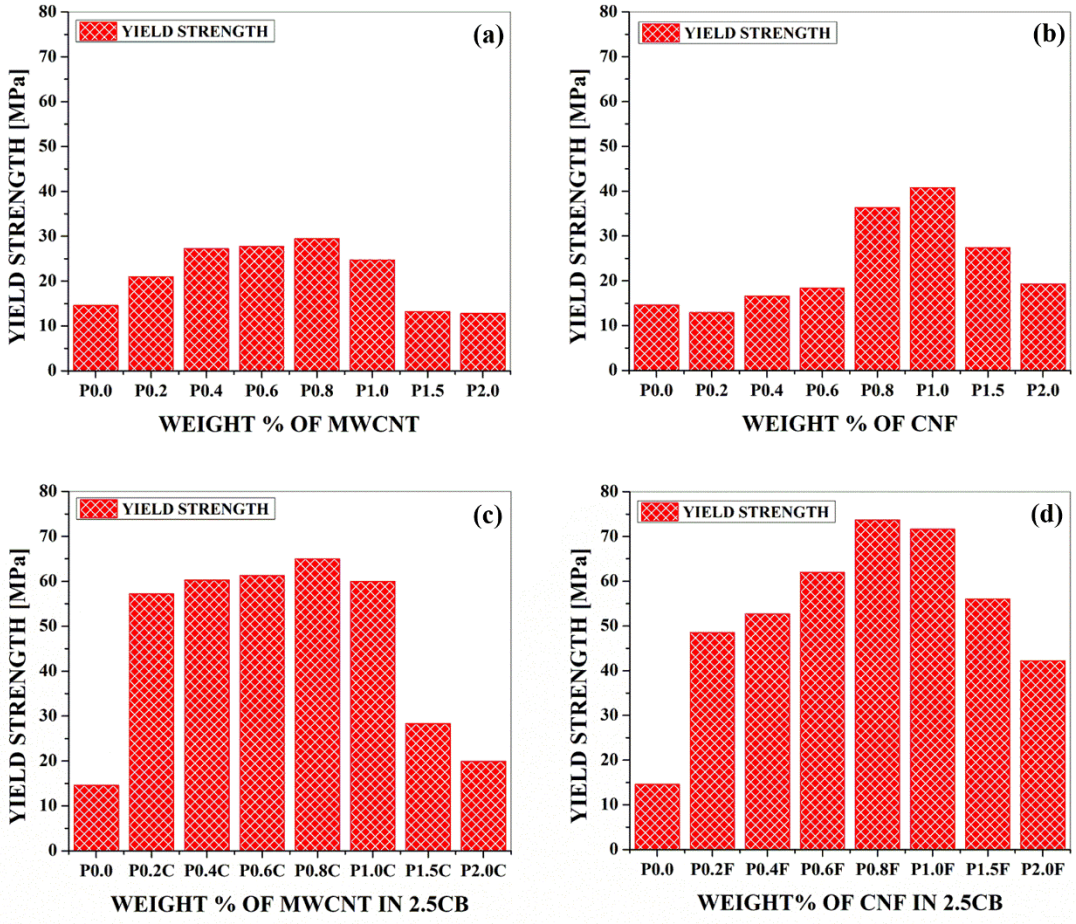

Figure 8.8.Yield strength for poly (lactic acid) composites filled with (a) multiwalled carbon nanotubes (b) cellulose nanofibers (c) multiwalled carbon nanotubes + 2.5carbon black (d) cellulose nanofibers + 2.5carbon black

Table 8.21. Descriptive Statistics of tensile strength for cellulose nanofibers filled Poly (lactic acid) composites

Sample Code	Sample Size	Mean	Standard Dev	SE of mean

P0.0	10	14.68	0.32931	0.10414
P0.2	10	17.28	0.44422	0.14048
P0.4	10	19.65	0.27988	0.08851
P0.6	10	22.7	0.82327	0.26034
P0.8	10	52.09	1.52494	0.48223
P1.0	10	56.21	1.13377	0.35853
P1.5	10	44.57	0.83273	0.26333
P2.0	10	30.31	1.24584	0.39397

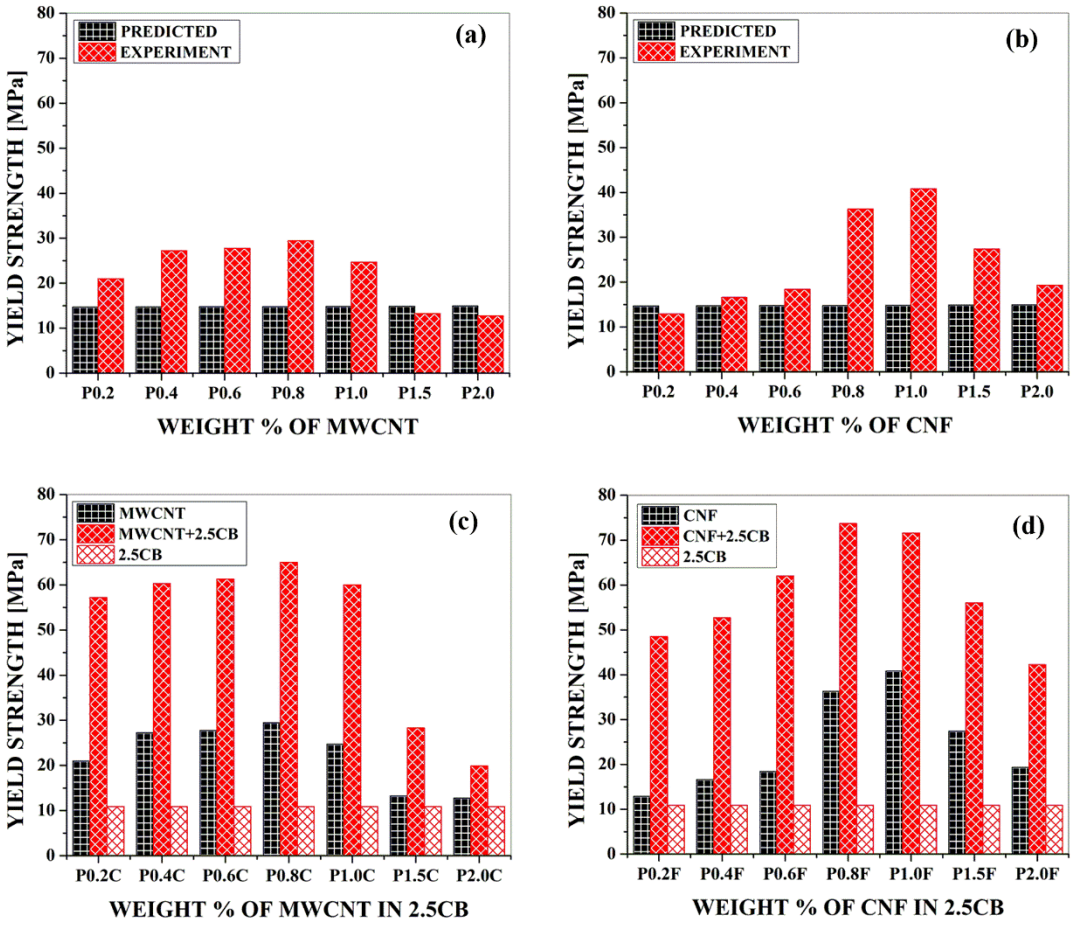

Figure 8.9.Comparative yield strength for (a) multiwalled carbon nanotubes (b) cellulose nanofibers (c) multiwalled carbon nanotubes + 2.5 carbon black (d) cellulose nanofibers + 2.5 carbon black with predicted values for multiwalled carbon nanotubes and cellulose nanofibers filled poly (lactic acid) composites and 2.5carbon black poly (lactic acid) composites and specific nanofiller loaded poly (lactic acid) composites.

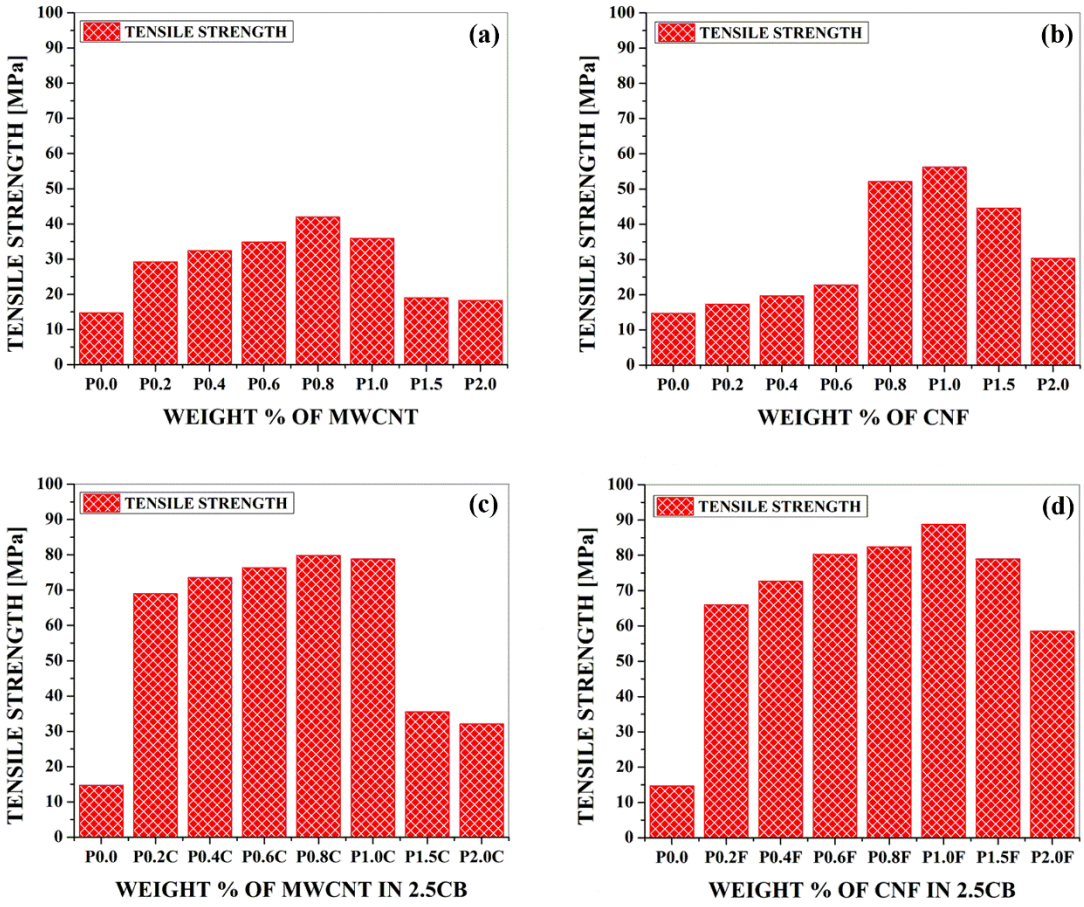

Figure 8.10.Tensile strength for poly (lactic acid) composites filled with (a) multiwalled carbon nanotubes (b) cellulose nanofibers (c) multiwalled carbon nanotubes + 2.5carbon black (d) cellulose nanofibers + 2.5carbon black

Table 8.22. Descriptive Statistics of tensile strength for 2.5carbon black + multiwalled carbon nanotubes and 2.5carbon black + cellulose nanofibers filled Poly (lactic acid) composites

Sample Code	Sample Size	Mean	Standard Dev	SE of mean
P0.0	10	14.68	0.32931	0.10414
P0.2C	10	69	1.05409	0.33333
P0.4C	10	73.5	0.84984	0.26874
P0.6C	10	76.3	1.25167	0.39581
P0.8C	10	79.8	1.98886	0.62893
P1.0C	10	78.8	1.75119	0.55377
P1.5C	10	35.5	1.84089	0.58214

P2.0C	10	32.1	2.42441	0.76667
P0.2F	10	66	1.03172	0.32626
P0.4F	10	72.63	1.41896	0.44871
P0.6F	10	80.3	1.33749	0.42295
P0.8F	10	82.44	1.25716	0.39755
P1.0F	10	88.76	1.13451	0.35876
P1.5F	10	78.96	1.30571	0.4129
P2.0F	10	58.5	1.71594	0.54263

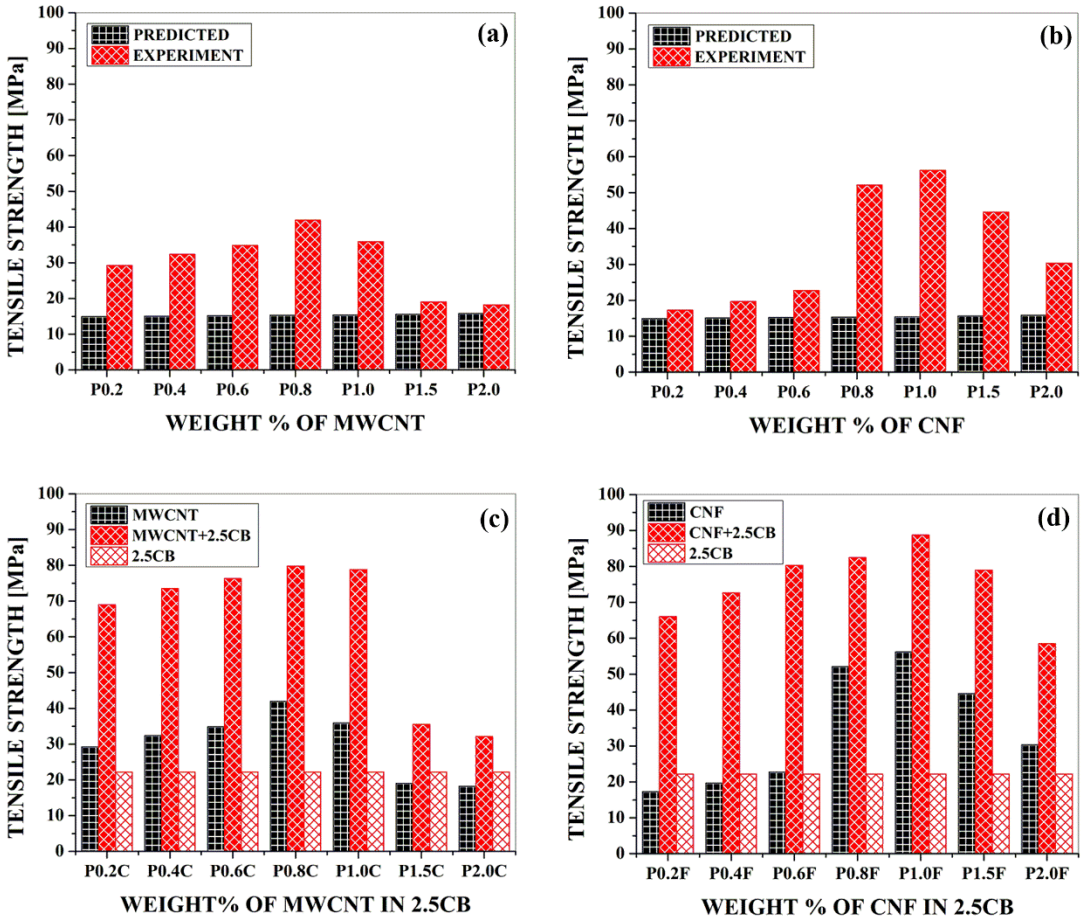

Figure 8.11.Comparative tensile strength for (a) multiwalled carbon nanotubes (b) cellulose nanofibers (c) multiwalled carbon nanotubes + 2.5 carbon black (d) cellulose nanofibers + 2.5 carbon black with predicted values for multiwalled carbon nanotubes and cellulose nanofibers filled poly (lactic acid) composites and 2.5carbon black poly (lactic acid) composites and specific nanofiller loaded poly (lactic acid) composites.

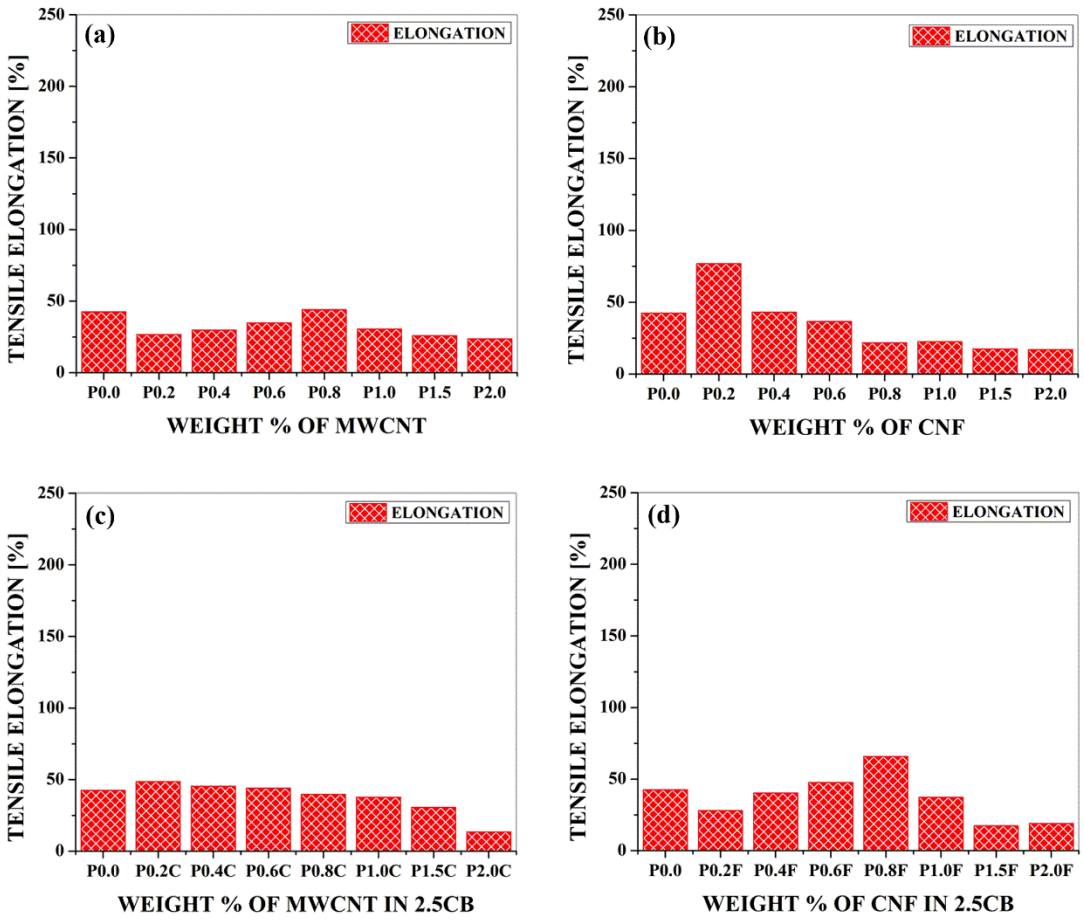

Figure 8.12.Tensile elongation for poly (lactic acid) composites filled with (a) multiwalled carbon nanotubes (b) cellulose nanofibers (c) multiwalled carbon nanotubes + 2.5carbon black (d) cellulose nanofibers + 2.5carbon black

Table 8.23. Descriptive Statistics of tensile elongation for multiwalled carbon nanotubes filled Poly (lactic acid) composites

Sample Code	Sample Size	Mean	Standard Dev	SE of mean
P0.0	10	42.5	0.97183	0.30732
P0.2	10	26.56	0.42646	0.13486
P0.4	10	29.775	0.76494	0.2419
P0.6	10	34.814	0.52806	0.16699
P0.8	10	43.891	0.7505	0.23733
P1.0	10	30.381	1.43699	0.45442
P1.5	10	25.747	0.63603	0.20113

P2.0	10	23.617	0.64308	0.20336

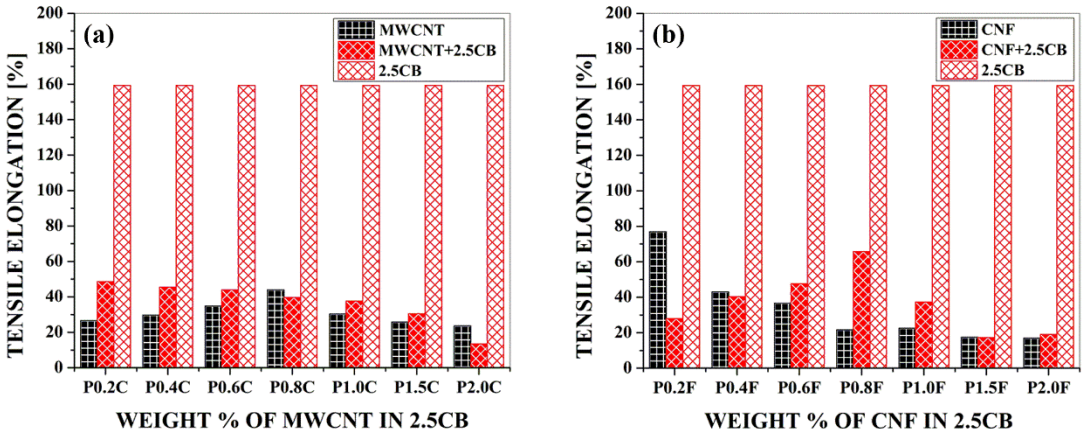

Figure 8.13. Comparative tensile elongation for (a) multiwalled carbon nanotubes + 2.5 carbon black (b) cellulose nanofibers + 2.5 carbon black with 2.5carbon black poly (lactic acid) composites and specific nanofiller loaded poly (lactic acid) composites.

Table 8.24. Descriptive Statistics of tensile elongation for cellulose nanofibers filled Poly (lactic acid) composites

Sample Code	Sample Size	Mean	Standard Dev	SE of mean
P0.0	10	42.5	0.97183	0.30732
P0.2	10	76.9	0.99443	0.31447
P0.4	10	43	1.05409	0.33333
P0.6	10	36.6	1.26491	0.4
P0.8	10	21.64	5.50236	1.74
P1.0	10	22.51	0.47714	0.15089
P1.5	10	17.41	0.1792	0.05667
P2.0	10	16.93	0.27101	0.0857

Table 8.25. Descriptive Statistics of tensile elongation for 2.5carbon black + multiwalled carbon nanotubes and 2.5carbon black + cellulose nanofibers filled Poly (lactic acid) composites

Sample Code	Sample Size	Mean	Standard Dev	SE of mean
P0.0	10	42.5	0.97183	0.30732
P0.2C	10	48.6	1.3499	0.42687
P0.4C	10	45.4	2.41293	0.76303

P0.6C	10	43.9	0.99443	0.31447
P0.8C	10	39.7	1.94651	0.61554
P1.0C	10	37.6	2.01108	0.63596
P1.5C	10	30.5	1.08012	0.34157
P2.0C	10	13.5	1.64992	0.52175
P0.2F	10	28	1.24722	0.39441
P0.4F	10	40.3	1.82878	0.57831
P0.6F	10	47.6	1.57762	0.49889
P0.8F	10	65.8	1.54919	0.4899
P1.0F	10	37.3	1.41814	0.44845
P1.5F	10	17.3	0.82327	0.26034
P2.0F	10	19	0.94281	0.29814

Table 8.26. Means Comparison of tensile modulus by Bonferroni Test for carbon black filled poly (lactic acid) composites

Sample Code	Mean Diff	t Value	Alpha	Sigma
P0.5 P0.0	149.3	16.90177	0.05	1
P1.0 P0.0	363.4	41.13933	0.05	1
P1.0 P0.5	214.1	24.23756	0.05	1
P1.5 P0.0	459.9	52.06378	0.05	1
P1.5 P0.5	310.6	35.16201	0.05	1
P1.5 P1.0	96.5	10.92445	0.05	1
P2.0 P0.0	521.1	58.99203	0.05	1
P2.0 P0.5	371.8	42.09027	0.05	1
P2.0 P1.0	157.7	17.8527	0.05	1
P2.0 P1.5	61.2	6.92825	0.05	1
P2.5 P0.0	563.4	63.78068	0.05	1
P2.5 P0.5	414.1	46.87891	0.05	1
P2.5 P1.0	200	22.64135	0.05	1
P2.5 P1.5	103.5	11.7169	0.05	1
P2.5 P2.0	42.3	4.78865	0.05	1
P5.0 P0.0	663.9	75.15796	0.05	1

P5.0 P0.5	514.6	58.25619	0.05	1
P5.0 P1.0	300.5	34.01863	0.05	1
P5.0 P1.5	204	23.09418	0.05	1
P5.0 P2.0	142.8	16.16592	0.05	1
P5.0 P2.5	100.5	11.37728	0.05	1
P10.0 P0.0	804.4	91.0635	0.05	1
P10.0 P0.5	655.1	74.16174	0.05	1
P10.0 P1.0	441	49.92417	0.05	1
P10.0 P1.5	344.5	38.99972	0.05	1
P10.0 P2.0	283.3	32.07147	0.05	1
P10.0 P2.5	241	27.28282	0.05	1
P10.0 P5.0	140.5	15.90555	0.05	1

Table 8.27. Means Comparison of tensile modulus by Bonferroni Test for multiwalled carbon nanotubes filled poly (lactic acid) composites

Sample Code	Mean Diff	t Value	Alpha	Sigma
P0.2 P0.0	124.3	18.92132	0.05	1
P0.4 P0.0	153.5	23.36623	0.05	1
P0.4 P0.2	29.2	4.44491	0.05	1
P0.6 P0.0	215.5	32.80405	0.05	1
P0.6 P0.2	91.2	13.88274	0.05	1
P0.6 P0.4	62	9.43783	0.05	1
P0.8 P0.0	319.4	48.62002	0.05	1
P0.8 P0.2	195.1	29.69871	0.05	1
P0.8 P0.4	165.9	25.25379	0.05	1
P0.8 P0.6	103.9	15.81597	0.05	1
P1.0 P0.0	466.4	70.9968	0.05	1
P1.0 P0.2	342.1	52.07548	0.05	1
P1.0 P0.4	312.9	47.63057	0.05	1
P1.0 P0.6	250.9	38.19275	0.05	1
P1.0 P0.8	147	22.37678	0.05	1
P1.5 P0.0	607.7	92.50591	0.05	1

P1.5 P0.2	483.4	73.58459	0.05	1
P1.5 P0.4	454.2	69.13968	0.05	1
P1.5 P0.6	392.2	59.70186	0.05	1
P1.5 P0.8	288.3	43.88589	0.05	1
P1.5 P1.0	141.3	21.50911	0.05	1
P2.0 P0.0	813.3	123.80296	0.05	1
P2.0 P0.2	689	104.88164	0.05	1
P2.0 P0.4	659.8	100.43673	0.05	1
P2.0 P0.6	597.8	90.9989	0.05	1
P2.0 P0.8	493.9	75.18293	0.05	1
P2.0 P1.0	346.9	52.80616	0.05	1
P2.0 P1.5	205.6	31.29705	0.05	1

Table 8.28. Means Comparison of tensile modulus by Bonferroni Test for cellulose nanofibers filled poly (lactic acid) composites

Sample Code	Mean Diff	t Value	Alpha	Sigma
P0.2 P0.0	133.3	75.85218	0.05	1
P0.4 P0.0	205.6	116.99331	0.05	1
P0.4 P0.2	72.3	41.14113	0.05	1
P0.6 P0.0	232.8	132.47102	0.05	1
P0.6 P0.2	99.5	56.61884	0.05	1
P0.6 P0.4	27.2	15.47771	0.05	1
P0.8 P0.0	434	246.96058	0.05	1
P0.8 P0.2	300.7	171.10841	0.05	1
P0.8 P0.4	228.4	129.96728	0.05	1
P0.8 P0.6	201.2	114.48956	0.05	1
P1.0 P0.0	475.1	270.34787	0.05	1
P1.0 P0.2	341.8	194.49569	0.05	1
P1.0 P0.4	269.5	153.35456	0.05	1
P1.0 P0.6	242.3	137.87684	0.05	1
P1.0 P0.8	41.1	23.38728	0.05	1
P1.5 P0.0	629	357.92214	0.05	1

P1.5 P0.2	495.7	282.06996	0.05	1
P1.5 P0.4	423.4	240.92883	0.05	1
P1.5 P0.6	396.2	225.45111	0.05	1
P1.5 P0.8	195	110.96155	0.05	1
P1.5 P1.0	153.9	87.57427	0.05	1
P2.0 P0.0	915.6	521.00717	0.05	1
P2.0 P0.2	782.3	445.15499	0.05	1
P2.0 P0.4	710	404.01386	0.05	1
P2.0 P0.6	682.8	388.53615	0.05	1
P2.0 P0.8	481.6	274.04658	0.05	1
P2.0 P1.0	440.5	250.6593	0.05	1
P2.0 P1.5	286.6	163.08503	0.05	1

Table 8.29. Means Comparison of tensile modulus by Bonferroni Test for 2.5carbon black + multiwalled carbon nanotubes filled poly (lactic acid) composites

Sample Code	Mean Diff	t Value	Alpha	Sigma
P0.2C P0.0	509.9	46.87812	0.05	1
P0.4C P0.0	670.4	61.63384	0.05	1
P0.4C P0.2C	160.5	14.75571	0.05	1
P0.6C P0.0	823.7	75.72761	0.05	1
P0.6C P0.2C	313.8	28.84949	0.05	1
P0.6C P0.4C	153.3	14.09378	0.05	1
P0.8C P0.0	888.2	81.65748	0.05	1
P0.8C P0.2C	378.3	34.77936	0.05	1
P0.8C P0.4C	217.8	20.02364	0.05	1
P0.8C P0.6C	64.5	5.92987	0.05	1
P1.0C P0.0	990.7	91.08091	0.05	1
P1.0C P0.2C	480.8	44.20279	0.05	1
P1.0C P0.4C	320.3	29.44707	0.05	1
P1.0C P0.6C	167	15.3533	0.05	1
P1.0C P0.8C	102.5	9.42343	0.05	1
P1.5C P0.0	1215.2	111.72052	0.05	1

P1.5C P0.2C	705.3	64.8424	0.05	1
P1.5C P0.4C	544.8	50.08669	0.05	1
P1.5C P0.6C	391.5	35.99291	0.05	1
P1.5C P0.8C	327	30.06304	0.05	1
P1.5C P1.0C	224.5	20.63961	0.05	1
P2.0C P0.0	1236.7	113.69714	0.05	1
P2.0C P0.2C	726.8	66.81902	0.05	1
P2.0C P0.4C	566.3	52.06331	0.05	1
P2.0C P0.6C	413	37.96953	0.05	1
P2.0C P0.8C	348.5	32.03967	0.05	1
P2.0C P1.0C	246	22.61623	0.05	1
P2.0C P1.5C	21.5	1.97662	0.05	0

Table 8.30. Means Comparison of tensile modulus by Bonferroni Test for 2.5carbon black + cellulose nanofibers filled poly (lactic acid) composites

Sample Code	Mean Diff	t Value	Alpha	Sigma
P0.2F P0.0	561.4	60.6911	0.05	1
P0.4F P0.0	704.5	76.16117	0.05	1
P0.4F P0.2F	143.1	15.47007	0.05	1
P0.6F P0.0	821.5	88.80966	0.05	1
P0.6F P0.2F	260.1	28.11855	0.05	1
P0.6F P0.4F	117	12.64848	0.05	1
P0.8F P0.0	875.9	94.69066	0.05	1
P0.8F P0.2F	314.5	33.99956	0.05	1
P0.8F P0.4F	171.4	18.52949	0.05	1
P0.8F P0.6F	54.4	5.881	0.05	1
P1.0F P0.0	1135.1	122.71192	0.05	1
P1.0F P0.2F	573.7	62.02082	0.05	1
P1.0F P0.4F	430.6	46.55075	0.05	1
P1.0F P0.6F	313.6	33.90226	0.05	1
P1.0F P0.8F	259.2	28.02126	0.05	1
P1.5F P0.0	1401.8	151.54398	0.05	1

P1.5F P0.2F	840.4	90.85287	0.05	1
P1.5F P0.4F	697.3	75.3828	0.05	1
P1.5F P0.6F	580.3	62.73432	0.05	1
P1.5F P0.8F	525.9	56.85332	0.05	1
P1.5F P1.0F	266.7	28.83206	0.05	1
P2.0F P0.0	1604.7	173.47883	0.05	1
P2.0F P0.2F	1043.3	112.78772	0.05	1
P2.0F P0.4F	900.2	97.31766	0.05	1
P2.0F P0.6F	783.2	84.66917	0.05	1
P2.0F P0.8F	728.8	78.78817	0.05	1
P2.0F P1.0F	469.6	50.76691	0.05	1
P2.0F P1.5F	202.9	21.93485	0.05	1

Table 8.31. Means Comparison of yield strength by Bonferroni Test for carbon black filled poly (lactic acid) composites

Sample Code	Mean Diff	t Value	Alpha	Sigma
P0.5 P0.0	-6.16	-35.84129	0.05	1
P1.0 P0.0	-1.96	-11.40405	0.05	1
P1.0 P0.5	4.2	24.43724	0.05	1
P1.5 P0.0	-3.4	-19.78253	0.05	1
P1.5 P0.5	2.76	16.05876	0.05	1
P1.5 P1.0	-1.44	-8.37848	0.05	1
P2.0 P0.0	-3.75	-21.81897	0.05	1
P2.0 P0.5	2.41	14.02232	0.05	1
P2.0 P1.0	-1.79	-10.41492	0.05	1
P2.0 P1.5	-0.35	-2.03644	0.05	0
P2.5 P0.0	-3.72	-21.64442	0.05	1
P2.5 P0.5	2.44	14.19687	0.05	1
P2.5 P1.0	-1.76	-10.24037	0.05	1
P2.5 P1.5	-0.32	-1.86189	0.05	0
P2.5 P2.0	0.03	0.17455	0.05	0
P5.0 P0.0	-3.81	-22.16807	0.05	1

P5.0 P0.5	2.35	13.67322	0.05	1
P5.0 P1.0	-1.85	-10.76402	0.05	1
P5.0 P1.5	-0.41	-2.38554	0.05	0
P5.0 P2.0	-0.06	-0.3491	0.05	0
P5.0 P2.5	-0.09	-0.52366	0.05	0
P10.0 P0.0	-6.12	-35.60855	0.05	1
P10.0 P0.5	0.04	0.23274	0.05	0
P10.0 P1.0	-4.16	-24.20451	0.05	1
P10.0 P1.5	-2.72	-15.82602	0.05	1
P10.0 P2.0	-2.37	-13.78959	0.05	1
P10.0 P2.5	-2.4	-13.96414	0.05	1
P10.0 P5.0	-2.31	-13.44048	0.05	1

Table 8.32. Means Comparison of yield strength by Bonferroni Test for multiwalled carbon nanotubes filled poly (lactic acid) composites

Sample Code	Mean Diff	t Value	Alpha	Sigma
P0.2 P0.0	6.39	13.94745	0.05	1
P0.4 P0.0	12.617	27.53913	0.05	1
P0.4 P0.2	6.227	13.59167	0.05	1
P0.6 P0.0	13.126	28.65012	0.05	1
P0.6 P0.2	6.736	14.70267	0.05	1
P0.6 P0.4	0.509	1.11099	0.05	0
P0.8 P0.0	14.867	32.4502	0.05	1
P0.8 P0.2	8.477	18.50275	0.05	1
P0.8 P0.4	2.25	4.91108	0.05	1
P0.8 P0.6	1.741	3.80008	0.05	1
P1.0 P0.0	10.111	22.06928	0.05	1
P1.0 P0.2	3.721	8.12183	0.05	1
P1.0 P0.4	-2.506	-5.46985	0.05	1
P1.0 P0.6	-3.015	-6.58084	0.05	1
P1.0 P0.8	-4.756	-10.38092	0.05	1
P1.5 P0.0	-1.365	-2.97939	0.05	0

P1.5 P0.2	-7.755	-16.92684	0.05	1
P1.5 P0.4	-13.982	-30.51851	0.05	1
P1.5 P0.6	-14.491	-31.62951	0.05	1
P1.5 P0.8	-16.232	-35.42959	0.05	1
P1.5 P1.0	-11.476	-25.04867	0.05	1
P2.0 P0.0	-1.819	-3.97033	0.05	1
P2.0 P0.2	-8.209	-17.91779	0.05	1
P2.0 P0.4	-14.436	-31.50946	0.05	1
P2.0 P0.6	-14.945	-32.62046	0.05	1
P2.0 P0.8	-16.686	-36.42054	0.05	1
P2.0 P1.0	-11.93	-26.03961	0.05	1
P2.0 P1.5	-0.454	-0.99095	0.05	0

Table 8.33. Means Comparison of yield strength by Bonferroni Test for cellulose nanofibers filled poly (lactic acid) composites

Sample Code	Mean Diff	t Value	Alpha	Sigma
P0.2 P0.0	-1.7	-3.69265	0.05	1
P0.4 P0.0	2	4.34429	0.05	1
P0.4 P0.2	3.7	8.03694	0.05	1
P0.6 P0.0	3.8	8.25415	0.05	1
P0.6 P0.2	5.5	11.9468	0.05	1
P0.6 P0.4	1.8	3.90986	0.05	1
P0.8 P0.0	21.7	47.13556	0.05	1
P0.8 P0.2	23.4	50.82821	0.05	1
P0.8 P0.4	19.7	42.79127	0.05	1
P0.8 P0.6	17.9	38.88141	0.05	1
P1.0 P0.0	26.2	56.91022	0.05	1
P1.0 P0.2	27.9	60.60287	0.05	1
P1.0 P0.4	24.2	52.56593	0.05	1
P1.0 P0.6	22.4	48.65607	0.05	1
P1.0 P0.8	4.5	9.77466	0.05	1
P1.5 P0.0	12.8	27.80347	0.05	1

P1.5 P0.2	14.5	31.49611	0.05	1
P1.5 P0.4	10.8	23.45918	0.05	1
P1.5 P0.6	9	19.54931	0.05	1
P1.5 P0.8	-8.9	-19.3321	0.05	1
P1.5 P1.0	-13.4	-29.10675	0.05	1
P2.0 P0.0	4.7	10.20909	0.05	1
P2.0 P0.2	6.4	13.90173	0.05	1
P2.0 P0.4	2.7	5.86479	0.05	1
P2.0 P0.6	0.9	1.95493	0.05	0
P2.0 P0.8	-17	-36.92648	0.05	1
P2.0 P1.0	-21.5	-46.70114	0.05	1
P2.0 P1.5	-8.1	-17.59438	0.05	1

Table 8.34. Means Comparison of yield strength by Bonferroni Test for 2.5carbon black + multiwalled carbon nanotubes filled poly (lactic acid) composites

Sample Code	Mean Diff	t Value	Alpha	Sigma
P0.2C P0.0	42.6	45.38311	0.05	1
P0.4C P0.0	45.7	48.68564	0.05	1
P0.4C P0.2C	3.1	3.30253	0.05	1
P0.6C P0.0	46.7	49.75097	0.05	1
P0.6C P0.2C	4.1	4.36786	0.05	1
P0.6C P0.4C	1	1.06533	0.05	0
P0.8C P0.0	50.4	53.69269	0.05	1
P0.8C P0.2C	7.8	8.30958	0.05	1
P0.8C P0.4C	4.7	5.00706	0.05	1
P0.8C P0.6C	3.7	3.94173	0.05	1
P1.0C P0.0	45.4	48.36604	0.05	1
P1.0C P0.2C	2.8	2.98293	0.05	0
P1.0C P0.4C	-0.3	-0.3196	0.05	0
P1.0C P0.6C	-1.3	-1.38493	0.05	0
P1.0C P0.8C	-5	-5.32666	0.05	1
P1.5C P0.0	13.7	14.59504	0.05	1

P1.5C P0.2C	-28.9	-30.78807	0.05	1
P1.5C P0.4C	-32	-34.0906	0.05	1
P1.5C P0.6C	-33	-35.15593	0.05	1
P1.5C P0.8C	-36.7	-39.09766	0.05	1
P1.5C P1.0C	-31.7	-33.771	0.05	1
P2.0C P0.0	5.3	5.64626	0.05	1
P2.0C P0.2C	-37.3	-39.73686	0.05	1
P2.0C P0.4C	-40.4	-43.03938	0.05	1
P2.0C P0.6C	-41.4	-44.10471	0.05	1
P2.0C P0.8C	-45.1	-48.04644	0.05	1
P2.0C P1.0C	-40.1	-42.71978	0.05	1
P2.0C P1.5C	-8.4	-8.94878	0.05	1

Table 8.35. Means Comparison of yield strength by Bonferroni Test for 2.5carbon black + cellulose nanofibers filled poly (lactic acid) composites

Sample Code	Mean Diff	t Value	Alpha	Sigma
P0.2F P0.0	33.9	39.80591	0.05	1
P0.4F P0.0	38.1	44.73761	0.05	1
P0.4F P0.2F	4.2	4.93171	0.05	1
P0.6F P0.0	47.4	55.65782	0.05	1
P0.6F P0.2F	13.5	15.85191	0.05	1
P0.6F P0.4F	9.3	10.9202	0.05	1
P0.8F P0.0	59.1	69.39614	0.05	1
P0.8F P0.2F	25.2	29.59023	0.05	1
P0.8F P0.4F	21	24.65853	0.05	1
P0.8F P0.6F	11.7	13.73832	0.05	1
P1.0F P0.0	57	66.93028	0.05	1
P1.0F P0.2F	23.1	27.12438	0.05	1
P1.0F P0.4F	18.9	22.19267	0.05	1
P1.0F P0.6F	9.6	11.27247	0.05	1
P1.0F P0.8F	-2.1	-2.46585	0.05	0
P1.5F P0.0	41.4	48.61252	0.05	1

P1.5F P0.2F	7.5	8.80662	0.05	1
P1.5F P0.4F	3.3	3.87491	0.05	1
P1.5F P0.6F	-6	-7.04529	0.05	1
P1.5F P0.8F	-17.7	-20.78361	0.05	1
P1.5F P1.0F	-15.6	-18.31776	0.05	1
P2.0F P0.0	27.6	32.40835	0.05	1
P2.0F P0.2F	-6.3	-7.39756	0.05	1
P2.0F P0.4F	-10.5	-12.32926	0.05	1
P2.0F P0.6F	-19.8	-23.24947	0.05	1
P2.0F P0.8F	-31.5	-36.98779	0.05	1
P2.0F P1.0F	-29.4	-34.52194	0.05	1
P2.0F P1.5F	-13.8	-16.20417	0.05	1

Table 8.36. Means Comparison of tensile strength by Bonferroni Test for carbon black filled poly (lactic acid) composites

Sample Code	Mean Diff	t Value	Alpha	Sigma
P0.5 P0.0	0.03	0.28457	0.05	0
P1.0 P0.0	2.66	25.23182	0.05	1
P1.0 P0.5	2.63	24.94725	0.05	1
P1.5 P0.0	6.09	57.76759	0.05	1
P1.5 P0.5	6.06	57.48302	0.05	1
P1.5 P1.0	3.43	32.53577	0.05	1
P2.0 P0.0	7.15	67.82238	0.05	1
P2.0 P0.5	7.12	67.53781	0.05	1
P2.0 P1.0	4.49	42.59056	0.05	1
P2.0 P1.5	1.06	10.05479	0.05	1
P2.5 P0.0	7.52	71.33207	0.05	1
P2.5 P0.5	7.49	71.0475	0.05	1
P2.5 P1.0	4.86	46.10025	0.05	1
P2.5 P1.5	1.43	13.56448	0.05	1
P2.5 P2.0	0.37	3.50969	0.05	1
P5.0 P0.0	4.79	45.43625	0.05	1

P5.0 P0.5	4.76	45.15168	0.05	1
P5.0 P1.0	2.13	20.20443	0.05	1
P5.0 P1.5	-1.3	-12.33134	0.05	1
P5.0 P2.0	-2.36	-22.38613	0.05	1
P5.0 P2.5	-2.73	-25.89582	0.05	1
P10.0 P0.0	-0.19	-1.80227	0.05	0
P10.0 P0.5	-0.22	-2.08684	0.05	0
P10.0 P1.0	-2.85	-27.03409	0.05	1
P10.0 P1.5	-6.28	-59.56987	0.05	1
P10.0 P2.0	-7.34	-69.62465	0.05	1
P10.0 P2.5	-7.71	-73.13434	0.05	1
P10.0 P5.0	-4.98	-47.23852	0.05	1

Table 8.37. Means Comparison of tensile strength by Bonferroni Test for multiwalled carbon nanotubes filled poly (lactic acid) composites

Sample Code	Mean Diff	t Value	Alpha	Sigma
P0.2 P0.0	14.548	73.87919	0.05	1
P0.4 P0.0	17.687	89.81999	0.05	1
P0.4 P0.2	3.139	15.9408	0.05	1
P0.6 P0.0	20.15	102.32785	0.05	1
P0.6 P0.2	5.602	28.44867	0.05	1
P0.6 P0.4	2.463	12.50787	0.05	1
P0.8 P0.0	27.286	138.56664	0.05	1
P0.8 P0.2	12.738	64.68745	0.05	1
P0.8 P0.4	9.599	48.74665	0.05	1
P0.8 P0.6	7.136	36.23879	0.05	1
P1.0 P0.0	21.184	107.57882	0.05	1
P1.0 P0.2	6.636	33.69963	0.05	1
P1.0 P0.4	3.497	17.75883	0.05	1
P1.0 P0.6	1.034	5.25097	0.05	1
P1.0 P0.8	-6.102	-30.98782	0.05	1
P1.5 P0.0	4.329	21.98398	0.05	1

P1.5 P0.2	-10.219	-51.8952	0.05	1
P1.5 P0.4	-13.358	-67.836	0.05	1
P1.5 P0.6	-15.821	-80.34387	0.05	1
P1.5 P0.8	-22.957	-116.58266	0.05	1
P1.5 P1.0	-16.855	-85.59484	0.05	1
P2.0 P0.0	3.53	17.92642	0.05	1
P2.0 P0.2	-11.018	-55.95277	0.05	1
P2.0 P0.4	-14.157	-71.89357	0.05	1
P2.0 P0.6	-16.62	-84.40143	0.05	1
P2.0 P0.8	-23.756	-120.64022	0.05	1
P2.0 P1.0	-17.654	-89.6524	0.05	1
P2.0 P1.5	-0.799	-4.05757	0.05	1

Table 8.38. Means Comparison of tensile strength by Bonferroni Test for cellulose nanofibers filled poly (lactic acid) composites

Sample Code	Mean Diff	t Value	Alpha	Sigma
P0.2 P0.0	2.6	6.25176	0.05	1
P0.4 P0.0	4.97	11.95049	0.05	1
P0.4 P0.2	2.37	5.69872	0.05	1
P0.6 P0.0	8.02	19.28429	0.05	1
P0.6 P0.2	5.42	13.03252	0.05	1
P0.6 P0.4	3.05	7.3338	0.05	1
P0.8 P0.0	37.41	89.95327	0.05	1
P0.8 P0.2	34.81	83.70151	0.05	1
P0.8 P0.4	32.44	78.00278	0.05	1
P0.8 P0.6	29.39	70.66898	0.05	1
P1.0 P0.0	41.53	99.85991	0.05	1
P1.0 P0.2	38.93	93.60815	0.05	1
P1.0 P0.4	36.56	87.90943	0.05	1
P1.0 P0.6	33.51	80.57562	0.05	1
P1.0 P0.8	4.12	9.90664	0.05	1
P1.5 P0.0	29.89	71.87125	0.05	1

P1.5 P0.2	27.29	65.61948	0.05	1
P1.5 P0.4	24.92	59.92076	0.05	1
P1.5 P0.6	21.87	52.58696	0.05	1
P1.5 P0.8	-7.52	-18.08203	0.05	1
P1.5 P1.0	-11.64	-27.98867	0.05	1
P2.0 P0.0	15.63	37.58272	0.05	1
P2.0 P0.2	13.03	31.33096	0.05	1
P2.0 P0.4	10.66	25.63223	0.05	1
P2.0 P0.6	7.61	18.29843	0.05	1
P2.0 P0.8	-21.78	-52.37055	0.05	1
P2.0 P1.0	-25.9	-62.27719	0.05	1
P2.0 P1.5	-14.26	-34.28852	0.05	1

Table 8.39. Means Comparison of tensile strength by Bonferroni Test for 2.5carbon black + multiwalled carbon nanotubes filled poly (lactic acid) composites

Sample Code	Mean Diff	t Value	Alpha	Sigma
P0.2C P0.0	54.32	77.21229	0.05	1
P0.4C P0.0	58.82	83.60874	0.05	1
P0.4C P0.2C	4.5	6.39645	0.05	1
P0.6C P0.0	61.62	87.58875	0.05	1
P0.6C P0.2C	7.3	10.37647	0.05	1
P0.6C P0.4C	2.8	3.98001	0.05	1
P0.8C P0.0	65.12	92.56377	0.05	1
P0.8C P0.2C	10.8	15.35149	0.05	1
P0.8C P0.4C	6.3	8.95503	0.05	1
P0.8C P0.6C	3.5	4.97502	0.05	1
P1.0C P0.0	64.12	91.14234	0.05	1
P1.0C P0.2C	9.8	13.93005	0.05	1
P1.0C P0.4C	5.3	7.5336	0.05	1
P1.0C P0.6C	2.5	3.55358	0.05	1
P1.0C P0.8C	-1	-1.42143	0.05	0
P1.5C P0.0	20.82	29.59425	0.05	1

P1.5C P0.2C	-33.5	-47.61803	0.05	1
P1.5C P0.4C	-38	-54.01449	0.05	1
P1.5C P0.6C	-40.8	-57.9945	0.05	1
P1.5C P0.8C	-44.3	-62.96952	0.05	1
P1.5C P1.0C	-43.3	-61.54808	0.05	1
P2.0C P0.0	17.42	24.76138	0.05	1
P2.0C P0.2C	-36.9	-52.45091	0.05	1
P2.0C P0.4C	-41.4	-58.84736	0.05	1
P2.0C P0.6C	-44.2	-62.82738	0.05	1
P2.0C P0.8C	-47.7	-67.80239	0.05	1
P2.0C P1.0C	-46.7	-66.38096	0.05	1
P2.0C P1.5C	-3.4	-4.83288	0.05	1

Table 8.40. Means Comparison of tensile strength by Bonferroni Test for 2.5carbon black + cellulose nanofibers filled poly (lactic acid) composites

Sample Code	Mean Diff	t Value	Alpha	Sigma
P0.2F P0.0	51.32	91.83299	0.05	1
P0.4F P0.0	57.95	103.69684	0.05	1
P0.4F P0.2F	6.63	11.86385	0.05	1
P0.6F P0.0	65.62	117.42168	0.05	1
P0.6F P0.2F	14.3	25.58869	0.05	1
P0.6F P0.4F	7.67	13.72484	0.05	1
P0.8F P0.0	67.76	121.25104	0.05	1
P0.8F P0.2F	16.44	29.41805	0.05	1
P0.8F P0.4F	9.81	17.5542	0.05	1
P0.8F P0.6F	2.14	3.82936	0.05	1
P1.0F P0.0	74.08	132.56017	0.05	1
P1.0F P0.2F	22.76	40.72718	0.05	1
P1.0F P0.4F	16.13	28.86333	0.05	1
P1.0F P0.6F	8.46	15.13849	0.05	1
P1.0F P0.8F	6.32	11.30913	0.05	1
P1.5F P0.0	64.28	115.02386	0.05	1

P1.5F P0.2F	12.96	23.19087	0.05	1
P1.5F P0.4F	6.33	11.32702	0.05	1
P1.5F P0.6F	-1.34	-2.39782	0.05	0
P1.5F P0.8F	-3.48	-6.22718	0.05	1
P1.5F P1.0F	-9.8	-17.53631	0.05	1
P2.0F P0.0	43.82	78.41235	0.05	1
P2.0F P0.2F	-7.5	-13.42064	0.05	1
P2.0F P0.4F	-14.13	-25.28449	0.05	1
P2.0F P0.6F	-21.8	-39.00934	0.05	1
P2.0F P0.8F	-23.94	-42.83869	0.05	1
P2.0F P1.0F	-30.26	-54.14782	0.05	1
P2.0F P1.5F	-20.46	-36.61152	0.05	1

Table 8.41. Means Comparison of tensile elongation by Bonferroni Test for carbon black filled poly (lactic acid) composites

Sample Code	Mean Diff	t Value	Alpha	Sigma
P0.5 P0.0	181.8	113.3976	0.05	1
P1.0 P0.0	171.9	107.22248	0.05	1
P1.0 P0.5	-9.9	-6.17512	0.05	1
P1.5 P0.0	131	81.71114	0.05	1
P1.5 P0.5	-50.8	-31.68646	0.05	1
P1.5 P1.0	-40.9	-25.51134	0.05	1
P2.0 P0.0	123.9	77.28252	0.05	1
P2.0 P0.5	-57.9	-36.11508	0.05	1
P2.0 P1.0	-48	-29.93996	0.05	1
P2.0 P1.5	-7.1	-4.42862	0.05	1
P2.5 P0.0	116.8	72.8539	0.05	1
P2.5 P0.5	-65	-40.54369	0.05	1
P2.5 P1.0	-55.1	-34.36858	0.05	1
P2.5 P1.5	-14.2	-8.85724	0.05	1
P2.5 P2.0	-7.1	-4.42862	0.05	1
P5.0 P0.0	108.9	67.92628	0.05	1

P5.0 P0.5	-72.9	-45.47131	0.05	1
P5.0 P1.0	-63	-39.2962	0.05	1
P5.0 P1.5	-22.1	-13.78486	0.05	1
P5.0 P2.0	-15	-9.35624	0.05	1
P5.0 P2.5	-7.9	-4.92762	0.05	1
P10.0 P0.0	81.4	50.77318	0.05	1
P10.0 P0.5	-100.4	-62.62442	0.05	1
P10.0 P1.0	-90.5	-56.4493	0.05	1
P10.0 P1.5	-49.6	-30.93796	0.05	1
P10.0 P2.0	-42.5	-26.50934	0.05	1
P10.0 P2.5	-35.4	-22.08072	0.05	1
P10.0 P5.0	-27.5	-17.1531	0.05	1

Table 8.42. Means Comparison of tensile elongation by Bonferroni Test for multiwalled carbon nanotubes filled poly (lactic acid) composites

Sample Code	Mean Diff	t Value	Alpha	Sigma
P0.2 P0.0	-15.94	-43.23696	0.05	1
P0.4 P0.0	-12.725	-34.51633	0.05	1
P0.4 P0.2	3.215	8.72063	0.05	1
P0.6 P0.0	-7.686	-20.84813	0.05	1
P0.6 P0.2	8.254	22.38882	0.05	1
P0.6 P0.4	5.039	13.66819	0.05	1
P0.8 P0.0	1.391	3.77306	0.05	1
P0.8 P0.2	17.331	47.01002	0.05	1
P0.8 P0.4	14.116	38.28939	0.05	1
P0.8 P0.6	9.077	24.6212	0.05	1
P1.0 P0.0	-12.119	-32.87256	0.05	1
P1.0 P0.2	3.821	10.36439	0.05	1
P1.0 P0.4	0.606	1.64376	0.05	0
P1.0 P0.6	-4.433	-12.02443	0.05	1
P1.0 P0.8	-13.51	-36.64563	0.05	1
P1.5 P0.0	-16.753	-45.4422	0.05	1

P1.5 P0.2	-0.813	-2.20525	0.05	0
P1.5 P0.4	-4.028	-10.92588	0.05	1
P1.5 P0.6	-9.067	-24.59407	0.05	1
P1.5 P0.8	-18.144	-49.21527	0.05	1
P1.5 P1.0	-4.634	-12.56964	0.05	1
P2.0 P0.0	-18.883	-51.21979	0.05	1
P2.0 P0.2	-2.943	-7.98283	0.05	1
P2.0 P0.4	-6.158	-16.70346	0.05	1
P2.0 P0.6	-11.197	-30.37166	0.05	1
P2.0 P0.8	-20.274	-54.99285	0.05	1
P2.0 P1.0	-6.764	-18.34723	0.05	1
P2.0 P1.5	-2.13	-5.77759	0.05	1

Table 8.43. Means Comparison of tensile elongation by Bonferroni Test for cellulose nanofibers filled poly (lactic acid) composites

Sample Code	Mean Diff	t Value	Alpha	Sigma
P0.2 P0.0	34.4	36.6426	0.05	1
P0.4 P0.0	0.5	0.5326	0.05	0
P0.4 P0.2	-33.9	-36.11	0.05	1
P0.6 P0.0	-5.9	-6.28463	0.05	1
P0.6 P0.2	-40.3	-42.92723	0.05	1
P0.6 P0.4	-6.4	-6.81723	0.05	1
P0.8 P0.0	-20.86	-22.2199	0.05	1
P0.8 P0.2	-55.26	-58.8625	0.05	1
P0.8 P0.4	-21.36	-22.7525	0.05	1
P0.8 P0.6	-14.96	-15.93527	0.05	1
P1.0 P0.0	-19.99	-21.29319	0.05	1
P1.0 P0.2	-54.39	-57.93579	0.05	1
P1.0 P0.4	-20.49	-21.82578	0.05	1
P1.0 P0.6	-14.09	-15.00855	0.05	1
P1.0 P0.8	0.87	0.92672	0.05	0
P1.5 P0.0	-25.09	-26.72566	0.05	1

P1.5 P0.2	-59.49	-63.36827	0.05	1
P1.5 P0.4	-25.59	-27.25826	0.05	1
P1.5 P0.6	-19.19	-20.44103	0.05	1
P1.5 P0.8	-4.23	-4.50576	0.05	1
P1.5 P1.0	-5.1	-5.43248	0.05	1
P2.0 P0.0	-25.57	-27.23696	0.05	1
P2.0 P0.2	-59.97	-63.87956	0.05	1
P2.0 P0.4	-26.07	-27.76955	0.05	1
P2.0 P0.6	-19.67	-20.95232	0.05	1
P2.0 P0.8	-4.71	-5.01705	0.05	1
P2.0 P1.0	-5.58	-5.94377	0.05	1
P2.0 P1.5	-0.48	-0.51129	0.05	0

Table 8.44. Means Comparison of tensile elongation by Bonferroni Test for 2.5carbon black + multiwalled carbon nanotubes filled poly (lactic acid) composites

Sample Code	Mean Diff	t Value	Alpha	Sigma
P0.2C P0.0	6.1	8.3593	0.05	1
P0.4C P0.0	2.9	3.97409	0.05	1
P0.4C P0.2C	-3.2	-4.38521	0.05	1
P0.6C P0.0	1.4	1.91853	0.05	0
P0.6C P0.2C	-4.7	-6.44077	0.05	1
P0.6C P0.4C	-1.5	-2.05557	0.05	0
P0.8C P0.0	-2.8	-3.83706	0.05	1
P0.8C P0.2C	-8.9	-12.19636	0.05	1
P0.8C P0.4C	-5.7	-7.81115	0.05	1
P0.8C P0.6C	-4.2	-5.75559	0.05	1
P1.0C P0.0	-4.9	-6.71485	0.05	1
P1.0C P0.2C	-11	-15.07415	0.05	1
P1.0C P0.4C	-7.8	-10.68894	0.05	1
P1.0C P0.6C	-6.3	-8.63338	0.05	1
P1.0C P0.8C	-2.1	-2.87779	0.05	0
P1.5C P0.0	-12	-16.44453	0.05	1

P1.5C P0.2C	-18.1	-24.80383	0.05	1
P1.5C P0.4C	-14.9	-20.41862	0.05	1
P1.5C P0.6C	-13.4	-18.36306	0.05	1
P1.5C P0.8C	-9.2	-12.60747	0.05	1
P1.5C P1.0C	-7.1	-9.72968	0.05	1
P2.0C P0.0	-29	-39.74095	0.05	1
P2.0C P0.2C	-35.1	-48.10025	0.05	1
P2.0C P0.4C	-31.9	-43.71504	0.05	1
P2.0C P0.6C	-30.4	-41.65947	0.05	1
P2.0C P0.8C	-26.2	-35.90389	0.05	1
P2.0C P1.0C	-24.1	-33.0261	0.05	1
P2.0C P1.5C	-17	-23.29642	0.05	1

Table 8.45. Means Comparison of tensile elongation by Bonferroni Test for 2.5carbon black + cellulose nanofibers filled poly (lactic acid) composites

Sample Code	Mean Diff	t Value	Alpha	Sigma
P0.2F P0.0	-14.5	-24.2416	0.05	1
P0.4F P0.0	-2.2	-3.67804	0.05	1
P0.4F P0.2F	12.3	20.56357	0.05	1
P0.6F P0.0	5.1	8.52636	0.05	1
P0.6F P0.2F	19.6	32.76796	0.05	1
P0.6F P0.4F	7.3	12.20439	0.05	1
P0.8F P0.0	23.3	38.95375	0.05	1
P0.8F P0.2F	37.8	63.19535	0.05	1
P0.8F P0.4F	25.5	42.63178	0.05	1
P0.8F P0.6F	18.2	30.42739	0.05	1
P1.0F P0.0	-5.2	-8.69354	0.05	1
P1.0F P0.2F	9.3	15.54806	0.05	1
P1.0F P0.4F	-3	-5.0155	0.05	1
P1.0F P0.6F	-10.3	-17.2199	0.05	1
P1.0F P0.8F	-28.5	-47.64729	0.05	1
P1.5F P0.0	-25.2	-42.13023	0.05	1

P1.5F P0.2F	-10.7	-17.88863	0.05	1
P1.5F P0.4F	-23	-38.4522	0.05	1
P1.5F P0.6F	-30.3	-50.65659	0.05	1
P1.5F P0.8F	-48.5	-81.08398	0.05	1
P1.5F P1.0F	-20	-33.43669	0.05	1
P2.0F P0.0	-23.5	-39.28811	0.05	1
P2.0F P0.2F	-9	-15.04651	0.05	1
P2.0F P0.4F	-21.3	-35.61008	0.05	1
P2.0F P0.6F	-28.6	-47.81447	0.05	1
P2.0F P0.8F	-46.8	-78.24186	0.05	1
P2.0F P1.0F	-18.3	-30.59457	0.05	1
P2.0F P1.5F	1.7	2.84212	0.05	0

Table 8.10 to **Table 8.13** represents the descriptive statistics for tensile modulus, yield strength, tensile strength and tensile elongation of carbon black filled poly (lactic acid) composites. **Table 8.26**, **Table 8.31**, **Table 8.36** and **Table 8.41** represents the means comparison within the batch for tensile modulus, yield strength, tensile strength and tensile elongation of carbon black filled poly (lactic acid) composites. **Figure 8.3** graphically represents the tensile modulus, yield strength, tensile strength and tensile elongation of carbon black filled poly (lactic acid) composites. **Figure 8.4** represents stress strain curve and comparative graphs of experimental values versus theoretical values for tensile modulus, yield strength and tensile strength of carbon black filled poly (lactic acid) composites. One can observe increase in tensile modulus values with increasing concentration of carbon black; this increase in tensile modulus values can be attributed to strong intermolecular forces of attraction (physical and chemical interactions) between poly (lactic acid) and surface of carbon black at initial stages of stress. Yield point, is a point on stress strain curve, wherein movement of poly (lactic acid) chains within the carbon black filled composites sets in. Numerical values in **Table 8.11** shows a decrease in yield strength; with increasing concentration of carbon black, this decrease can be attributed to weak physical interactions of filler – filler dominating the strong physical interactions and chemical interactions between polymer – filler. Tensile strength is the ultimate strength that a materials withstands before its failure, from **Table 8.12** one can observe that tensile strength gradually increases till 2.5wt%CB and decreases thereafter. Increase in tensile strength values till 2.5wt% CB can be attributed to initiation of strong intermolecular forces within carbon black filled poly (lactic

acid) composites during tensile mode. Decrease in tensile strength values, after 2.5wt% CB can be attributed to weak forces of attraction existing between poly (lactic acid) chains and surface of carbon black owing to increased filler – filler interaction. Elongation at break shows a decreasing trend with increasing concentration of carbon black; this decrease can be attributed to restriction on mobility of polymer chains. Higher values of elongation at break can be attributed to uncoiling and slippage of polymeric chains, due to reduction of restriction from carbon black within poly (lactic acid) composites. The difference in predicted values and experimental values of tensile modulus, yield strength and tensile strength for carbon black filled poly (lactic acid) composites ; (**see Figure 8.4**) can be attributed to difference in real contact surface between the phases (as contact surface is greater than the predicted from a theoretical model).**Figure 8.6**, **Figure 8.8**, **Figure 8.10** and **Figure 8.12** represents the tensile modulus, yield strength, tensile strength and tensile elongation of carbon black, multiwalled carbon nanotubes, MWCNT+2.5CB and CNF+2.5CB. **Figure 8.7**, **Figure 8.9**, **Figure 8.11** and **Figure 8.13** represents the comparative data for tensile modulus, yield strength, tensile strength and tensile elongation of carbon black, multiwalled carbon nanotubes, MWCNT+2.5CB and CNF+2.5CB. **Table 8.16**, **Table 8.19**, **Table 8.22** and **Table 8.25** indicates the descriptive statistics data for tensile modulus, yield strength, tensile strength and tensile elongation of MWCNT+2.5CB and CNF+2.5CB. **Table 8.29**, **Table 8.34**, **Table 8.39** and **Table 8.44** indicates the means comparison statistics data for tensile modulus, yield strength, tensile strength and tensile elongation of MWCNT+2.5CB. **Table 8.30**, **Table 8.35**, **Table 8.40** and **Table 8.45** indicates the means comparison statistics data for tensile modulus, yield strength, tensile strength and tensile elongation of CNF+2.5CB. From the data represented in form of tables and figures one can observe that tensile modulus increases with increase in concentration of filler (irrespective of filler used in the present study), with maximum for CNF filled poly (lactic acid) composites. Addition of 2.5CB to specific quantities of MWCNT and CNF increases the tensile modulus with maximum for CNF filled poly (lactic acid) composites. Increase in the tensile modulus values can be attributed to increase in stiffness of the poly (lactic acid) composites with hybrid effect of fillers. Yield strength of MWCNT filled poly (lactic acid) composites increases till 0.6wt%, whereas shows a decreasing trend for CNF filled poly (lactic acid) composites ; with increase in concentration (<<0.6wt%) of MWCNT yield strength shows a decreasing trend; whereas increases for CNF filled poly (lactic acid) composites. Similar trend is observed for hybrid filler poly (lactic acid) composites specific to MWCNT and CNF. Tensile strength for MWCNT as well as CNF filled poly (lactic acid) composites shows an increasing trend till 0.8wt% MWCNT and 1.0wt% CNF,

after which a decrease is observed; decrease in tensile strength after a specific concentration of fillers can be attributed to increase in number of weak physical forces of filler – filler interaction, which dominates the polymer – filler interaction. Increasing tensile strength in hybrid poly (lactic acid) composites in comparison to their singly filled composites can be attributed to strong interaction initiated between hybrid structure of fillers and poly (lactic acid) chains during stretching in tensile mode, which has the ability to develop strong chemical and physical interactions within the hybrid filler poly (lactic acid) composites. Usually elongation at break shows a decreasing trend with increasing concentration of filler – which is opposite to the trend of tensile strength; in present study poly (lactic acid) composites filled with MWCNT depicts its tensile elongation lower than CNF filled poly (lactic acid) till 0.6wt% (irrespective of filler used); after which tensile elongation increases for MWCNT filled poly (lactic acid) composites. Decrease in tensile elongation for CNF filled poly (lactic acid) composites after 0.6wt% can be attributed to strong physical and chemical interaction between hydroxyl groups of CNF and carbonyl group of poly (lactic acid) which makes the composites more strong but reduces the polymer chain mobility and is responsible for decrease in tensile elongation. Hybrid filler poly (lactic acid) filled with MWCNT shows an inverted bell curve, whereas CNF filled hybrid filler poly (lactic acid) composite shows a bell curve ; this irregularity in the trend of tensile elongation can be attributed to mobility of poly (lactic acid) in tensile mode. Fillers decrease the chain mobility, which is a general concept; but addition of fillers leading to increase in tensile elongation as observed in hybrid filler poly (lactic acid) filled with 1.5wt% and 2.0wt% MWCNT can be attributed to weak physical forces of interaction between filler – filler at higher concentration, leading to mobility of polymer chains thereby increasing the tensile elongation. The difference in predicted values and experimental values of tensile modulus, yield strength and tensile strength for carbon black filled poly (lactic acid) composites; can be attributed to difference in real contact surface between the phases (as contact surface is greater than the predicted from a theoretical model)[133][132][131][165][166].

Tensile test determined the mechanical strength of the singly filled poly (lactic acid) composites and hybrid filler poly (lactic acid) composites Descriptive statistics data and means comparison data as mentioned in above tables, can be used to determine the mean value, standard error and significance of the numerical values of tensile test.

Let us now determine the effect of CB, MWCNT and CNF in single and hybrid form in poly (lactic acid) composites on notched Izod impact property of the poly (lactic acid) composites and hybrid filler poly (lactic acid) composites .

8.4 NOTCHED IZOD IMPACT

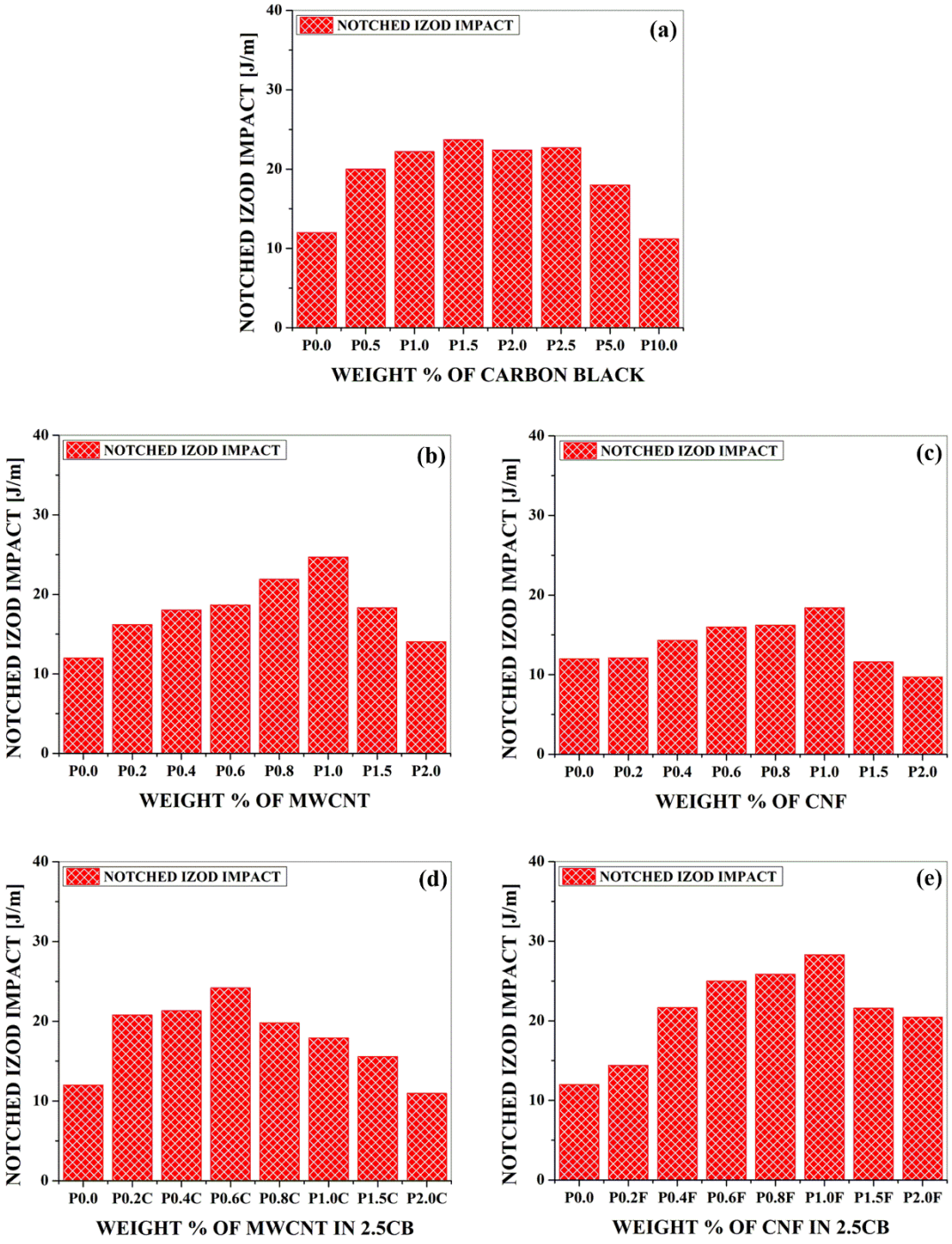

Figure 8.14. Notched Izod Impact for poly (lactic acid) composites filled with (a) carbon black (b) multiwalled carbon nanotubes (c) cellulose nanofibers (d) multiwalled carbon nanotubes + 2.5carbon black (e) cellulose nanofibers + 2.5carbon black

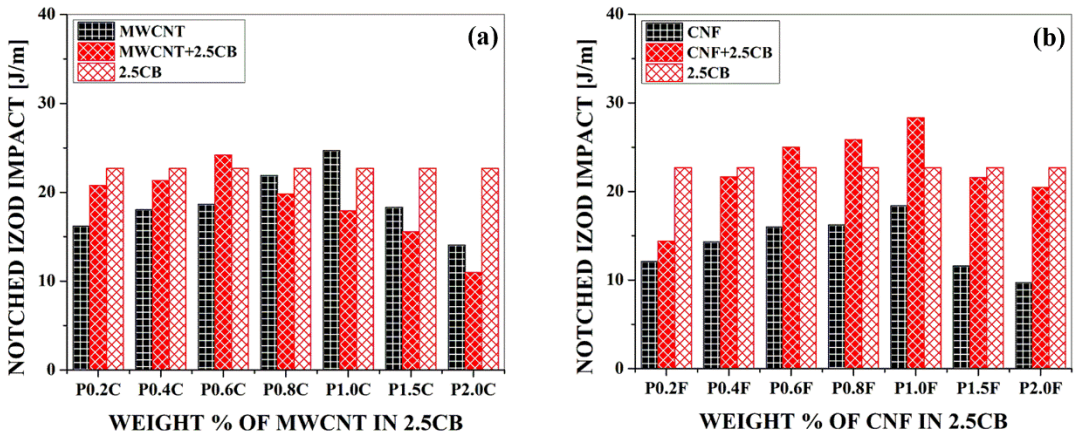

Figure 8.15. Comparative notched Izod impact for (a) multiwalled carbon nanotubes + 2.5 carbon black (b) cellulose nanofibers + 2.5 carbon black with 2.5carbon black poly (lactic acid) composites and specific nanofiller loaded poly (lactic acid) composites.

Table 8.46. Descriptive Statistics of notched Izod impact for Carbon black filled Poly (lactic acid) composites

Sample Code	Sample Size	Mean	Standard Dev	SE of mean
P0.0	10	12	1.1547	0.36515
P0.5	10	20	1.1547	0.36515
P1.0	10	22.2	0.91894	0.29059
P1.5	10	23.7	0.94868	0.3
P2.0	10	22.4	0.5164	0.1633
P2.5	10	22.7	0.82327	0.26034
P5.0	10	18	1.33333	0.42164
P10.0	10	11.2	0.91894	0.29059

Table 8.47. Descriptive Statistics of notched Izod impact for Multiwalled carbon nanotubes filled Poly (lactic acid) composites

Sample Code	Sample Size	Mean	Standard Dev	SE of mean
P0.0	10	12	1.1547	0.36515
P0.2	10	16.19	0.92189	0.29153
P0.4	10	18.02	0.66966	0.21177
P0.6	10	18.66	0.24129	0.0763

P0.8	10	21.9	0.09428	0.02981
P1.0	10	24.69	0.30714	0.09713
P1.5	10	18.31	0.11972	0.03786
P2.0	10	14.04	0.34705	0.10975

Table 8.48. Descriptive Statistics of notched Izod impact for Cellulose nanofibers filled Poly (lactic acid) composites

Sample Code	Sample Size	Mean	Standard Dev	SE of mean
P0.0	10	12	1.1547	0.36515
P0.2	10	12.1	0.73786	0.23333
P0.4	10	14.3	1.05935	0.335
P0.6	10	16	0.8165	0.2582
P0.8	10	16.2	1.0328	0.3266
P1.0	10	18.4	1.17379	0.37118
P1.5	10	11.6	0.84327	0.26667
P2.0	10	9.7	1.25167	0.39581

Table 8.49. Descriptive Statistics of notched Izod impact for 2.5carbon black + multiwalled carbon nanotubes and 2.5carbon black + cellulose nanofibers filled Poly (lactic acid) composites

Sample Code	Sample Size	Mean	Standard Dev	SE of mean
P0.0	10	12	1.1547	0.36515
P0.2C	10	20.77	0.32677	0.10333
P0.4C	10	21.32	0.37653	0.11907
P0.6C	10	24.19	0.1792	0.05667
P0.8C	10	19.79	0.32813	0.10376
P1.0C	10	17.91	0.42282	0.13371
P1.5C	10	15.57	0.2406	0.07608
P2.0C	10	10.97	0.3802	0.12023
P0.2F	10	14.4	0.30912	0.09775
P0.4F	10	21.65	0.66875	0.21148
P0.6F	10	24.99	0.37253	0.1178
P0.8F	10	25.84	0.18974	0.06

P1.0F	10	28.3	0.18257	0.05774
P1.5F	10	21.59	0.18529	0.05859
P2.0F	10	20.45	0.21731	0.06872

Table 8.50. Means Comparison of notched Izod impact by Bonferroni Test for carbon black filled poly (lactic acid) composites

Sample Code	Mean Diff	t Value	Alpha	Sigma
P0.5 P0.0	8	17.91344	0.05	1
P1.0 P0.0	10.2	22.83964	0.05	1
P1.0 P0.5	2.2	4.9262	0.05	1
P1.5 P0.0	11.7	26.19841	0.05	1
P1.5 P0.5	3.7	8.28497	0.05	1
P1.5 P1.0	1.5	3.35877	0.05	1
P2.0 P0.0	10.4	23.28747	0.05	1
P2.0 P0.5	2.4	5.37403	0.05	1
P2.0 P1.0	0.2	0.44784	0.05	0
P2.0 P1.5	-1.3	-2.91093	0.05	0
P2.5 P0.0	10.7	23.95923	0.05	1
P2.5 P0.5	2.7	6.04579	0.05	1
P2.5 P1.0	0.5	1.11959	0.05	0
P2.5 P1.5	-1	-2.23918	0.05	0
P2.5 P2.0	0.3	0.67175	0.05	0
P5.0 P0.0	6	13.43508	0.05	1
P5.0 P0.5	-2	-4.47836	0.05	1
P5.0 P1.0	-4.2	-9.40456	0.05	1
P5.0 P1.5	-5.7	-12.76333	0.05	1
P5.0 P2.0	-4.4	-9.85239	0.05	1
P5.0 P2.5	-4.7	-10.52415	0.05	1
P10.0 P0.0	-0.8	-1.79134	0.05	0
P10.0 P0.5	-8.8	-19.70478	0.05	1
P10.0 P1.0	-11	-24.63098	0.05	1
P10.0 P1.5	-12.5	-27.98975	0.05	1

P10.0 P2.0	-11.2	-25.07882	0.05	1
P10.0 P2.5	-11.5	-25.75057	0.05	1
P10.0 P5.0	-6.8	-15.22642	0.05	1

Table 8.51. Means Comparison of notched Izod impact by Bonferroni Test for multiwalled carbon nanotubes filled poly (lactic acid) composites

Sample Code	Mean Diff	t Value	Alpha	Sigma
P0.2 P0.0	4.19	15.48698	0.05	1
P0.4 P0.0	6.02	22.25098	0.05	1
P0.4 P0.2	1.83	6.764	0.05	1
P0.6 P0.0	6.66	24.61654	0.05	1
P0.6 P0.2	2.47	9.12956	0.05	1
P0.6 P0.4	0.64	2.36555	0.05	0
P0.8 P0.0	9.9	36.59215	0.05	1
P0.8 P0.2	5.71	21.10517	0.05	1
P0.8 P0.4	3.88	14.34116	0.05	1
P0.8 P0.6	3.24	11.97561	0.05	1
P1.0 P0.0	12.69	46.90448	0.05	1
P1.0 P0.2	8.5	31.4175	0.05	1
P1.0 P0.4	6.67	24.6535	0.05	1
P1.0 P0.6	6.03	22.28794	0.05	1
P1.0 P0.8	2.79	10.31233	0.05	1
P1.5 P0.0	6.31	23.32287	0.05	1
P1.5 P0.2	2.12	7.83589	0.05	1
P1.5 P0.4	0.29	1.07189	0.05	0
P1.5 P0.6	-0.35	-1.29366	0.05	0
P1.5 P0.8	-3.59	-13.26927	0.05	1
P1.5 P1.0	-6.38	-23.58161	0.05	1
P2.0 P0.0	2.04	7.5402	0.05	1
P2.0 P0.2	-2.15	-7.94678	0.05	1
P2.0 P0.4	-3.98	-14.71078	0.05	1
P2.0 P0.6	-4.62	-17.07634	0.05	1

P2.0 P0.8	-7.86	-29.05195	0.05	1
P2.0 P1.0	-10.65	-39.36428	0.05	1
P2.0 P1.5	-4.27	-15.78267	0.05	1

Table 8.52. Means Comparison of notched Izod impact by Bonferroni Test for cellulose nanofibers filled poly (lactic acid) composites

Sample Code	Mean Diff	t Value	Alpha	Sigma
P0.2 P0.0	0.1	0.21836	0.05	0
P0.4 P0.0	2.3	5.02233	0.05	1
P0.4 P0.2	2.2	4.80397	0.05	1
P0.6 P0.0	4	8.73449	0.05	1
P0.6 P0.2	3.9	8.51613	0.05	1
P0.6 P0.4	1.7	3.71216	0.05	1
P0.8 P0.0	4.2	9.17122	0.05	1
P0.8 P0.2	4.1	8.95286	0.05	1
P0.8 P0.4	1.9	4.14888	0.05	1
P0.8 P0.6	0.2	0.43672	0.05	0
P1.0 P0.0	6.4	13.97519	0.05	1
P1.0 P0.2	6.3	13.75683	0.05	1
P1.0 P0.4	4.1	8.95286	0.05	1
P1.0 P0.6	2.4	5.2407	0.05	1
P1.0 P0.8	2.2	4.80397	0.05	1
P1.5 P0.0	-0.4	-0.87345	0.05	0
P1.5 P0.2	-0.5	-1.09181	0.05	0
P1.5 P0.4	-2.7	-5.89578	0.05	1
P1.5 P0.6	-4.4	-9.60794	0.05	1
P1.5 P0.8	-4.6	-10.04467	0.05	1
P1.5 P1.0	-6.8	-14.84864	0.05	1
P2.0 P0.0	-2.3	-5.02233	0.05	1
P2.0 P0.2	-2.4	-5.2407	0.05	1
P2.0 P0.4	-4.6	-10.04467	0.05	1
P2.0 P0.6	-6.3	-13.75683	0.05	1

P2.0 P0.8	-6.5	-14.19355	0.05	1
P2.0 P1.0	-8.7	-18.99753	0.05	1
P2.0 P1.5	-1.9	-4.14888	0.05	1

Table 8.53. Means Comparison of notched Izod impact by Bonferroni Test for 2.5carbon black + multiwalled carbon nanotubes filled poly (lactic acid) composites

Sample Code	Mean Diff	t Value	Alpha	Sigma
P0.2C P0.0	8.77	38.24912	0.05	1
P0.4C P0.0	9.32	40.64787	0.05	1
P0.4C P0.2C	0.55	2.39875	0.05	0
P0.6C P0.0	12.19	53.16497	0.05	1
P0.6C P0.2C	3.42	14.91585	0.05	1
P0.6C P0.4C	2.87	12.5171	0.05	1
P0.8C P0.0	7.79	33.97499	0.05	1
P0.8C P0.2C	-0.98	-4.27413	0.05	1
P0.8C P0.4C	-1.53	-6.67288	0.05	1
P0.8C P0.6C	-4.4	-19.18998	0.05	1
P1.0C P0.0	5.91	25.77563	0.05	1
P1.0C P0.2C	-2.86	-12.47349	0.05	1
P1.0C P0.4C	-3.41	-14.87223	0.05	1
P1.0C P0.6C	-6.28	-27.38933	0.05	1
P1.0C P0.8C	-1.88	-8.19935	0.05	1
P1.5C P0.0	3.57	15.57005	0.05	1
P1.5C P0.2C	-5.2	-22.67907	0.05	1
P1.5C P0.4C	-5.75	-25.07781	0.05	1
P1.5C P0.6C	-8.62	-37.59491	0.05	1
P1.5C P0.8C	-4.22	-18.40493	0.05	1
P1.5C P1.0C	-2.34	-10.20558	0.05	1
P2.0C P0.0	-1.03	-4.4922	0.05	1
P2.0C P0.2C	-9.8	-42.74132	0.05	1
P2.0C P0.4C	-10.35	-45.14007	0.05	1
P2.0C P0.6C	-13.22	-57.65717	0.05	1

P2.0C P0.8C	-8.82	-38.46719	0.05	1
P2.0C P1.0C	-6.94	-30.26783	0.05	1
P2.0C P1.5C	-4.6	-20.06225	0.05	1

Table 8.54. Means Comparison of notched Izod impact by Bonferroni Test for 2.5carbon black + cellulose nanofibers filled poly (lactic acid) composites

Sample Code	Mean Diff	t Value	Alpha	Sigma
P0.2F P0.0	2.4	10.31417	0.05	1
P0.4F P0.0	9.65	41.47156	0.05	1
P0.4F P0.2F	7.25	31.15739	0.05	1
P0.6F P0.0	12.99	55.82545	0.05	1
P0.6F P0.2F	10.59	45.51128	0.05	1
P0.6F P0.4F	3.34	14.35389	0.05	1
P0.8F P0.0	13.84	59.47838	0.05	1
P0.8F P0.2F	11.44	49.16421	0.05	1
P0.8F P0.4F	4.19	18.00682	0.05	1
P0.8F P0.6F	0.85	3.65294	0.05	1
P1.0F P0.0	16.3	70.05041	0.05	1
P1.0F P0.2F	13.9	59.73624	0.05	1
P1.0F P0.4F	6.65	28.57885	0.05	1
P1.0F P0.6F	3.31	14.22496	0.05	1
P1.0F P0.8F	2.46	10.57202	0.05	1
P1.5F P0.0	9.59	41.2137	0.05	1
P1.5F P0.2F	7.19	30.89953	0.05	1
P1.5F P0.4F	-0.06	-0.25785	0.05	0
P1.5F P0.6F	-3.4	-14.61174	0.05	1
P1.5F P0.8F	-4.25	-18.26468	0.05	1
P1.5F P1.0F	-6.71	-28.8367	0.05	1
P2.0F P0.0	8.45	36.31447	0.05	1
P2.0F P0.2F	6.05	26.0003	0.05	1
P2.0F P0.4F	-1.2	-5.15709	0.05	1
P2.0F P0.6F	-4.54	-19.51097	0.05	1

P2.0F P0.8F	-5.39	-23.16391	0.05	1
P2.0F P1.0F	-7.85	-33.73593	0.05	1
P2.0F P1.5F	-1.14	-4.89923	0.05	1

Figure 8.14 and **Figure 8.15** represents the graphical form of the numerical values and comparative values of notched Izod test for poly (lactic acid) composites filled with CB, MWCNT, CNF, MWCNT + 2.5CB and CNF + 2.5CB. Descriptive statistical data for notched Izod impact for poly (lactic acid) composites filled with CB, MWCNT, CNF and MWCNT + 2.5CB, CNF + 2.5CB are noted in **Table 8.46**, **Table 8.47**, **Table 8.48** and **Table 8.49**. **Table 8.50**, **Table 8.51**, **Table 8.52**, **Table 8.53** and **Table 8.54** gives the means comparison within the batches for CB, MWCNT, CNF, MWCNT + 2.5CB and CNF + 2.5CB. On basis of the numerical data presented in figures and tables, one can observe that notched Izod impact values increases till a specific filler concentration after which a decrease in notched Izod impact value is observed (irrespective of the filler). Poly (lactic acid) composites filled with MWCNT possess higher values of notched Izod impact than CNF filled poly (lactic acid) composites at equal concentration of MWCNT and CNF; hence cannot be compared with poly (lactic acid) composites filled with CB. Lower values of notched Izod impact for CNF filled poly (lactic acid) composites in comparison to MWCNT filled poly (lactic acid) composites can be attributed to embrittlement induced within CNF filled poly (lactic acid) composites owing to the strong physical and chemical interactions. Hybrid filler poly (lactic acid) composites filled with CNF showed notched Izod impact values slightly higher than singly filled CNF poly (lactic acid) composites; this increase in hybrid filler poly (lactic acid) composites filled with CNF can be attributed to the sliding effect developed between spherical CB and short CNF; thereon for hybrid filler poly (lactic acid) composites with MWCNT the spherical CB and long curvy MWCNT does not induce any sliding effect thereby making the hybrid filler poly (lactic acid) filled with MWCNT embrittle; which reduces the capacity of hybrid filler poly (lactic acid) composites (MWCNT) to absorb and dissipate energy. Control over interparticle distance within poly (lactic acid) composites is also a determinantal factor for fluctuation in notched Izod impact; hence agglomeration at higher concentrations are responsible for decrease in notched Izod impact values. Notched Izod impact test determines the toughness of the singly filled and hybrid filler poly (lactic acid) composites . The energy absorbed during fracture by the singly filled and hybrid filler poly (lactic acid) composites is proportional to the numerical values of notched Izod impact[133][122][167][129].

8.5 FLEXURAL TEST

8.5.1 FLEXURAL STRENGTH

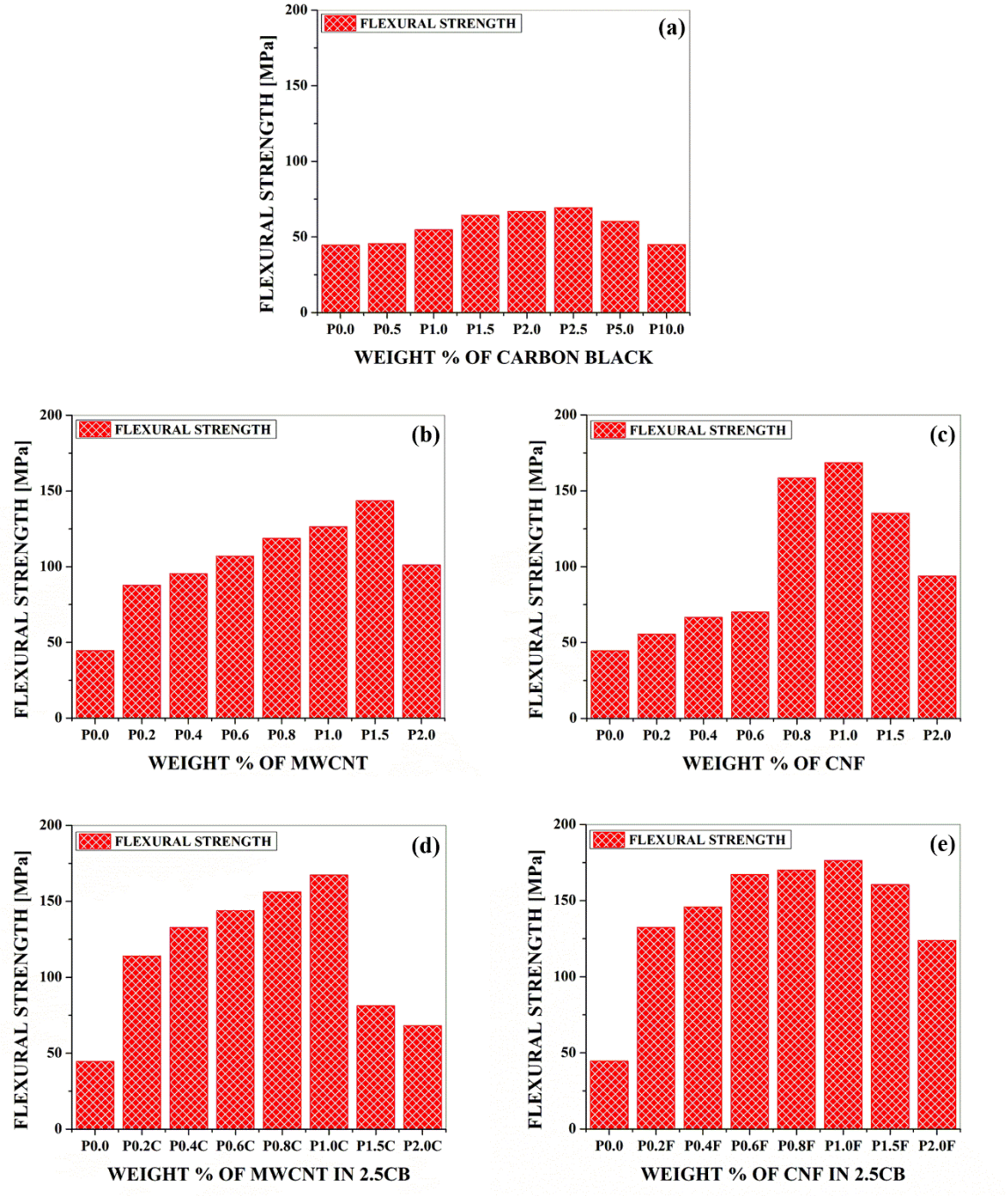

Figure 8.16. Flexural Strength for poly (lactic acid) composites filled with (a) carbon black (b) multiwalled carbon nanotubes (c) cellulose nanofibers (d) multiwalled carbon nanotubes + 2.5carbon black (e) cellulose nanofibers + 2.5carbon black

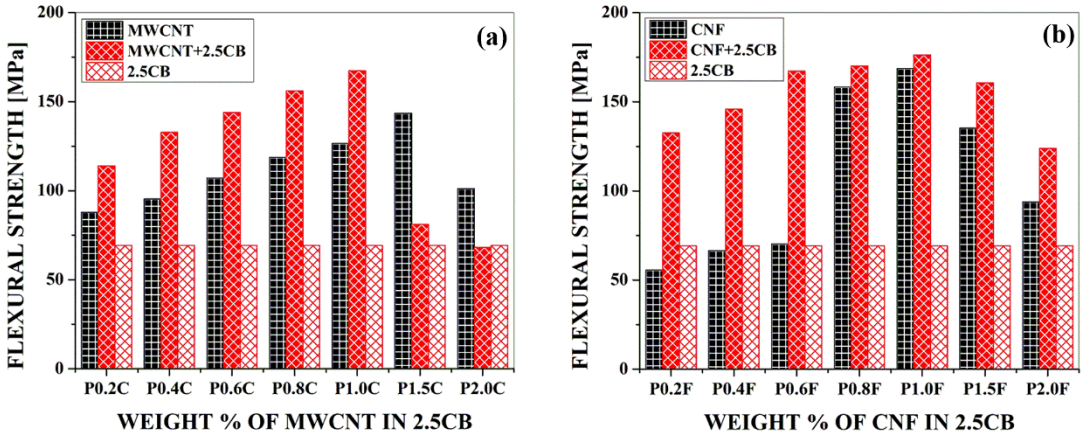

Figure 8.17. Comparative flexural strength for (a) multiwalled carbon nanotubes + 2.5 carbon black (b) cellulose nanofibers + 2.5 carbon black with 2.5carbon black poly (lactic acid) composites and specific nanofiller loaded poly (lactic acid) composites.

Table 8.55. Descriptive Statistics of flexural strength for Carbon black filled Poly (lactic acid) composites

Sample Code	Sample Size	Mean	Standard Dev	SE of mean
P0.0	10	44.5	1.08012	0.34157
P0.5	10	45.5	0.84984	0.26874
P1.0	10	54.8	0.78881	0.24944
P1.5	10	64.3	1.25167	0.39581
P2.0	10	67	0.8165	0.2582
P2.5	10	69.3	0.94868	0.3
P5.0	10	60.4	1.17379	0.37118
P10.0	10	45	0.8165	0.2582

Table 8.56. Descriptive Statistics of flexural strength for multiwalled carbon nanotubes filled Poly (lactic acid) composites

Sample Code	Sample Size	Mean	Standard Dev	SE of mean
P0.0	10	44.5	1.08012	0.34157
P0.2	10	87.86	0.74267	0.23485
P0.4	10	95.36	0.87331	0.27616

P0.6	10	107.07	0.74841	0.23667
P0.8	10	118.75	1.31762	0.41667
P1.0	10	126.52	1.17075	0.37023
P1.5	10	143.51	1.07543	0.34008
P2.0	10	101.1	5.17365	1.63605

Table 8.57. Descriptive Statistics of flexural strength for cellulose nanofibers filled Poly (lactic acid) composites

Sample Code	Sample Size	Mean	Standard Dev	SE of mean
P0.0	10	44.5	1.08012	0.34157
P0.2	10	55.6	1.26491	0.4
P0.4	10	66.5	1.08012	0.34157
P0.6	10	70.2	2.09762	0.66332
P0.8	10	158.4	3.27278	1.03494
P1.0	10	168.6	2.22111	0.70238
P1.5	10	135.2	1.68655	0.53333
P2.0	10	93.8	1.22927	0.38873

Table 8.58. Descriptive Statistics of flexural strength for 2.5carbon black + multiwalled carbon nanotubes and 2.5carbon black + cellulose nanofibers filled Poly (lactic acid) composites

Sample Code	Sample Size	Mean	Standard Dev	SE of mean
P0.0	10	44.5	1.08012	0.34157
P0.2C	10	113.97	1.656	0.52367
P0.4C	10	132.75	1.35913	0.42979
P0.6C	10	143.84	1.45694	0.46072
P0.8C	10	156.07	4.39749	1.39061
P1.0C	10	167.37	2.45223	0.77546
P1.5C	10	81.15	2.13503	0.67515
P2.0C	10	68.15	2.53914	0.80295
P0.2F	10	132.54	1.30996	0.41425
P0.4F	10	145.88	1.59499	0.50438
P0.6F	10	167.18	1.87723	0.59363

P0.8F	10	170.09	1.78665	0.56499
P1.0F	10	176.27	1.55496	0.49172
P1.5F	10	160.61	1.84056	0.58204
P2.0F	10	123.89	1.44872	0.45812

Table 8.59. Means Comparison of flexural strength by Bonferroni Test for carbon black filled poly (lactic acid) composites

Sample Code	Mean Diff	t Value	Alpha	Sigma
P0.5 P0.0	1	2.28086	0.05	0
P1.0 P0.0	10.3	23.49283	0.05	1
P1.0 P0.5	9.3	21.21198	0.05	1
P1.5 P0.0	19.8	45.16098	0.05	1
P1.5 P0.5	18.8	42.88013	0.05	1
P1.5 P1.0	9.5	21.66815	0.05	1
P2.0 P0.0	22.5	51.3193	0.05	1
P2.0 P0.5	21.5	49.03844	0.05	1
P2.0 P1.0	12.2	27.82646	0.05	1
P2.0 P1.5	2.7	6.15832	0.05	1
P2.5 P0.0	24.8	56.56527	0.05	1
P2.5 P0.5	23.8	54.28441	0.05	1
P2.5 P1.0	14.5	33.07244	0.05	1
P2.5 P1.5	5	11.40429	0.05	1
P2.5 P2.0	2.3	5.24597	0.05	1
P5.0 P0.0	15.9	36.26564	0.05	1
P5.0 P0.5	14.9	33.98478	0.05	1
P5.0 P1.0	5.6	12.7728	0.05	1
P5.0 P1.5	-3.9	-8.89535	0.05	1
P5.0 P2.0	-6.6	-15.05366	0.05	1
P5.0 P2.5	-8.9	-20.29963	0.05	1
P10.0 P0.0	0.5	1.14043	0.05	0
P10.0 P0.5	-0.5	-1.14043	0.05	0
P10.0 P1.0	-9.8	-22.35241	0.05	1

P10.0 P1.5	-19.3	-44.02055	0.05	1
P10.0 P2.0	-22	-50.17887	0.05	1
P10.0 P2.5	-24.3	-55.42484	0.05	1
P10.0 P5.0	-15.4	-35.12521	0.05	1

Table 8.60. Means Comparison of flexural strength by Bonferroni Test for multiwalled carbon nanotubes filled poly (lactic acid) composites

Sample Code	Mean Diff	t Value	Alpha	Sigma
P0.2 P0.0	43.36	46.98149	0.05	1
P0.4 P0.0	50.86	55.10791	0.05	1
P0.4 P0.2	7.5	8.12641	0.05	1
P0.6 P0.0	62.57	67.79594	0.05	1
P0.6 P0.2	19.21	20.81445	0.05	1
P0.6 P0.4	11.71	12.68804	0.05	1
P0.8 P0.0	74.25	80.45148	0.05	1
P0.8 P0.2	30.89	33.46998	0.05	1
P0.8 P0.4	23.39	25.34357	0.05	1
P0.8 P0.6	11.68	12.65553	0.05	1
P1.0 P0.0	82.02	88.87044	0.05	1
P1.0 P0.2	38.66	41.88894	0.05	1
P1.0 P0.4	31.16	33.76253	0.05	1
P1.0 P0.6	19.45	21.07449	0.05	1
P1.0 P0.8	7.77	8.41896	0.05	1
P1.5 P0.0	99.01	107.27947	0.05	1
P1.5 P0.2	55.65	60.29797	0.05	1
P1.5 P0.4	48.15	52.17156	0.05	1
P1.5 P0.6	36.44	39.48353	0.05	1
P1.5 P0.8	24.76	26.82799	0.05	1
P1.5 P1.0	16.99	18.40903	0.05	1
P2.0 P0.0	56.6	61.32732	0.05	1
P2.0 P0.2	13.24	14.34583	0.05	1
P2.0 P0.4	5.74	6.21941	0.05	1

P2.0 P0.6	-5.97	-6.46862	0.05	1
P2.0 P0.8	-17.65	-19.12416	0.05	1
P2.0 P1.0	-25.42	-27.54312	0.05	1
P2.0 P1.5	-42.41	-45.95215	0.05	1

Table 8.61. Means Comparison of flexural strength by Bonferroni Test for cellulose nanofibers filled poly (lactic acid) composites

Sample Code	Mean Diff	t Value	Alpha	Sigma
P0.2 P0.0	11.1	13.18877	0.05	1
P0.4 P0.0	22	26.1399	0.05	1
P0.4 P0.2	10.9	12.95113	0.05	1
P0.6 P0.0	25.7	30.53615	0.05	1
P0.6 P0.2	14.6	17.34738	0.05	1
P0.6 P0.4	3.7	4.39626	0.05	1
P0.8 P0.0	113.9	135.33337	0.05	1
P0.8 P0.2	102.8	122.1446	0.05	1
P0.8 P0.4	91.9	109.19347	0.05	1
P0.8 P0.6	88.2	104.79722	0.05	1
P1.0 P0.0	124.1	147.45277	0.05	1
P1.0 P0.2	113	134.26401	0.05	1
P1.0 P0.4	102.1	121.31288	0.05	1
P1.0 P0.6	98.4	116.91662	0.05	1
P1.0 P0.8	10.2	12.11941	0.05	1
P1.5 P0.0	90.7	107.76766	0.05	1
P1.5 P0.2	79.6	94.57889	0.05	1
P1.5 P0.4	68.7	81.62776	0.05	1
P1.5 P0.6	65	77.23151	0.05	1
P1.5 P0.8	-23.2	-27.56571	0.05	1
P1.5 P1.0	-33.4	-39.68511	0.05	1
P2.0 P0.0	49.3	58.57713	0.05	1
P2.0 P0.2	38.2	45.38836	0.05	1
P2.0 P0.4	27.3	32.43723	0.05	1

P2.0 P0.6	23.6	28.04098	0.05	1
P2.0 P0.8	-64.6	-76.75624	0.05	1
P2.0 P1.0	-74.8	-88.87564	0.05	1
P2.0 P1.5	-41.4	-49.19053	0.05	1

Table 8.62. Means Comparison of flexural strength by Bonferroni Test for 2.5carbon black + multiwalled carbon nanotubes filled poly (lactic acid) composites

Sample Code	Mean Diff	t Value	Alpha	Sigma
P0.2C P0.0	69.47	66.06029	0.05	1
P0.4C P0.0	88.25	83.91853	0.05	1
P0.4C P0.2C	18.78	17.85824	0.05	1
P0.6C P0.0	99.34	94.46421	0.05	1
P0.6C P0.2C	29.87	28.40393	0.05	1
P0.6C P0.4C	11.09	10.54568	0.05	1
P0.8C P0.0	111.57	106.09394	0.05	1
P0.8C P0.2C	42.1	40.03366	0.05	1
P0.8C P0.4C	23.32	22.17541	0.05	1
P0.8C P0.6C	12.23	11.62973	0.05	1
P1.0C P0.0	122.87	116.83932	0.05	1
P1.0C P0.2C	53.4	50.77903	0.05	1
P1.0C P0.4C	34.62	32.92079	0.05	1
P1.0C P0.6C	23.53	22.37511	0.05	1
P1.0C P0.8C	11.3	10.74538	0.05	1
P1.5C P0.0	36.65	34.85115	0.05	1
P1.5C P0.2C	-32.82	-31.20914	0.05	1
P1.5C P0.4C	-51.6	-49.06738	0.05	1
P1.5C P0.6C	-62.69	-59.61306	0.05	1
P1.5C P0.8C	-74.92	-71.24279	0.05	1
P1.5C P1.0C	-86.22	-81.98817	0.05	1
P2.0C P0.0	23.65	22.48922	0.05	1
P2.0C P0.2C	-45.82	-43.57107	0.05	1
P2.0C P0.4C	-64.6	-61.42932	0.05	1

P2.0C P0.6C	-75.69	-71.975	0.05	1
P2.0C P0.8C	-87.92	-83.60473	0.05	1
P2.0C P1.0C	-99.22	-94.3501	0.05	1
P2.0C P1.5C	-13	-12.36194	0.05	1

Table 8.63. Means Comparison of flexural strength by Bonferroni Test for 2.5carbon black + cellulose nanofibers filled poly (lactic acid) composites

Sample Code	Mean Diff	t Value	Alpha	Sigma
P0.2F P0.0	88.04	124.36098	0.05	1
P0.4F P0.0	101.38	143.20441	0.05	1
P0.4F P0.2F	13.34	18.84343	0.05	1
P0.6F P0.0	122.68	173.29174	0.05	1
P0.6F P0.2F	34.64	48.93076	0.05	1
P0.6F P0.4F	21.3	30.08733	0.05	1
P0.8F P0.0	125.59	177.40226	0.05	1
P0.8F P0.2F	37.55	53.04129	0.05	1
P0.8F P0.4F	24.21	34.19786	0.05	1
P0.8F P0.6F	2.91	4.11052	0.05	1
P1.0F P0.0	131.77	186.13183	0.05	1
P1.0F P0.2F	43.73	61.77085	0.05	1
P1.0F P0.4F	30.39	42.92742	0.05	1
P1.0F P0.6F	9.09	12.84009	0.05	1
P1.0F P0.8F	6.18	8.72956	0.05	1
P1.5F P0.0	116.11	164.01128	0.05	1
P1.5F P0.2F	28.07	39.6503	0.05	1
P1.5F P0.4F	14.73	20.80687	0.05	1
P1.5F P0.6F	-6.57	-9.28046	0.05	1
P1.5F P0.8F	-9.48	-13.39098	0.05	1
P1.5F P1.0F	-15.66	-22.12055	0.05	1
P2.0F P0.0	79.39	112.14241	0.05	1
P2.0F P0.2F	-8.65	-12.21857	0.05	1
P2.0F P0.4F	-21.99	-31.06199	0.05	1

P2.0F P0.6F	-43.29	-61.14933	0.05	1
P2.0F P0.8F	-46.2	-65.25985	0.05	1
P2.0F P1.0F	-52.38	-73.98941	0.05	1
P2.0F P1.5F	-36.72	-51.86887	0.05	1

Figure 8.16 and **Figure 8.17** represents the graphical form of the numerical values and comparative values of flexural strength for poly (lactic acid) composites filled with CB, MWCNT, CNF, MWCNT + 2.5CB and CNF + 2.5CB. Descriptive statistical data for flexural strength for poly (lactic acid) composites filled with CB, MWCNT, CNF and MWCNT + 2.5CB, CNF + 2.5CB are noted in **Table 8.55**, **Table 8.56**, **Table 8.57** and **Table 8.58**. **Table 8.59**, **Table 8.60**, **Table 8.61**, **Table 8.62** and **Table 8.63** gives the means comparison within the batches for CB, MWCNT, CNF, MWCNT + 2.5CB and CNF + 2.5CB. Poly (lactic acid) composites filled with CB possess the lower resistance to bending during flexural test, hence has the lower values of flexural strength in comparison to poly (lactic acid) composites filled with MWCNT and CNF. Poly (lactic acid) composites filled with CNF possess high resistance to flexural bending than poly (lactic acid) composites filled with MWCNT; and hence flexural strength for MWCNT decreases. Decrease in the flexural strength for singly filled poly (lactic acid) composites can be attributed to debonding between the filler – filler interaction. Hybrid filler poly (lactic acid) composites filled with CNF possessed high resistance to bending than hybrid filler poly (lactic acid) composites filled with MWCNT; due to which hybrid filler poly (lactic acid) composites filled with CNF possessed flexural strength higher than hybrid filler poly (lactic acid) composites filled with MWCNT. Increase in flexural strength for hybrid filler poly (lactic acid) filled with CNF can be attributed to bridging between surfaces of CB and CNF in vicinity. A significant increase in flexural strength of hybrid filler poly (lactic acid) composites filled with CNF in comparison to 2.5CB and singly filled CNF poly (lactic acid) composites is observed, which can be attributed to the transmission of energy across the polymer chains producing intensified vibrations of the segments. Decrease in flexural strength of hybrid filler poly (lactic acid) composites at higher concentration of nanofillers (it be MWCNT or CNF) can be attributed to the debonding between nanofillers and CB. Flexural strength determines the bending ability of the singly filled and hybrid filler filled poly (lactic acid) composites; and their resistance to bending determines the flexural strength. In further discussion we shall look into the modulus, in flexural mode; thereby indicating the stiffness of poly (lactic acid) composites at initial stages of bending[131][140][125][124].

8.5.2 FLEXURAL MODULUS

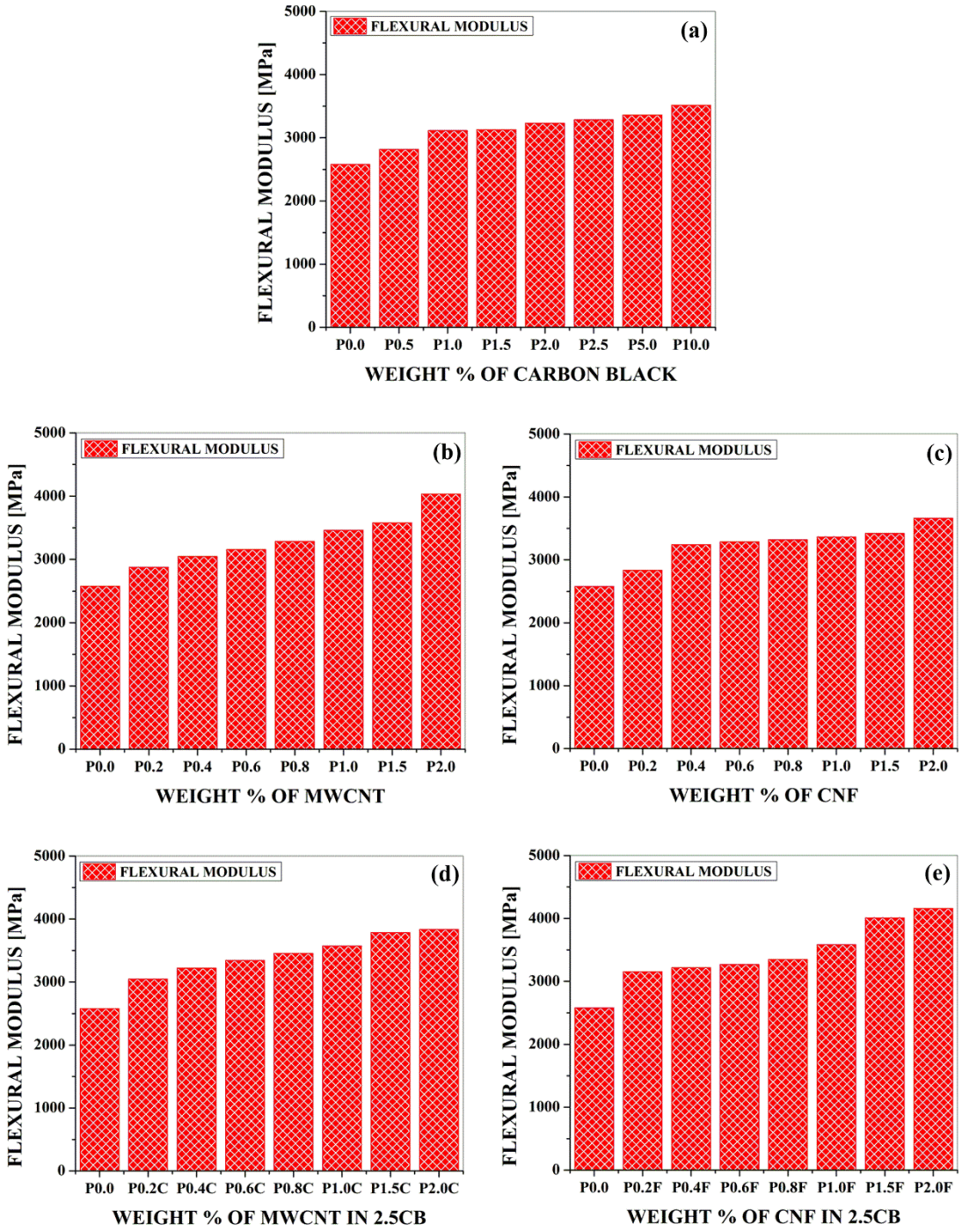

Figure 8.18. Flexural Modulus for poly (lactic acid) composites filled with (a) carbon black (b) multiwalled carbon nanotubes (c) cellulose nanofibers (d) multiwalled carbon nanotubes + 2.5carbon black (e) cellulose nanofibers + 2.5carbon black

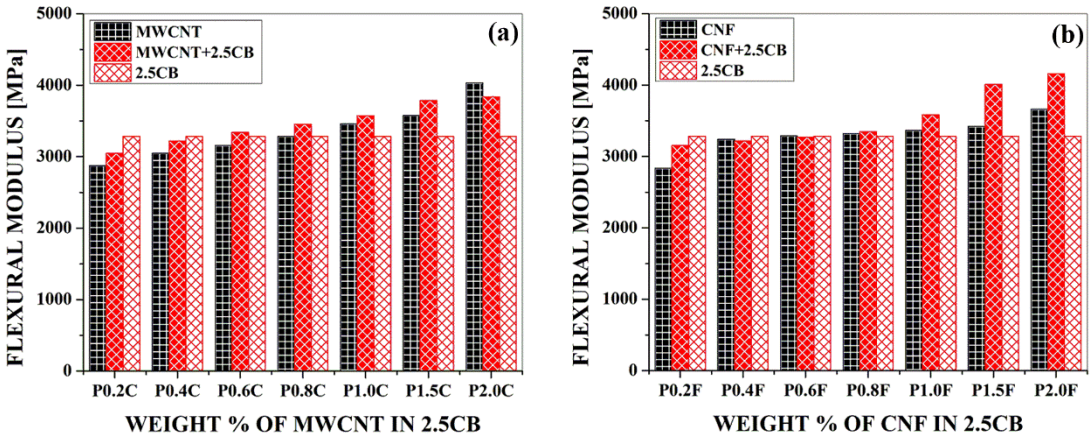

Figure 8.19. Comparative flexural modulus for (a) multiwalled carbon nanotubes + 2.5 carbon black (b) cellulose nanofibers + 2.5 carbon black with 2.5carbon black poly (lactic acid) composites and specific nanofiller loaded poly (lactic acid) composites.

Table 8.64. Descriptive Statistics of flexural modulus for Carbon black filled Poly (lactic acid) composites

Sample Code	Sample Size	Mean	Standard Dev	SE of mean
P0.0	10	2576.7	9.23821	2.92138
P0.5	10	2816.5	4.74342	1.5
P1.0	10	3112.9	3.31495	1.04828
P1.5	10	3128.1	5.04315	1.59478
P2.0	10	3231.7	1.49443	0.47258
P2.5	10	3285.4	2.1187	0.66999
P5.0	10	3358.3	1.88856	0.59722
P10.0	10	3513.5	4.22295	1.33542

Table 8.65. Descriptive Statistics of flexural modulus for multiwalled carbon nanotubes filled Poly (lactic acid) composites

Sample Code	Sample Size	Mean	Standard Dev	SE of mean
P0.0	10	2576.7	9.23821	2.92138
P0.2	10	2875.4	2.27058	0.71802
P0.4	10	3048.1	2.42441	0.76667
P0.6	10	3156.1	2.28279	0.72188

P0.8	10	3285	2.16025	0.68313
P1.0	10	3459.3	1.76698	0.55877
P1.5	10	3576.8	3.01109	0.95219
P2.0	10	4033.5	59.78341	18.90517

Table 8.66. Descriptive Statistics of flexural modulus for cellulose nanofibers filled Poly (lactic acid) composites

Sample Code	Sample Size	Mean	Standard Dev	SE of mean
P0.0	10	2576.7	9.23821	2.92138
P0.2	10	2834.4	9.37135	2.96348
P0.4	10	3241.1	3.69534	1.16857
P0.6	10	3287.1	1.37032	0.43333
P0.8	10	3320.1	2.80674	0.88757
P1.0	10	3365.5	2.41523	0.76376
P1.5	10	3422.1	4.25441	1.34536
P2.0	10	3661.8	5.53373	1.74992

Table 8.67. Descriptive Statistics of flexural modulus for 2.5carbon black + multiwalled carbon nanotubes and 2.5carbon black + cellulose nanofibers filled Poly (lactic acid) composites

Sample Code	Sample Size	Mean	Standard Dev	SE of mean
P0.0	10	2576.7	9.23821	2.92138
P0.2C	10	3047.35	3.10957	0.98333
P0.4C	10	3219.55	4.03078	1.27465
P0.6C	10	3342.28	9.98808	3.15851
P0.8C	10	3455.38	3.48004	1.10048
P1.0C	10	3572.94	3.77601	1.19408
P1.5C	10	3785.16	2.43821	0.77103
P2.0C	10	3835.3	8.87005	2.80496
P0.2F	10	3153.33	1.98329	0.62717
P0.4F	10	3217.39	2.37321	0.75047
P0.6F	10	3269.47	8.49236	2.68552
P0.8F	10	3348.16	3.43032	1.08476

P1.0F	10	3583.38	1.71904	0.54361
P1.5F	10	4009.76	48.91942	15.46968
P2.0F	10	4159.08	2.4444	0.77299

Table 8.68. Means Comparison of flexural modulus by Bonferroni Test for carbon black filled poly (lactic acid) composites

Sample Code	Mean Diff	t Value	Alpha	Sigma
P0.5 P0.0	239.8	115.51132	0.05	1
P1.0 P0.0	536.2	258.28678	0.05	1
P1.0 P0.5	296.4	142.77546	0.05	1
P1.5 P0.0	551.4	265.60859	0.05	1
P1.5 P0.5	311.6	150.09728	0.05	1
P1.5 P1.0	15.2	7.32182	0.05	1
P2.0 P0.0	655	315.51257	0.05	1
P2.0 P0.5	415.2	200.00125	0.05	1
P2.0 P1.0	118.8	57.22579	0.05	1
P2.0 P1.5	103.6	49.90397	0.05	1
P2.5 P0.0	708.7	341.37978	0.05	1
P2.5 P0.5	468.9	225.86846	0.05	1
P2.5 P1.0	172.5	83.093	0.05	1
P2.5 P1.5	157.3	75.77119	0.05	1
P2.5 P2.0	53.7	25.86721	0.05	1
P5.0 P0.0	781.6	376.49561	0.05	1
P5.0 P0.5	541.8	260.98429	0.05	1
P5.0 P1.0	245.4	118.20883	0.05	1
P5.0 P1.5	230.2	110.88701	0.05	1
P5.0 P2.0	126.6	60.98304	0.05	1
P5.0 P2.5	72.9	35.11583	0.05	1
P10.0 P0.0	936.8	451.25522	0.05	1
P10.0 P0.5	697	335.74391	0.05	1
P10.0 P1.0	400.6	192.96845	0.05	1
P10.0 P1.5	385.4	185.64663	0.05	1

P10.0 P2.0	281.8	135.74266	0.05	1
P10.0 P2.5	228.1	109.87544	0.05	1
P10.0 P5.0	155.2	74.75962	0.05	1

Table 8.69. Means Comparison of flexural modulus by Bonferroni Test for multiwalled carbon nanotubes filled poly (lactic acid) composites

Sample Code	Mean Diff	t Value	Alpha	Sigma
P0.2 P0.0	298.7	31.08887	0.05	1
P0.4 P0.0	471.4	49.06359	0.05	1
P0.4 P0.2	172.7	17.97472	0.05	1
P0.6 P0.0	579.4	60.30429	0.05	1
P0.6 P0.2	280.7	29.21542	0.05	1
P0.6 P0.4	108	11.2407	0.05	1
P0.8 P0.0	708.3	73.72028	0.05	1
P0.8 P0.2	409.6	42.63141	0.05	1
P0.8 P0.4	236.9	24.65669	0.05	1
P0.8 P0.6	128.9	13.41599	0.05	1
P1.0 P0.0	882.6	91.86153	0.05	1
P1.0 P0.2	583.9	60.77266	0.05	1
P1.0 P0.4	411.2	42.79794	0.05	1
P1.0 P0.6	303.2	31.55723	0.05	1
P1.0 P0.8	174.3	18.14125	0.05	1
P1.5 P0.0	1000.1	104.091	0.05	1
P1.5 P0.2	701.4	73.00213	0.05	1
P1.5 P0.4	528.7	55.02741	0.05	1
P1.5 P0.6	420.7	43.7867	0.05	1
P1.5 P0.8	291.8	30.37072	0.05	1
P1.5 P1.0	117.5	12.22947	0.05	1
P2.0 P0.0	1456.8	151.6246	0.05	1
P2.0 P0.2	1158.1	120.53573	0.05	1
P2.0 P0.4	985.4	102.56101	0.05	1
P2.0 P0.6	877.4	91.32031	0.05	1

P2.0 P0.8	748.5	77.90432	0.05	1
P2.0 P1.0	574.2	59.76307	0.05	1
P2.0 P1.5	456.7	47.53361	0.05	1

Table 8.70. Means Comparison of flexural modulus by Bonferroni Test for cellulose nanofibers filled poly (lactic acid) composites

Sample Code	Mean Diff	t Value	Alpha	Sigma
P0.2 P0.0	257.7	102.84714	0.05	1
P0.4 P0.0	664.4	265.15965	0.05	1
P0.4 P0.2	406.7	162.31251	0.05	1
P0.6 P0.0	710.4	283.51809	0.05	1
P0.6 P0.2	452.7	180.67094	0.05	1
P0.6 P0.4	46	18.35843	0.05	1
P0.8 P0.0	743.4	296.68827	0.05	1
P0.8 P0.2	485.7	193.84112	0.05	1
P0.8 P0.4	79	31.52862	0.05	1
P0.8 P0.6	33	13.17018	0.05	1
P1.0 P0.0	788.8	314.80724	0.05	1
P1.0 P0.2	531.1	211.9601	0.05	1
P1.0 P0.4	124.4	49.64759	0.05	1
P1.0 P0.6	78.4	31.28916	0.05	1
P1.0 P0.8	45.4	18.11898	0.05	1
P1.5 P0.0	845.4	337.3961	0.05	1
P1.5 P0.2	587.7	234.54896	0.05	1
P1.5 P0.4	181	72.23645	0.05	1
P1.5 P0.6	135	53.87801	0.05	1
P1.5 P0.8	102	40.70783	0.05	1
P1.5 P1.0	56.6	22.58886	0.05	1
P2.0 P0.0	1085.1	433.05951	0.05	1
P2.0 P0.2	827.4	330.21237	0.05	1
P2.0 P0.4	420.7	167.89986	0.05	1
P2.0 P0.6	374.7	149.54142	0.05	1

P2.0 P0.8	341.7	136.37124	0.05	1
P2.0 P1.0	296.3	118.25226	0.05	1
P2.0 P1.5	239.7	95.66341	0.05	1

Table 8.71. Means Comparison of flexural modulus by Bonferroni Test for 2.5carbon black + multiwalled carbon nanotubes filled poly (lactic acid) composites

Sample Code	Mean Diff	t Value	Alpha	Sigma
P0.2C P0.0	470.65	165.87861	0.05	1
P0.4C P0.0	642.85	226.56977	0.05	1
P0.4C P0.2C	172.2	60.69116	0.05	1
P0.6C P0.0	765.58	269.82544	0.05	1
P0.6C P0.2C	294.93	103.94683	0.05	1
P0.6C P0.4C	122.73	43.25567	0.05	1
P0.8C P0.0	878.68	309.68706	0.05	1
P0.8C P0.2C	408.03	143.80845	0.05	1
P0.8C P0.4C	235.83	83.11729	0.05	1
P0.8C P0.6C	113.1	39.86162	0.05	1
P1.0C P0.0	996.24	351.12059	0.05	1
P1.0C P0.2C	525.59	185.24198	0.05	1
P1.0C P0.4C	353.39	124.55082	0.05	1
P1.0C P0.6C	230.66	81.29514	0.05	1
P1.0C P0.8C	117.56	41.43353	0.05	1
P1.5C P0.0	1208.46	425.91663	0.05	1
P1.5C P0.2C	737.81	260.03802	0.05	1
P1.5C P0.4C	565.61	199.34686	0.05	1
P1.5C P0.6C	442.88	156.09119	0.05	1
P1.5C P0.8C	329.78	116.22957	0.05	1
P1.5C P1.0C	212.22	74.79604	0.05	1
P2.0C P0.0	1258.6	443.58826	0.05	1
P2.0C P0.2C	787.95	277.70966	0.05	1
P2.0C P0.4C	615.75	217.01849	0.05	1
P2.0C P0.6C	493.02	173.76282	0.05	1

P2.0C P0.8C	379.92	133.9012	0.05	1
P2.0C P1.0C	262.36	92.46768	0.05	1
P2.0C P1.5C	50.14	17.67163	0.05	1

Table 8.72. Means Comparison of flexural modulus by Bonferroni Test for 2.5carbon black + cellulose nanofibers filled poly (lactic acid) composites

Sample Code	Mean Diff	t Value	Alpha	Sigma
P0.2F P0.0	576.63	71.78719	0.05	1
P0.4F P0.0	640.69	79.7623	0.05	1
P0.4F P0.2F	64.06	7.97511	0.05	1
P0.6F P0.0	692.77	86.24597	0.05	1
P0.6F P0.2F	116.14	14.45878	0.05	1
P0.6F P0.4F	52.08	6.48367	0.05	1
P0.8F P0.0	771.46	96.04243	0.05	1
P0.8F P0.2F	194.83	24.25524	0.05	1
P0.8F P0.4F	130.77	16.28013	0.05	1
P0.8F P0.6F	78.69	9.79646	0.05	1
P1.0F P0.0	1006.68	125.326	0.05	1
P1.0F P0.2F	430.05	53.53881	0.05	1
P1.0F P0.4F	365.99	45.5637	0.05	1
P1.0F P0.6F	313.91	39.08003	0.05	1
P1.0F P0.8F	235.22	29.28357	0.05	1
P1.5F P0.0	1433.06	178.40791	0.05	1
P1.5F P0.2F	856.43	106.62072	0.05	1
P1.5F P0.4F	792.37	98.64561	0.05	1
P1.5F P0.6F	740.29	92.16194	0.05	1
P1.5F P0.8F	661.6	82.36548	0.05	1
P1.5F P1.0F	426.38	53.08191	0.05	1
P2.0F P0.0	1582.38	196.99741	0.05	1
P2.0F P0.2F	1005.75	125.21022	0.05	1
P2.0F P0.4F	941.69	117.23511	0.05	1
P2.0F P0.6F	889.61	110.75144	0.05	1

P2.0F P0.8F	810.92	100.95498	0.05	1
P2.0F P1.0F	575.7	71.67141	0.05	1
P2.0F P1.5F	149.32	18.5895	0.05	1

Figure 8.18 and **Figure 8.19** represents the graphical form of the numerical values and comparative values of flexural modulus for poly (lactic acid) composites filled with CB, MWCNT, CNF, MWCNT + 2.5CB and CNF + 2.5CB. Descriptive statistical data for flexural modulus for poly (lactic acid) composites filled with CB, MWCNT, CNF and MWCNT + 2.5CB, CNF + 2.5CB are noted in **Table 8.64**, **Table 8.65**, **Table 8.66** and **Table 8.67**. **Table 8.68**, **Table 8.69**, **Table 8.70**, **Table 8.71** and **Table 8.72** gives the means comparison within the batches for CB, MWCNT, CNF, MWCNT + 2.5CB and CNF + 2.5CB. From the data presented in form of graphs and tables, one may observe that flexural modulus increases with increasing concentration of filler (irrespective of the choice of filler – single or hybrid). Increase in flexural modulus with increasing concentration of fillers can be attributed to the connectivity between fillers in single form and hybrid form with the poly (lactic acid) matrix; thereby inducing strain energy and increasing the flexural modulus of singly filled and hybrid filler poly (lactic acid) composites[131][168][166][169].

8.6 HEAT DEFLECTION TEST

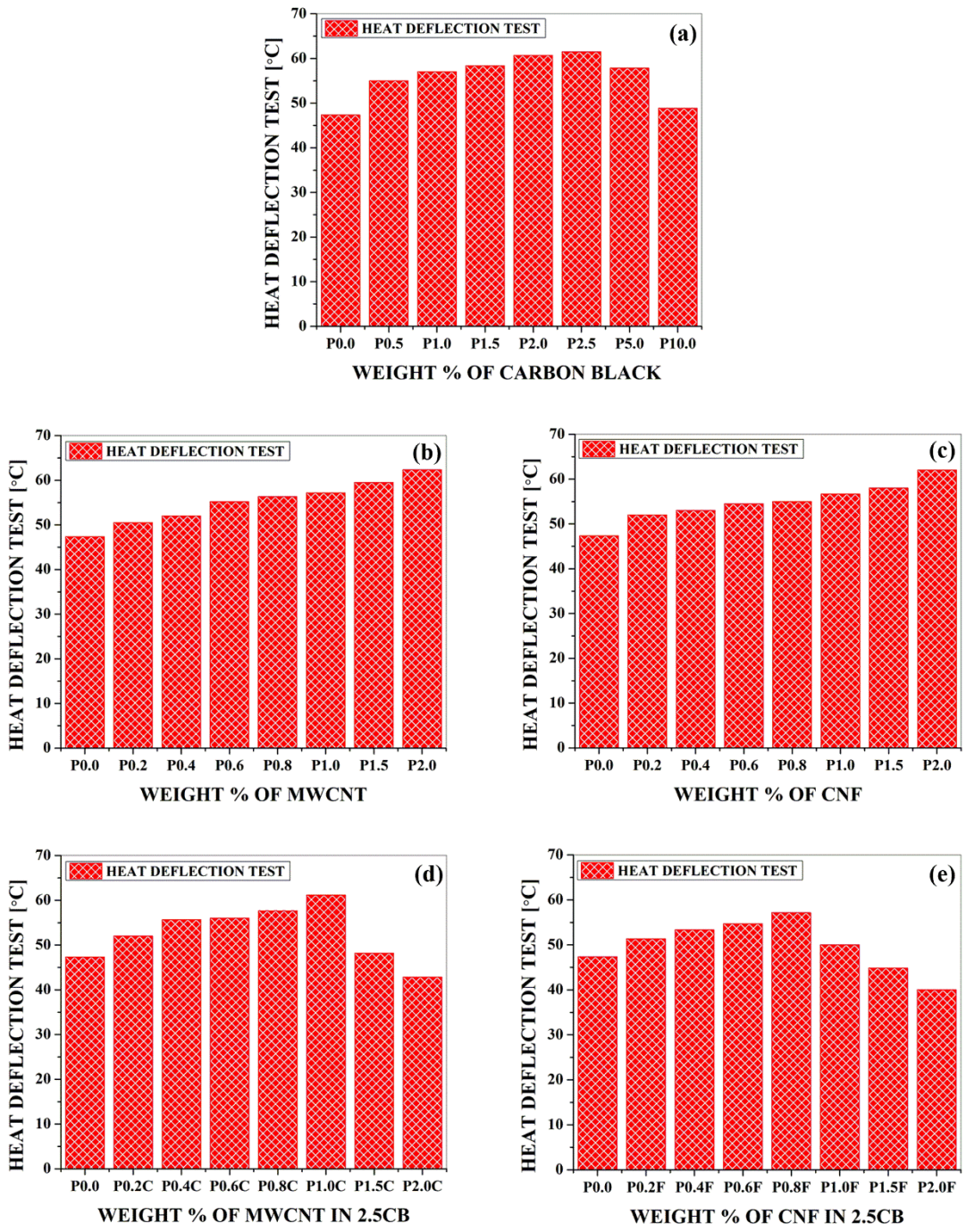

Figure 8.20. Heat Deflection Test for poly (lactic acid) composites filled with (a) carbon black (b) multiwalled carbon nanotubes (c) cellulose nanofibers (d) multiwalled carbon nanotubes + 2.5carbon black (e) cellulose nanofibers + 2.5carbon black.

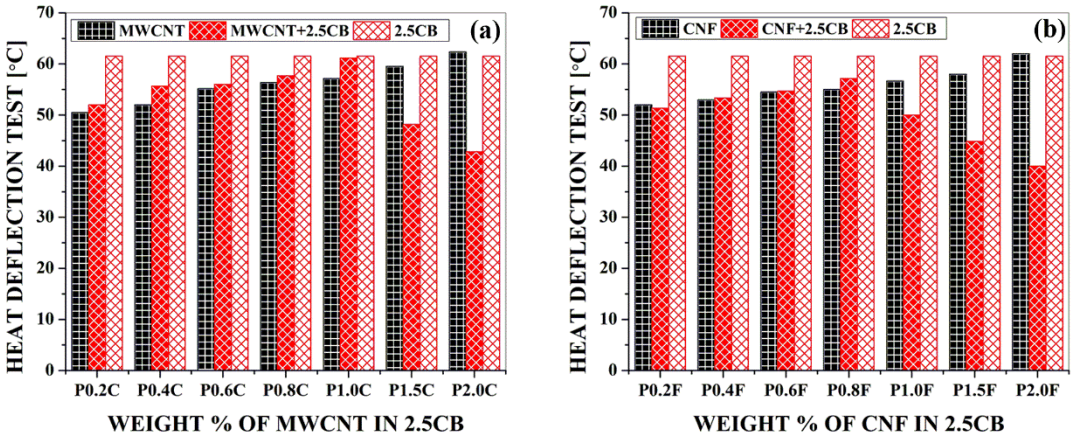

Figure 8.21.Comparative heat deflection test for (a) multiwalled carbon nanotubes + 2.5 carbon black (b) cellulose nanofibers + 2.5 carbon black with 2.5carbon black poly (lactic acid) composites and specific nanofiller loaded poly (lactic acid) composites.

Table 8.73. Descriptive Statistics of heat deflection test for Carbon black filled Poly (lactic acid) composites

Sample Code	Sample Size	Mean	Standard Dev	SE of mean
P0.0	10	47.33333	0.8165	0.33333
P0.5	10	55	0.63246	0.2582
P1.0	10	57	0.63246	0.2582
P1.5	10	58.33333	0.5164	0.21082
P2.0	10	60.66667	0.8165	0.33333
P2.5	10	61.5	1.04881	0.42817
P5.0	10	57.83333	0.75277	0.30732
P10.0	10	48.83333	0.98319	0.40139

Table 8.74. Descriptive Statistics of heat deflection test for multiwalled carbon nanotubes filled Poly (lactic acid) composites

Sample Code	Sample Size	Mean	Standard Dev	SE of mean
P0.0	10	47.33333	0.8165	0.33333
P0.2	10	50.5	1.3784	0.56273
P0.4	10	52	0.63246	0.2582

P0.6	10	55.16667	0.75277	0.30732
P0.8	10	56.33333	0.5164	0.21082
P1.0	10	57.16667	0.75277	0.30732
P1.5	10	59.5	0.54772	0.22361
P2.0	10	62.33333	0.8165	0.33333

Table 8.75. Descriptive Statistics of heat deflection test for cellulose nanofibers filled Poly (lactic acid) composites

Sample Code	Sample Size	Mean	Standard Dev	SE of mean
P0.0	10	47.33333	0.8165	0.33333
P0.2	10	52	0.63246	0.2582
P0.4	10	53	0.63246	0.2582
P0.6	10	54.5	0.83666	0.34157
P0.8	10	55	0.63246	0.2582
P1.0	10	56.66667	1.0328	0.42164
P1.5	10	58	0.63246	0.2582
P2.0	10	62	0.63246	0.2582

Table 8.76. Descriptive Statistics of heat deflection test for 2.5carbon black + multiwalled carbon nanotubes and 2.5carbon black + cellulose nanofibers filled Poly (lactic acid) composites

Sample Code	Sample Size	Mean	Standard Dev	SE of mean
P0.0	10	47.33333	0.8165	0.33333
P0.2C	10	52	0.63246	0.2582
P0.4C	10	55.66667	0.5164	0.21082
P0.6C	10	56	0.63246	0.2582
P0.8C	10	57.66667	0.5164	0.21082
P1.0C	10	61.16667	0.75277	0.30732
P1.5C	10	48.16667	0.98319	0.40139
P2.0C	10	42.83333	0.75277	0.30732
P0.2F	10	51.33333	0.8165	0.33333
P0.4F	10	53.33333	1.0328	0.42164
P0.6F	10	54.66667	0.8165	0.33333

P0.8F	10	57.16667	0.75277	0.30732
P1.0F	10	50	0.63246	0.2582
P1.5F	10	44.83333	0.75277	0.30732
P2.0F	10	40	1.09545	0.44721

Table 8.77. Means Comparison of heat deflection test by Bonferroni Test for carbon black filled poly (lactic acid) composites

Sample Code	Mean Diff	t Value	Alpha	Sigma
P0.5 P0.0	7.66667	16.74111	0.05	1
P1.0 P0.0	9.66667	21.10836	0.05	1
P1.0 P0.5	2	4.36725	0.05	1
P1.5 P0.0	11	24.01986	0.05	1
P1.5 P0.5	3.33333	7.27875	0.05	1
P1.5 P1.0	1.33333	2.9115	0.05	0
P2.0 P0.0	13.33333	29.11498	0.05	1
P2.0 P0.5	5.66667	12.37387	0.05	1
P2.0 P1.0	3.66667	8.00662	0.05	1
P2.0 P1.5	2.33333	5.09512	0.05	1
P2.5 P0.0	14.16667	30.93467	0.05	1
P2.5 P0.5	6.5	14.19355	0.05	1
P2.5 P1.0	4.5	9.82631	0.05	1
P2.5 P1.5	3.16667	6.91481	0.05	1
P2.5 P2.0	0.83333	1.81969	0.05	0
P5.0 P0.0	10.5	22.92805	0.05	1
P5.0 P0.5	2.83333	6.18693	0.05	1
P5.0 P1.0	0.83333	1.81969	0.05	0
P5.0 P1.5	-0.5	-1.09181	0.05	0
P5.0 P2.0	-2.83333	-6.18693	0.05	1
P5.0 P2.5	-3.66667	-8.00662	0.05	1
P10.0 P0.0	1.5	3.27544	0.05	0
P10.0 P0.5	-6.16667	-13.46568	0.05	1
P10.0 P1.0	-8.16667	-17.83293	0.05	1

P10.0 P1.5	-9.5	-20.74442	0.05	1
P10.0 P2.0	-11.83333	-25.83955	0.05	1
P10.0 P2.5	-12.66667	-27.65923	0.05	1
P10.0 P5.0	-9	-19.65261	0.05	1

Table 8.78. Means Comparison of heat deflection test by Bonferroni Test for multiwalled carbon nanotubes filled poly (lactic acid) composites

Sample Code	Mean Diff	t Value	Alpha	Sigma
P0.2 P0.0	3.16667	6.71751	0.05	1
P0.4 P0.0	4.66667	9.89949	0.05	1
P0.4 P0.2	1.5	3.18198	0.05	0
P0.6 P0.0	7.83333	16.61701	0.05	1
P0.6 P0.2	4.66667	9.89949	0.05	1
P0.6 P0.4	3.16667	6.71751	0.05	1
P0.8 P0.0	9	19.09188	0.05	1
P0.8 P0.2	5.83333	12.37437	0.05	1
P0.8 P0.4	4.33333	9.19239	0.05	1
P0.8 P0.6	1.16667	2.47487	0.05	0
P1.0 P0.0	9.83333	20.85965	0.05	1
P1.0 P0.2	6.66667	14.14214	0.05	1
P1.0 P0.4	5.16667	10.96016	0.05	1
P1.0 P0.6	2	4.24264	0.05	1
P1.0 P0.8	0.83333	1.76777	0.05	0
P1.5 P0.0	12.16667	25.8094	0.05	1
P1.5 P0.2	9	19.09188	0.05	1
P1.5 P0.4	7.5	15.9099	0.05	1
P1.5 P0.6	4.33333	9.19239	0.05	1
P1.5 P0.8	3.16667	6.71751	0.05	1
P1.5 P1.0	2.33333	4.94975	0.05	1
P2.0 P0.0	15	31.81981	0.05	1
P2.0 P0.2	11.83333	25.10229	0.05	1
P2.0 P0.4	10.33333	21.92031	0.05	1

P2.0 P0.6	7.16667	15.2028	0.05	1
P2.0 P0.8	6	12.72792	0.05	1
P2.0 P1.0	5.16667	10.96016	0.05	1
P2.0 P1.5	2.83333	6.01041	0.05	1

Table 8.79. Means Comparison of heat deflection test by Bonferroni Test for cellulose nanofibers filled poly (lactic acid) composites

Sample Code	Mean Diff	t Value	Alpha	Sigma
P0.2 P0.0	4.66667	10.85793	0.05	1
P0.4 P0.0	5.66667	13.18463	0.05	1
P0.4 P0.2	1	2.3267	0.05	0
P0.6 P0.0	7.16667	16.67468	0.05	1
P0.6 P0.2	2.5	5.81675	0.05	1
P0.6 P0.4	1.5	3.49005	0.05	1
P0.8 P0.0	7.66667	17.83803	0.05	1
P0.8 P0.2	3	6.9801	0.05	1
P0.8 P0.4	2	4.6534	0.05	1
P0.8 P0.6	0.5	1.16335	0.05	0
P1.0 P0.0	9.33333	21.71587	0.05	1
P1.0 P0.2	4.66667	10.85793	0.05	1
P1.0 P0.4	3.66667	8.53123	0.05	1
P1.0 P0.6	2.16667	5.04118	0.05	1
P1.0 P0.8	1.66667	3.87783	0.05	1
P1.5 P0.0	10.66667	24.81814	0.05	1
P1.5 P0.2	6	13.9602	0.05	1
P1.5 P0.4	5	11.6335	0.05	1
P1.5 P0.6	3.5	8.14345	0.05	1
P1.5 P0.8	3	6.9801	0.05	1
P1.5 P1.0	1.33333	3.10227	0.05	0
P2.0 P0.0	14.66667	34.12494	0.05	1
P2.0 P0.2	10	23.267	0.05	1
P2.0 P0.4	9	20.9403	0.05	1

P2.0 P0.6	7.5	17.45025	0.05	1
P2.0 P0.8	7	16.2869	0.05	1
P2.0 P1.0	5.33333	12.40907	0.05	1
P2.0 P1.5	4	9.3068	0.05	1

Table 8.80. Means Comparison of heat deflection test by Bonferroni Test for 2.5carbon black + multiwalled carbon nanotubes filled poly (lactic acid) composites

Sample Code	Mean Diff	t Value	Alpha	Sigma
P0.2C P0.0	4.66667	11.29069	0.05	1
P0.4C P0.0	8.33333	20.16195	0.05	1
P0.4C P0.2C	3.66667	8.87126	0.05	1
P0.6C P0.0	8.66667	20.96842	0.05	1
P0.6C P0.2C	4	9.67773	0.05	1
P0.6C P0.4C	0.33333	0.80648	0.05	0
P0.8C P0.0	10.33333	25.00081	0.05	1
P0.8C P0.2C	5.66667	13.71012	0.05	1
P0.8C P0.4C	2	4.83887	0.05	1
P0.8C P0.6C	1.66667	4.03239	0.05	1
P1.0C P0.0	13.83333	33.46883	0.05	1
P1.0C P0.2C	9.16667	22.17814	0.05	1
P1.0C P0.4C	5.5	13.30688	0.05	1
P1.0C P0.6C	5.16667	12.50041	0.05	1
P1.0C P0.8C	3.5	8.46802	0.05	1
P1.5C P0.0	0.83333	2.01619	0.05	0
P1.5C P0.2C	-3.83333	-9.2745	0.05	1
P1.5C P0.4C	-7.5	-18.14575	0.05	1
P1.5C P0.6C	-7.83333	-18.95223	0.05	1
P1.5C P0.8C	-9.5	-22.98462	0.05	1
P1.5C P1.0C	-13	-31.45264	0.05	1
P2.0C P0.0	-4.5	-10.88745	0.05	1
P2.0C P0.2C	-9.16667	-22.17814	0.05	1
P2.0C P0.4C	-12.83333	-31.0494	0.05	1

P2.0C P0.6C	-13.16667	-31.85587	0.05	1
P2.0C P0.8C	-14.83333	-35.88826	0.05	1
P2.0C P1.0C	-18.33333	-44.35628	0.05	1
P2.0C P1.5C	-5.33333	-12.90365	0.05	1

Table 8.81. Means Comparison of heat deflection test by Bonferroni Test for 2.5carbon black + cellulose nanofibers filled poly (lactic acid) composites

Sample Code	Mean Diff	t Value	Alpha	Sigma
P0.2F P0.0	4	8.13676	0.05	1
P0.4F P0.0	6	12.20514	0.05	1
P0.4F P0.2F	2	4.06838	0.05	1
P0.6F P0.0	7.33333	14.9174	0.05	1
P0.6F P0.2F	3.33333	6.78064	0.05	1
P0.6F P0.4F	1.33333	2.71225	0.05	0
P0.8F P0.0	9.83333	20.00287	0.05	1
P0.8F P0.2F	5.83333	11.86611	0.05	1
P0.8F P0.4F	3.83333	7.79773	0.05	1
P0.8F P0.6F	2.5	5.08548	0.05	1
P1.0F P0.0	2.66667	5.42451	0.05	1
P1.0F P0.2F	-1.33333	-2.71225	0.05	0
P1.0F P0.4F	-3.33333	-6.78064	0.05	1
P1.0F P0.6F	-4.66667	-9.49289	0.05	1
P1.0F P0.8F	-7.16667	-14.57837	0.05	1
P1.5F P0.0	-2.5	-5.08548	0.05	1
P1.5F P0.2F	-6.5	-13.22224	0.05	1
P1.5F P0.4F	-8.5	-17.29062	0.05	1
P1.5F P0.6F	-9.83333	-20.00287	0.05	1
P1.5F P0.8F	-12.33333	-25.08835	0.05	1
P1.5F P1.0F	-5.16667	-10.50998	0.05	1
P2.0F P0.0	-7.33333	-14.9174	0.05	1
P2.0F P0.2F	-11.33333	-23.05416	0.05	1
P2.0F P0.4F	-13.33333	-27.12254	0.05	1

P2.0F P0.6F	-14.66667	-29.83479	0.05	1
P2.0F P0.8F	-17.16667	-34.92027	0.05	1
P2.0F P1.0F	-10	-20.34191	0.05	1
P2.0F P1.5F	-4.83333	-9.83192	0.05	1

Figure 8.20 and **Figure 8.21** represents the graphical form of the numerical values and comparative values of heat deflection temperature for poly (lactic acid) composites filled with CB, MWCNT, CNF, MWCNT + 2.5CB and CNF + 2.5CB. Descriptive statistical data for heat deflection temperature for poly (lactic acid) composites filled with CB, MWCNT, CNF and MWCNT + 2.5CB, CNF + 2.5CB are noted in **Table 8.73**, **Table 8.74**, **Table 8.75** and **Table 8.76**. **Table 8.77**, **Table 8.78**, **Table 8.79**, **Table 8.80** and **Table 8.81** gives the means comparison within the batches for CB, MWCNT, CNF, MWCNT + 2.5CB and CNF + 2.5CB. From the numerical data presented in above figures and tables, one may observe that poly (lactic acid) composites filled with 2.5wt% CB shows maximum heat deflection temperature amongst the poly (lactic acid) composites filled with CB. CB filled poly (lactic acid) composites at 5.0wt% and above decreases heat deflection temperature, and can be attributed to debonding of filler – filler network at increasing temperature. Poly (lactic acid) composites filled with MWCNT and CNF shows similar trend; addition of 2.5wt% CB increases heat deflection temperature till 1.0wt% MWCNT and 0.8wt% CNF; after which heat deflection temperature decreases; increase in heat deflection temperature can be attributed to strong physical forces and chemical interaction between filler – filler, polymer – filler interactions; decrease in polymer – filler interactions, owing to which weak filler – filler interactions rise and decrease the heat deflection temperature[139][133][131][1].

8.7 CONCLUSION

Mechanical strength for singly filled and hybrid filler poly (lactic acid) composites were calculated using hardness, tensile test, impact test, flexural test and heat deflection test. Hybrid filler poly (lactic acid) composites possessed increase in mechanical strength in comparison to singly filled poly (lactic acid) composites; increase in the mechanical strength for hybrid filler poly (lactic acid) composites can be attributed to hybrid structure (**Chapter 7**), physical forces and chemical interactions (**Chapter 6**) and modification of interphases (**Chapter 5**) within hybrid filler poly (lactic acid) composites. Concept of constrained region is also important and is presented in short in **Chapter 9** of the thesis.

9 CONSTRAINED REGION ESTIMATION

Spectroscopic studies using ATR - Fourier Transform Infrared Spectroscopy (**Chapter 6**) and Ultraviolet – Visible spectroscopy (**Chapter 5**) were performed to determine the interactions and interphase modifications within singly filled poly (lactic acid) and hybrid filler poly (lactic acid) composites; the extent of interactions were confirmed by estimating constrained region. Constrained region within singly filled and hybrid filler poly (lactic acid) composites are derived result from tan∂ curve of dynamic mechanical analysis.

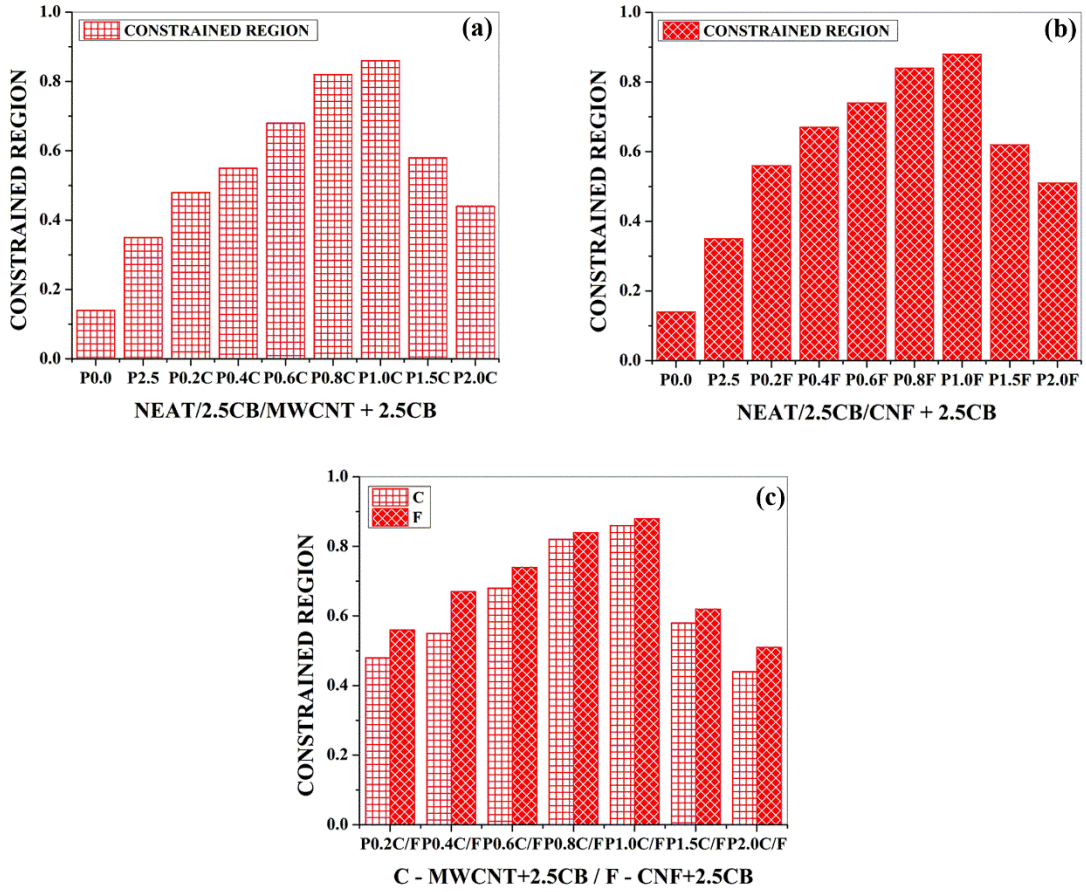

Figure 9.1. Constrained region (a) MWCNT filled hybrid poly (lactic acid) composites (b) CNF filled hybrid poly (lactic acid) composites (c) Comparative between MWCNT and CNF filled hybrid poly (lactic acid) composites

9.1 DISCUSSION

Constrained regions are severely restricted regions within polymer composites; the restriction is imposed due to interaction between surface of filler and the polymer matrix. Constrained region determines the mechanical strength of the polymer composites. In this chapter,

constrained region of hybrid filler poly (lactic acid) composites is compared with neat poly (lactic acid) and 2.5wt%CB filled poly (lactic acid) composites. Comparison between the constrained regions of neat poly (lactic acid), 2.5wt% of carbon black filled poly (lactic acid) composites and hybrid filler poly (lactic acid) composites (MWCNT+2.5CB and CNF+2.5CB) is graphically represented in **Figure 9.1**. One may observe that constrained region increases till 1.0wt% of MWCT as well as CNF in hybrid filler poly (lactic acid); but slightly increases for hybrid filler composites filled with CNF; which can be attributed to the hydroxyl functional group. These hydroxyl group with CNF is responsible for the strong chemical interactions with poly (lactic acid) thereby strengthening the interface and contributing to the constrained region[170][171].

9.2 CONCLUSION

Constrained regions are those regimes within polymer composites; wherein polymer chains are restricted on surface of fillers. Constrained regions in singly poly (lactic acid) composites and hybrid filler poly (lactic acid) composites determines its mechanical strength. Numerical values of mechanical strength closely matches the values of constrained region within singly filler and hybrid filler poly (lactic acid) composites.

General conclusion and future outlook with respect to current research attempt is presented in **Chapter 10**.

10 GENERAL CONCLUSION AND FUTURE OUTLOOK

10.1 GENERAL CONCLUSION

Poly (lactic acid) [PLA] is the abundantly available biopolymer and is core candidate for functional applications, the designing of nanocomposites aiming further improvement in structural properties is important for poly (lactic acid) to be used in structural component, hence poly (lactic acid) composites for structural applications should be mechanically strong, thermally stable. Current research problem was an attempt to modify poly (lactic acid) [PLA] with micro and nanofillers to fabricate and characterize singly filled poly (lactic acid) composites and hybrid filler poly (lactic acid) composites to fabricate a material with optimized strength and toughness, i.e. balancing the tensile strength and elongation. Hence it was important to explore the mechanisms playing in property improvement of PLA hybrid composites to reveal the mystery behind the positive trends in properties: special morphology and micro structural development due to the dispersion of nanofillers, the major role of interface, effect of nanofillers on polymer crystallization as heterogeneous nucleating agents, altered polymer chain dynamics .

One of the main challenges in the field of hybrid composites was processing i.e. it's difficult to disperse inorganic nanoparticles in polymers due to the incompatibility in surface characteristics between organic, hydrophobic, non-polar polymer and inorganic, hydrophilic, polar nanofillers. Hence the use of specific processing methods was required to reach a good dispersion of the filler in the polymeric matrix. The synergistic effect of nanoparticles as fillers in PLA, and the extent of polymer-filler interaction on structural behaviour, morphological and mechanical behaviour of poly (lactic acid) composites are addressed. No thrust has been given so far to this aspect of PLA hybrid filler system.

Hybrid systems, having binary nanofillers was found promising in enhancing the dispersion of nanoparticles and hybrid microstructure development by the synergism between the nanofillers, extending increased mechanical, structural and thermal characteristics. This was absolutely a new idea to have hybrid fillers in PLA system for proper distribution and superior micro structural development. It is worthy to notice that many works claim large improvement of mechanical stiffness with the addition of very small amount of fillers. Such stiffness increases cannot be explained as a simple mechanical reinforcement, as shown by classical mechanical coupling equations. So it is essential to search the change in mobility and nature of polymer chains in the presence of binary nanoparticles. In fact, a well dispersed minor

phase of nanomaterials can affect the crystallization characteristics of its continuous polymeric matrix since it creates a very large interfacial area.

In a nutshell, oligomeric dispersion was used to process poly (lactic acid) composites and hybrid composites, cellulose nanofibers were extracted from raw kenaf fibers and characterized. UV – Visible spectroscopy and ATR – FTIR Spectroscopy were performed to determine the interphase (absorbance height) and intermolecular interactions (peak height, peak position and peak width) within poly (lactic acid) composites. Absorbance increased for hybrid composites in comparison to singly filled poly (lactic acid) composites, which attributes to increase in interphase thickness for hybrid composites; hybrid composites showed closer absorbance values till 1.5wt% (CNF/MWCNT in hybrid composites), a slight decrease at 2.0wt% CNF in comparison to 2.0wt% MWCNT in hybrid composites was observed which can be attributed to decrease in interphase thickness. Hybrid composites showed increased modulus, (tensile and flexural), yield strength, strength (tensile and flexural) values in comparison to single filled poly (lactic acid) composites with maximum for hybrid composites filled with CNF. Although hybrid composites showed improvement in notched Izod impact, in comparison to singly filled composites but decrease after 0.6wt% MWCNT and 1.0wt% CNF in hybrid composites was observed, which can be attributed to sliding effect between fillers and embrittlement in hybrid composites. Hybrid composites showed a decrease in heat deflection temperature in comparison to singly filled composites. Considering the magnitude of mechanical strength, the fabricated hybrid composites could be used in structural applications where balance between stiffness and toughness is required. Filler networkability in hybrid composites also makes it a successful candidate for functional applications like EMI shielding, shape memory effect, agriculture mulch films and electrical sensors.

This thesis aimed at a detailed evaluation of PLA hybrid filler composites for crucial understanding on the system, its property enhancements and the structural alteration leading to that positive property variation. Detailed conclusions on the results for process selection, structural activity, morphological analysis and physio – mechanical properties are mentioned in line with the respective chapters.

10.2 FUTURE OUTLOOK

Possibilities are unlimited, but further investigations in use of nanofillers of different shapes/sizes and concentration and processing techniques would be interesting, which would be a interesting study. Studies in crystallization and its effect on mechanical strength of the polymer composites.

APPENDIX 1 – SYNTHESIZED CELLULOSE NANOFIBERS

Cellulose nanofibers [CNF] – Properties discussed in Section 4.2

APPENDIX 2 – PERCENT CHANGE

HARDNESS

CB	MWCNT	CNF	CB+MWCNT	CB+CNF
0.3983486	0.7766124	0.3358625	0.9272484	0.9216693
0.8201294	1.1202857	0.4864985	1.2363312	1.2843115
0.9372908	1.1359072	0.559027	1.3624191	1.4025887
1.0544521	1.2653426	0.8948895	1.8366436	1.614595
1.1258648	1.375809	0.9506807	1.9549208	2.0151752
1.2988172	1.7451462	1.1158224	2.1557688	2.1702745
1.4583798	2.2372238	1.614595	2.3421111	2.2885517

TENSILE MODULUS

CB	MWCNT	CNF	CB+MWCNT	CB+CNF
5.63694027	4.693045382	5.032847542	19.25168013	21.1961036
13.72045609	5.795514611	7.762591558	25.31148531	26.59895794
17.36389036	8.136373933	8.789549196	31.09944877	31.01638602
19.67454504	12.05920109	16.38601525	33.53469758	33.07030129
21.27161519	17.60930303	17.93777845	37.40466662	42.85660349
25.06607264	22.94419693	23.74839538	45.88084271	52.92607415
30.37076191	30.70678849	34.56920637	46.69259231	60.58672506

YIELD STRENGTH

CB	MWCNT	CNF	CB+MWCNT	CB+CNF
-42.19178082	43.76712329	-11.64383562	291.7808219	232.1917808
-13.42465753	86.43835616	13.69863014	313.0136986	260.9589041
-23.28767123	89.93150685	26.02739726	319.8630137	324.6575342
-25.68493151	101.8493151	148.630137	345.2054795	404.7945205
-25.47945205	69.24657534	179.4520548	310.9589041	390.4109589
-26.09589041	-9.315068493	87.67123288	93.83561644	283.5616438
-41.91780822	-12.46575342	32.19178082	36.30136986	189.0410959

TENSILE ELONGATION

CB	MWCNT	CNF	CB+MWCNT	CB+CNF
427.7647059	-37.50588235	80.94117647	14.35294118	-34.11764706
404.4705882	-29.92941176	1.176470588	6.823529412	-5.176470588
308.2352941	-18.09411765	-13.88235294	3.294117647	12
291.5294118	3.270588235	-49.08235294	-6.588235294	54.82352941
274.8235294	-28.51764706	-47.03529412	-11.52941176	-12.23529412
256.2352941	-39.41176471	-59.03529412	-28.23529412	-59.29411765
191.5294118	-44.42352941	-60.09411765	-68.23529412	-55.29411765

TENSILE STRENGTH

CB	MWCNT	CNF	CB+MWCNT	CB+CNF
0.2043597	99.114441	17.711172	370.02725	349.59128
18.119891	120.50409	33.855586	400.6812	394.75477
41.485014	137.26158	54.632153	419.75477	447.00272
48.705722	185.89918	254.83651	443.59673	461.58038
51.226158	144.27793	282.90191	436.78474	504.63215
32.629428	29.495913	203.61035	141.82561	437.87466
0.2043597	24.046322	106.47139	118.66485	298.50136

IMPACT STRENGTH

CB	MWCNT	CNF	CB+MWCNT	CB+CNF
66.666667	34.916667	0.8333333	73.083333	20
85	50.166667	19.166667	77.666667	80.416667
97.5	55.5	33.333333	101.58333	108.25
86.666667	82.5	35	64.916667	115.33333
89.166667	105.75	53.333333	49.25	135.83333
50	52.583333	-3.333333	29.75	79.916667
-6.666667	17	-19.16667	-8.583333	70.416667

FLEXURAL STRENGTH

CB	MWCNT	CNF	CB+MWCNT	CB+CNF
2.247191	97.438202	24.94382	156.11236	197.8427
23.146067	114.29213	49.438202	198.31461	227.82022
44.494382	140.60674	57.752809	223.23596	275.68539
50.561798	166.85393	255.95506	250.7191	282.22472
55.730337	184.31461	278.8764	276.11236	296.11236
35.730337	222.49438	203.82022	82.359551	260.92135
1.1235955	127.19101	110.78652	53.146067	178.40449

FLEXURAL MODULUS

CB	MWCNT	CNF	CB+MWCNT	CB+CNF
9.3064773	11.592347	10.001164	18.265611	22.378624
20.809563	18.294718	25.784919	24.948578	24.864749
21.399464	22.486126	27.570148	29.711647	26.885939
25.420111	27.488648	28.850856	34.100982	29.939846
27.504172	34.253114	30.612799	38.663407	39.068576
30.333372	38.813211	32.809407	46.899523	55.616098
36.35658	56.537432	42.112004	48.845422	61.411107

HEAT DEFLECTION TEST

CB	MWCNT	CNF	CB+MWCNT	CB+CNF
16.197191	6.6901484	9.8591627	9.8591627	8.4507048
20.422544	9.8591627	11.971839	17.605649	12.676057
23.239438	16.549311	15.140853	18.309867	15.492973
28.16903	19.014086	16.197191	21.831002	20.774663
29.929587	20.774663	19.718325	29.225368	5.6338103
22.1831	25.704234	22.53522	1.7605776	-5.281691
3.1690143	31.690143	30.985925	-9.507043	-15.49295

Note: % CHANGE is calculated on basis of “mean values” of physio – mechanical properties of neat poly (lactic acid) i.e. P(0.0) and singly filled poly (lactic acid) composites and hybrid composites.

REFERENCES

[1] A. V. Rane, K. Kanny, A. Mathew, T.P. Mohan, S. Thomas, Comparitive Analysis of Processing Techniques' Effect on the strength of carbon black (N220) filled poly (lactic acid) composites, Strength Mater. 51 (2019) 476–489. doi:10.1007/s11223-019-00093-6.

[2] S K Hajra Choudhury and A K Hajra Choudhury, Materials Science and Process, Indian Book Distributing Co, 2009.

[3] M. Nardin, E. Papirer, Powders and Fibers, Interfacial Science and Applications., 1st ed., CRC Press, Taylor and Francis Group, 2006.

[4] Y.S. Lipatov, Polymer Reinforcement, First, Chem Tech Publishing, Canada, 1995.

[5] G. Wypych, Handbook of Fillers, 2nd ed., Rapra, Toronto - Newyork, 2000.

[6] I.P. Singh, S. Chander, R.K. Prasad, Materials Science and Engineering, 1st ed., Jain Brothers, New Delhi, India, 2007.

[7] A.R. Ajitha, S. Thomas, Compatibilization of polymer blends, Micro and nanoscale morphologies, interphase characterization and properties, 1st ed., Elsevier Ltd, 2020.

[8] R. Auras, L.T. Lim, S.E.. Selke, H. Tsuji, Poly(Lactic Acid): Synthesis, Structures, Properties, Processing, and Applications, 1st ed., Wiley, A John Wiley & Sons, Inc., Publication, United States of America, 2010.

[9] L.T. Sin, A.R. Rahmat, W.. W.. Rahman, Poly(lactic acid): PLA Biopolymer Technology and Applications, 1st ed., Elsevier Ltd, Great Britain, 2012.

[10] C. Bastioli, Handbook of Biodegradable Polymers, 1st ed., Rapra Technology, United Kingdom, 2005.

[11] H.Y. Cheung, K.T. Lau, X.M. Tao, D. Hui, A potential material for tissue engineering: Silkworm silk/PLA biocomposite, Compos. Part B Eng. 39 (2008) 1026–1033. doi:10.1016/j.compositesb.2007.11.009.

[12] X. Xu, Q. Yang, Y. Wang, H. Yu, X. Chen, X. Jing, Biodegradable electrospun poly(l-lactide) fibers containing antibacterial silver nanoparticles, Eur. Polym. J. 42 (2006) 2081–2087. doi:10.1016/j.eurpolymj.2006.03.032.

[13] Y. Liu, G. Huang, C. Gao, L. Zhang, M. Chen, X. Xu, J. Gao, C. Pan, N. Yang, Y. Liu, Biodegradable polylactic acid porous monoliths as effective oil sorbents, Compos. Sci. Technol. 118 (2015) 9–15. doi:10.1016/j.compscitech.2015.08.005.

[14] E. Petinakis, X. Liu, L. Yu, C. Way, P. Sangwan, K. Dean, S. Bateman, G. Edward, Biodegradation and thermal decomposition of poly(lactic acid)-based materials

reinforced by hydrophilic fillers, Polym. Degrad. Stab. 95 (2010) 1704–1707. doi:10.1016/j.polymdegradstab.2010.05.027.

[15] J. Chen, W. Shi, A.J. Norman, P. Ilavarasan, Electrical impact of high-speed bus crossing plane split, IEEE Int. Symp. Electromagn. Compat. 2 (2002) 861–865. doi:10.1109/isemc.2002.1032709.

[16] K. Oksman, M. Skrifvars, J.F. Selin, Natural fibres as reinforcement in polylactic acid (PLA) composites, Compos. Sci. Technol. 63 (2003) 1317–1324. doi:10.1016/S0266-3538(03)00103-9.

[17] J. Xu, J. Zhang, W. Gao, H. Liang, H. Wang, J. Li, Preparation of chitosan/PLA blend micro/nanofibers by electrospinning, Mater. Lett. 63 (2009) 658–660. doi:10.1016/j.matlet.2008.12.014.

[18] M. Liu, Y. Yin, Z. Fan, X. Zheng, S. Shen, P. Deng, C. Zheng, H. Teng, W. Zhang, The effects of gamma-irradiation on the structure, thermal resistance and mechanical properties of the PLA/EVOH blends, Nucl. Instruments Methods Phys. Res. Sect. B Beam Interact. with Mater. Atoms. 274 (2012) 139–144. doi:10.1016/j.nimb.2011.12.020.

[19] W.J.E.M. Habraken, J.G.C. Wolke, J.A. Jansen, Ceramic composites as matrices and scaffolds for drug delivery in tissue engineering, Adv. Drug Deliv. Rev. 59 (2007) 234–248. doi:10.1016/j.addr.2007.03.011.

[20] R. Saiwaew, P. Suppakul, W. Boonsupthip, C. Pechyen, Development and characterization of Poly (lactic acid)/fish water soluble protein composite sheets: A potential approach for biodegradable packaging, Energy Procedia. 56 (2014) 280–288. doi:10.1016/j.egypro.2014.07.159.

[21] I. Stefani, J.J. Cooper-White, Development of an in-process UV-crosslinked, electrospun PCL/aPLA-co-TMC composite polymer for tubular tissue engineering applications, Acta Biomater. 36 (2016) 231–240. doi:10.1016/j.actbio.2016.03.013.

[22] S. Girdthep, N. Komrapit, R. Molloy, S. Lumyong, W. Punyodom, P. Worajittiphon, Effect of plate-like particles on properties of poly(lactic acid)/poly(butylene adipate-co-terephthalate) blend: A comparative study between modified montmorillonite and graphene nanoplatelets, Compos. Sci. Technol. 119 (2015) 115–123. doi:10.1016/j.compscitech.2015.10.005.

[23] G. Liao, S. Jiang, X. Xu, Y. Ke, Electrospun aligned PLLA/PCL/HA composite fibrous membranes and their in vitro degradation behaviors, Mater. Lett. 82 (2012) 159–162. doi:10.1016/j.matlet.2012.05.085.

[24] X. Song, F. Ling, L. Ma, C. Yang, X. Chen, Electrospun hydroxyapatite grafted poly(l-lactide)/poly(lactic-co-glycolic acid) nanofibers for guided bone regeneration membrane, Compos. Sci. Technol. 79 (2013) 8–14. doi:10.1016/j.compscitech.2013.02.014.

[25] X. Xu, X. Chen, A. Liu, Z. Hong, X. Jing, Electrospun poly(l-lactide)-grafted hydroxyapatite/poly(l-lactide) nanocomposite fibers, Eur. Polym. J. 43 (2007) 3187–3196. doi:10.1016/j.eurpolymj.2007.05.024.

[26] Q.H. Li, Q.H. Zhou, D. Deng, Q.Z. Yu, L. Gu, K. Da Gong, K.H. Xu, Enhanced thermal and electrical properties of poly (D,L-lactide)/multi- walled carbon nanotubes composites by in-situ polymerization, Trans. Nonferrous Met. Soc. China (English Ed. 23 (2013) 1421–1427. doi:10.1016/S1003-6326(13)62612-6.

[27] N. Sutivisedsak, H.N. Cheng, M.K. Dowd, G.W. Selling, A. Biswas, Evaluation of cotton byproducts as fillers for poly(lactic acid) and low density polyethylene, Ind. Crops Prod. 36 (2012) 127–134. doi:10.1016/j.indcrop.2011.08.016.

[28] T. Qiao, P. Song, H. Guo, X. Song, B. Zhang, X. Chen, Reinforced electrospun PLLA fiber membrane via chemical crosslinking, Eur. Polym. J. 74 (2016) 101–108. doi:10.1016/j.eurpolymj.2015.11.012.

[29] O. Gil-Castell, J.D. Badia, T. Kittikorn, E. Strömberg, A. Martínez-Felipe, M. Ek, S. Karlsson, A. Ribes-Greus, Hydrothermal ageing of polylactide/sisal biocomposites. Studies of water absorption behaviour and Physico-Chemical performance, Polym. Degrad. Stab. 108 (2014) 212–222. doi:10.1016/j.polymdegradstab.2014.06.010.

[30] B. Bax, J. Müssig, Impact and tensile properties of PLA/Cordenka and PLA/flax composites, Compos. Sci. Technol. 68 (2008) 1601–1607. doi:10.1016/j.compscitech.2008.01.004.

[31] A. Le Duigou, A. Bourmaud, E. Balnois, P. Davies, C. Baley, Improving the interfacial properties between flax fibres and PLLA by a water fibre treatment and drying cycle, Ind. Crops Prod. 39 (2012) 31–39. doi:10.1016/j.indcrop.2012.02.001.

[32] D. Chen, J. Li, J. Ren, Influence of fiber surface-treatment on interfacial property of poly(l-lactic acid)/ramie fabric biocomposites under UV-irradiation hydrothermal aging, Mater. Chem. Phys. 126 (2011) 524–531. doi:10.1016/j.matchemphys.2011.01.035.

[33] A.P. Johari, S.K. Kurmvanshi, S. Mohanty, S.K. Nayak, Influence of surface modified cellulose microfibrils on the improved mechanical properties of poly (lactic acid), Int. J. Biol. Macromol. 84 (2016) 329–339. doi:10.1016/j.ijbiomac.2015.12.038.

[34] X. Gong, C.Y. Tang, L. Pan, Z. Hao, C.P. Tsui, J. Liu, In vitro degradation of porous

poly(lactic acid)/quantum dots scaffolds, Compos. Part B Eng. 55 (2013) 234–239. doi:10.1016/j.compositesb.2013.06.034.

[35] C. Prapruddivongs, N. Sombatsompop, Roles and evidence of wood flour as an antibacterial promoter for triclosan-filled poly(lactic acid), Compos. Part B Eng. 43 (2012) 2730–2737. doi:10.1016/j.compositesb.2012.04.032.

[36] N. Petchwattana, S. Covavisaruch, Mechanical and morphological properties of wood plastic biocomposites prepared from toughened poly(lactic acid) and rubber wood sawdust (hevea brasiliensis), J. Bionic Eng. 11 (2014) 630–637. doi:10.1016/S1672-6529(14)60074-3.

[37] S. Ochi, Mechanical properties of kenaf fibers and kenaf/PLA composites, Mech. Mater. 40 (2008) 446–452. doi:10.1016/j.mechmat.2007.10.006.

[38] A. Kiziltas, B. Nazari, E. Erbas Kiziltas, D.J. Gardner, Y. Han, T.S. Rushing, Method to reinforce polylactic acid with cellulose nanofibers via a polyhydroxybutyrate carrier system, Carbohydr. Polym. 140 (2016) 393–399. doi:10.1016/j.carbpol.2015.12.059.

[39] A. Le Duigou, P. Davies, C. Baley, Seawater ageing of flax/poly(lactic acid) biocomposites, Polym. Degrad. Stab. 94 (2009) 1151–1162. doi:10.1016/j.polymdegradstab.2009.03.025.

[40] N. Wu, Y. Liang, K. Zhang, W. Xu, L. Chen, Preparation and bending properties of three dimensional braided single poly (lactic acid) composite, Compos. Part B Eng. 52 (2013) 106–113. doi:10.1016/j.compositesb.2013.02.047.

[41] N. Le Bolay, V. Santran, G. Dechambre, C. Combes, C. Drouet, A. Lamure, C. Rey, Production, by co-grinding in a media mill, of porous biodegradable polylactic acid-apatite composite materials for bone tissue engineering, Powder Technol. 190 (2009) 89–94. doi:10.1016/j.powtec.2008.04.043.

[42] E. de M. Teixeira, A.A.S. Curvelo, A.C. Corrêa, J.M. Marconcini, G.M. Glenn, L.H.C. Mattoso, Properties of thermoplastic starch from cassava bagasse and cassava starch and their blends with poly (lactic acid), Ind. Crops Prod. 37 (2012) 61–68. doi:10.1016/j.indcrop.2011.11.036.

[43] G. Yang, C. Geng, J. Su, W. Yao, Q. Zhang, Q. Fu, Property reinforcement of poly(propylene carbonate) by simultaneous incorporation of poly(lactic acid) and multiwalled carbon nanotubes, Compos. Sci. Technol. 87 (2013) 196–203. doi:10.1016/j.compscitech.2013.08.010.

[44] M. Reinhardt, J. Kaufmann, M. Kausch, L. Kroll, PLA-Viscose-Composites with Continuous Fibre Reinforcement for Structural Applications, Procedia Mater. Sci. 2

(2013) 137–143. doi:10.1016/j.mspro.2013.02.016.

[45] V.C. Pinto, T. Ramos, S. Alves, J. Xavier, P. Tavares, P.M.G.P. Moreira, R.M. Guedes, Comparative Failure Analysis of PLA, PLA/GNP and PLA/CNT-COOH Biodegradable Nanocomposites thin Films, Procedia Eng. 114 (2015) 635–642. doi:10.1016/j.proeng.2015.08.004.

[46] M. Luddee, S. Pivsa-Art, S. Sirisansaneeyakul, P. Chiravootpechyen, Particle size of ground bacterial cellulose affecting mechanical, thermal, and moisture barrier properties of PLA/BC biocomposites, Energy Procedia. 56 (2014) 211–218. doi:10.1016/j.egypro.2014.07.151.

[47] W. Nuthong, P. Uawongsuwan, W. Pivsa-Art, H. Hamada, Impact property of flexible epoxy treated natural fiber reinforced PLA composites, Energy Procedia. 34 (2013) 839–847. doi:10.1016/j.egypro.2013.06.820.

[48] W. Sujaritjun, P. Uawongsuwan, W. Pivsa-Art, H. Hamada, Mechanical property of surface modified natural fiber reinforced PLA biocomposites, Energy Procedia. 34 (2013) 664–672. doi:10.1016/j.egypro.2013.06.798.

[49] W.Y. Lin, Y.F. Shih, C.H. Lin, C.C. Lee, Y.H. Yu, The preparation of multi-walled carbon nanotube/poly(lactic acid) composites with excellent conductivity, J. Taiwan Inst. Chem. Eng. 44 (2013) 489–496. doi:10.1016/j.jtice.2012.12.012.

[50] S. Tanpichai, W.W. Sampson, S.J. Eichhorn, Stress-transfer in microfibrillated cellulose reinforced poly(lactic acid) composites using Raman spectroscopy, Compos. Part A Appl. Sci. Manuf. 43 (2012) 1145–1152. doi:10.1016/j.compositesa.2012.02.006.

[51] Y.S. Song, J.T. Lee, D.S. Ji, M.W. Kim, S.H. Lee, J.R. Youn, Viscoelastic and thermal behavior of woven hemp fiber reinforced poly(lactic acid) composites, Compos. Part B Eng. 43 (2012) 856–860. doi:10.1016/j.compositesb.2011.10.021.

[52] H. Zhou, J.G. Lawrence, S.B. Bhaduri, Fabrication aspects of PLA-CaP/PLGA-CaP composites for orthopedic applications: A review, Acta Biomater. 8 (2012) 1999–2016. doi:10.1016/j.actbio.2012.01.031.

[53] A.A. Mamun, H.P. Heim, D.H. Beg, T.S. Kim, S.H. Ahmad, PLA and PP composites with enzyme modified oil palm fibre: A comparative study, Compos. Part A Appl. Sci. Manuf. 53 (2013) 160–167. doi:10.1016/j.compositesa.2013.06.010.

[54] B. Imre, D. Bedo, A. Domján, P. Schön, G.J. Vancso, B. Pukánszky, Structure, properties and interfacial interactions in poly(lactic acid)/polyurethane blends prepared by reactive processing, Eur. Polym. J. 49 (2013) 3104–3113.

doi:10.1016/j.eurpolymj.2013.07.007.

[55] T. Yu, J. Ren, S. Li, H. Yuan, Y. Li, Effect of fiber surface-treatments on the properties of poly(lactic acid)/ramie composites, Compos. Part A Appl. Sci. Manuf. 41 (2010) 499–505. doi:10.1016/j.compositesa.2009.12.006.

[56] M.S. Islam, K.L. Pickering, N.J. Foreman, Influence of alkali treatment on the interfacial and physico-mechanical properties of industrial hemp fibre reinforced polylactic acid composites, Compos. Part A Appl. Sci. Manuf. 41 (2010) 596–603. doi:10.1016/j.compositesa.2010.01.006.

[57] L. Qin, J. Qiu, M. Liu, S. Ding, L. Shao, S. Lü, G. Zhang, Y. Zhao, X. Fu, Mechanical and thermal properties of poly(lactic acid) composites with rice straw fiber modified by poly(butyl acrylate), Chem. Eng. J. 166 (2011) 772–778. doi:10.1016/j.cej.2010.11.039.

[58] J. Leng, P.J. Purohit, N. Kang, D.Y. Wang, J. Falkenhagen, F. Emmerling, A.F. Thünemann, A. Schönhals, Structure-property relationships of nanocomposites based on polylactide and MgAl layered double hydroxides, Eur. Polym. J. 68 (2015) 338–354. doi:10.1016/j.eurpolymj.2015.05.008.

[59] M.A.S. Anwer, H.E. Naguib, Study on the morphological, dynamic mechanical and thermal properties of PLA carbon nanofibre composites, Compos. Part B Eng. 91 (2016) 631–639. doi:10.1016/j.compositesb.2016.01.039.

[60] J.F. Balart, V. Fombuena, O. Fenollar, T. Boronat, L. Sánchez-Nacher, Processing and characterization of high environmental efficiency composites based on PLA and hazelnut shell flour (HSF) with biobased plasticizers derived from epoxidized linseed oil (ELO), Compos. Part B Eng. 86 (2016) 168–177. doi:10.1016/j.compositesb.2015.09.063.

[61] M.P. Ho, K.T. Lau, H. Wang, D. Hui, Improvement on the properties of polylactic acid (PLA) using bamboo charcoal particles, Compos. Part B Eng. 81 (2015) 14–25. doi:10.1016/j.compositesb.2015.05.048.

[62] I. Spiridon, K. Leluk, A.M. Resmerita, R.N. Darie, Evaluation of PLA-lignin bioplastics properties before and after accelerated weathering, Compos. Part B Eng. 69 (2015) 342–349. doi:10.1016/j.compositesb.2014.10.006.

[63] W. Jia, R.H. Gong, P.J. Hogg, Poly (lactic acid) fibre reinforced biodegradable composites, Compos. Part B Eng. 62 (2014) 104–112. doi:10.1016/j.compositesb.2014.02.024.

[64] N.C. Loureiro, J.L. Esteves, J.C. Viana, S. Ghosh, Development of polyhydroxyalkanoates/poly(lactic acid) composites reinforced with cellulosic fibers,

Compos. Part B Eng. 60 (2014) 603–611. doi:10.1016/j.compositesb.2014.01.001.

[65] T. Gobi Kannan, C.M. Wu, K.B. Cheng, Effect of different knitted structure on the mechanical properties and damage behavior of Flax/PLA (Poly Lactic acid) double covered uncommingled yarn composites, Compos. Part B Eng. 43 (2012) 2836–2842. doi:10.1016/j.compositesb.2012.04.047.

[66] H.Y. Cheung, K.T. Lau, Y.F. Pow, Y.Q. Zhao, D. Hui, Biodegradation of a silkworm silk/PLA composite, Compos. Part B Eng. 41 (2010) 223–228. doi:10.1016/j.compositesb.2009.09.004.

[67] S. Cheng, K. tak Lau, T. Liu, Y. Zhao, P.M. Lam, Y. Yin, Mechanical and thermal properties of chicken feather fiber/PLA green composites, Compos. Part B Eng. 40 (2009) 650–654. doi:10.1016/j.compositesb.2009.04.011.

[68] P.J. Jandas, S. Mohanty, S.K. Nayak, Surface treated banana fiber reinforced poly (lactic acid) nanocomposites for disposable applications, J. Clean. Prod. 52 (2013) 392–401. doi:10.1016/j.jclepro.2013.03.033.

[69] K. Madhavan Nampoothiri, N.R. Nair, R.P. John, An overview of the recent developments in polylactide (PLA) research, Bioresour. Technol. 101 (2010) 8493–8501. doi:10.1016/j.biortech.2010.05.092.

[70] Z. Ying-Chen, W. Hong-Yan, Q. Yi-Ping, Morphology and properties of hybrid composites based on polypropylene/polylactic acid blend and bamboo fiber, Bioresour. Technol. 101 (2010) 7944–7950. doi:10.1016/j.biortech.2010.05.007.

[71] E. Llorens, S. Calderón, L.J. Del Valle, J. Puiggalí, Polybiguanide (PHMB) loaded in PLA scaffolds displaying high hydrophobic, biocompatibility and antibacterial properties, Mater. Sci. Eng. C. 50 (2015) 74–84. doi:10.1016/j.msec.2015.01.100.

[72] A. Morawska-Chochół, P. Domalik-Pyzik, J. Chłopek, B. Szaraniec, J. Sterna, M. Rzewuska, M. Boguń, R. Kucharski, P. Mielczarek, Gentamicin release from biodegradable poly-l-lactide based composites for novel intramedullary nails, Mater. Sci. Eng. C. 45 (2014) 15–20. doi:10.1016/j.msec.2014.08.059.

[73] C.E. Tanase, I. Spiridon, PLA/chitosan/keratin composites for biomedical applications, Mater. Sci. Eng. C. 40 (2014) 242–247. doi:10.1016/j.msec.2014.03.054.

[74] T. Maharana, S. Pattanaik, A. Routaray, N. Nath, A.K. Sutar, Synthesis and characterization of poly(lactic acid) based graft copolymers, React. Funct. Polym. 93 (2015) 47–67. doi:10.1016/j.reactfunctpolym.2015.05.006.

[75] F.O. Bakare, D. Åkesson, M. Skrifvars, T. Bashir, P. Ingman, R. Srivastava, Synthesis and characterization of unsaturated lactic acid based thermoset bio-resins, Eur. Polym.

J. 67 (2015) 570–582. doi:10.1016/j.eurpolymj.2014.11.045.

[76] V. Fiore, L. Botta, R. Scaffaro, A. Valenza, A. Pirrotta, PLA based biocomposites reinforced with Arundo donax fillers, Compos. Sci. Technol. 105 (2014) 110–117. doi:10.1016/j.compscitech.2014.10.005.

[77] P. Wan, C. Yuan, L.L. Tan, Q. Li, K. Yang, Fabrication and evaluation of bioresorbable PLLA/magnesium and PLLA/magnesium fluoride hybrid composites for orthopedic implants, Compos. Sci. Technol. 98 (2014) 36–43. doi:10.1016/j.compscitech.2014.04.011.

[78] A.K. Bledzki, A. Jaszkiewicz, Mechanical performance of biocomposites based on PLA and PHBV reinforced with natural fibres - A comparative study to PP, Compos. Sci. Technol. 70 (2010) 1687–1696. doi:10.1016/j.compscitech.2010.06.005.

[79] Q. Lv, K. Hu, Q. Feng, F. Cui, C. Cao, Preparation and characterization of PLA/fibroin composite and culture of HepG2 (human hepatocellular liver carcinoma cell line) cells, Compos. Sci. Technol. 67 (2007) 3023–3030. doi:10.1016/j.compscitech.2007.05.003.

[80] J.H. Wu, M.S. Yen, M.C. Kuo, B.H. Chen, Physical properties and crystallization behavior of silica particulates reinforced poly(lactic acid) composites, Mater. Chem. Phys. 142 (2013) 726–733. doi:10.1016/j.matchemphys.2013.08.031.

[81] G. Gorrasi, C. Milone, E. Piperopoulos, M. Lanza, A. Sorrentino, Hybrid clay mineral-carbon nanotube-PLA nanocomposite films. Preparation and photodegradation effect on their mechanical, thermal and electrical properties, Appl. Clay Sci. 71 (2013) 49–54. doi:10.1016/j.clay.2012.11.004.

[82] A. Awal, M. Rana, M. Sain, Thermorheological and mechanical properties of cellulose reinforced PLA bio-composites, Mech. Mater. 80 (2015) 87–95. doi:10.1016/j.mechmat.2014.09.009.

[83] Z. Song, H. Xiao, Y. Zhao, Hydrophobic-modified nano-cellulose fiber/PLA biodegradable composites for lowering water vapor transmission rate (WVTR) of paper, Carbohydr. Polym. 111 (2014) 442–448. doi:10.1016/j.carbpol.2014.04.049.

[84] G. Faludi, G. Dora, K. Renner, J. Móczó, B. Pukánszky, Biocomposite from polylactic acid and lignocellulosic fibers: Structure-property correlations, Carbohydr. Polym. 92 (2013) 1767–1775. doi:10.1016/j.carbpol.2012.11.006.

[85] A.N. Frone, S. Berlioz, J.F. Chailan, D.M. Panaitescu, Morphology and thermal properties of PLA-cellulose nanofibers composites, Carbohydr. Polym. 91 (2013) 377–384. doi:10.1016/j.carbpol.2012.08.054.

[86] E. Fortunati, M. Peltzer, I. Armentano, L. Torre, A. Jiménez, J.M. Kenny, Effects of

modified cellulose nanocrystals on the barrier and migration properties of PLA nano-biocomposites, Carbohydr. Polym. 90 (2012) 948–956. doi:10.1016/j.carbpol.2012.06.025.

[87] C.S. Wu, Polylactide-based renewable composites from natural products residues by encapsulated film bag: Characterization and biodegradability, Carbohydr. Polym. 90 (2012) 583–591. doi:10.1016/j.carbpol.2012.05.081.

[88] A. Marais, J.J. Kochumalayil, C. Nilsson, L. Fogelström, E.K. Gamstedt, Toward an alternative compatibilizer for PLA/cellulose composites: Grafting of xyloglucan with PLA, Carbohydr. Polym. 89 (2012) 1038–1043. doi:10.1016/j.carbpol.2012.03.051.

[89] X. Li, C.L. Chu, L. Liu, X.K. Liu, J. Bai, C. Guo, F. Xue, P.H. Lin, P.K. Chu, Biodegradable poly-lactic acid based-composite reinforced unidirectionally with high-strength magnesium alloy wires, Biomaterials. 49 (2015) 135–144. doi:10.1016/j.biomaterials.2015.01.060.

[90] Y. Jin, J. Wang, H. Ke, S. Wang, Z. Dai, Graphene oxide modified PLA microcapsules containing gold nanoparticles for ultrasonic/CT bimodal imaging guided photothermal tumor therapy, Biomaterials. 34 (2013) 4794–4802. doi:10.1016/j.biomaterials.2013.03.027.

[91] T. Kasuga, Y. Ota, M. Nogami, Y. Abe, Preparation and mechanical properties of polylactic acid composites containing hydroxyapatite fibers, Biomaterials. 22 (2000) 19–23. doi:10.1016/S0142-9612(00)00091-0.

[92] Y.N. Wang, Y.X. Weng, L. Wang, Characterization of interfacial compatibility of polylactic acid and bamboo flour (PLA/BF) in biocomposites, Polym. Test. 36 (2014) 119–125. doi:10.1016/j.polymertesting.2014.04.001.

[93] M.P. Arrieta, J. López, D. López, J.M. Kenny, L. Peponi, Effect of chitosan and catechin addition on the structural, thermal, mechanical and disintegration properties of plasticized electrospun PLA-PHB biocomposites, Polym. Degrad. Stab. 132 (2016) 145–156. doi:10.1016/j.polymdegradstab.2016.02.027.

[94] F. Luzi, E. Fortunati, D. Puglia, R. Petrucci, J.M. Kenny, L. Torre, Study of disintegrability in compost and enzymatic degradation of PLA and PLA nanocomposites reinforced with cellulose nanocrystals extracted from Posidonia Oceanica, Polym. Degrad. Stab. 121 (2015) 105–115. doi:10.1016/j.polymdegradstab.2015.08.016.

[95] O. Gordobil, I. Egüés, R. Llano-Ponte, J. Labidi, Physicochemical properties of PLA lignin blends, Polym. Degrad. Stab. 108 (2014) 330–338.

doi:10.1016/j.polymdegradstab.2014.01.002.

[96] K. Bocz, B. Szolnoki, A. Marosi, T. Tábi, M. Wladyka-Przybylak, G. Marosi, Flax fibre reinforced PLA/TPS biocomposites flame retarded with multifunctional additive system, Polym. Degrad. Stab. 106 (2014) 63–73. doi:10.1016/j.polymdegradstab.2013.10.025.

[97] C. Man, C. Zhang, Y. Liu, W. Wang, W. Ren, L. Jiang, F. Reisdorffer, T.P. Nguyen, Y. Dan, Poly (lactic acid)/titanium dioxide composites: Preparation and performance under ultraviolet irradiation, Polym. Degrad. Stab. 97 (2012) 856–862. doi:10.1016/j.polymdegradstab.2012.03.039.

[98] C. Way, K. Dean, D.Y. Wu, E. Palombo, Biodegradation of sequentially surface treated lignocellulose reinforced polylactic acid composites: Carbon dioxide evolution and morphology, Polym. Degrad. Stab. 97 (2012) 430–438. doi:10.1016/j.polymdegradstab.2011.11.013.

[99] M. Gardette, S. Thérias, J.L. Gardette, M. Murariu, P. Dubois, Photooxidation of polylactide/calcium sulphate composites, Polym. Degrad. Stab. 96 (2011) 616–623. doi:10.1016/j.polymdegradstab.2010.12.023.

[100] B. Zou, X. Li, H. Zhuang, W. Cui, J. Zou, J. Chen, Degradation behaviors of electrospun fibrous composites of hydroxyapatite and chemically modified poly(dl-lactide), Polym. Degrad. Stab. 96 (2011) 114–122. doi:10.1016/j.polymdegradstab.2010.10.012.

[101] M. Murariu, A.L. Dechief, L. Bonnaud, Y. Paint, A. Gallos, G. Fontaine, S. Bourbigot, P. Dubois, The production and properties of polylactide composites filled with expanded graphite, Polym. Degrad. Stab. 95 (2010) 889–900. doi:10.1016/j.polymdegradstab.2009.12.019.

[102] M. Murariu, L. Bonnaud, P. Yoann, G. Fontaine, S. Bourbigot, P. Dubois, New trends in polylactide (PLA)-based materials: “Green” PLA-Calcium sulfate (nano)composites tailored with flame retardant properties, Polym. Degrad. Stab. 95 (2010) 374–381. doi:10.1016/j.polymdegradstab.2009.11.032.

[103] M.S. Islam, K.L. Pickering, N.J. Foreman, Influence of accelerated ageing on the physico-mechanical properties of alkali-treated industrial hemp fibre reinforced poly(lactic acid) (PLA) composites, Polym. Degrad. Stab. 95 (2010) 59–65. doi:10.1016/j.polymdegradstab.2009.10.010.

[104] C.S. Wu, Renewable resource-based composites of recycled natural fibers and maleated polylactide bioplastic: Characterization and biodegradability, Polym. Degrad. Stab. 94 (2009) 1076–1084. doi:10.1016/j.polymdegradstab.2009.04.002.

[105] R.T. De Silva, P. Pasbakhsh, K.L. Goh, L. Mishnaevsky, 3-D computational model of poly (lactic acid)/halloysite nanocomposites: Predicting elastic properties and stress analysis, Polymer (Guildf). 55 (2014) 6418–6425. doi:10.1016/j.polymer.2014.09.057.

[106] P.K. Bajpai, I. Singh, J. Madaan, Tribological behavior of natural fiber reinforced PLA composites, Wear. 297 (2013) 829–840. doi:10.1016/j.wear.2012.10.019.

[107] S. Perinović, B. Andriić, M. Erceg, Thermal properties of poly(l-lactide)/olive stone flour composites, Thermochim. Acta. 510 (2010) 97–102. doi:10.1016/j.tca.2010.07.002.

[108] A.F. Koutsomitopoulou, J.C. Bénézet, A. Bergeret, G.C. Papanicolaou, Preparation and characterization of olive pit powder as a filler to PLA-matrix bio-composites, Powder Technol. 255 (2014) 10–16. doi:10.1016/j.powtec.2013.10.047.

[109] A. Le Duigou, A. Bourmaud, P. Davies, C. Baley, Long term immersion in natural seawater of Flax/PLA biocomposite, Ocean Eng. 90 (2014) 140–148. doi:10.1016/j.oceaneng.2014.07.021.

[110] I.S.M.A. Tawakkal, M.J. Cran, S.W. Bigger, Release of thymol from poly(lactic acid)-based antimicrobial films containing kenaf fibres as natural filler, LWT - Food Sci. Technol. 66 (2016) 629–637. doi:10.1016/j.lwt.2015.11.011.

[111] I. Armentano, E. Fortunati, N. Burgos, F. Dominici, F. Luzi, S. Fiori, A. Jiménez, K. Yoon, J. Ahn, S. Kang, J.M. Kenny, Bio-based PLA_PHB plasticized blend films: Processing and structural characterization, LWT - Food Sci. Technol. 64 (2015) 980–988. doi:10.1016/j.lwt.2015.06.032.

[112] N. Zhao, S. Shi, G. Lu, M. Wei, Polylactide (PLA)/layered double hydroxides composite fibers by electrospinning method, J. Phys. Chem. Solids. 69 (2008) 1564–1568. doi:10.1016/j.jpcs.2007.10.046.

[113] A. Abdal-Hay, F.A. Sheikh, J.K. Lim, Air jet spinning of hydroxyapatite/poly(lactic acid) hybrid nanocomposite membrane mats for bone tissue engineering, Colloids Surfaces B Biointerfaces. 102 (2013) 635–643. doi:10.1016/j.colsurfb.2012.09.017.

[114] B. Imre, G. Keledi, K. Renner, J. Móczó, M. Murariu, P. Dubois, B. Pukánszky, Adhesion and micromechanical deformation processes in PLA/CaSO 4 composites, Carbohydr. Polym. 89 (2012) 759–767. doi:10.1016/j.carbpol.2012.04.005.

[115] J. Hughes, R. Thomas, Y. Byun, S. Whiteside, Improved flexibility of thermally stable poly-lactic acid (PLA), Carbohydr. Polym. 88 (2012) 165–172. doi:10.1016/j.carbpol.2011.11.078.

[116] Á. Csikós, G. Faludi, A. Domján, K. Renner, J. Móczó, B. Pukánszky, Modification of interfacial adhesion with a functionalized polymer in PLA/wood composites, Eur.

Polym. J. 68 (2015) 592–600. doi:10.1016/j.eurpolymj.2015.03.032.

[117] D. Wu, M. Hakkarainen, Recycling PLA to multifunctional oligomeric compatibilizers for PLA/starch composites, Eur. Polym. J. 64 (2015) 126–137. doi:10.1016/j.eurpolymj.2015.01.004.

[118] R. Al-Itry, K. Lamnawar, A. Maazouz, Reactive extrusion of PLA, PBAT with a multi-functional epoxide: Physico-chemical and rheological properties, Eur. Polym. J. 58 (2014) 90–102. doi:10.1016/j.eurpolymj.2014.06.013.

[119] H. Zhang, Q.W. Fu, T.W. Sun, F. Chen, C. Qi, J. Wu, Z.Y. Cai, Q.R. Qian, Y.J. Zhu, Amorphous calcium phosphate, hydroxyapatite and poly(d,l-lactic acid) composite nanofibers: Electrospinning preparation, mineralization and in vivo bone defect repair, Colloids Surfaces B Biointerfaces. 136 (2015) 27–36. doi:10.1016/j.colsurfb.2015.08.015.

[120] V. Guarino, L. Ambrosio, The synergic effect of polylactide fiber and calcium phosphate particle reinforcement in poly ε-caprolactone-based composite scaffolds, Acta Biomater. 4 (2008) 1778–1787. doi:10.1016/j.actbio.2008.05.013.

[121] Y. Wang, B. Tong, S. Hou, M. Li, C. Shen, Transcrystallization behavior at the poly(lactic acid)/sisal fibre biocomposite interface, Compos. Part A Appl. Sci. Manuf. 42 (2011) 66–74. doi:10.1016/j.compositesa.2010.10.006.

[122] W.D. Biggs, The Mechanical Behaviour of Engineering Materials, (1965) 148.

[123] D. Francois, P. Andre, Z. Andre, Mechanical Behaviour of Materials: Micro- and Macroscopic Constitutive Behaviour, Springer, 2012.

[124] D. Francois, P. Andre, Z. Andre, Mechanical Behaviour of Materials: Elasticity and Plasticity, 1st ed., Springer, 1993.

[125] D. Francois, P. Andre, Z. Andre, Mechanical Behaviour of Materials: Fracture Mechanics and Damage, 1st ed., Springer, London, 2013.

[126] D. Francois, P. Andre, Z. Andre, Mechanical Behaviour of Materials: Viscoplasticity, Damage, Fracture and Contact Mechanics, 1st ed., Springer, 1993.

[127] A. Dufresene, Nanocellulose: From Nature to High performance tailored materials, 1st ed., De Gruyter, Boston, 2012.

[128] B.P. GRADY, Carbon Nanotube - Polymer Composites, Manufacture, Properties and Applications, 1st ed., Wiley, A John Wiley & Sons, Inc., Publication, Hoboken, New Jersey, 2011.

[129] S.G. Advani, Processing and properties of nanocomposites, 1st ed., World Scientific, 2007.

[130] ASTM, Standard Test Methods for Density and Specific gravity (Relative Density) of Plastics by Displacement., 792, 2000.

[131] G. Wypych, Handbook of Fillers, 1st ed., Chem Tech Publishing, Toronto, 2010.

[132] J. Roesler, H. Harders, M. Baeker, Mechanical Behaviour of Engineering Materials: Metals, Ceramics, Polymers and Composites, 1st ed., Springer-Verlag Berlin Heidelberg New York, 2007.

[133] V. Shah, Handbook of Plastics Testing and Failure Analysis, 3rd ed., Wiley, A John Wiley & Sons, Inc., Publication, 2007.

[134] S. Qian, H. Zhang, W. Yao, K. Sheng, Effects of bamboo cellulose nanowhisker content on the morphology, crystallization, mechanical, and thermal properties of PLA matrix biocomposites, Compos. Part B Eng. 133 (2018) 203–209. doi:10.1016/j.compositesb.2017.09.040.

[135] P.S. Theocaris, The Mesophase Concept in Composites, 1st ed., Springer-Verlag Berlin Heidelberg New York, 1987.

[136] G. Wypych, Atlas of Material Damage, 1st ed., ChemTec Publishing, Toronto, 2012.

[137] L. Ma, J. Zhao, X. Wang, M. Chen, Y. Liang, Z. Wang, Z. Yu, R.C. Hedden, Effects of carbon black nanoparticles on two-way reversible shape memory in crosslinked polyethylene, Polymer (Guildf). 56 (2015) 490–497. doi:10.1016/j.polymer.2014.11.036.

[138] J. Wang, H. Li, R. Liu, L. Li, Y.H. Lin, C.W. Nan, Thermoelectric and mechanical properties of PLA/Bi0·5Sb1·5Te3 composite wires used for 3D printing, Compos. Sci. Technol. 157 (2018) 1–9. doi:10.1016/j.compscitech.2018.01.013.

[139] ASTM, Standard Test Method for Deflection Temperature of Plastics using Flexural Load in the Edgewise position, 648, 2001.

[140] J.E. Mark, Physical Properties of Polymers Handbook, 2nd ed., Springer, 2007.

[141] M. Ahmadi, A. Shojaei, Cure kinetic and network structure of NR/SBR composites reinforced by multiwalled carbon nanotube and carbon blacks, Thermochim. Acta. 566 (2013) 238–248. doi:10.1016/j.tca.2013.06.004.

[142] X. Wen, Y. Wang, J. Gong, J. Liu, N. Tian, Y. Wang, Z. Jiang, J. Qiu, T. Tang, Thermal and flammability properties of polypropylene/carbon black nanocomposites, Polym. Degrad. Stab. 97 (2012) 793–801. doi:10.1016/j.polymdegradstab.2012.01.031.

[143] H.S. B Cappella, M.Geuss, M .Kluppel, M.Munz, E.Schulz, Filler-Reinforced Elastomers Scanning Force Microscopy;Springer-Verlag Berlin Heidelberg New York, Springer-Verlag Berlin Heidelberg New York, 2003. doi:10.1007/b10953.

[144] J.K. Pandey, H. Takagi, A.N. Nakagaito, H.-J. Kim, eds., Handbook of Polymer Nanocomposites. Processing, Performance and Application, 1st ed., Springer, Newyork, 2015.

[145] B. Neher, M.A. Gafur, M.A. Al-Mansur, M.M.R. Bhuiyan, M.R. Qadir, F. Ahmed, Investigation of the Surface Morphology and Structural Characterization of Palm Fiber Reinforced Acrylonitrile Butadiene Styrene (PF-ABS) Composites, Mater. Sci. Appl. 05 (2014) 378–386. doi:10.4236/msa.2014.56043.

[146] E. Chukwunyelu Christian, S. Metu Chidiebere, C. Ojukwu Martin, Fourier Transform Infrared (FTIR) Spectroscopy Study on Coir Fibre Reinforced Polyester (CFRP) Composites, Int. J. Civil, Mech. Energy Sci. 2 (2016) 20–28.

[147] B. Ruxanda, Carmen.A.T, Iuliana.s, Preparation and characterisation of composites comprising modified hardwood and wood polymers/polyvinyl chlodide, Bioresources. 4 (2009) 1285–1304.

[148] V.S. Giita Silverajah, N.A. Ibrahim, N. Zainuddin, W.M.Z. Wan Yunus, H.A. Hassan, Mechanical, thermal and morphological properties of poly(lactic acid)/epoxidized palm olein blend, Molecules. 17 (2012) 11729–11747. doi:10.3390/molecules171011729.

[149] K. Ayyasamy, S. Eswaran, P. Kandasamy, Subraman, Polyester Clay Composite: Preparation and Characterization, J. Chem. 2 (2014) 1–6.

[150] E.L.M. Pereira, A.S.M. Batista, F.A.S. Ribeiro, A.P. Santos, A. Clascídia, L.O. Faria, Preliminary Studies of MWCNT / PVDF Polymer Composites, 10 (2016) 144–147.

[151] L. Bokobza, Spectroscopic techniques for the characterization of polymer nanocomposites: A review, Polymers (Basel). 10 (2017). doi:10.3390/polym10010007.

[152] E.E. Popa, M. Rapa, O. Popa, G. Mustatea, V.I. Popa, A.C. Mitelut, M.E. Popa, Polylactic acid/cellulose fibres based composites for food packaging applications, Mater. Plast. 54 (2017).

[153] F. Rositani, P.L. Antonucci, M. Minutoli, N. Giordano, A. Villari, Infrared analysis of carbon blacks, Carbon N. Y. 25 (1987) 325–332. doi:10.1016/0008-6223(87)90002-9.

[154] W. Kemp, Organic Spectroscopy, Third, Palgrave, Newyork, 2012.

[155] S. Zhao, W. Zhai, N. Li, K. Dai, G. Zheng, C. Liu, J. Chen, C. Shen, Liquid sensing properties of carbon black/polypropylene composite with a segregated conductive network, Sensors Actuators, A Phys. 217 (2014) 13–20. doi:10.1016/j.sna.2014.06.013.

[156] S. Xu, M. Wen, J. Li, S. Guo, M. Wang, Q. Du, J. Shen, Y. Zhang, S. Jiang, Structure and properties of electrically conducting composites consisting of alternating layers of

pure polypropylene and polypropylene with a carbon black filler, Polymer (Guildf). 49 (2008) 4861–4870. doi:10.1016/j.polymer.2008.08.056.

[157] H. Yui, G. Wu, H. Sano, M. Sumita, K. Kino, Morphology and electrical conductivity of injection-molded polypropylene/carbon black composites with addition of high-density polyethylene, Polymer (Guildf). 47 (2006) 3599–3608. doi:10.1016/j.polymer.2006.03.064.

[158] K. Chrissafis, K.M. Paraskevopoulos, S.Y. Stavrev, A. Docoslis, A. Vassiliou, D.N. Bikiaris, Characterization and thermal degradation mechanism of isotactic polypropylene/carbon black nanocomposites, Thermochim. Acta. 465 (2007) 6–17. doi:10.1016/j.tca.2007.08.007.

[159] E.A. Zaragoza-Contreras, C.A. Hernández-Escobar, A. Navarrete-Fontes, S.G. Flores-Gallardo, Synthesis of carbon black/polystyrene conductive nanocomposite. Pickering emulsion effect characterized by TEM, Micron. 42 (2011) 263–270. doi:10.1016/j.micron.2010.10.005.

[160] A.S. Alghamdi, I.A. Ashcroft, M. Song, D. Cai, Morphology and strain rate effects on heat generation during the plastic deformation of polyethylene/carbon black nanocomposites, Polym. Test. 32 (2013) 1105–1113. doi:10.1016/j.polymertesting.2013.06.013.

[161] A. Vayyaprontavida Kaliyathan, K.M. Varghese, A.S. Nair, S. Thomas, Rubber - rubber blends: A critical review, Prog. Rubber, Plast. Recycl. Technol. (2019) 1–47. doi:10.1177/1477760619895002.

[162] N. Yao, Z.L. Wang, Handbook of Microscopy for Nanotechnology, 1st ed., Kluwer Academic Press, 2005.

[163] M.A. Hayat, Basic Techniques for Transmission Electron Microscopy, 1st ed., Academic Press, 1986.

[164] K.C. Khulbe, C.Y. Feng, T. Matsuura, Synthetic Polymeric Membranes: Characterization by Atomic Force Microscopy, 1st ed., Springer-Verlag Berlin Heidelberg New York, 2008.

[165] J. Pelleg, Mechanical Properties of Materials, 1st ed., Springer-Verlag Berlin Heidelberg New York, 2013.

[166] H. Altenbach, J. Altenbach, W. Kissing, Mechanics of Composite Structural Elements, 1st ed., Springer-Verlag Berlin Heidelberg New York, 2004.

[167] R.N. Rothon, Particulate Filled Polymer Composites, 2nd ed., Rapra Technology, 2003.

[168] J.E. Mark, C. Y - C Lee, P.A. Bianconi, Hybrid Organic - Inorganic Composites, 1st ed., American Chemical Society, Washington, DC, 1995.

[169] R.M. German, Particulate Composites: Fundamentals and Applications, 1st ed., Springer-Verlag Berlin Heidelberg New York, 2016.

[170] P. Bindu, S. Thomas, Viscoelastic Behavior and Reinforcement Mechanism in Rubber Nanocomposites in the Vicinity of Spherical Nanoparticles, J. Phys. Chem. - B. 117 (2013) 12632–12648. doi:dx.doi.org/10.1021/jp4039489.

[171] Y. Rao, J.M. Pochan, Mechanics of Polymer - Clay Nanocomposites, Macromolecules. 40 (2007) 290–296. doi:10.1021/ma061445w.